Pharmacological stimulation of amyloid-ß (Aß) peptide uptake by macrophages and microglia cells

Inaugural-Dissertation

zur Erlangung des Doktorgrades
der Mathematisch-Naturwissenschaftlichen Fakultät
der Heinrich-Heine-Universität Düsseldorf

vorgelegt von

Isabella Ogorek
aus Laurahütte

Düsseldorf, April 2018

aus dem Institut für Neuropathologie
der Heinrich-Heine-Universität Düsseldorf

Gedruckt mit der Genehmigung der
Mathematisch-Naturwissenschaftlichen Fakultät der
Heinrich-Heine-Universität Düsseldorf

Berichterstatter:

1. Prof. Dr. Sascha Weggen

2. Prof. Dr. Lutz Schmitt

Tag der mündlichen Prüfung:

Ich versichere an Eides Statt, dass die vorgelegte Dissertation

Pharmacological stimulation of amyloid-ß (Aß) peptide uptake by macrophages and microglia cells

von mir selbständig und ohne unzulässige fremde Hilfe unter Beachtung der „Grundsätze zur Sicherung guter wissenschaftlicher Praxis an der Heinrich-Heine-Universität Düsseldorf" erstellt worden ist.

Des Weiteren versichere ich, dass die Dissertation zuvor keiner anderen Universität oder Fakultät vorgelegt wurde und ich bislang keinerlei andere Promotionsversuche getätigt habe.

Düsseldorf, 16.04.2018

Ort, Datum	Isabella Ogorek

Contents

Summary

Alzheimer's disease (AD) is the most common neurodegenerative disorder in the elderly and responsible for up to 75 % of all dementia cases. Imaging studies indicate that the accumulation of amyloid-ß (Aß) peptides in the brain and their deposition into insoluble amyloid plaques is a triggering event in the disease process. Microglia are the resident immune cells of the brain, and they surround Aß deposits in the brains of AD patients. Microglia have the ability to internalize Aß and numerous studies support that this cell population is involved in the removal of Aß peptides from the brain. This clearance pathway appears to be impaired in AD patients, and boosting salutary microglia functions is a putative treatment option for AD. At the beginning of this thesis project, preliminary evidence indicated that small molecule inhibitors of the glycogen synthase kinase 3 (GSK3) might promote the capacity of cells to take up and internalize Aß peptides. In this study, we show that structurally divergent GSK3 inhibitors (GSKi) stimulated Aß uptake by human THP-1 macrophages and primary murine microglia cells in a dose-dependent fashion, without negative effects on the cellular degradation rate of Aß. In primary microglia, treatment with GSKi was accompanied by a ramified morphology and upregulation of CD36 and IL-4R surface receptors, indicating the transition to an anti-inflammatory activation state. GSKi similarly enhanced the uptake of *E. coli* particles suggesting a receptor-independent, macropinocytic uptake mechanism. Importantly, both siRNA knockdown and CRISPR/Cas9 knockout experiments in THP-1 cells confirmed that the stimulatory effect of GSKi was mediated by their primary target GSK3 with a critical role for the GSK3ß isoform. Further studies showed that, while GSK3-dependent Wnt/ß-catenin signalling was not involved, the stimulation of Aß uptake by GSKi did require *de novo* transcription. Consequently, a microarray-based gene expression analysis of THP-1 cells was performed and identified a subset of genes similarly altered by three different GSKi, including cytokines and surface receptors implicated in the regulation of microglia activation and endocytosis. Finally, extensive CRISPR/Cas9 candidate gene analysis revealed a role for CDC42, a small Rho family GTPase, in the stimulation of Aß uptake. GSKi have been demonstrated to improve cognition in AD animal models. Our findings that GSKi stimulate the uptake of Aß peptides by microglia cells suggest a novel molecular explanation for their beneficial effects and further indicate that pharmacological targeting of GSK3 or its downstream effectors could provide a way to overcome impaired Aß clearance and limit its accumulation in AD.

Zusammenfassung

Die Alzheimer Erkrankung ist die häufigste neurodegenerative Erkrankung des Alters und verantwortlich für bis zu 75% aller Demenzfälle. Bildgebende Verfahren haben gezeigt, dass die Akkumulation von Amyloid-ß (Aß) Peptiden im Gehirn und die Ausbildung von unlöslichen amyloiden Plaques eine Schlüsselrolle in der Pathogenese der Erkrankung spielen. Mikroglia sind die Immunzellen des Gehirns und finden sich im Gehirn von Alzheimer Patienten vermehrt in der Umgebung der amyloiden Plaques. Mikroglia können Aß aufnehmen und sie tragen zur Beseitigung von Aß aus dem Gehirn bei, eine Funktion, die bei Alzheimer Patienten gestört ist. Zu Beginn dieses Dissertationsprojektes deuteten vorläufige Ergebnisse darauf hin, dass Inhibitoren der Glykogensynthase-Kinase 3 (GSK3) die Aufnahme von Aß Peptiden durch Zellen steigern können. Nachfolgend konnten wir zeigen, dass strukturell divergierende GSK3 Inhibitoren (GSKi) die Aufnahme von Aß durch humane THP-1 Makrophagen und primäre murine Mikroglia dosisabhängig stimulieren, ohne den zellulären Abbau der Peptide negativ zu beeinflussen. GSKi behandelte primäre Mikroglia zeigten einen anti-inflammatorischen Aktivierungszustand mit einer verzweigten Morphologie und einer erhöhten Expression der Oberflächenrezeptoren CD36 und IL-4R. GSKi stimulierten auch die zelluläre Aufnahme von *E. coli* Partikeln, was auf einen Rezeptor-unabhängigen, makropinozytotischen Mechanismus hindeutet. Knockout Experimente mittels siRNA und CRISPR/Cas9 bestätigten, dass der stimulierende Effekt der GSKi auf einer Inhibition der GSK3 Enzymaktivität beruht, mit einer zentralen Rolle der GSK3ß Isoform. Weitere Untersuchungen ergaben keine Hinweise auf eine Beteiligung des GSK3-abhängigen Wnt/ß-Catenin Signalweges, die Stimulation der Aß-Aufnahme war jedoch transkriptionsabhängig. Eine Transkriptomanalyse von THP-1 Zellen identifizierte eine Gruppe von Genen, die gleichermaßen von drei unterschiedlichen GSKi reguliert wurden. Diese umfassten Zytokine und Rezeptoren, welche den Aktivierungszustand von Mikroglia und den Prozess der Endozytose beeinflussen. Schließlich konnte durch eine umfassende CRISPR/Cas9 Analyse dieser Kandidatengene gezeigt werden, dass die Rho-GTPase CDC42 (cell division cycle 42) für die Stimulation der Aß-Aufnahme durch GSKi erforderlich ist. In Alzheimer-Tiermodellen hatten GSKi in früheren Studien kognitionsverbessernde Effekte gezeigt. Die in dieser Arbeit nachgewiesene, gesteigerte Aufnahme von Aß durch Mikroglia bietet einen neuen molekularen Erklärungsansatz für die beobachteten positiven Effekte der GSKi. Folglich könnten GSKi oder eine pharmakologische Beeinflussung von GSK3 Effektorproteinen der toxischen Akkumulation von Aß Peptiden bei der Alzheimer Erkrankung entgegenwirken.

Abbreviations

°C	Degree Celsius
AD	Alzheimer`s disease
ADAM	A Disintegrin And Metalloprotease
AICD	APP intracellular domain
APH	Anterior Pharynx Defective
APLP	Amyloid Precursor Protein-like Protein
ApoE	Apolipoprotein E
APP	Amyloid Precursor Protein
APPs	Soluble APP
APS	Ammoniumpersulfate
ARF1	Adenosyl Ribosylation Factor-1
Aß	Amyloid-ß
BACE1	ß-site APP Cleaving Enzyme 1
BCA	Bicinchoninic acid
BSA	Bovine Serum Albumin
Cas9	CRISPR associated protein 9
CCL	CC-chemokine ligand
CDC42	Cell division cycle 42
cDNA	Complementary DNA
CDK	Cyclin-dependent Kinase
CNS	Central Nervous System
CSF	Cerebrospinal Fluid
C-terminal	Carboxy-terminal
CRISPR	Clustered Regularly Interspaced Short Palindromic Repeats
CTF	Carboxy-terminal fragment
DAPI	4',6-diamidino-2-phenylindole
ddH_20	Double-distilled water
DMEM	Dulbecco`s Modified Eagle`s Medium
DMSO	Dimethylsulfoxid
DNA	Deoxyribonucleic acid
DSB	Double-strand break
DTT	Dithiothreitol
ECM	Extracellular Matrix
E. coli	*Escherichia coli*

EDTA	Ethylenediaminetetraacetic acid
EGFP	Enhanced Green Fluorescent Protein
e.g.	*exempli gratia* = for example
ELISA	Enzyme-linked Immunosorbent Assay
ER	Endoplasmic Reticulum
esiRNA	Endoribonuclease-prepared siRNA
et al.	and others
FAD	Familial Alzheimer`s disease
FAM-$A\beta_{42}$	Carboxyfluorescein-labeled amyloid beta 1-42
fAß	Fibrillar Aß
FCS	Fetal Calf Serum
g	gram
GM-CSF	Granulocyte Macrophage Colony-Stimulating Factor
GSK3	Glycogen Synthase Kinase 3
GWAS	Genome-Wide Association Study
h	hour(s)
HRP	Horse-Raddish Peroxidase
Iba1	Ionized calcium binding adaptor molecule 1
IC_{50}	Half maximal inhibitory concentration
IDE	Insulin-Degrading Enzyme
IgG	Immunoglobulin G
IL	Interleukin
kDa	kiloDalton
l	liter
LB	Lysogeny Broth
LDLR	Low Density Lipoprotein Receptor
LPS	Lipopolysaccharide
LTP	Long-term Potentiation
M	molar
m	meter
mA	milliampere
M-CSF	Macrophage Colony-Stimulating Factor
MES	2-(N-morpholino)ethanesulfonic acid
MilliQ	Double-distilled water
min	minute
MMP	Matrix Metallopeptidase

mRNA	Messenger RNA
MTT	(3-(4,5-dimethylthiazol-2-yl)-2,5-diphenyltetrazolium bromide)
n	nano
NEP	Neprilysin
NFT	Neurofibrillary tangle
NHEJ	Non-homologous end joining
NLRP3	NLR family, pyrin domain containing 3
N-terminal	Amino-terminal
NSAID	Non-Steroidal Anti-Inflammatory Drug
PAMPs	Pathogen-associated molecular patterns
PBS	Phosphate-Buffered Saline
PCR	Polymerase Chain Reaction
PEN	Presenilin Enhancer
PFA	Paraformaldehyde
PHF	Paired Helical Filaments
PKC	Proteinkinase C
PMA	Phorbol-12-myristat-13-acetat
PRRs	Pattern Recognition Receptors
PSEN	Presenilin
PVDF	Polyvinylidene fluoride
qPCR	Quantitative Real-Time PCR
RAGE	Receptor for Advanced Glycosylation Endproducts
RIPA	Radioimmunoprecipitation assay buffer
RNA	Ribonucleic acid
ROS	Reactive Oxygen Species
rpm	Revolutions Per Minute
RT	Room Temperature
s	second
sAPP	Soluble Amyloid Precursor Protein Ectodomain
SD	Standard Deviation
SDS	Sodium Dodecyle Sulfate
SDS PAGE	SDS-Polyacrylamide Gel Electrophoresis
sgRNA	Single guide RNA
siRNA	Small interfering RNA
SpCas9	*Streptococcus pyogenes* Cas9
SR	Scavenger Receptor

STAB1	Stabilin 1
TAE	TRIS-Acetic acid-EDTA
TBS	Tris Buffered Saline
TEMED	Tetramethylethylenediamine
THBS1	Thrombospondin 1
TLR	Toll Like Receptor
TNF-α	Tumor Necrosis Factor α
TREM	Triggering receptor expressed on myeloid cells
Tris	Tris(hydroxymethyl)aminomethane
V	Volt
v/v	volume/volume
w/v	weight/volume
WHO	World Health Organization
x g	Multiple of gravitational acceleration, g = 9.81 m/s^2

1 Introduction

1.1 Alzheimer`s Disease

Alzheimer`s disease (AD) is a progressive neurodegenerative disorder and the predominant type of dementia in the elderly, accounting for 60-70 % of all cases. Worldwide, over 47 million people are living with dementia, with approximately 7.7 million new patients being diagnosed with dementia every year (WHO 2016). Due to increasing life expectancy the number of dementia cases is expected to increase to 135.5 million by 2050 (WHO 2016). AD is clinically characterized by gradual loss of cognitive abilities including early memory impairment and language difficulties (Burns & Iliffe 2009). In addition, patients suffer from psychiatric symptoms and behavioural disturbances that may involve depression, hallucinations, delusions and agitation (Burns *et al.* 1990). Eventually, AD patients lose their ability to independently perform activities of daily living. The disease ultimately leads to death mostly within 8 to 10 years after clinical onset, but it can last in excess of 20 years. Age is the strongest risk factor for AD. In addition, genetic, medical and environmental factors have been implicated, including cardiovascular risk factors, psychosocial factors (e.g. depression) and lifestyle choices (e.g. physical activity and smoking) (Daviglus *et al.* 2010). Based on the age of onset, the disease can be divided into early-onset and late-onset AD (sporadic AD). Late-onset, sporadic AD accounts for about 90 % of cases and usually occurs after the age of 65. While early-onset AD with onset ages younger than 65 years is almost exlusively determined by genetic causes, only around 10 % of early-onset and < 1% of all AD cases are due to mutations in known genes and are inherited within families in an autosomal-dominant fashion (Bertram & Tanzi 2005, Cacace *et al.* 2016). The first-line medication for the treatment of AD are cholinesterase inhibitors, which raise the level of the neurotransmitter acetylcholine and thus alleviate symptoms without treating the underlying pathology (Winslow *et al.* 2011). To date, no effective cure or preventive treatment has been developed yet. One major barrier to an effective therapy is the lack of a full understanding of the pathomechanisms of AD.

1.2 Neuropathological hallmarks of Alzheimer`s Disease

AD is named after the psychiatrist Alois Alzheimer, who originally described the clinical and neuropathological characteristics of the disease in 1906. He examined the brain of a 51-year-old woman who died of an unusual mental disorder, and made the assertion that

her dementia was related to abnormal changes that he observed in her brain tissue (Alzheimer 1907). At present, the definitive diagnosis of AD is still based on a *post mortem* histological confirmation. The most significant neuropathological findings in autopsy brain tissues of AD patients are extensive neuronal loss and the presence of amyloid plaques and neurofibrillary tangles (NFT). Amyloid plaques are composed of the amyloid-ß peptide (Aß) (Masters *et al.* 1985, Gorevic *et al.* 1986), which is produced through proteolytic cleavage of the amyloid precursor protein (APP), a type I transmembrane protein. Aß is a 4 kDa peptide (Glenner & Wong 1984) and comprises part of the extracellular and part of the transmembrane domain of APP (Vassar *et al.* 1999b). Aß accumulates in the brain and forms soluble oligomers as well as ß-sheet pleated insoluble amyloid fibrils that are the main component of the amyloid plaques (Meyer-Luehmann *et al.* 2008). Based on their morphology and immunohistochemical staining properties amyloid plaques are commonly classified in neuritic Aß plaques and diffuse plaques. Neuritic plaques are fibrillar amyloid deposits associated with degenerating neuronal processes, which can be axons or dendrites. These dystrophic neurites, which are located within or in the immediate vicinity of amyloid plaques, are characterized by abnormal cellular structures including enlarged lysosomes and numerous mitochondria and are believed to be signs of neuronal injury (Selkoe 2001a). In contrast, diffuse plaques lack the compact structure of the classical neuritic plaques and are not associated with neuritic dystrophy. Several studies suggest that cognition is affected primarily by neuritic plaques, whereas diffuse plaques appear to be age-related changes and are also frequently found in the brains of cognitively intact elderly people (Aizenstein *et al.* 2008, Malek-Ahmadi *et al.* 2016). Besides its presence in parenchymal plaques, Aß accumulation is also found in the walls of cerebral capillaries and arteries, which has been named cerebral amyloid angiopathy (CAA) (Ghiso & Frangione 2002, Greenberg *et al.* 2004). NFT are intracellular paired helical filaments that are composed of a hyperphosphorylated form of the Tau protein (Kosik *et al.* 1986, Grundke-Iqbal *et al.* 1986, Lee *et al.* 1991). Tau was originally discovered as a microtubule-associated protein that stimulates tubulin assembly into microtubules and plays an important role in the stabilization of the microtubule network (Weingarten *et al.* 1975). The phosphorylation of Tau isolated from AD brains is 3- to 4-fold higher compared to Tau isolated from normal human brains (Kopke *et al.* 1993). Abnormal hyperphosphorylation of Tau leads to its dissociation from microtubules (Sengupta *et al.* 1998), promotes its self-aggregation into insoluble filaments (Abraha *et al.* 2000), and the formation of NFT in neuronal cell bodies as well as in dystrophic neurites associated with amyloid plaques (Grundke-Iqbal et al. 1986, Kosik et al. 1986, Wood *et al.* 1986).

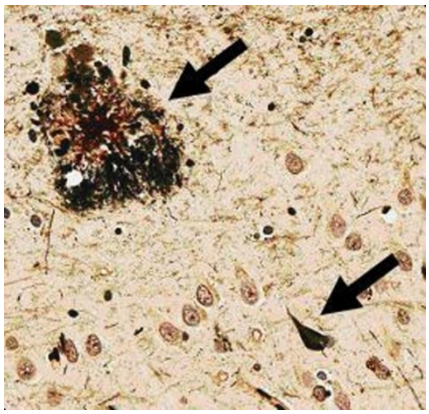

Figure 1: The two hallmark features of Alzheimer's disease. Neuritic plaque (upper arrow) and neurofibrillary tangle (lower arrow) visualized by silver staining in the brain of an 85-year old patient with histologically confirmed AD (histological picture adopted from Clifford 2012).

Specific regions in the brain are more susceptible to neuronal loss and formation of amyloid plaques and NFT than others. The cognitive impairment in AD patients is closely correlated with the progressive degeneration of the limbic system, neocortical regions and the basal forebrain (Serrano-Pozo *et al.* 2011). Within the cortex, the most severely affected brain regions include the hippocampal formation and association cortices (Arnold *et al.* 1991). The loss of neurons and synapses in the cerebral cortex and subcortical areas leads to severe atrophy of the affected regions.

Although autopsy of the brain is still required for a definitive AD diagnosis, newly developed diagnostic methods allow an early prediction of the disease in living patients with high accuracy. Imaging techniques have been developed to detect overall changes in brain size, to measure glucose metabolism in the brain, and to visualize Aß deposits and NFT using positron emission tomography imaging. Moreover, Aß and Tau concentration changes in the cerebrospinal fluid (CSF) are currently used to help in the diagnosis of AD (Jack *et al.* 2013, Blennow *et al.* 2015, Da Mesquita *et al.* 2016).

1.3 Proteolytic processing of APP

The amyloid precursor protein (APP) is a ubiquitously expressed type I transmembrane protein. The human *APP* gene is located on chromosome 21. Alternative splicing of the human APP mRNA leads to the expression of multiple APP protein isoforms of different sizes (Sandbrink *et al.* 1996, Matsui *et al.* 2007). The most common APP splice forms contain 751, 770 and 695 amino acids. In humans, the APP751 and APP770 isoforms are widely expressed in tissues, while the 695-residue isoform is predominantly expressed in neurons (Matsui et al. 2007). APP belongs to the family of amyloid

precursor-like proteins (APLPs), together with the APP like proteins 1 and 2 (APLP1 and 2), two proteins that share high sequence homology with APP, except in the Aß peptide region (Slunt *et al.* 1994). The subcellular localization of APP is dynamic: in the secretory pathway APP shuttles from the endoplasmic reticulum (ER) through the Golgi complex to the plasma membrane. During its transit, APP undergoes a variety of posttranslational modifications, which include N- or O- linked glycosylation, tyrosine sulphation and phosphorylation (De Strooper & Annaert 2000). Based on APP overexpression studies in cultured cells it has been reported that only a small fraction of APP (10%) is trafficked to the plasma membrane, while the majority of APP molecules are localized to the Golgi complex (Haass *et al.* 2012). APP at the cell surface can be rapidly internalized via the endosomal/lysosomal pathway, and endocytosed APP molecules are partly recycled back to the cell surface (Lai *et al.* 1995, Haass et al. 2012).

Three proteases called α-, β-, and γ-secretase are involved in the proteolytic processing of APP. The predominant APP processing pathways are divided into the non-amyloidogenic pathway, preventing Aß generation, and the amyloidogenic pathway, which leads to the generation of Aß (Wilquet & De Strooper 2004). The non-amyloidogenic pathway starts with α-secretase-mediated cleavage of APP, which leads to the release of a large ectodomain fragment, soluble APP α (APPsα), and the retention of an 83-residue C-terminal fragment (CTFα or C83) in the plasma membrane. The α-secretase cuts APP within the Aß domain and therefore prevents Aß formation (Lammich *et al.* 1999). Subsequent intramembrane cleavage of C83 by γ-secretase results in a small peptide called p3 and the APP intracellular domain (AICD) (Chow *et al.* 2010). In the amyloidogenic pathway full-length APP is initially cleaved by ß-secretase, yielding a slightly smaller ectodomain (APPsß) and retaining a fragment of 99 amino acids (C99) in the plasma membrane (Seubert *et al.* 1993, Vassar *et al.* 1999a). The C99 fragment includes the complete Aß region. Finally, cleavage of C99 by γ-secretase releases Aβ into the luminal/extracellular space, whereas the AICD is released into the cytoplasm.

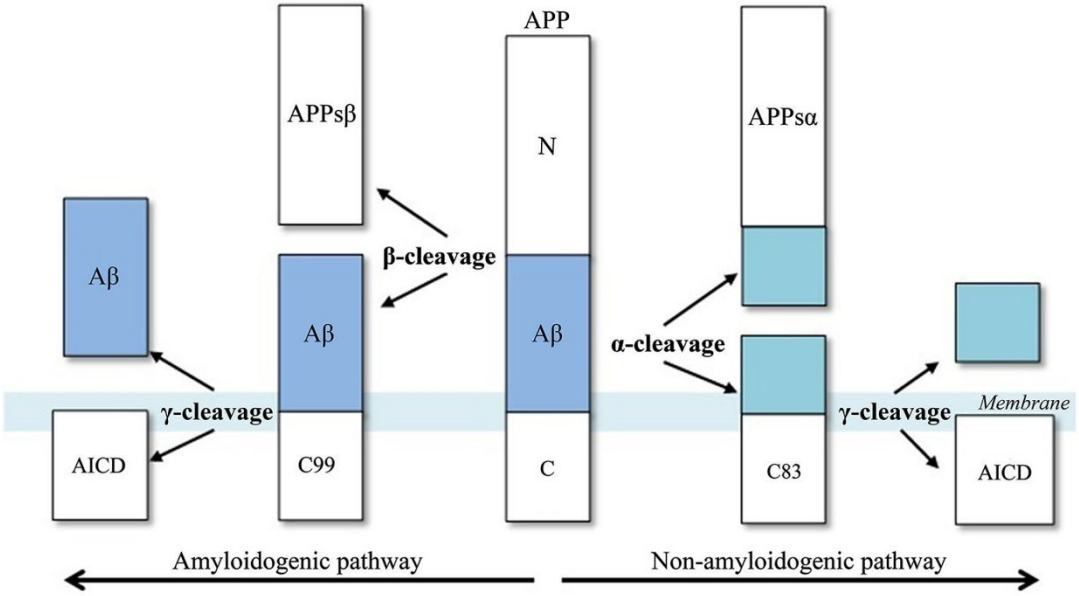

Figure 2: APP processing pathways. The non-amyloidogenic pathway starts with cleavage of APP by α-secretase, generating the soluble ectodomain APPsα and membrane bound C83. C83 is then cleaved by γ-secretase, which leads to the release of p3 into the extracellular space and AICD into the cytoplasm. Alternatively, some APP molecules are cleaved by ß-secretase, yielding extracellular APPsß and membrane bound C99. Aβ and AICD are released upon cleavage by γ-secretase of the C99 fragment (schema adopted from K. W. Menting 2014).

The α-secretase is a membrane-bound protease and a member of the A Disintegrin And Metalloprotease (ADAM) family. ADAM10 has been identified as the constitutive α-secretase that cleaves APP predominantly at the plasma membrane (Kuhn *et al.* 2010). BACE1 (ß-site APP Cleaving Enzyme 1) is the ß-secretase and the rate limiting enzyme for the generation of Aß. Knockout of BACE1 completely blocks the generation of Aβ (Cai *et al.* 2001, Luo *et al.* 2003). It is a membrane-bound aspartyl protease with highest activity in acidic environments like the endosome (Vassar et al. 1999a, Yan & Vassar 2014). The majority of body tissues express BACE1, with highest activity in brain and pancreas. The concurrent high expression of BACE1 and APP makes the brain susceptible for high Aß generation and provides an explanation why AD is a disease of the brain (Haass et al. 2012, Yan & Vassar 2014). The Aß liberating γ-secretase, another aspartyl protease, is a high molecular weight complex consisting of four subunits. These include presenilin (PSEN), nicastrin, anterior pharynx defective (APH-1), and PS enhancer (PEN2) (Kimberly *et al.* 2003, Bergmans & De Strooper 2010). In mammals two presenilin homologs exist, PSEN1 and PSEN2, that can both function as the crucial catalytic domain of γ-secretase. However, each of the four γ-secretase components seems to be necessary for enzymatic activity, since deficiency in any of them leads to impaired γ-secretase function (Bergmans & De Strooper 2010, Zhang *et al.* 2011). Since both BACE1 and γ-secretase are located in endosomes, it is thought that Aß is mainly

generated in this subcellular compartment and secreted through exocytosis. Intracellular Aß has also been found, both in animal models of AD and in human brains (Wirths *et al.* 2001, Gouras *et al.* 2000, Oakley *et al.* 2006). In addition to the three secretases, other proteins have been identified that might be involved in APP proteolysis and Aß production (Andrew *et al.* 2016). However, their potential contribution to AD pathogenesis remains to be established.

The exact functions of APP and its proteolytic fragments are still largely unclear (Zheng & Koo 2011). A number of possible functions of APP have been proposed, including neuroprotective and neurotrophic effects (Mattson *et al.* 1993). Since APP interacts with laminin and collagen and co-localizes with integrins, it has been implicated in cell adhesion (Yamazaki *et al.* 1997, Young-Pearse *et al.* 2008). APP was also found to play a role in cell growth. Downregulation of APP expression in fibroblasts resulted in slow cell growth and division, which could be rescued by restoring APPsα levels (Saitoh *et al.* 1989). APP knock-out mice are viable but show cerebral gliosis and decreased locomotor activity in adult animals (Zheng *et al.* 1995). These abnormalities of APP-deficient mice could be restored by expression of APPsα (Ring *et al.* 2007), which further supported an important physiological function of this APP cleavage fragment. In addition, the AICD fragment has been implicated in the modulation of gene expression and apoptosis (Muller *et al.* 2008). Although most studies are directed at determining how and why Aß forms aggregates, limited data indicate that Aß may also have a physiological function. Regulation of neuronal cell survival and protection of organisms from microbial infections have been proposed as putative physiological functions of Aß (Plant *et al.* 2003, Soscia *et al.* 2010, Kumar *et al.* 2016).

1.4 The amyloid hypothesis

The amyloid hypothesis has become the leading model to explain how AD pathology develops and progresses. This hypothesis states that the accumulation and aggregation of Aß peptides in the brain is the critical factor initiating and driving the pathological cascade in AD (Hardy & Higgins 1992, Hardy & Selkoe 2002, Selkoe & Hardy 2016). The cleavage of APP catalyzed by γ-secretase results in the secretion of Aß peptides of variable length. Peptides consisting of 40 amino acids (Aß40) are the predominant Aß species that are produced by cells. However, a two amino acids longer Aß42 form is the major component of the amyloid material in neuritic plaques and is believed to be the key pathogenic species affecting memory and cell survival (Haass & Selkoe 2007, Selkoe

2011). Aß42 is particularly prone to aggregation as a result of its higher hydrophobicity (Glabe 2001). Fibrils consisting of Aß42 are formed more rapidly and are more stable than those consisting of shorter Aß peptides (Jarrett *et al.* 1993, Burdick *et al.* 1992). Soluble Aß oligomers rather than insoluble plaques have been proposed to be the primary synaptotoxic species (Gong *et al.* 2003, Haass & Selkoe 2007, Shankar *et al.* 2008). Distinct oligomeric Aß forms have been isolated from brains of AD mouse models as well as human AD brains (Lesne *et al.* 2006, Shankar et al. 2008). According to the amyloid hypothesis, these oligomers act as a pathological trigger and might directly causes synaptic and neuritic injury. In addition, Aß oligomers are believed to induce the formation of neurofibrillary tangles, eventually leading to neuronal dysfunction and cell death (Hardy & Higgins 1992, Lewis *et al.* 2001, Gotz *et al.* 2001). Furthermore, Aß deposition and amyloid plaque formation promote the activation of microglia cells and astrocytes and the release of cytokines, resulting in widespread neuroinflammation (Eikelenboom *et al.* 1994, Rogers *et al.* 1996).

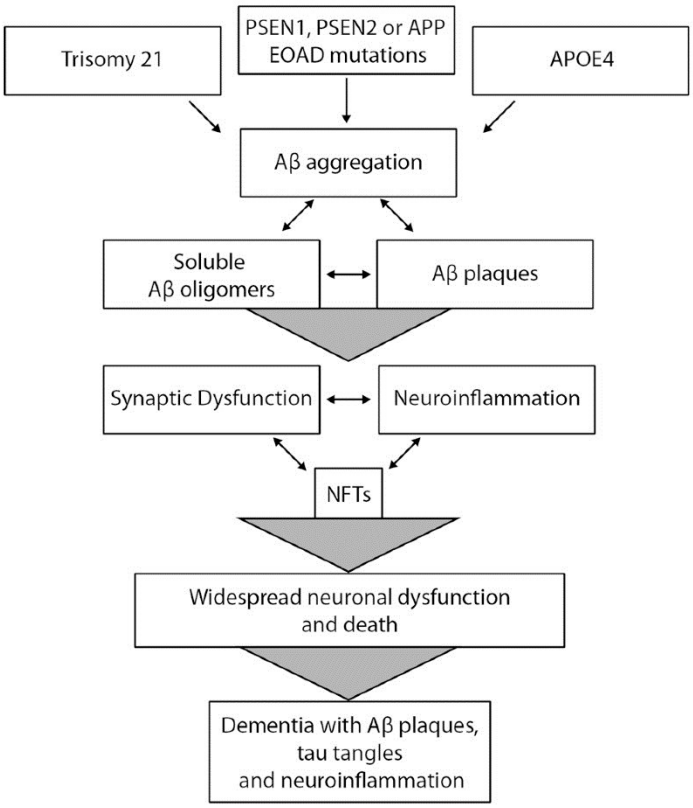

Figure 3: The amyloid cascade hypothesis of AD. Proposed cascade of pathogenic events ultimately leading to neuronal cell death and dementia (schema adopted from Morris *et al.* 2014).

Strong support for the amyloid hypothesis results from cases of early-onset familial AD (FAD). FAD is caused by autosomal-dominantly inherited missense mutations that occur

either in the gene encoding APP or in the two homologous PSEN1 and PSEN2 genes that encode the catalytic subunit of the γ-secretase complex. Mutations in PSEN1 or PSEN2 impair the γ-secretase mediated cleavage of APP and lead to an elevation of the Aß42/Aß40 ratio, by increasing Aß42 production, decreasing Aß40 production, or by a combination of both mechanisms (Weggen & Beher 2012). Numerous mutations have also been identified within and around the Aß sequence of the APP gene (Chartier *et al.* 1991, Goate *et al.* 1991, Haass et al. 2012). These missense mutations in APP can increase total Aß production by converting APP into a better substrate for the β-secretase, or they can lead to increased generation of longer Aß42 species similar to PSEN mutations. In addition, mutations in the central region of Aß can increase the self-aggregation of the produced peptides (Citron *et al.* 1992, Cai *et al.* 1993, Suzuki *et al.* 1994, Nilsberth *et al.* 2001, Weggen & Beher 2012). Another finding strongly supporting the amyloid hypothesis is that patients with Down's syndrome (trisomy 21) suffer from AD. Down's syndrome patients have an additional copy of the APP gene, which is located on chromosome 21. Duplication of the APP gene results in higher Aß levels and eventually leads to Aß deposition and an AD-like dementia in middle adult years (Teller *et al.* 1996, Tokuda *et al.* 1997). Conversely, patients, who harbor a rare microduplication of chromosome 21 involving the distal part of the chromosome but not the APP gene, have Down's syndrome features but do not develop AD (Prasher *et al.* 1998). More recently, an APP missense mutation (A673T) within the Aß region has been identified, which has been shown to reduce amyloid deposition and to protect against AD. These beneficial effects are thought to result from decreased APP cleavage by ß-secretase and altered aggregation properties of the mutant Aß peptides (Jonsson *et al.* 2012, Benilova *et al.* 2014, Zheng *et al.* 2015). Together, these findings provide overwhelming evidence that Aß is crucial for the initiation of AD pathogenesis. The relatively rare FAD cases are characterized by an early disease onset and a strong genetic disposition, but otherwise exhibit a similar progression of clinical symptoms and the same amyloid plaque and neurofibrillary tangle pathology as sporadic late-onset AD (De Strooper 2012). Nevertheless, the reasons for brain Aß accumulation in the much more common sporadic AD cases are less well understood. Numerous contributing factors have been suggested, including the age-dependent downregulation of Aß degrading enzymes like the metalloprotease neprilysin (Selkoe 2001b), increased ß-secretase activity (Li *et al.* 2004, Willem *et al.* 2009) and reduced Aß clearance due to the presence of the apolipoprotein E4 (*APOE4*) allele (Kim *et al.* 2009). The *APOE4* allele is the strongest genetic risk factor for late-onset AD (Corder *et al.* 1993). *APOE4* carriers displayed a significantly higher amyloid plaque burden than patients lacking this allele (Rebeck *et al.*

1993). ApoE is a glycoprotein that is involved in lipid metabolism by regulating cholesterol and triglyceride transport and distribution in the brain (Mahley 1988, Mahley & Rall 2000). Interestingly, ApoE binds Aß and the ApoE4 isoform was found to enhance Aß aggregation and to impair clearance of Aß in the brain (Ma *et al.* 1994, Castano *et al.* 1995, Castellano *et al.* 2011). In recent years, numerous additional genetic risk factors have been identified for AD, although these are much rarer and weaker in effect than ApoE4 (Lambert *et al.* 2013, Selkoe & Hardy 2016). These discovered genes are associated with three types of cellular processes that have emerged as particularly important: cholesterol and lipid metabolism, immune system function and inflammation, and endosomal vesicle recycling (Van Cauwenberghe *et al.* 2016). Among the multiple genetic and environmental risk factors that have been linked to AD pathogenesis, the overall failure of Aß clearance in the brain is likely a major contributor to the late-onset form of AD (Mawuenyega *et al.* 2010).

1.5 Microglia – Immune defense of the brain

Microglia are the resident immune cells of the central nervous system (CNS). They are part of the glial system of non-neuronal cells supporting and protecting neuronal functions. Nearly 90 % of the human brain is composed of glial cells which consist of two main populations: the macroglia, comprising astrocytes and oligodendrocytes, and the microglia (Greter & Merad 2013). Microglia are widely distributed in the brain and spinal cord and represent approximately 10 % of the total glial cell population within the CNS parenchyma (Perry 1998, Lawson *et al.* 1990). Microglia were originally described and named by the Spanish neuroscientist Pio del Rio-Hortega who characterized them using silver carbonate staining almost 100 years ago (del Rio-Hortega 1919). The origin of microglia has been a matter of much debate (Katsumoto *et al.* 2014), but it is now accepted that microglia in the adult CNS are derived from myeloid precursors (primitive macrophages) in the yolk sac, that migrate into the neuroepithelium during early embryogenesis prior to formation of the blood-brain-barrier (Ginhoux *et al.* 2010). Moreover, it was shown that under steady-state conditions microglia are predominantly maintained via local self-renewal independently of input from hematopoietic stem cells (Ajami *et al.* 2007, Bruttger *et al.* 2015). However, the potential contribution of bone marrow-derived precursors to the resident microglial pool in the course of a lifetime and after repeated immune challenges remains controversial (Mildner *et al.* 2007, Ajami *et al.* 2011, Perry & Teeling 2013).

Immune defense and CNS maintenance are the two main functions of microglia. In the steady-state, microglia exhibit a specific morphology with a small cell body and numerous ramified processes. Like macrophages in other tissues, these ramified or “resting” microglia have been recognized as surveying cells in the healthy brain. They constantly scan the brain environment for signs of tissue damage or pathogenic invasion by extending their highly motile processes (Davalos *et al.* 2005, Nimmerjahn *et al.* 2005). Besides their surveillance function, microglia have an impact on neural networks via removal of cellular and subcellular elements and secretion of factors mediating transmitter, trophic or neuroprotective functions (Kohsaka *et al.* 1996, Morgan *et al.* 2004, Kettenmann *et al.* 2013). It was shown that microglial processes transiently contact neuronal synapses and contribute to the modification or elimination of synaptic structures (Tremblay *et al.* 2010, Kettenmann et al. 2013). This interaction with synapses seems to play an important role for synapse formation and plasticity during development and also in the adult brain (Wu *et al.* 2015, Paolicelli *et al.* 2011).

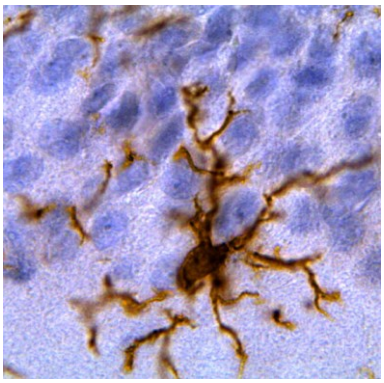

Figure 4: Microglia in the rat hippocampus. Immunocytochemical staining for the microglia marker and calcium binding protein Iba-1 reveals a microglia cell endowed with numerous processes. Counterstaining with hematoxylin (picture adopted from Korzhevskii & Kirik 2016).

Microglia remove cellular particles and internalize solutes from the surrounding environment via endocytosis. The term endocytosis comprises various mechanisms that are used by cells to take up molecules, including phagocytosis, receptor-mediated endocytosis and pinocytosis (Mandrekar *et al.* 2009). The uptake of large particles such as microorganisms and dead cells across the plasma membrane by phagocytosis is an active process that involves the interaction with specific cell surface receptors and is dependent on actin as part of the cell cytoskeleton (Stuart & Ezekowitz 2005). Receptor-mediated endocytosis enables the uptake of selected macromolecules and is induced upon binding of a ligand to a receptor on the cell surface, resulting in the incorporation of the ligand-receptor complex within clathrin-coated or uncoated vesicles (Sorkin & von Zastrow 2009). Pinocytosis is associated with the non-specific uptake of soluble

molecules from the extracellular space and can occur either by macropinocytosis or micropinocytosis. Macropinocytosis allows the uptake of larger particles and is actin-dependent while micropinocytosis is an actin-independent process (Swanson & Watts 1995).

Microglia are considered the most sensitive sensors of brain pathology. They express diverse pattern recognition receptors (PRRs) that sense microbial molecules, including highly conserved pathogen-associated molecular patterns (PAMPs). Other sets of PRRs on microglia recognize damage-associated molecular patterns (DAMPs), which comprise cell components released during tissue damage and cell death (Wolf *et al.* 2016). Upon detection of signs for brain injury or pathogen infection, microglia cells acquire a new morphology characterized by an amoeboid shape, and undergo a complex activation process (Stence *et al.* 2001, Colton & Wilcock 2010). Activated microglia have an enlarged cell body with several short processes. They are capable of performing macrophage-like immune functions, including the release of multiple factors with pro-inflammatory and immunoregulatory effects like cytokines, chemokines and reactive oxygen species (ROS) that contribute to the clearance of pathogen infections (Block *et al.* 2007, Saijo & Glass 2011). In parallel to their change in morphology, the cells undergo changes in the expression of cell membrane receptors and intracellular enzymes (Raivich *et al.* 1999, Kettenmann *et al.* 2011).

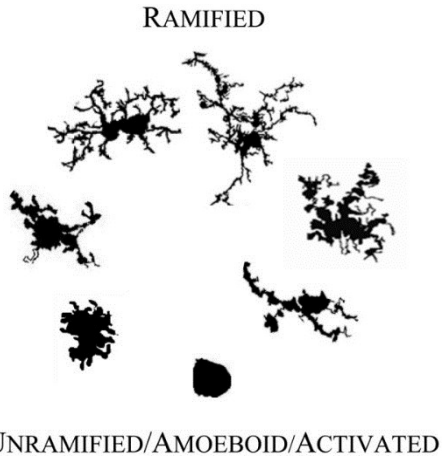

Figure 5: Illustration of microglia cell morphologies. Microglia cells can switch reversibly from a simple roundish form to a complex branched morphology. Morphology and function of microglia are highly related and depend on complex environmental signals. In their ramified form, microglia are associated with a “resting” state, primarily serving physiological functions. Amoeboid forms of microglia are considered to represent a “reactive” or “activated” state (schema adopted from Karperien *et al.* 2013).

In the active state, microglia become professional phagocytes, which proliferate and migrate to the site of injury where they phagocytose damaged cells and debris, and

present antigens to infiltrating lymphocytes. Once activated, microglia can acquire diverse functional phenotypes ranging between two extremes: the classically activated M1 phenotype that is mainly pro-inflammatory, and an alternatively activated M2 phenotype that is involved in anti-inflammatory actions promoting regeneration (Colton & Wilcock 2010, Prinz & Priller 2014). Classically activated microglia are associated with the production of pro-inflammatory cytokines such as tumor necrosis factor-α (TNF-α), interleukin-1β (IL-1β) and IL-6, as well as superoxide, nitric oxide (NO) and ROS (Block et al. 2007). The alternatively activated M2 phenotype is linked to the activation state induced by the cytokines IL-4 and IL-13 and is closely associated with the expression of M2 genes promoting tissue repair, extracellular matrix (ECM) reconstruction and the release of neurotrophic factors (Ponomarev *et al.* 2007, Martinez *et al.* 2009, Colton 2009). M2 microglia are driven by multiple anti-inflammatory factors and antagonize the pro-inflammatory responses, which eventually results in immunosuppression and neuronal protection. However, the M1/M2 classification represents a simplified model to describe just two contrasting sides of the immune response. More likely, microglia activation states represent a complex continuum highly dependent on the environment, in which the cells become activated, and the factors by which they are stimulated (Tang & Le 2016).

1.6 Microglia in Alzheimer`s disease

The deposition of amyloid plaques in the AD brain is accompanied by a chronic inflammatory response involving astrocytes and, in particular, microglia. While the microglia response to injury is commonly beneficial, it can become detrimental, particularly in cases of chronic injury and long-term inflammation such as in AD. In AD patients as well as in AD mouse models, microglia are phenotypically activated and are found in close proximity to amyloid deposits (Itagaki *et al.* 1989, Perlmutter *et al.* 1990, Frautschy *et al.* 1998).

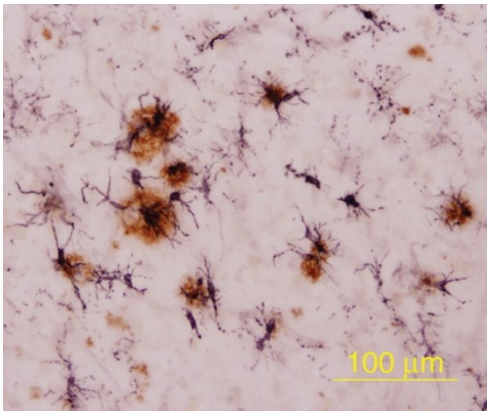

Figure 6: Microglia clustering around Aß plaques in the AD brain. Immunostaining of the temporal cortex of an AD brain reveals Aß plaques visualized with a monoclonal anti-Aß antibody (brown). Microglia are found in close proximity to the amyloid deposits, as shown by immunostaining with an antibody against the microglial marker Iba-1 (black) (picture adopted from McGeer & McGeer 2015).

The interaction of microglia with Aß can trigger their activation resulting in the secretion of inflammatory cytokines (Meda *et al.* 1995, Giulian *et al.* 1996, Combs *et al.* 1999, Manocha *et al.* 2016). Increased levels of pro-inflammatory cytokines such as TNFα, IL-1β and IL-6 have been measured in the brains of APP transgenic mouse models of AD, and the production of these cytokines was increased in microglia cell cultures upon exposure to aggregated synthetic Aß (Lue *et al.* 2001a, Patel *et al.* 2005). Elevated levels of pro-inflammatory cytokines were also found in the brains and CSF of AD patients, whereas anti-inflammatory factors were decreased (Griffin *et al.* 1989, Cacabelos *et al.* 1991, Blum-Degen *et al.* 1995). Aß-stimulated microglia also release ROS and reactive nitrogen species, as well as a number of other immune mediators including macrophage colony stimulating factor (M-CSF) and members of the complement system (Lue *et al.* 1996). Products of the complement system, including the membrane attack complex, have been found to colocalize with amyloid plaques and neurons containing neurofibrillary tangles in AD (Webster *et al.* 1997). The secretion of multiple proinflammatory molecules by microglia is believed to contribute to the chronic inflammatory response and neurotoxicity observed in the AD brain (Combs *et al.* 2001, Yates *et al.* 2000). In support of this hypothesis some studies reported a lower incidence of AD in humans and a reduction of AD pathogenic features in AD mouse models following long term treatment with nonsteroidal anti-inflammatory drugs (NSAIDs) (Anthony *et al.* 2000, Zandi *et al.* 2002, Heneka *et al.* 2005, Yip *et al.* 2005). However, on the contrary, overexpression of the proinflammatory cytokine IL-1β in transgenic mice was shown to decrease amyloid deposition. It was observed that sustained IL-1ß activation led to increased numbers of activated plaque-associated microglia and IL-1ß-stimulated recruitment of bone marrow-derived cells into the brain (Shaftel *et al.* 2007).

Similarly, the overexpression of the proinflammatory cytokine IL-6 in the brain of AD mice was found to increase gliosis and attenuate Aß deposition. In addition, IL-6 expression was associated with the upregulation of glial phagocytic markers *in vivo* and increased microglia-mediated phagocytosis of Aß aggregates *in vitro*, without affecting APP expression or processing (Chakrabarty *et al.* 2010). These studies point to a more beneficial role of microglia in AD pathogenesis and illustrate the complexity of the inflammatory response. Microglia are able to recognize Aß and numerous studies indicate that microglia and bone marrow-derived macrophages are involved in the clearance of Aß (Rogers *et al.* 2002, Simard *et al.* 2006, El Khoury *et al.* 2007, Bolmont *et al.* 2008, Liu *et al.* 2010). There is clear evidence that microglia in culture are able to internalize aggregated Aß (Paresce *et al.* 1996, Paresce *et al.* 1997, Li *et al.* 2000, Koenigsknecht-Talboo & Landreth 2005). Microglia can take up soluble forms of Aß by macropinocytosis and are capable of internalizing fibrillary Aß via phagocytosis (Koenigsknecht & Landreth 2004, Mandrekar et al. 2009). Several microglial cell surface receptors have been proposed to cooperate in the recognition, internalization and clearance of Aß as well as cell activation. Fibrillar forms of Aß can be recognized by a complex of cell surface receptors composed of CD36 (a B-class scavenger receptor), α6β1 integrin, the integrin associated protein CD47 and the scavenger receptor A (Bamberger *et al.* 2003). Upon binding of Aß, the complex triggers the activation of tyrosine kinase-based intracellular signaling cascades, which lead to the activation of microglia, increased phagocytosis and cytokine production (Koenigsknecht & Landreth 2004, Combs et al. 1999). Microglia from CD36 knock-out mice showed decreased production of cytokines and less microglia recruitment after exposure to fibrillar Aß species (El Khoury *et al.* 2003). Furthermore, innate immune toll-like receptors (TLRs) and the coreceptor CD14 were reported to play a role as members of the Aß receptor complex (Reed-Geaghan *et al.* 2009). Stimulation of TLR2, TLR4 and its coreceptor CD14 were required for microglial activation in response to fibrillar Aß, and deficiency in any of these receptors resulted in impaired fibrillar Aß-stimulated phagocytosis of microglia (Fassbender *et al.* 2004, Reed-Geaghan et al. 2009). In line with that, Tahara *et al*. have reported increased Aß phagocytosis after activation of microglial TLR2 and TLR4 receptors (Tahara *et al.* 2006). Another cell surface receptor that has been postulated to interact with Aß is the receptor for advanced glycosylation endproducts (RAGE). Several studies indicate that the RAGE-Aß interaction mediates microglia activation and the production of proinflammatory molecules (Lue *et al.* 2001b, Fang *et al.* 2010, Doens & Fernandez 2014).

The link between microglia function and AD pathology is further supported by the identification of immune receptors as risk factors for AD. Several genome-wide association studies (GWAS) of sporadic AD cases have identified disease-associated single nucleotide polymorphisms (SNPs) and rare mutations in genes that may be implicated in microglial phagocytosis and Aß clearance. Variants of genes encoding for CD33, the triggering receptor expressed on myeloid 2 (TREM2) and the complement receptor (CR1) were identified as susceptibility loci for late-onset AD (Lambert *et al.* 2009, Naj *et al.* 2011, Guerreiro *et al.* 2013, Jonsson *et al.* 2013). CD33 is a transmembrane protein that was found to be highly expressed on microglia in human AD brains. A variant of the *CD33* gene is associated with increased CD33 levels, leading to higher plaque burden in AD brains due to inhibition of Aß uptake by microglia (Griciuc *et al.* 2013). TREM2 is a transmembrane receptor found on myeloid cells such as monocytes and microglia (Sessa *et al.* 2004), and has previously been shown to be involved in the regulation of phagocytosis (Takahashi *et al.* 2005, Hsieh *et al.* 2009, N'Diaye *et al.* 2009). Very rare mutations in the *TREM2* gene increase the risk for AD to a similar extent as variants of the *APOE4* gene (Guerreiro et al. 2013, Jonsson et al. 2013). In AD, TREM2 was found to be upregulated in amyloid plaque-associated microglia (Frank *et al.* 2008). The most common AD-associated *TREM2* mutation, R47H, has been shown to reduce the phagocytic activity of microglia cells and to impair the detection of lipid ligands known to associate with fibrillar Aß (Kleinberger *et al.* 2014, Wang *et al.* 2015). This indicates that impaired clearance of Aß may at least contribute to the increased risk of AD in carriers of *TREM2* gene variants (Hickman & El Khoury 2014). However, recent studies of the impact of *TREM2* deficiency on Aß accumulation in AD mouse models resulted in contradictory outcomes and further investigations are required (Jiang *et al.* 2014, Ulrich *et al.* 2014, Wang et al. 2015, Jay *et al.* 2015). Another GWAS also found rare variants in *TREM1*, another TREM family receptor, to be associated with susceptibility to AD (Replogle *et al.* 2015). In this study, variants of *TREM1* were related to an increased Aß burden and an increased rate of cognitive decline. In support of that, Jiang *et al.* have reported that a *TREM1* variant was associated with a decline in monocytic TREM1 expression and a reduced ability of human monocytes for Aß phagocytosis (Jiang *et al.* 2016). On the contrary, increased microglial phagocytosis of Aß and a reduced amyloid burden in brains of AD mice was observed upon TREM1 overexpression (Jiang et al. 2016). In other studies silencing of TREM1 expression has also been linked to an impaired phagocytosis activity of immune cells (Hommes *et al.* 2014, Li *et al.* 2016), further supporting the role of TREM1 as a positive modulator of phagocytosis. The identification of AD risk-associated variants in

microglia-specific genes supports the concept of altered microglial function in AD. Despite their interaction with Aß, microglia fail to clear Aß deposits in the brain of AD patients. Several studies provided evidence that microglia in AD become chronically altered, including phagocytic and physiological functions like secretion of cytokines and growth factors (Lue et al. 2001a, Hanisch & Kettenmann 2007, Solito & Sastre 2012, Orre *et al.* 2014). It has further been reported that myeloid cells of AD patients displayed reduced Aß phagocytosis compared to healthy controls (Fiala *et al.* 2005). Similarly, microglia from adult AD mice were shown to ingest less Aß compared to microglia from young AD mice (Hellwig *et al.* 2015). In line with that, Hickman *et al.* have reported that microglia from aged AD mice showed a decrease in the expression of Aß-binding receptors including the scavenger receptor A, CD36 and RAGE. Moreover, a reduction in the Aß degrading enzymes insulysin, neprilysin, and matrix metallopeptidase 9 (MMP9) has been observed (Hickman *et al.* 2008). Likewise, Orre *et al*. have shown a reduced expression of genes involved in phagocytosis in microglia isolated from aged AD brains (Orre et al. 2014). These findings suggest that a compromised phagocytic function of microglia in AD and a diminished ability to degrade Aß might, at least partly, explain the failure of Aß clearance in AD brains (Mawuenyega *et al.* 2010). Indeed, experiments with organotypic brain slices of AD mice demonstrated that a decrease in the phagocytic capacity of microglia correlated with an increased Aß plaque burden, indicating a close connection between Aß plaque deposition and microglial function (Krabbe *et al.* 2013). Furthermore, studies by Streit *et al.* revealed age-related microglial structural deterioration, with more prevalent dystrophic (senescent) microglia especially in older subjects (Streit *et al.* 2004, Streit 2006), suggesting a functional impairment of microglia during aging. Morphological changes, including increased soma size and thickening of processes, have also been observed in plaque-associated microglia of AD mouse models (Brawek *et al.* 2014). These morphological differences may represent different functional states, but further studies are required to clarify the connection between microglia morphology and functional impairment in AD.

1.7 Targeting microglia for the treatment of Alzheimer`s disease

Despite the findings of age-related changes and compromised microglial function in AD, under particular circumstances microglia are able to phagocytose or degrade Aß. Interestingly, immunization studies with anti-Aß antibodies resulted in a reduction in amyloid deposition in AD mouse models (Schenk *et al.* 1999, Bard *et al.* 2000, Bacskai *et al.* 2001, Wilcock *et al.* 2004). Several mechanisms have been proposed, including the

antibody-mediated activation of microglia. It is assumed that microglial activation and clearance of amyloid plaques is triggered through Fcγ-receptor binding of antibody opsonized Aß aggregates (Bard et al. 2000, Bard *et al.* 2003, Wilcock et al. 2004, Koenigsknecht-Talboo *et al.* 2008). A reduction in amyloid deposits was subsequently reproduced in AD patients after Aß immunotherapy, through both active and passive immunization (Nicoll *et al.* 2003, Nicoll *et al.* 2006, Sevigny *et al.* 2016). These findings indicate that the *in vivo* stimulation of microglia can trigger an efficient phagocytic response and clearance of insoluble Aß aggregates. However, vaccination approaches have repeatedly failed in clinical trials due to lack of efficacy (Morkuniene *et al.* 2013). Nevertheless, a large number of active and passive immunotherapies are still in clinical development (Sevigny et al. 2016, Rygiel 2016, Hull *et al.* 2017).

Studies with bone-marrow derived monocytes that can infiltrate the brain during the disease process and differentiate into macrophages or microglia have shown that these cells might be more effective in Aß phagocytosis compared to resident microglia that were highly exposed to Aß (Simard et al. 2006). In addition, transplantation of bone-marrow derived mesenchymal stem cells into brains of AD mice was shown to reduce amyloid deposition and enhance cognitive functions (Lee *et al.* 2010). The beneficial effects of transplanted cells seem not only to arise from the differentiation into microglia-like cells but also from the modulation of the microenvironment of resident microglia (Kim *et al.* 2012, Ma *et al.* 2013a). Thus, the transplantation of bone-marrow derived progenitor cells from healthy individuals into AD patients might represent a potential therapeutic approach (Theriault *et al.* 2015).

Other therapeutic strategies attempt to revert the phenotype that microglia adopt in the disease state to a healthy, physiological phenotype. Several studies have addressed the question whether microglial dysfunction in AD is reversible and whether their phagocytic ability can be restored. In this regard, modulation of the inflammatory state via cytokines such as TGF-ß, IL-10 and TNF-α was reported to modify amyloid plaque deposition and to improve outcomes in AD mouse models (Town *et al.* 2008, Chakrabarty *et al.* 2011, Chakrabarty *et al.* 2015, Guillot-Sestier *et al.* 2015). Furthermore, it has been proposed that a shift from the classically activated M1 phenotype that seems to aggravate the inflammatory response towards the alternatively activated M2 phenotype promoting tissue repair would increase Aß clearance (Heneka *et al.* 2013). In support of this idea, it has been reported that the PPARγ agonist pioglitazone enhanced phagocytosis and degradation of Aß by microglia. The effect was attributed to a switch from M1 to M2 microglia phenotype (Mandrekar-Colucci *et al.* 2012). In another study, reduced amyloid plaque size was observed when brain slices from old AD mice were cultured together

with slices from young wild type mice in a novel *ex vivo* model (Daria *et al.* 2016). Co-culturing resulted in increased proliferation and clustering of old microglia around amyloid plaques, suggesting that dysfunction of old microglia might be restored by factors secreted by young microglia (Daria et al. 2016). Similarly, treatment of an AD mouse model with the growth factor M-CSF resulted in a reduced Aß burden and improved cognitive functions (Boissonneault *et al.* 2009). M-CSF treatment increased the number of plaque-associated microglia, which was accompanied by an increased uptake of Aß by these cells (Boissonneault et al. 2009). Taken together, these studies suggest that the modulation of microglia phenotypes *in vivo* might be of benefit for the treatment of AD.
In 2005 it was discovered that glycogen synthase kinase 3 (GSK3) is a positive regulator of inflammatory pathways in immune cells (Martin *et al.* 2005). GSK3 is a highly conserved serine/threonine kinase, which exists in two closely related isoforms (GSK3α and GSK3ß) (Embi *et al.* 1980, Woodgett 1990). In the brain, GSK3ß regulates numerous signalling pathways, including innate and adaptive immune responses (Beurel *et al.* 2010). The activation of several subtypes of Toll-like receptors revealed that GSK3 is required for the inflammatory response in human monocytes (Martin et al. 2005). GSK3 has been found to promote the production of pro-inflammatory cytokines such as IL-6, IL-1ß and TNFα (Martin et al. 2005, Cheng *et al.* 2009, Beurel & Jope 2009, Yuskaitis & Jope 2009, Wang *et al.* 2010). Inhibition of GSK3 has been subsequently found to reduce inflammation in the CNS (Cuzzocrea *et al.* 2006, De Sarno *et al.* 2008, Yuskaitis & Jope 2009). GSK3 inhibitors decreased the production of pro-inflammatory cytokines and were shown to increase the secretion of the anti-inflammatory cytokine interleukin 10 (IL-10) (Martin et al. 2005, Beurel 2011). Furthermore, administration of GSK3 inhibitors protected mice from sepsis induced by an otherwise lethal dose of the inflammatory stimulans lipopolysaccharide (LPS) (Martin et al. 2005). The data indicated that GSK3 inhibitors could shift the inflammatory response from pro-inflammatory toward an anti-inflammatory state. Given that inflammation and microglia activation are contributing factors in AD, inhibition of GSK3 might provide a novel therapeutic approach to control inflammation. However, the full impact of GSK3 inhibitors on microglial functions and, in particular, on Aß uptake and degradation remains to be determined.

1.8 Aims of this study

The modulation of microglial phenotypes has become a major focus of interest in the area of AD therapy development. The identification of cellular targets that promote Aß clearance by microglia while in parallel limiting potentially detrimental inflammatory

responses may be key to develop effective disease-modifying drugs. However, the knowledge is limited with regard to the molecular mechanisms that control different microglia phenotypes and their ability to internalize and degrade Aß peptides. GSK3 has been identified as an important mediator of inflammatory responses and has been recognized as a potential therapeutic target in AD (Martin et al. 2005, Jope *et al.* 2007). In preliminary studies, we had observed that treatment with GSK3 inhibitors might be able to promote the uptake of Aß by macrophages derived from the human monocytic cell line THP-1 (Ogorek 2011, unpublished Master`s thesis). Therefore, the objectives of this doctoral thesis were as follows:

(1) To rigorously validate the effects of GSK3 inhibitors on Aß uptake and degradation using the human monocytic cell line THP-1, human primary macrophages, and primary mouse microglia cells.

(2) To confirm that the stimulatory effect of GSK3 inhibitors is mediated by their primary targets GSK3α and GSK3ß, and to exclude off-target effects.

(3) To investigate the molecular mechanism(s) by which GSK3 inhibition might stimulate Aß uptake and degradation.

2 Materials

2.1 Cell lines

THP-1	human acute monocytic leukemia cell line	(Tsuchiya *et al.* 1980)
L929	murine fibroblast cell line	(Earle 1943)
GP2-293	HEK293-based cell line with stable expression of the viral gag and pol proteins.	(Emi *et al.* 1991, Burns *et al.* 1993)
HEK293FT	HEK293-based cell line transformed with the SV40 large T antigen.	(Naldini *et al.* 1996)

2.2 Bacterial strains

Strain	**Genotype**
DH5α	F^- Φ80*lac*ZΔM15 Δ(*lac*ZYA-*arg*F) U169 *rec*A1 *end*A1 *hsd*R17 (r_K^-, m_K^+) *pho*A *sup*E44 λ– *thi*-1 *gyr*A96 *rel*A1
STBL3	F^- *mcr*B *mrrhsd*S20(r_B^-, m_B^-) *rec*A13 *sup*E44 *ara*-14 *gal*K2 *lac*Y1 *pro*A2 *rps*L20(Str^R) *xyl*-5 λ^- *leumtl*-1

2.3 Plasmids

Name	
E(beta)P	Addgene, #24313 (Fuerer & Nusse 2010)
lentiCRISPRv2	Addgene, #52961 (Sanjana *et al.* 2014)
pLHCX	Clontech
pLHCX-ß-catenin	
pCMV-VSV-G	Addgene, #8454 (Stewart *et al.* 2003)
pMD2.G	Addgene, #12259
pMDLg/pRRE	Addgene, #12251 (Dull *et al.* 1998)
pRSV-Rev	Addgene, #12253 (Dull et al. 1998)
pVSVG	Clontech

2.4 Primer

Name	Sequence
hARF1_RT_for	GAC CAC GAT CCT CTA CAA GC
hARF1_RT_rev	TCC CAC ACA GTG AAG CTG ATG
betaCat_XhoI_for	AAA TCT CGA GAT GGC TAC TCA AGC TGA CCT GA
betaCat_NotI_rev	AAA TGC GGC CGC TTA CAG GTC AGT ATC AAA CCA G
hCCL2_RT_for	AGA ATC ACC AGC AGC AAG TGT
hCCL2_RT_rev	CAG ATC TCC TTG GCC ACA AT
hCCL3_RT_for	TGC TCA GAA TCA TGC AGG TC
hCCL3_RT_rev	TGA TGC AGA GAA CTG GTT GC
hCCL7_RT_for	CCA CCA GTA GCC ACT GTC C
hCCL7_RT_rev	CAG CAC AGA TCT CCT TGT CC
hCD163_RT_for	TTG CCA GCA GCT TAA ATG TG
hCD163_RT_rev	AGG ACA GTG TTT GGG ACT GG
hCDC42_RT_for	TAA CTC ACC ACT GTC CAA AGA CTC C
hCDC42_RT_rev	CCT CAT CAA ACA CAT TCT TCA GAC C
mCDC42_RT_for	ACG ACC GCT AAG TTA TCC ACA
mCDC42_RT_rev	GGC TTC TGT TTG TTC TTG GCA
hLDLR_RT_for	TTT CCA GCT AGG ACA CAG CA
hLDLR_RT_rev	CTC CTG GGA CTC ATC AGA GC
hMMP10_RT_for	AGT GGA GGA AAA CCC ACC TT
hMMP10_RT_rev	CCT GGG CCA TCA AAA GAG TA
hNLRP3_RT_for	GAT CTT CGC TGC GAT CAA CAG
hNLRP3_RT_rev	CGT GCA TTA TCT GAA CCC CAC
mRPL32_RT_for	GCC TCT GGT GAA GCC CAA G
mRPL32_RT_rev	TTG TTG CTC CCA TAA CCG ATG T
Sequencing_hU6-F	GAG GGC CTA TTT CCC ATG ATT
hSTAB1_RT_for	CAT AGG CCC TTC ACA ATG CT
hSTAB1_RT_rev	CTG CAG GAG AAA GAG ATG GG
hTHBS1_RT_for	TTG TCT TTG GAA CCA CAC CA
hTHBS1_RT_rev	GGG TGA GGA GGA CAC TGG TA
hTREM1_RT_for	TCC AAG TGG GGA GGA TCA TA
hTREM1_RT_rev	AAG GCC TTA GTG GTG GTA GGA
mTREM1_RT_for	CTG CTG TGC GTG TTC TTT GT
mTREM1_RT_rev	TAA AGG GCC TCT GTG TGA CC
hTREM2_RT_for	GGC ACT CTC ACC ATT ACG CT
hTREM2_RT_rev	GGC ATC CTC GAA GCT CTC AG
mTREM2_RT_for	GGA ACC GTC ACC ATC ACT CT
mTREM2_RT_rev	GGA GGT GCT GTG TTC CAC TT

2.5 siRNA and esiRNA

Name	Target	Source
Hs_GSK3A_5 siRNA	human GSK3α	Qiagen
Hs_GSK3B_8 siRNA	human GSK3ß	Qiagen
GSK3B esiRNA	human GSK3ß	Sigma Aldrich
AllStars negative control siRNA	-	Qiagen

2.6 CRISPR/Cas9 sgRNA

Gene/sgRNA name	Target exon	sgRNA sequence $(N)_{20}$
CCL2 Ex1	Exon 1	AGC GAG CCC TTG GGG AAT GA
CCL2 Ex2	Exon 2	ATT GGT GAA GTT ATA ACA GC
CCL3 Ex1	Exon 1	GGT GCA GAG GAG GAC AGC AA
CCL3 Ex3	Exon 3	CCT AAC CAA GCG AAG CCG GC
CCL7 Ex2	Exon 2	TTC CCG GGG ACA GTG GCT AC
CCL7 Ex3	Exon3	CCA GGT GCT TCA TAA AGT CC
CD44 Ex2	Exon 2	CTA CAG CAT CTC TCG GAC GG
CD44 Ex3	Exon 3	AAG GGC ACG TGG TGA TTC CC
CD163 Ex1	Exon 1	ATG GTG CTA CTT GAA GAC TC
CD163 Ex2	Exon 2	GAG TCC CTT CAC CAT TAC TG
CDC42 Ex1	Exon 1	GTC TCC TGC GCG CTG ACG TC
CDC42 Ex1.2	Exon 1	ACA ATT AAG TGT GTT GTT GT
CTNNB1/ ßCat Ex2	Exon 2	GAA AAG CGG CTG TTA GTC AC
CTNNB1/ ßCat Ex3	Exon 3	TCC CAC TAA TGT CCA GCG TT
EGFP control	(Shalem *et al.* 2014)	GGT GAA CCG CAT CGA GCT GA
GSK3B/ GSK3ß Ex1	Exon 1	CGG CTT GCA GCT CTC CGC AA
GSK3B/ GSK3ß Ex4	Exon 4	TTT GGC TCG ACT ATA GTG TC
LDLR Ex1	Exon 1	GCC TTG CTC CTC GCC GCG GC
LDLR Ex2	Exon 2	TCC TAC AAG TGG GTC TGC GA
MMP10 Ex2	Exon 2	GAG CTG AAG TGA CCA ACG TC
MMP10 Ex4	Exon 4	TTG GCT CAT GCC TAC CCA CC
NLRP3 Ex1	Exon 1	ATT GAA GTC GAT CAT TAG CG
NLRP3 Ex2	Exon 2	GTC TTC CTG GCA TAT CAC AG
STAB1 Ex1	Exon 1	CAG AGT GGG AGG AGG CCC CG
STAB1 Ex2	Exon 2	CTT CTT GAT GGC CGC GCA CG
THBS1 Ex1	Exon 1	GAA CAG GAC GCC TAG TCC CC
THBS1 Ex2	Exon 2	CAG CCC AGC TTT CCG CAT CG
TREM1 Ex1	Exon 1	CCG AAG CCT CTA GGT CAT TG
TREM1 Ex1.2	Exon 1	CCA CAA TGA CCT AGA GGC TT
TREM1 Ex2	Exon 2	TGG TTT ACT GCG CGT CCG AA

2.7 Antibodies

2.7.1 Primary antibodies

Name	Host	Dilution	Clonality	Source
anti-Actin	rabbit	1:2000	polyclonal	Sigma Aldrich
anti-ß-catenin	mouse	1:1000	monoclonal	BD Biosciences
anti-CDC42	mouse	1:500	monoclonal	Santa Cruz
Anti-CD36 (phycoerythrin conjugate)	rat	1:75	monoclonal	eBioscience
anti-CD44	rabbit	1:1000	polyclonal	Sigma Aldrich
anti-CD163	rabbit	1:1000	polyclonal	Santa Cruz
anti-GSK3α	rabbit	1:2000	polyclonal	Cell Signaling Technology
anti-GSK3ß	rabbit	1:5000	polyclonal	Cell Signaling Technology
anti-Iba1	rabbit	1:350	polyclonal	Wako
IC16 (anti-Aß)	mouse	1:1000	monoclonal	unpublished
anti-IL-4R (biotinylated)	goat	1:50	polyclonal	R&D Systems
anti-NLRP3	mouse	1:1000	monoclonal	Adipogen

2.7.2 Secondary antibodies

Antigen	Conjugate	Dilution	Species	Source
Goat IgG	IRDye 800CW	1:10000	donkey	LI-COR Biosciences
Mouse IgG	IRDye 800CW	1:10000	goat	LI-COR Biosciences
Rabbit IgG	IRDye 800CW	1:10000	goat	LI-COR Biosciences
Rabbit IgG	Alexa Fluor 594	1:500	goat	Thermo Fisher Scientific

2.8 Reagents

2.8.1 Chemicals

1-Step Ultra TMB ELISA	Pierce, Bonn
30 % Acrylamide 37.5:1, Bis-Acrylamide	National Diagnostics, USA
Agar	Roth, Karlsruhe
Agarose	Bio-Budget, Krefeld
AlamarBlue	Invitrogen, Karlsruhe
Ammoniumpersulfate (APS)	Sigma Aldrich, USA

Beta-amyloid (1-42)	JPT, Berlin
BisTris	Calbiochem, Darmstadt
Boric Acid	Sigma Aldrich, USA
Bromphenolblue	Roth, Karlsruhe
BSA	Sigma Aldrich, USA
Desoxynucleotide-tri-phosphate (dNTP)	New England Biolabs, USA
Dimethylsulfoxide (DMSO)	Sigma Aldrich, USA
Dithiothreitol (DTT)	Sigma Aldrich, USA
Dry-milk	Oxoid, GB
Ethylendiaminetetraacetic acid (EDTA)	Roth, Karlsruhe
Ethanol	Roth, Karlsruhe
FAM-Aß	Peptide Specialty Lab., Heidelberg
Fetal calf serum (FCS)	Invitrogen, Karlsruhe
Gene Juice	Merck, Darmstadt
Glycerine	Roth, Karlsruhe
Glycine	Roth, Karlsruhe
HiPerfect transfection reagent	Qiagen, Hilden
Hoechst 33342	Cayman Chemical, USA
Hydrochloric acid (HCl)	Sigma Aldrich, USA
Isopropanol	Roth, Karlsruhe
Lymphoprep	Stemcell Technologies, Vancouver
Lipofectamine 2000	Thermo Fisher Scientific, USA
Lipopolysaccharide (LPS)	Sigma Aldrich, USA
Magnesium-chloride ($MgCl_2$)	Roth, Karlsruhe
2-β-mercaptoethanol	Invitrogen, Karlsruhe
Methanol	Roth, Karlsruhe
Methylthialazole Tetrazolium (MTT)	Cayman Chemical, USA
Midori Green Advance DNA Stain	Biozym, Oldendorf
2-(N-morpholino)ethanesulfonic acid (MES)	Roth, Karlsruhe
Paraformaldehyde (PFA)	Sigma Aldrich, USA
PBS	Invitrogen, Karlsruhe
Phorbol 12-myristate 13-acetate (PMA)	Cayman Chemical, USA
Polybrene	Sigma Aldrich, USA
Potassium chloride (KCl)	Sigma Aldrich, USA
Potassium di-hydrogen phosphate (KH_2PO_4)	Roth, Karlsruhe
Protease Inhibitor cocktail tablets	Roche, Mannheim

Random Hexamers (pd(N_6))	Thermo Fisher Scientific, USA
RPMI1640	Invitrogen, Karlsruhe
Sodium azide (NaN_3)	Merck, Darmstadt
Sodium chloride (NaCl)	Roth, Karlsruhe
Sodium di-hydrogen phosphate (NaH_2PO_4)	Merck, Darmstadt
Sodium dodecyl sulfate (SDS)	BioRad, Munich
Sodium hydroxide (NaOH)	Merck, Darmstadt
Sulfuric acid	Merck, Darmstadt
TEMED (Tetramethylendiamine)	BioRad, Munich
Tris hydrochloride	Roth, Karlsruhe
Tris-Base	Roth, Karlsruhe
Triton-X 100	Pierce, Bonn
Trypan blue	Invitrogen, Karlsruhe
Tryptone	Roth, Karlsruhe
Trypsin/EDTA	Invitrogen, Karlsruhe
Tween-20	Roth, Karlsruhe
Yeast Extract	Roth. Karlsruhe

2.8.2 Cell culture reagents

CCL2 (human)	Peprotech, London
DMEM	Thermo Fisher Scientific, USA
DPBS	Thermo Fisher Scientific, USA
Fetal Bovine Serum	Thermo Fisher Scientific, USA
GM-CSF (human)	Peprotech, London
IL-34 (human)	Peprotech, London
L-Glutamine	Thermo Fisher Scientific, USA
Opti-MEM	Thermo Fisher Scientific, USA
Poly-L-Lysine	Sigma Aldrich, USA
RPMI 1640	Thermo Fisher Scientific, USA
Sodium pyruvate	Thermo Fisher Scientific, USA
Trypsin 0.25 % (no EDTA)	Thermo Fisher Scientific, USA
Trypsin/EDTA	Thermo Fisher Scientific, USA
Wnt-3a (human)	R&D Systems, USA

2.8.3 Inhibitors

Name	Target	IC_{50}	Source
SB216763	GSK3	GSK3α: 34 nM; GSK3ß: 12 nM (Coghlan *et al.* 2000)	Cayman Chemical
Bio-Acetoxime	GSK3	GSK3α/ß: 10 nM (Polychronopoulos *et al.* 2004)	Cayman Chemical
CHIR99021	GSK3	GSK3α: 10 nM; GSK3ß: 6.7 nM (Ring *et al.* 2003)	Cayman Chemical
Cytochalasin D	Actin polymerization		Cayman Chemical
Roscovitine	CDKs	CDK1: 0.65 µM (Meijer *et al.* 1997)	Cell Signaling
Purvalanol A	CDKs	CDK1: 4 nM (Gray *et al.* 1998)	Santa Cruz

2.8.4 Antibiotics

Actinomycin D	Cayman Chemical, USA
Ampicillin	Sigma Aldrich, USA
Hygromycin	Roth, Karlsruhe
Penicillin/ Streptomycin	Thermo Fisher Scientific, USA
Puromycin	Merck, Darmstadt

2.8.5 Size standards

PageRuler Plus Prestained Protein Ladder	Thermo Fisher Scientific, USA
Quick-Load 2-log DNA Ladder	New England Biolabs, USA

2.8.6 Enzymes

Antarctic phosphatase	New England Biolabs, USA
DNase	Sigma Aldrich, USA
M-MLV Reverse Transcriptase	Promega, USA
NotI Restriction Endonuclease	New England Biolabs, USA
Phusion High-Fidelity DNA-Polymerase	Thermo Fisher Scientific, USA
Quick Ligase	New England Biolabs, USA
T4 DNA Ligase	New England Biolabs, USA

T4 Polynucleotide Kinase	New England Biolabs, USA
XhoI Restriction Endonuclease	New England Biolabs, USA

2.8.7 Kits

BCA Protein Assay Kit	Pierce, Bonn
Cell Mask Plasma Membrane Stain	Thermo Fisher Scientific, USA
E. coli BioParticles	Thermo Fisher Scientific, USA
EasySep Human Monocyte Enrichment Kit	Stemcell Technologies, Vancouver
Platinum SYBR Green	Invitrogen, Karlsruhe
QIAquick Gel Extraction Kit	Qiagen, Hilden
QIAquick PCR purification Kit	Qiagen, Hilden
ReliaPrep RNA Cell Miniprep System	Promega, USA
Wizard Plus SV Minipreps DNA Purification System	Promega, USA

2.9 Laboratory equipment

Centrifuges	Eppendorf, Hamburg
	Hettich, Tuttingen
Electronic multi channel pipette	Brand, UK
Electrophoresis power supply	Consort, Belgium
Flat bed shaker	Heidolph, Kehlheim
Fluorescence microscope	Zeiss, Oberkochen
Freezers and fridges	-80°C Heraeus
	-20°C Liebherr
	4°C Liebherr
Glassware	Schott, Mainz
Heating block	HLC BioTech, Bovenden
Incubator, Cell culture	Binder, Tuttlingen
Incubator, bacteria	New Brunswick Scientific, USA
Laminar flow	Gelaire, Kottenforst
LI-COR Odyssey CLx	LI-COR Biotechnology, USA
Light-optical microscope	Olympus, Hamburg
Magnetic stirrer	Heidolph, Kehlheim
NanoDrop ND-1000 Spectrophotometer	Peqlab, Erlangen

Novex Mini-Cell Electrophoresis chamber	Thermo Fisher Scientific, USA
Paradigm microtiterplate reader	Beckman Coulter, Krefeld
Pasteur pipettes	Roth, Karlsruhe
pH meter	inoLab, Weinheim
Pipettes 0.2 µl-1ml	Gilson, USA
Pipettor AccuJet	Brand, UK
Scale (max=110 g)	Sartorius, Goettingen
Semi Dry Blotter	Hoefer, USA
Scale (max= 2000 g)	KERN, Balingen
StepOne Plus Real Time PCR System	Thermo Fisher Scientific, USA
T3 Thermocycler	Biometra, Goettingen
Tank Blotter	CBS Scientific, USA
Vi-Cell XR cell counter	Beckman Coulter, Krefeld
Vortexer	IKA, Staufen
Waterbath	Julabo, Seelbach
XCell SureLock™ Mini-Cell Electrophoresis System	Invitrogen, Karlsruhe

2.10 Consumables

0.2 ml reaction tubes	Eppendorf, Hamburg
1.5 ml reaction tubes	Eppendorf, Hamburg
2 ml reaction tubes	Eppendorf, Hamburg
10 cm petri dishes	Nunc, Wiesbaden
15 ml tubes	Sarstedt, Nürnbrecht
50 ml tubes	Sarstedt, Nürnbrecht
6-well plates	Nunc, Wiesbaden
12-well plates	Nunc, Wiesbaden
24-well plates	Nunc, Wiesbaden
96-well plates	Nunc, Wiesbaden
96-well plates (black)	Greiner, Frickenhausen
Aluminium-foil	Aro, Metro
Cassettes	Thermo Fisher Scientific, USA
Cell Scraper	TPP, Schweiz
Centrifugal Filter Units	Sartorius, Goettingen
Coverslips	VWR, Darmstadt

Cryotubes	Nunc, Wiesbaden
Disposable gloves, Latex	Maimed, Neuenkirchen
Disposable gloves, Nitril	Ansell, UK
Immobilion-FL Transfer Membrane (PVDF)	Millipore, USA
Microscope cover glasses	VWR, Darmstadt
Needles	Becton Dickinson, USA
Pipet tips (10 µl – 1000 µl)	Starlab, Ahrensburg
Pipettes (5 ml-25ml)	Sarstedt, Nürnbrecht
Syringes (5 ml, 10 ml)	Braun, Melsung
T25, T75 flask	Nunc, Wiesbaden
Whatman paper	Whatman, Dassel

2.11 Software

Adobe Illustrator CS3
Adobe Photoshop CS3
CLC DNA Workbench 6
EndNote X5
GraphPad Prism 5.0
Image Studio Software 2.1
Microsoft Office Professional Plus 2010

3 Methods

3.1 Cell culture

3.1.1 Passaging of immortalized cell lines

Routine cell culture was performed under sterile working conditions in S1 or S2 qualified laboratories. Cell lines were cultured in the appropriate medium supplemented with selection antibiotics as necessary and incubated in a humidified incubator at 37°C in the presence of 5 % CO_2. Monocyte THP-1 cells were cultured in RPMI 1640 medium supplemented with 10 % FCS, 1 mM sodium pyruvate, antibiotics (5 units/ml penicillin, 5 µg/ml streptomycin), 2 mM L-glutamine and 50 µM 2-ß-mercaptoethanol. For passaging, every 3 or 4 days a portion of the cell suspension was transferred into a new 75 cm^2 cell culture flask containing fresh medium. For the differentiation of THP-1 monocytes into adherent macrophages the cells were grown for at least 24 h in the presence of 10 nM phorbol myristate acetate (PMA). In general, adherent cell lines (HEK293, L929) were cultured in 10 cm cell culture dishes in DMEM (high glucose, + L-glutamine) supplemented with 10 % FCS, antibiotics (5 units/ml penicillin, 5 µg/ml streptomycin) and 1 mM sodium pyruvate. For passaging, cells were washed with PBS and subsequently incubated in 1 ml 0.05 % trypsin/EDTA. The trypsination reaction was stopped by addition of 9 ml fresh medium. A desired amount of the cell suspension was transferred into a new 10 cm culture dish with fresh medium.

3.1.2 Freezing and thawing of cells

For long-term storage of cell lines the cells were frozen and stored at -80 °C or in liquid nitrogen. The cells were trypsinized (3.1.1) and centrifuged for 5 min at 1000 rpm. After centrifugation the cells were resuspended in freezing medium (1 ml per 10 cm dish/ 75 cm^2 flask) containing 95 % FCS and 5 % DMSO. The cell suspension was aliquoted in 1 ml cryo-vials and frozen at -80 °C. For long-term storage the vials were transferred into a liquid nitrogen tank. For thawing of cells, the cryo-vials were placed in a 37 °C water bath. The cell suspension was diluted in medium and centrifuged at 1000 rpm for 5 min. The cell pellet was resuspended in fresh medium and transferred onto a culture dish or into a culture flask.

3.1.3 Primary microglia cell culture

Primary microglia were isolated from mixed glial cultures prepared from newborn wildtype C57BL/6 mice. After decapitation, brains were isolated and collected on ice in Hank's Balanced Salt solution (HBSS, Biochrom). Blood vessels and meninges were removed and brains were washed three times with HBSS. Next, 1 ml trypsin (0.25 %, no EDTA) was added to 10 ml HBSS containing the brain tissue and incubated for 10 min at 37 °C. After 5 min of incubation cells were vortexed. In the meantime, 75 cm^2 flasks were coated with 10 ml poly-L-lysine (0.01 % in MilliQ) for at least 20 min. Flasks were washed with 10 ml PBS and 10 ml complete growth medium were added per flask. The trypsin reaction was stopped by addition of 10 ml complete growth medium (DMEM supplemented with 5 % heat-inactivated FCS, 1 mM sodium pyruvate, 5 units/ml penicillin and 5 µg/ml streptomycin). 200 µl of DNase (2000 U/ml) were added and the tissue was dissociated by pipetting up and down with a 10 ml pipette. For further dissociation of cells, a 1000 µl tip was mounted on the top of the 10 ml pipette and the procedure was repeated. The cell suspension was centrifuged at 1200 rpm and 4 °C for 10 min. Cells were then resuspended in 5 ml fresh DMEM per two brains and transferred to a 75 cm^2 flask (5 ml/flask) already containing 10 ml pre-warmed DMEM. After 48 h cells were washed three times with pre-warmed PBS to remove cell debris and 9 ml fresh DMEM and 1 ml L929 conditioned media (3.1.4) were added to each flask. After approximately eight days in culture microglia cells were harvested and separated from the underlying astrocytic layer by shake-off. Supernatants were centrifuged at 1200 rpm for 10 min at 4 °C. Cells were resuspended in fresh medium and plated at appropriate numbers on poly-L-lysine coated glass coverslips in 24-well plates, in 6-well plates or 96-well plates for following experiments. Flasks were refilled with 5 ml fresh DMEM, 5 ml of the old supernatant and 500 µl of L929 conditioned media. Cells could be shaken-off every two to four days and the procedure was repeated up to three times per flask.

3.1.4 Preparation of L929 conditioned media

Conditioned media from L929 fibroblasts were used for microglia cultures as a source of Macrophage-Colony-Stimulating Factor (M-CSF). A confluent 10 cm culture dish of L929 cells was splitted 1 : 8 to 75 cm^2 flasks. After 24 h, 30 ml of complete DMEM were added to the cells. Supernatant was harvested after four days by centrifugation and sterile filtration through a 0.2 µm filter. Conditioned media were aliquoted and stored at -20 °C.

3.1.5 Isolation and differentiation of human monocytes

Monocytes were prepared from buffy coats from healthy blood donors in a two-step procedure. Firstly, Lymphoprep (Stemcell Technologies) density gradient centrifugation was used to isolate peripheral blood mononuclear cells (PBMCs). 15 ml of blood were diluted with 15 ml PBS containing 2 % FCS/ 5mM EDTA and layered on top of 15 ml of the Lymphoprep density gradient medium. The tube was centrifuged at 800 x g for 30 min at RT with the brake off. After centrifugation the cells were kept on ice and the white cell layer containing mononuclear cells was removed and transferred into a new tube. The mononuclear cell fraction was filled up with PBS to a total volume of 20 ml and centrifuged at 120 x g for 10 min at RT with the brake off. The supernatant was removed and the cell pellet was resuspended in 20 ml PBS. The centrifugation step was repeated twice and the purified PBMC pellet was resuspended in 1 ml of PBS containing 2 % FCS/ 1 mM EDTA. In the second purification step, monocytes were isolated from PBMCs using the EasySep™ Human Monocyte Enrichment Kit without CD16 Depletion (Stemcell Technologies) and the Purple EasySep™ Magnet (Stemcell Technologies). The method is based on negative selection to isolate monocytes and CD14+CD16+ monocytes. Non-monocytes are removed by magnetic labelling with monoclonal antibodies and subsequent separation in the EasySep™ magnet. The isolation was performed according to the manufacturer`s instructions. Following isolation, the monocytes were differentiated into macrophages under conditions described by Ohgidani *et al.* (Ohgidani *et al.* 2014). Monocytes were transferred into growth medium (RPMI 1640 supplemented with 10 % heat-inactivated FCS, 1 mM sodium pyruvate, 5 units/ml penicillin and 5 µg/ml streptomycin, 1 mM L-glutamine and 50 µM 2-ß-mercaptoethanol) and seeded at a density of 50.000 cells/well in poly-L-lysine (0.01 % in MilliQ) coated black and clear 96-well plates. After 24 h medium was changed to growth medium containing 10 ng/ml GM-CSF and 100 ng/ml IL-34. After seven days in culture, medium was changed to fresh growth medium containing 10 ng/ml GM-CSF and 100 ng/ml IL-34 and the cells were cultured for another 7 days. The morphology of cells that were seeded in clear 96-well plates was monitored using light microscopy. After 14 days of differentiation, the cells were treated for 48 h with the GSK3 inhibitor CHIR99021 and a FAM-A$ß_{42}$ uptake assay was performed (3.1.14).

3.1.6 Determination of cell concentrations

Cell concentrations were determined using the Vi-CELL™ cell viability analyzer (Beckman Coulter). The system uses the trypan blue cell counting method to determine the percentage of viable and non-viable cells.

3.1.7 Generation of retroviral particles

A confluent 10 cm culture plate of the HEK293-based packaging cell line GP2-293 was splitted 1 : 4 to 75 cm^2 flasks. After 24 h (cell density 70 - 80 %) cells were transfected by lipid transfection using Gene Juice® (Millipore). A transfection mixture was prepared containing 45 µl Gene Juice® in 800 µl Opti-MEM™ (Invitrogen). Following incubation for 5 min at RT, 7.5 µg of a retroviral shuttle vector containing the gene of interest and 7.5 µg of the envelope plasmid pCMV-VSVG were added to the transfection mixture and incubated for 20 min at RT. Medium on the GP2-293 cells was replaced by fresh complete DMEM and the transfection mixture was added dropwise onto the cells. The next day, the supernatant was removed and 5 ml fresh medium were added to the cells for 24 h. To harvest the retroviral particles, the supernatant was drawn into a 10 ml syringe and filter sterilized through a 0.45 µm filter. Filtered supernatants were aliquoted into screw cap cryovials and stored at -80 °C.

3.1.8 Generation of lentiviral particles

A confluent 10 cm culture plate of the packaging cell line HEK293FT was splitted 1 : 2 to 75 cm^2 flasks. After 24 h (cell density 90-100 %) medium was changed to 5 ml Opti-MEM™ (Invitrogen) 1 h before transfection. A transfection mixture was prepared containing 27 µl Lipofectamine™ 2000 (Thermo Fisher) in 640 µl Opti-MEM™ (Invitrogen) and incubated for 5 min a RT. For the transfection of HEK293FT cells a 3rd generation lentivirus system comprising the two packaging plasmids pMDLg/pRRE and pRSV_Rev and the envelope plasmid pMD2.G was used. 4 µg of each plasmid and 7 µg of a lentiviral shuttle vector containing the gene of interest were added to a final volume of 667 µl Opti-MEM™. After incubation for 5 min at RT the mixture was combined with the transfection mixture and incubated for another 20 min at RT. The mixture was added dropwise onto the cells. The next morning, medium was changed to 6 ml DMEM without antibiotics for 24 h. Lentiviral particles were harvested as described in 3.1.7.

3.1.9 Infection with viral particles

To generate THP-1 cells stably expressing a gene of interest, cells were infected with retro- or lentiviral particles. THP-1 cells were seeded in 25 cm^2 flasks at a density of 750.000 cells in 5 ml complete RPMI. The next day, cells were centrifuged at 1000 rpm for 5 min and resuspended in 1 ml fresh medium. Next, 2 µl of a polybrene stock solution (5 mg/ml) were added to the cells. Viral particles were thawed in a waterbath at 37 °C and 1 ml was added to the cells. Control cells were treated with 1 ml RPMI instead of viral particles. After incubation for 24 h, cells were centrifuged at 1000 rpm for 5 min and the supernatant containing the viral particles was removed. Cells were washed once with 5 ml PBS followed by another centrifugation step. Then, 5 ml of fresh complete RPMI were added to the cells. After 24 h an appropriate concentration of a selection antibiotic was added. Selection was maintained at least until the control cells not expressing antibiotic selection markers were dead and stable clones appeared.

3.1.10 Dose-response curve for antibiotic selection

To determine the minimum concentration of antibiotics needed for the selection of stable THP-1 cell clones after lentiviral or retroviral transduction, non-transduced THP-1 cells were subjected to increasing concentrations of the selection antibiotic. Cells were seeded in 6-well plates at a density of 500.000 cells/well. After 24 h medium was changed to medium containing the selection antibiotic. One well served as control without the addition of antibiotics. Medium was exchanged every 2 – 3 days and fresh antibiotic was added. The lowest antibiotic concentration that killed 100 % of cells over the course of one week was determined. For THP-1 cells, 1 µg/ml puromycin and 300 µg/ml hygromycin were used for selection.

3.1.11 Compound treatment

To evaluate the effect of compounds, cells were treated for indicated time periods with the respective compounds and vehicle control and an uptake assay was performed or lysates were prepared. Inhibitors were dissolved in DMSO. Wnt3-a was dissolved in sterile PBS containing 0.1 % BSA. THP-1 cells, primary macrophages and primary microglia were seeded and treated in complete growth medium. For seeding and treatment of THP-1 cells, 10 nM PMA was added to the medium.

3.1.12 AlamarBlue cell viability assay

The alamarBlue® dye (Invitrogen) monitors cell viability and was used to test for compound toxicity. AlamarBlue® (resazurin) undergoes a colorimetric change in response to the metabolic reduction by living cells. Cells were seeded in clear 96-well plates at a concentration of 5000 cells/50 µl medium per well. Appropriate dilutions of the inhibitors in medium were added to the cells (50 µl/well). Cells treated with DMSO only served as a control. After 24 h, 48 h or 72 h of treatment, 10 µl of the AlamarBlue® solution were added to each well. Cells were incubated for at least 4 h at 37 °C until a color change appeared. Absorbance was measured on a Paradigm™ plate reader (Beckman Coulter) at 570 nm and 600 nm as a reference wavelength.

3.1.13 MTT assay

MTT (3-(4,5-dimethylthiazol-2-yl)-2,5-diphenyltetrazolium bromide) was used to test for compound toxicity. The method is based on the conversion of the yellow MTT reagent to insoluble purple formazan by living cells. Cells were seeded in clear 96-well plates at a concentration of 20.000 cells/100 µl medium per well. After 24 h, cells were treated with increasing compound concentrations for 24 h – 72 h. Cells treated with DMSO only served as a control. Following compound treatment, 20 µl of the MTT solution (5 mg/ml MTT in PBS) were added to each well and the cells were incubated for 3.5 h at 37 °C. The media was carefully removed prior to the addition of 150 µl MTT solvent (4 mM HCl, 0.1 % Nonidet P-40 in isopropanol) per well. The plate was incubated for 15 min in the dark at RT with shaking to dissolve formazan crystals. Absorbance was measured on a Paradigm™ plate reader (Beckman Coulter) at 590 nm with a reference filter of 620 nm.

3.1.14 Uptake assay for FAM-labeled Aß$_{42}$

The uptake assay was used to quantify the ability of cells to internalize carboxyfluorescein (FAM)-labeled amyloid beta 1-42 (FAM-Aß$_{42}$). FAM-Aß$_{42}$ was diluted in PBS/10% DMSO and incubated for three days at 37 °C. Cells were seeded in black 96-well plates at a density of 20.000 cells/well (primary monocytes: 50.000 cells/well). After 24 h, the cells were subjected to compound treatment in a total volume of 100 µl per well for the indicated time points. Following compound treatment, 50 µl medium and 50 µl medium containing 2 µM FAM-Aß$_{42}$ were added to the cells (total volume 200 µl containing 0.5 µM FAM-Aß$_{42}$ per well). Control wells contained 10 µM of the actin

polymerization inhibitor cytochalasin D. The cells were incubated for 4 h at 37 °C. The Aß-containing medium was removed and the fluorescence of extracellular FAM-$Aß_{42}$ was quenched by adding 100 µl/well of a 0.2 % trypan blue solution in PBS (pH 4.4). After an incubation time of 1 min, trypan blue was aspirated and the intracellular fluorescence was recorded on a Paradigm™ plate reader (Beckman Coulter) at 485 nm excitation/535 nm emission. The detected signal was used as a direct measure for the cellular uptake of FAM-$Aß_{42}$. To estimate cell numbers per well, 100 µl/well of the cell-permeable Hoechst dye 33342 (50 µg/ml in PBS) were added to the cells for 5 min. After removal of the dye, fluorescence was measured at 360 nm excitation/465 nm emission.

3.1.15 Uptake assay for *E. coli* particles

The uptake assay was used to determine the ability of cells to internalize fluorescently labeled *E. coli* BioParticles (Molecular Probes). These particles consist of fluorescein-conjugated heat-inactivated *E. coli*. The *E. coli* particles were resuspended in PBS containing 2 mM NaN_3 at a concentration of 20 mg/ml. For the uptake assay, the suspension was diluted 1:100 in the appropriate cell culture medium. 50 µl of this dilution were added to compound-treated cells seeded in 96-well plates in a final volume of 200 µl per well. After an incubation time of 45 min at 37 °C, the particle-containing medium was removed. Quenching of the extracellular fluorescence, recording of the intracellular fluorescence and Hoechst staining were performed as described for the FAM-$Aß_{42}$ uptake assay (3.1.14).

3.1.16 Preparation of THP-1 conditioned media

Conditioned media (CM) from CHIR99021-treated THP-1 cells were used to investigate the contribution of soluble factors in promoting Aß uptake. THP-1 cells were seeded at a density of 240.000 cells/well in a 24-well plate. After 24 h, medium was changed to 1 ml growth medium per well containing 5 µM CHIR99021 or DMSO vehicle control and the cells were incubated for 48 h. Supernatants were collected and centrifuged at 1000 x g for 5 min to remove cell debris. To purify the supernatants from remaining CHIR99021, the supernatants were transferred to an ultracentrifugal filter with a 3 kDa molecular weight cut-off (Sartorius) and centrifuged at 2800 x g for 35 min. The resulting concentrate was then diluted with fresh medium to the initial volume. The centrifugation and dilution steps were repeated twice and the conditioned media were used for treatment of THP-1 cells. For the preparation of conditioned media from THP-1 cells that

were pre-treated with CHIR99021, THP-1 cells were seeded as described above. After 24 h medium was changed to 1 ml growth medium per well containing 5 µM CHIR99021 or DMSO vehicle control and the cells were incubated for 48 h. Cells were then washed two times with PBS to remove the CHIR99021 containing medium prior to the addition of 500 µl fresh medium per well. After conditioning for 24 h, the supernatants were collected and centrifuged at 1000 x g for 5 min to remove cell debris. The 24 h conditioned media were used undiluted or 1:1 diluted with fresh medium for the treatment of THP-1 cells.

3.1.17 Aß$_{42}$ degradation assay

Aß$_{42}$ (JPT) was reconstituted in PBS/10 % DMSO. THP-1 cells were seeded in 12-well plates at a density of 700.000 cells/well. After 24 h medium was changed to 2 ml growth medium per well containing an appropriate concentration of the GSK3 inhibitor or DMSO vehicle control and incubated for 48 h. The medium was removed and 600 µl of fresh growth medium containing 2 µM Aß$_{42}$ were added per well and incubated for 2 h at 37 °C. Cells that were treated with medium without Aß$_{42}$ were used as control. The medium was removed, cells were washed twice with 1 ml PBS and 600 µl of fresh growth medium were added per well. After 0, 0.5, 1 and 4 hours of incubation at 37 °C the cells were washed once with PBS and cells were lysed in 70 µl RIPA buffer (table 3.2) per well. Protein concentrations of the lysates were determined by BCA (3.2.2) and the lysates were analyzed by ELISA (3.2.6) for Aß$_{42}$ levels. Furthermore, the 0 h samples were analyzed by SDS-PAGE and Western Blot (3.2.3 and 3.2.4).

3.1.18 Reverse transfection of siRNA

THP-1 cells were transiently transfected with either siRNAs or esiRNAs (section 2.5) by lipid transfection using HiPerfect transfection reagent (Qiagen). A non-targeting siRNA (AllStars negative control siRNA, Qiagen) served as a negative control. For a subsequent uptake assay, transfections were performed in 96-well plates. To determine the knock- down efficiencies of target proteins, the transfection was performed in 24-well plates. For the transfection of cells in 96-well plates 4.5 µl (27 µl for 24-well) of an esiRNA or siRNA dilution (1 µM in RNase free water) were spotted into each well. A transfection mixture was prepared by adding 1 µl HiPerfect (6 µl for 24-well) to a total volume of 25 µl (144 µl for 24-well) Opti-MEM™. Following incubation for 10 min at RT the mixture was transferred onto the spotted siRNA. The siRNA- transfection reagent mixture was then further incubated for 15 min at RT. In the meantime, a cell suspension

containing 20.000 cells/30 µl (120000 cell/180 µl for 24-well) in RPMI medium without antibiotics and supplemented with 10 nM PMA was prepared. 30 µl (180 µl for 24-well) of the cell suspension were added directly to the well containing the transfection complexes. After incubation for 2 h at 37 °C fresh medium without antibiotics and supplemented with 10 nM PMA was added to a final volume of 200 µl (1200 µl for 24-well) which resulted in a final siRNA/esiRNA concentration of 22.5 nM. On the next morning, medium was changed to 100 µl (500 µl for 24-well) complete growth medium containing 10 nM PMA. 72 h after transfection an uptake assay was performed (3.1.14) or cells were lysed for protein extraction (24-well).

3.1.19 RNA extraction, reverse transcription and quantitative PCR

For gene expression analysis total RNA was isolated from THP-1 cells and primary microglia using the ReliaPrep™ RNA Cell Miniprep System (Promega) according to the manufacturer`s protocol. THP-1 cells were seeded in 12-well plates in the presence of 10 nM PMA and allowed to differentiate for 24 h. The cells were then incubated in complete RPMI with or without GSK3 inhibitor or DMSO as control for up to 48 h. For primary microglia, an appropriate number of cells was seeded in 12-well plates and allowed to adhere for 24 h. Cells were then grown in DMEM with or without GSK3 inhibitor or DMSO as control for up to 72 h. RNA concentrations were measured by spectrophotometry at 260 nm. First-strand cDNA was synthesized from up to 3 µg RNA by reverse transcription reaction. For cDNA synthesis, the RNA was incubated with 0.5 mM dNTPs (Thermo Fisher) and 1.25 µM random hexamer primer (Thermo Fisher) in a volume of 15 µl for 5 min at 65 °C. The samples were cooled on ice before adding 4 µl M-MLV reverse transcriptase 5x reaction buffer (Promega) and 200 U M-MLV (H–) reverse transcriptase (Promega) to a final volume of 20 µl. The samples were placed in a thermocycler and the following program was run: 25 °C for 10 min, 40 °C for 50 min and 70 °C for 15 min. Appropriate dilutions of the cDNA were prepared. For subsequent quantitative PCR analysis the Platinum™ qPCR Super Mix (Thermo Fisher) based on the fluorescent nucleic acid dye SYBR™ Green was used. 10 µl of the SYBR™ Green Mix, 500 nM of each primer (section 2.4) and 0.5 µl ROX™ reference dye were mixed and RNase free water was added to a final volume of 17 µl. The SYBR™ green mix and 3 µl of the diluted cDNA were transferred into a 96-well reaction plate (Applied Biosystems). Quantitative PCR was performed in a StepOnePlus™ Real-Time PCR System (Applied Biosystems) using the following program: 10 min for 95 °C followed by 40 cycles of repeated denaturation and hybridzation/elongation at 95 °C for 15 sec and

60 °C for 1 min. After completing the whole run the wells were heated to 95 °C and stepwise cooled to 60 °C to measure the melting temperature of the amplified product to control for specificity. The results for the relative gene expression were calculated using the $2^{-\Delta\Delta CT}$-method. Human ARF and mouse MRPL32 served as housekeeping genes.

3.1.20 Morphometric analysis of primary microglia

For the evaluation of cell morphology of primary microglia that were treated for 72 h with DMSO vehicle control or GSK3 inhibitors, cells were examined by light microscopy. For morphometric quantification, the plasma membrane of cells was stained using the CellMask™ Green plasma membrane stain (Molecular Probes). 150.000 cells per well were seeded on cover slips in a 24-well plate and incubated overnight. The cells were treated for 72 h with DMSO or GSK3 inhibitors. After washing once with PBS, the cells were incubated with CellMask™ Green plasma membrane stain (1:250 in PBS) for 10 min at 37 °C. Cells were fixed with 1 ml fixation solution (3.1.21) for 10 min at RT. After washing 3 times with PBS the coverslips were mounted in ProLong™ Gold Antifade Mountant with DAPI (Thermo Fisher Scientific) onto microscope slides and stored overnight at RT in the dark. The next day fluorescence images were taken using a confocal microscope (Axio Imager 2, Zeiss). The images were sent to our collaborative partner at the group of Michael Heneka (Department of Neurodegenerative Diseases and Gerontopsychiatry at the University of Bonn) for analysis of cell morphology. The Schoenen ramification index (RI) was calculated by dividing the maximum process number by the number of primary branches originating at the cell soma (Schoenen 1982). Morphometric analysis was performed using the program ImageJ.

3.1.21 Immunocytochemistry

Immunocytochemistry was used to visualize the localization of a protein of interest in cells. The use of a fluorophore-conjugated secondary antibody that binds to a specific primary antibody allows the visualization of the target protein under a fluorescence microscope. Cells were seeded at a density of 5 x 10^4 cells per well on coverslips in a 24-well plate and incubated overnight at 37 °C. THP-1 cells were incubated for 48 h in the presence of 10 nM PMA. For the visualization of internalized FAM-Aβ_{42}, the cells were treated with 0.7 µM FAM-Aβ_{42} in 400 µl medium per well for 1 h. After washing three times for 5 min with PBST, the cells were fixed with 1 ml of the fixation solution per well for 10 min at RT. Cells were washed two times with TBS and 1 ml of the permeabilization

solution was added for 20 min at RT to permeabilize the cells. Cells were washed once with TBS before the addition of blocking solution for 1 h at RT. After blocking, cells were washed once with TBS and 350 µl of the primary antibody solution were added and incubated for 1 h at RT. Cells were washed three times with TBS and 350 µl of the secondary antibody were added and incubated for 1 h in the dark. After antibody incubation, cells were washed three times with TBS and 1 ml sterile water was added. The coverslips were mounted in ProLong™ Gold Antifade Mountant with DAPI (Thermo Fisher Scientific) onto microscope slides and stored overnight at RT in the dark. The next day the slides were analysed using a confocal fluorescence microscope (Axio Imager 2, Zeiss).

Table 3.1: Solutions for immunocytochemistry

TBS/ PBST	Fixation/ Permeabilization	Blocking solution	Antibody buffer
TBS:	Fixation:	5% BSA (w/v) in TBS	4% BSA (w/v) in TBS
see table 3.6	4% PFA (w/v) in ddH_2O	→ sterile filtration	→ sterile filtration
PBS:	Permeabilization:		
137 mM NaCl	1 % saponin (w/v) in ddH_2O		
2,7 mM KCl			
8 mM Na_2HPO_4			
1,5 mM KH_2PO_4			
pH 7.4			
PBST:			
PBS			
0.05 % Tween-20			

3.1.22 Flow cytometry analysis

FACS (Fluorescence-Activated Cell Sorting) analyses were carried out by our collaborative partner at the group of Michael Heneka (Department of Neurodegenerative Diseases and Gerontopsychiatry at the University of Bonn). Primary microglia were seeded at a density of 300.000 cells/well in a 6-well plate and incubated overnight. The cells were treated for 72 h with GSK3 inhibitors. After washing twice with PBS, cells were detached using 0.05 % trypsin at 37 °C. After addition of 1 ml PBS per well the cells were transferred into tubes and centrifuged for 3 min at 1000 x g. The supernatants were discarded and the pellets were resuspended in 50 µl Hank's Balanced Salt solution (HBSS, Biochrom) containing 1 % BSA and Fc blocking reagent, which prevents the

binding of antibodies to Fc-receptors. The cells were incubated for 10 min on ice and 500 µl HBSS/1% BSA were added. After centrifugation for 3 min at 1000 x g the cells were incubated in 50 µl antibody mix (CD36-PE 1:75/ biotinylated IL-4R 1:50 with streptavidin-PE/Cy7 conjugate 1:200) for 1 h on ice. After addition of 1 ml HBSS the cells were centrifuged for 5 min at 1000 rpm and the pellet was resuspended in 100 µl HBSS. Cells were measured on a FACSCanto II™ (BD Bioscience). As control, corresponding isotype control antibodies were used.

3.2 Protein Biochemistry

3.2.1 Protein extraction

To investigate intracellular proteins, cells were lysed in RIPA (Radio-Immunoprecipitation Assay) buffer. For protein extraction from cells grown in 12-well plates, the cells were washed with 1 ml ice-cold PBS. After removing PBS, an appropriate amount of RIPA buffer containing 1x protease inhibitor (Complete Protease Inhibitor, Roche) was added directly onto the cells in each well of the plate. Cells were scraped off the plate, transferred into 1.5 ml tubes and incubated for 20 min at 4 °C with vortexing every 5 min. Next, lysed cells were centrifuged at 4 °C with 13 000 x g for 15 min. Supernatants were transferred into fresh tubes and stored at -20 °C.

Table 3.2: RIPA lysis buffer.

5 x RIPA buffer
250 mM Tris-HCl, pH 8.0
750 mM NaCl
5 % Triton X
2.5 % Na-Desoxycholat
0.5 % SDS
in $_{dd}H_2O$
(add 1 x protease inhibitor prior to cell lysis)

3.2.2 Determination of protein concentrations

Protein concentrations of cell lysates were determined photometrically by using a bicinchoninic acid (BCA) protein assay kit (Pierce). This detection method is based on a two step colorimetric reaction starting with the reduction of Cu^{2+} ions to Cu^{+} by peptide

bonds (biuret reaction) followed by the chelation of BCA with Cu^{+}. The reaction results in purple-colored product with a strong linear absorbance at 562 nm. For the determination of protein concentrations BCA reagents A and B were mixed in a 50:1 ratio. Next, 2.5 µl of each protein sample were loaded onto a clear 96-well plate and filled up to a volume of 25 µl with RIPA buffer (table 3.2). As a standard curve 25 µl BSA standard diluted with RIPA buffer to a concentration of 100, 200, 300, 400, 500 and 600 µg/ml protein was used. Protein samples and standards were loaded in duplicates. Then, 200 µl of the BCA reagent mix were added to each sample and standard. After incubation at 60 °C for 20 min, absorbance was measured on a Paradigm™ plate reader (Beckman Coulter) at 562 nm.

3.2.3 SDS-PAGE

SDS-PAGE (sodium dodecylsulfate polyacrylamide gel electrophoresis) allows the separation of denatured proteins according to their molecular weight under the influence of an applied electrical field. SDS disrupts the tertiary and secondary structure of proteins resulting in an overall negative charge of the proteins. Separating gels were produced by preparing resolving and stacking gel mixtures listed in table 3.3.

Table 3.3: Composition of polyacrylamide gels.

	7.4 % stacking gel (2 gels)	10 % resolving gel (2 gels)	12 % resolving gel (2 gels)
30 % Acrylamide (37.5:1)	1 ml	4.4 ml	5.28 ml
1.6 M Bis-Tris, pH 6.4	1 ml	3.3 ml	3.3 ml
MilliQ-water	2 ml	5.4 ml	4.52 ml
10 % APS	40 µl	66 µl	66 µl
TEMED	10 µl	22 µl	22 µl

A Novex gel cassette was filled up to 3/4 with the resolving gel mixture. The gel mixture was covered with a layer of water until the polymerization was completed. Next, water was removed and the 7.4 % stacking gel mixture was poured onto the resolving gel. The gels were placed into the electrophoresis chamber and covered with 1 x MES running buffer (table 3.4). Protein samples were mixed with 4 x SDS sample buffer (table 3.4), heated to 95 °C for 5 min and loaded onto the gel. To determine the molecular weights of the proteins in the samples, the protein marker PageRuler™ Plus Prestained Protein Ladder (Thermo Fisher Scientific) was used. The gel was run at 150 V for approximately 1 h.

Table 3.4: Composition of buffers used for SDS-PAGE.

4 x SDS sample buffer	running buffer (20 x MES)
1.44 M Bis-Tris	1 M MES
0.64 M Bicine	1 M Tris-Base
4 % SDS	69.3 mM SDS
100 mM DTT	20.5 mM EDTA
0.05 % Bromphenol blue	

3.2.4 Western Blot

To enable the detection of specific proteins, protein samples were first separated by SDS-PAGE (3.2.3) and subsequently analyzed by Western Blotting. After electrophoresis, proteins were transferred from the gel to a polyvinylidene fluoride (PVDF) membrane by application of an electric field in a semi dry blotting apparatus. In semi-dry blotting a gel/PVDF membrane stack is placed directly in contact with the electrodes. First a piece of blot paper soaked with transfer buffer A was placed onto the anode of the blotting system. A second blot paper soaked with transfer buffer B was placed on the top of the first piece. Next, the PVDF membrane was pre-soaked in methanol/transfer buffer B and placed on top of the wetted blot papers. The gel was placed onto the membrane and was covered with two additional blot papers soaked with transfer buffer C. The stack was covered with the cathode plate and the transfer was run at 50 mA per gel for 1 h.

Table 3.5: Composition of buffers used for Western Blotting.

Transfer buffer A	Transfer buffer B	Transfer buffer C
210 mM Tris, pH 10.4	25 mM Tris, pH 10.4	25 mM Tris
30 % Methanol	30 % Methanol	0.025 % SDS
in $_{dd}H_2O$	in $_{dd}H_2O$	pH 9 (with boric acid)
		in $_{dd}H_2O$

3.2.5 Immunostaining of membranes

Following protein transfer by Western Blotting (3.2.4), the membrane was blocked in 5 % dry-milk in 1 x TBST for 1 h at RT. The membrane was then washed 3 x 5 min with 1 x TBST. An appropriate dilution of the primary antibody (section 2.7.1) was prepared in 1 x TBST with 0.02 % NaN_3 and incubated on the membrane at 4 °C overnight while

shaking. The membrane was washed 3 x 10 min with 1 x TBST and the secondary antibody (section 2.7.2) in the respective dilution and buffer was added. After incubation for 1h at RT, the membrane was washed 2 x 10 min with 1 x TBST and 1 x 5 min with 1 x TBS. The fluorescence signal of the antibody-labeled proteins was detected using the Odyssey® CLx near-infrared fluorescence imaging system (LI-COR® Biosciences). The fluorescence signal was quantified with the Image Studio Software 2.1 (LI-COR® Biosciences).

Table 3.6: Composition of buffers.

10 x TBS	1 x TBS	1 x TBST
1.37 M NaCl 27 mM KCl 0.25 M Tris-Base, pH 7.4 in $_{dd}H_2O$	1:10 dilution of 10 x TBS in $_{dd}H_2O$	1:10 dilution of 10 x TBS 0.1 % Tween-20 in $_{dd}H_2O$

3.2.6 Enzyme-linked immunorsorbent assay (ELISA)

For the detection of $Aß_{42}$ peptides in THP-1 protein lysates a cell-based sandwich ELISA assay was performed. As a capture antibody the monoclonal antibody IC16 diluted 1:250 in PBS (table 3.1) was used, which recognizes amino acids 1-15 of the Aß sequence. Synthetic $Aß_{42}$ peptides (JPT Peptide Technologies), solubilized in DMSO at a concentration of 1 mg/ml, were used to generate standard curves. 96-well high-binding microtiter plates were coated over night at 4 °C with the capture antibody. The capture antibody was removed and 5 µl of the THP-1 lysates (1 µg/ml in RIPA) and 145 µl assay buffer (PBS containing 0.05 % Tween-20, 1 % BSA) were added per well. Additionally, a freshly diluted standard containing $Aß_{42}$ concentrations ranging from 125 to 3000 pg/ml in assay buffer was transferred onto the plate. Subsequently, a C-terminal detection antibody specific for $Aß_{42}$ labeled with horseradish peroxidase (HRP) using the Pierce EZ-Link™ Plus Activated Peroxidase kit (Thermo Fisher Scientific) was diluted 1:1000 in assay buffer. 50 µl of the diluted detection antibody were added to each well. The plate was incubated overnight at 4°C. Plates were then washed 3 times with PBST (table 3.1) and once with PBS. Then, 50 µl of TMB ultrasubstrate (Thermo Fisher Scientific) were added to each well and incubated for 1-5 min at RT until a blue-colored reaction product appeared. The reaction was stopped with 50 µl of 2 M H_2SO_4 and the absorbance was measured at 450 nm using a Paradigm™ microplate reader (Beckman Coulter).

3.3 Molecular Biology

3.3.1 CRISPR/Cas9 sgRNA design and sgRNA vector cloning

CRISPR/Cas9 (clustered regularly interspaced short palindromic repeats)-mediated genome editing was used to introduce loss-of-function mutations at specific target genes in THP-1 cells. The CRISPR/Cas9 system utilizes a 20-bp single-guide RNA (sgRNA) sequence that directs the Cas9 nuclease to the target site. In the present study, the lentiviral plasmid lentiCRISPRv2 (#52961, Addgene), deposited by Feng Zhang, was used as sgRNA cloning vector (Sanjana et al. 2014). This plasmid enables the simultaneous expression of the sgRNA and Cas9 from *Streptococcus pyogenes* (SpCas9). In the target genome, the corresponding sgRNA sequence must precede a NGG protospacer adjacent motif (PAM) site to be recognized and cleaved by the SpCas9 nuclease. The online CRISPR design tool crispr.mit.edu was used to identify high-specificity sgRNAs that comply to the sequence $(N)_{20}$NGG and target a sequence located within the first exons of the gene of interest. For each gene, at least two sgRNA sequences with highest targeting score and lowest off-target hit score were chosen to be cloned in lentiCRISPRv2. A sgRNA targeting enhanced green fluorescent protein (EGFP) was used as control (Shalem et al. 2014). sgRNA sequences that were cloned into lentiCRISPRv2 are listed in section 2.6. Cloning steps to insert the sgRNA sequences into the lentiCRISPRv2 vector were performed according to the cloning protocol deposited by Feng Zhang on the Addgene website. Single strand oligonucleotides were designed as follows:

Forward oligo 5` - CACCG$(N)_{20}$ - 3`
Reverse oligo 3`- C$(N)_{20}$CAAA - 5`

For phosphorylation and annealing of the oligonucleotides, 1 µl of a 100 µM solution of each oligonucleotide was mixed with 1 x T4 ligation buffer (NEB) and 0.5 µl T4 polynucleotide kinase (NEB) in a total volume of 10 µl. The mixture was placed in a thermocycler and incubated under the following conditions:

37 °C 30 min
95 °C 5 min, then cool down to 25 °C at 5 °C/min

The annealed oligonucleotides were diluted 1:200 in sterile water. For the linearization and dephosphorylation of the lentiCRISPRv2 cloning vector the following mixture was prepared:

5 µg	lentiCRISPRv2
3 µl	FastDigest *Esp3I* (Thermo Fisher)
3 µl	Fast Antarctic phosphatase (NEB)
6 µl	FastDigest Buffer
0.6 µl	100 mM DTT

Total volume was adjusted to 60 µl with sterile water and the reaction was incubated for 30 min at 37 °C.
Annealed oligonucleotides (sgRNA inserts) and the linearized vector were ligated at room temperature for 10 min in the following reaction mixture:

50 ng	digested lentiCRISPRv2
1 µl	1:200 diluted, annealed oligonucleotides
5 µl	2 x Quick Ligase buffer (NEB)
1 µl	Quick Ligase (NEB)

Total volume was adjusted to 11 µl with sterile water.

5 µl of the ligation reaction were transformed into competent Stbl3™ bacteria as described in section 3.3.8. Transformed bacteria were plated on agar plates containing 50 µg/ml ampicillin and a selection of colonies was picked after overnight incubation at 37 °C. Colonies were grown in 4 ml LB medium containing 50 µg/ml ampicillin (table 3.9). Plasmid DNA was extracted (3.3.8) and sequenced to confirm the correct insertion of the sgRNA into the lentiCRISPRv2 vector using the hU6_for sequencing primer (section 2.4). Plasmids with proper sgRNA insertion were stored at -20 °C and used for lentiviral production and subsequent transduction of THP-1 cells (3.1.8 and 3.1.9). After transduction, puromycin was used as selection antibiotic to select for positive clones. Limited dilution of puromycin-selected cells was performed to obtain single cell clones. THP-1 cells were seeded in 96-well plates at a density of one cell per well. Cells were expanded and analysed for target gene knock-out by SDS-PAGE (3.2.3) and Western blotting (3.2.4) or qPCR (3.1.19).

3.3.2 Polymerase chain reaction (PCR)

Polymerase chain reaction (PCR) allows the amplification of a specific DNA fragment. PCR cycles consist of denaturation, annealing and elongation steps. During the denaturation and annealing phase, the DNA becomes thermally denatured and hybridizes with short oligonucleotides called primers. In the subsequent elongation phase, the DNA sequence that is flanked by the forward and reverse primer is amplified by a thermostable DNA polymerase. PCR was used to amplify the mutated *CTNNB1* gene encoding for constitutively active ß-catenin from the E(beta)P vector (Addgene #24313). For the amplification, the primers betaCat_XhoI_for and betaCat_NotI_rev (section 2.4) were used to introduce restriction sites on the 3'- and 5'- end of the DNA sequence.

PCR sample (50 µl):
1 µg template DNA
1 x Phusion GC reaction buffer (5x)
500 nM forward primer
500 nM reverse primer
200 µM dNTP mix
1 U Phusion® High-Fidelity DNA-Polymerase (2 U/ µl)
in ddH_2O

PCR program:

98 °C	30 sec	
98 °C	10 sec	
61,2 °C	20 sec	30 x
72 °C	59 sec	
72 °C	7 min	
4 °C		

3.3.3 Agarose gelelectrophoresis

For the analysis of DNA fragments they were separated according to their size on an agarose-gel matrix under the influence of an applied electrical field. The percentage of agarose (w/v) was adjusted depending on the size of the DNA fragments. Usually 1 % agarose in electrophoresis buffer (1 x TAE) was used. After boiling the agarose, an

appropriate amount of it was poured into a small glass and stirred for 2 min. For the visualization of DNA fragments 1.5 µl/ 20 ml Midori Green (Biozym) were added. The agarose was poured in a gel cassette and a comb was placed into the gel. The solid gel was then placed in a running chamber filled with 1 x TAE. Samples and a size standard (2-Log DNA Ladder, NEB) were loaded and the gel was run at 100 V for 20 – 25 min. When the run was finished, the gel was placed on an UV table to take pictures or excise fragments.

Table 3.7: Composition of the electrophoresis buffer.

10 x TAE	1 x TAE
0.8 M Tris-Base	1:10 dilution of 10 x TAE
20 mM EDTA	in $_{dd}H_2O$
1 % glacial acetic acid	
in $_{dd}H_2O$	

3.3.4 Gelelution

To purify PCR products or to isolate DNA fragments after restriction digest, the DNA was loaded onto an agarose gel and the respective band was excised after gel electrophoresis. The DNA was then extracted from the gel slice using the Qiagen Gel Extraction Kit according to the manufacturer´s protocol. The DNA was eluted in an appropriate amount of sterile MilliQ water.

3.3.5 Restriction-enzyme digest

Restriction endonucleases cut double stranded DNA within a specific recognition site generating blunt or sticky ends. Sticky ends have single stranded base overlaps, which anneal with the complementary sticky ends of a DNA fragment that has been cut with the same enzyme.
The amplified PCR fragment containing the mutated *CTNNB1* gene (3.3.2) encoding for constitutively active ß-catenin was cloned into the pLHCX vector using the XhoI and NotI restriction endonucleases (NEB) followed by ligation (3.3.6).

Digest (50 µl):
1 µg vector DNA or 20 µl PCR product
1 x NEB Buffer (10x)
100 µg/ml BSA
10 U of each restriction enzyme (XhoI/NotI)
in ddH_2O

3.3.6 Ligation

Ligation is used to integrate a DNA fragment into a vector plasmid. To create complementary ends, both, the DNA fragment and the vector, were digested with identical restriction enzymes. A molar ratio of 1:3 for the vector and insert was chosen for the sticky end ligation. The enzyme used for the ligation was the T4 DNA ligase which catalyzes the formation of a phosphodiester-bond between 5'- phosphate and the 3'-hydroxyl termini of the DNA.

Ligation sample (10 µl):
50 ng vector plasmid
x ng insert
1 x T4 DNA ligase buffer (10 x)
3 U T4 DNA ligase
in ddH_2O

The reaction was incubated overnight at 16 °C followed by heat inactivation at 65 °C for 10 minutes. The ligated construct was transformed into DH5α *E. coli* (3.3.8).

3.3.7 Preparation of chemically competent *E. coli*

For the generation of competent *E. coli* cells (DH5α and Stbl3) the Inoue method was used (Inoue *et al.* 1990). Bacteria were plated and incubated for 16 h at 37 °C. A 250 ml flask containing 25 ml SOB medium was inoculated with a freshly picked colony and incubated for 6 – 8 hours at 37 °C with shaking. 10, 4 and 2 ml of this starter culture were used to inoculate three 1 liter flasks containing 250 ml SOB medium. The cultures were incubated overnight at 18 - 22 °C with gently shaking. The first culture that reached an OD600 of 0.8 was cooled in an ice-water bath for 10 min and harvested by centrifugation at 2500 x g for 10 min at 4 °C. The remaining two cultures were discarded. The

harvested cells were resuspended in 80 ml ice-cold Inoue transformation buffer. The cell suspension was centrifuged at 2500 x g for 10 min at 4 °C and the pellet was resuspended in 20 ml ice-cold Inoue transformation buffer containing 1.5 ml DMSO. The cells were kept on ice for 10 min and aliquots were frozen in liquid nitrogen and stored at -80 °C.

Table 3.8: Composition of SOB medium and Inoue buffer.

SOB medium	Inoue buffer
2 % tryptone	55 mM $MnCl_2$
0.5 % yeast extract	15 mM $CaCl_2$
0.05 % NaCl	250 mM KCl
0.25 % KCl	10 mM PIPES (stock 0.5 M, pH 6.7)
Autoclave and store at 4 °C	Sterilize by filtration and store at -20°C

3.3.8 Bacterial transformation and plasmid purification

Plasmids were transformed into chemically competent bacteria to amplify the vector DNA. For the transformation of a ligated construct, 5 µl of the ligation reaction were transformed into selfmade chemically competent DH5α *E. coli*. For the transformation of ligated lentiCRISPRv2 constructs, selfmade competent Stbl3 *E. coli* were used. For the re-transformation of already existing constructs into DH5α, a maximum of 1 µl plasmid DNA was used. Competent bacteria were thawed on ice before the addition of the plasmid DNA. After 30 min incubation on ice, a heat shock was performed at 42 °C for 90 sec. The cells were placed on ice for 2 min and 1 ml LB medium was added. Following 1 h incubation at 37 °C with shaking, the bacteria were centrifuged at 1000 x g for 5 min. The pellet was resuspended in 100 µl LB medium and plated on agar plates containing the appropriate selection antibiotic. Colonies were picked after over-night incubation at 37 °C. For large scale plasmid DNA extraction from single colonies the Genopure Plasmid Maxi Kit (Roche) was used. For small scale DNA preparation from 4 ml bacterial culture the Wizard® Plus SV Miniprep DNA Purification System (Promega) was used. DNA extraction with both kits was performed according to the manufacturer`s protocol and DNA constructs were sequenced with the appropriate primers (StarSEQ, Mainz).

Table 3.9: Composition of LB medium and agar.

LB medium	LB-agar
1 % tryptone 0.5 % yeast extract 1 % NaCl Autoclave and store at 4 °C	1 % tryptone 0.5 % yeast extract 1 % NaCl 1.5 % agar Autoclave, pour plates and store at 4 °C

3.3.9 Microarray gene expression analysis

THP-1 cells were seeded in 6-well plates at a density of 700.000 cells in 3 ml medium per well. 24h after seeding the cells were treated for 48 h with GSK3 inhibitors. RNA was extracted from cells using the TRIzol™ Plus RNA Purification Kit (Thermo Fisher Scientific) according to the manufacturer's instructions. Microarray experiments and statistical data analysis were carried out by Dr. René Deenen at the group of Prof. Karl Köhrer (BMFZ Genomics and Transcriptomics Laboratory, University of Düsseldorf). RNA preparations were analysed for RNA integrity by using the Agilent 2100 Bioanalyzer (Agilent Technologies). All RNA samples showed high quality RNA Integrity Numbers (RIN 10). RNA was further analysed by photometric measurement using NanoDrop™ and quantified by fluorometric Qubit® RNA assays (Life Technologies). Synthesis of cDNA and subsequent biotin labeling of cRNA was performed according to the manufacturer`s instructions (3´ IVT Plus Kit; Affymetrix, Inc.). Briefly, 100 ng of total RNA were converted to cDNA, followed by *in vitro* transcription and biotin labeling of cRNA. After fragmentation the labeled cRNA was hybridized to Affymetrix PrimeView™ Human Gene Expression Microarrays for 16 h at 45 °C, stained by streptavidin/phycoerythrin conjugate and scanned as described in the manufacturers´ protocol. Data analyses on Affymetrix CEL files were carried out using the GeneSpring GX software (Vers. 12.5; Agilent Technologies). Probes within each probeset were summarized by GeneSpring`s RMA algorithm after quantile normalization of probe level signal intensities across all samples to reduce inter-array variability (Bolstad *et al.* 2003). Input data pre-processing was concluded by baseline transformation to the median of all samples. To further improve signal-to-noise ratio, a given probeset had to be expressed above background (i.e. fluorescence signal of a probeset was detected within the 20th and 100th percentiles of the raw signal distribution of a given array) in both replicates in at least one of two, or both conditions to be subsequently analysed in pairwise comparisons. Differential gene expression was statistically determined by moderated t-tests. Resulting p-values were corrected for multiple testing (Benjamini-Hochberg false discovery rate (FDR)). The

significance threshold was set to p(corr)<0.05. The Database for Annotation, Visualization, and Integrated Discovery (DAVID Bioinformatics database) was used to identify functional related categories within the group of differentially expressed genes regulated by all three inhibitors (p(corr)<0.01) (Huang da *et al.* 2009a, Huang da *et al.* 2009b). This allowed enriched genes to be clustered into biological process gene ontology (GO) terms. For the determination of enriched canonical pathways (differentially expressed genes with p<0.01 and fold change >5x) the Ingenuity Pathway Analysis (IPA) software (Qiagen) was used.

4 Results

4.1 Effects of GSK3 inhibitors on cellular uptake activity of macrophages and microglia

Glycogen synthase kinase 3 (GSK3) is a ubiquitous serine/threonine protein kinase that is expressed in two isoforms, GSK3α and GSK3ß. The isoforms share 98% sequence identity within their kinase domains and are highly expressed in the brain (Woodgett 1990, Yao *et al.* 2002). GSK3 is known to function in a wide spectrum of cellular processes including glycogen metabolism, apoptosis, transcription and microtubule stability (Hooper *et al.* 2008). Among its actions, GSK3 plays a central role in the inflammatory response of immune cells, including microglia (Beurel & Jope 2009, Yuskaitis & Jope 2009). In the present study the impact of GSK3 inhibition on the cellular uptake activity of primary mouse microglia cells, the human monocytic cell line THP-1, and of primary human macrophages was investigated. Primary mouse microglia were prepared from wild type postnatal mouse brains. THP-1 is a well-established *in vitro* model for mononuclear phagocytes. The cells were derived from an acute monocytic leukemia patient and differentiate into macrophage-like cells after treatment with phorbol myristate acetate (PMA) through activation of protein kinase C (PKC). Differentiated THP-1 cells are capable of releasing oxygen radicals and cytokines and have been extensively used in studies of phagocytosis (Tsuchiya et al. 1980, Nakamura *et al.* 1986, Friedland *et al.* 1993, Schiff *et al.* 1997, Kapetanovic *et al.* 2007). To quantify the Aß uptake capacity of cells after GSK3 inhibition, a microplate based uptake assay was established (Figure 7).

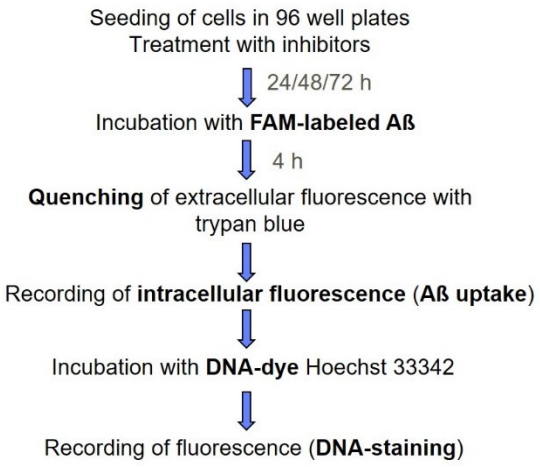

Figure 7: Flow chart of the FAM-Aß$_{42}$ uptake assay. Cells were seeded in black 96-well plates, treated with compounds and incubated with FAM-labeled Aß$_{42}$ peptides for 4 h. After quenching of the extracellular fluorescence, the intracellular fluorescence was recorded using a plate reader. To control for equal cell numbers per well, the cells were stained with the Hoechst dye 33342.

This assay is based on the uptake of 6-fluorescein amidite (FAM)-labeled synthetic Aß$_{42}$ peptides, which were pre-incubated for 3 days at 37°C to enable the formation of oligomers and aggregates (Fleisher-Berkovich *et al.* 2010, Floden & Combs 2006). Primary microglia and THP-1 cells were found to internalize FAM-Aß$_{42}$, as shown by fluorescence microscopy (Figure 8). The fluorescence images showed the spatial relation of internalized FAM-Aß$_{42}$ to the cell nucleus, indicating that FAM-Aß$_{42}$ was present in intracellular compartments and not only bound to the cell surface.

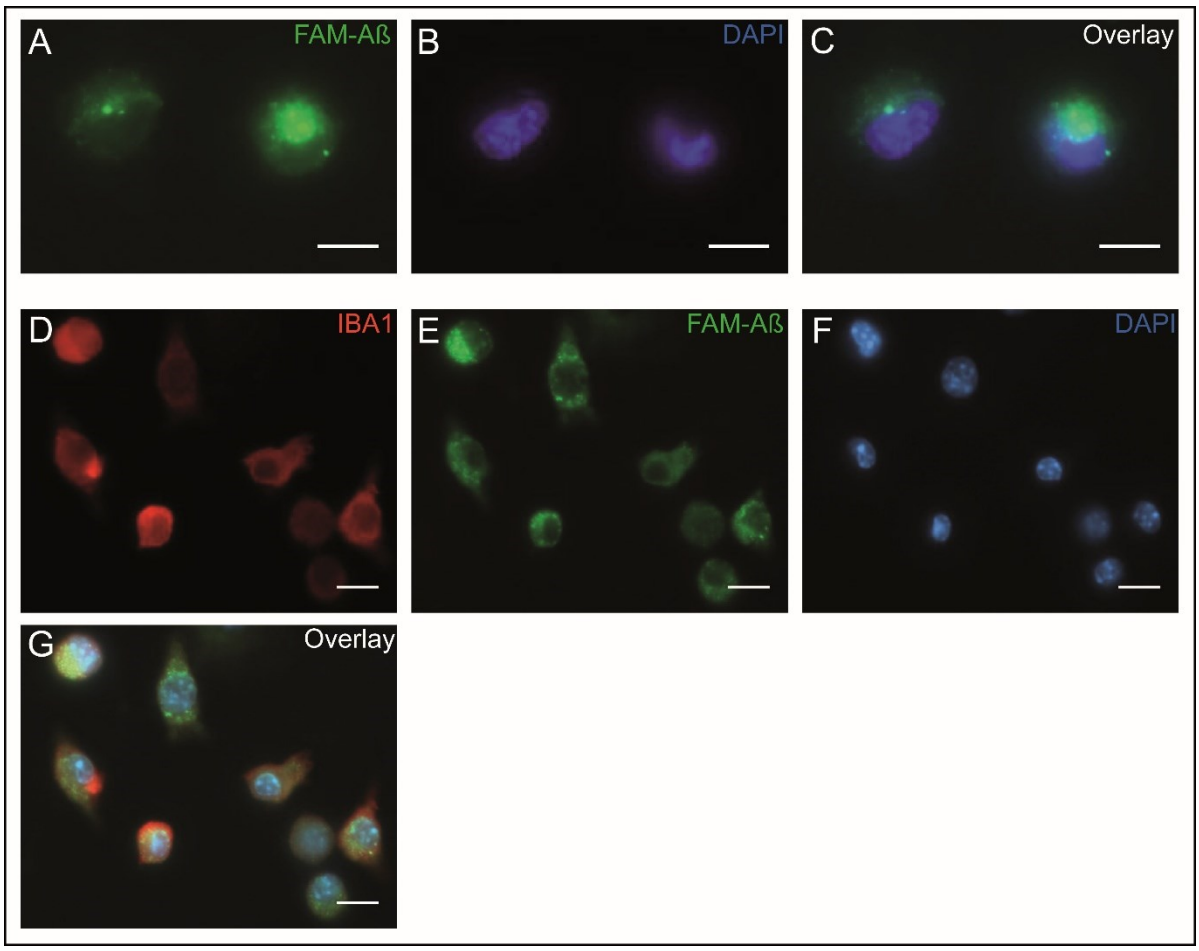

Figure 8: Uptake of FAM-Aß$_{42}$ peptides by THP-1 cells and primary mouse microglia. Cells were incubated for 1 h in the presence of 0.7 µM FAM-Aß$_{42}$. **(A-C)** Representative images of differentiated macrophage-like THP-1 cells with internalized FAM-Aß$_{42}$ peptides (green). Nuclei were stained with DAPI (blue). **(D-G)** Representative images of FAM-Aß$_{42}$ (green) uptake by primary mouse microglia. Primary cells were immunostained with the macrophage/microglia specific marker Iba-1 (red). Nuclei were stained with DAPI (blue). Scale bar 10 µm.

Three commercially available GSK3 inhibitors, CHIR99021, SB216763 and Bio-Acetoxime were used to inhibit GSK3 activity. These compounds inhibit GSK3 in an ATP-competitive manner and differ in their potency, selectivity and binding affinity. Especially the aminopyrimidine derivative CHIR99021 is a highly selective and potent inhibitor, inhibiting GSK3 at low nanomolar concentrations (IC_{50} = 6.7 nM for GSK3ß and IC_{50} = 10 nM for GSK3α) in *in vitro* kinase assays (Ring et al. 2003). Prior to the uptake

assay, the toxicity of the compounds was determined using both alamarBlue and MTT cell viability assays, to demonstrate that the cells tolerate the applied inhibitor concentrations (see subsection 4.3). Subsequently, THP-1 cells and primary microglia were incubated with non-toxic concentrations of the GSK3 inhibitors or DMSO vehicle, and the cellular uptake of FAM-Aß$_{42}$ was quantified in the uptake assay. Intracellular fluorescence was measured via a fluorescence plate reader as a readout for the cellular uptake of FAM-Aß$_{42}$. Cell nuclei were stained with the DNA-dye Hoechst 33342 to estimate cell numbers and control for equal cell plating as well as cytotoxicity.

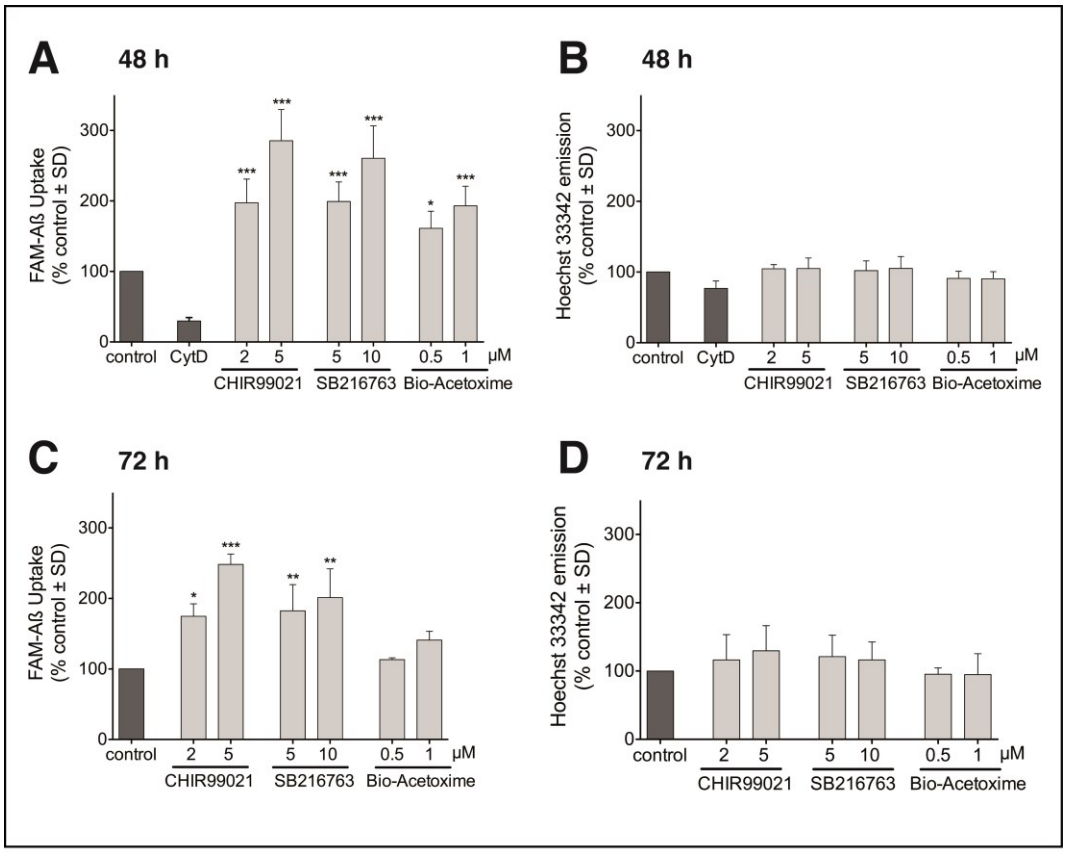

Figure 9: Inhibition of GSK3 promotes the uptake of FAM-Aß$_{42}$ by THP-1 cells. (A and C) FAM-Aß$_{42}$ uptake by THP-1 cells was quantified after 48-72 h of GSK3 inhibitor treatment. Control cells were treated with DMSO vehicle. Subsequently, cells were incubated in the presence of 0.5 µM FAM-Aß$_{42}$ for 4 h and the intracellular fluorescence was measured. Aß uptake was strongly impaired in the presence of 10 µM cytochalasin D (CytD), an inhibitor of actin polymerization. **(B and D)** Hoechst staining of cell nuclei was used to control for equal cell numbers per well. Bio-Acetoxime 72h: n=2, others: n=3-5 independent biological experiments, with 3 technical replicates for each experimental condition. Averaged values for each experimental condition were normalized to the control condition. Statistical analysis was performed by one-way ANOVA, followed by Dunnett`s multiple comparison test (* p<0.05, ** p<0.01, *** p<0.001). Error bars represent SD.

Treatment with the GSK3 inhibitors for 48-72 h resulted in a dose-dependent increase in the uptake of FAM-Aß$_{42}$ by THP-1 cells (Figure 9 A, C). FAM-Aß$_{42}$ uptake was enhanced approximately 2-3-fold after exposure to 5 µM CHIR99021 and 10 µM SB216763 as

compared to the DMSO control, whereas Bio-Acetoxime showed a weaker effect. A 48 h treatment with GSK3 inhibitors produced a greater change than the 72 h treatment. Endocytotic processes like phagocytosis and macropinocytosis are dependent on a functional actin cytoskeleton and are sensitive to cytochalasins (Araki *et al.* 1996, Aderem & Underhill 1999). Cytochalasin D, which inhibits actin polymerization, was used as a control to verify the endocytic uptake (Figure 9 A). The presence of 10 µM cytochalasin D blocked approximately 70 % of FAM-Aß$_{42}$ uptake. Nuclear staining with Hoechst 33342 indicated no significant changes in cell numbers after treatment with GSK3 inhibitors. In all follow-up experiments, Hoechst staining was solely used as an internal control to detect substantial differences in cell numbers.

Primary microglia cells treated with GSK3 inhibitors were also analyzed in the Aß uptake assay. Similar to the effects with THP-1 cells, inhibition of GSK3 in primary microglia increased the uptake of FAM-Aß$_{42}$ in a dose-dependent manner. While GSK3 inhibition in THP-1 cells resulted in the strongest increase after 48 h, treatment of primary microglia with GSK3 inhibitors showed the strongest effects after 72 h (Figure 10 A, C). CHIR99021 (5 µM) and SB261763 (10 µM) treatment of primary microglia for 72 h resulted in an approximately 2-fold increase of Aß uptake. As observed for the THP-1 cells, the effect of Bio-Acetoxime was less prominent. Internalization of Aß was reduced by around 70 % in the presence of cytochalasin D. Both primary microglia and THP-1 cells displayed the strongest effects with 5 µM CHIR99021. Taken together, these results showed that inhibition of GSK3 significantly increased the cellular uptake of Aß by primary microglia and macrophage-like THP-1 cells.

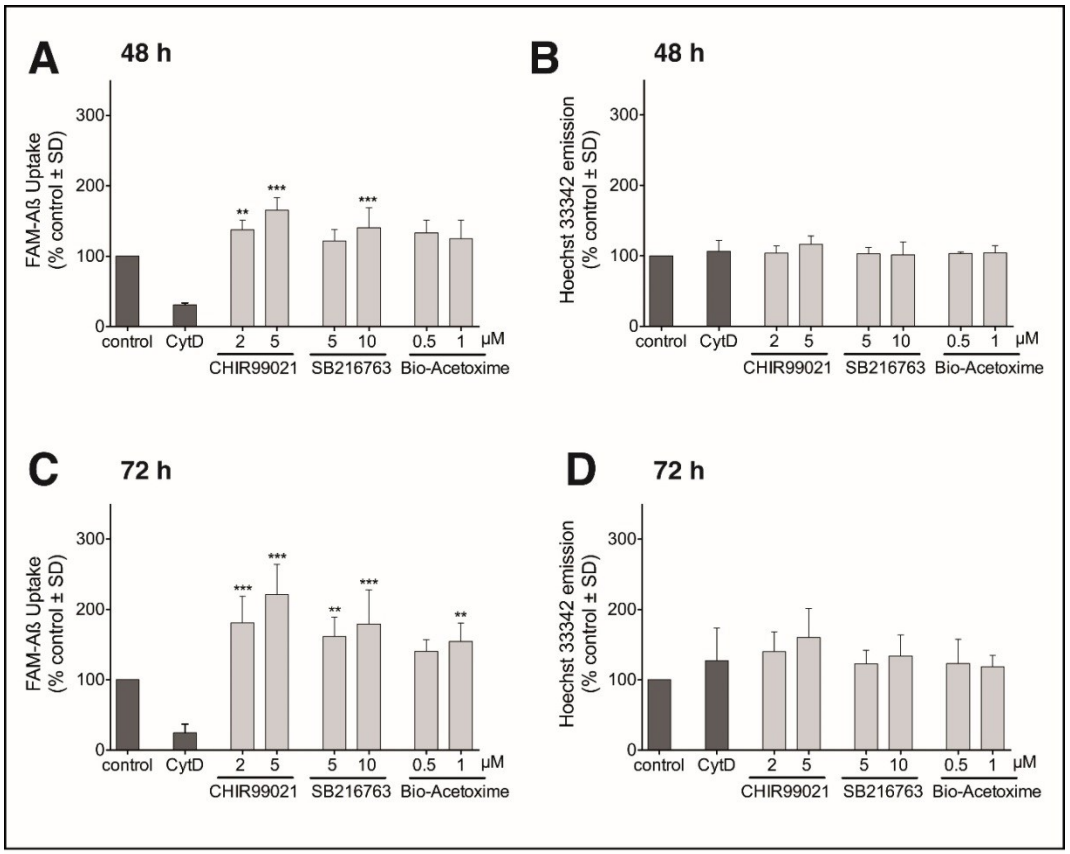

Figure 10: Inhibition of GSK3 promotes the uptake of FAM-Aß$_{42}$ by primary mouse microglia. (A and C) FAM-Aß$_{42}$ uptake by primary microglia was quantified after 48-72 h of GSK3 inhibitor treatment. Control cells were treated with DMSO vehicle. Aß uptake was impaired in the presence of 10 µM cytochalasin D (CytD), an inhibitor of actin polymerization. **(B and D)** Hoechst staining of cell nuclei was used to control for equal cell numbers per well. Bio-Acetoxime 0.5 µM: n=2-3, others: n=7-10 independent experiments, with 3 technical replicates for each experimental condition. Averaged values for each experimental condition were normalized to the control condition. Statistical analysis was performed by one-way ANOVA, followed by Dunnett`s multiple comparison test (* p<0.05, ** p<0.01, *** p<0.001). Error bars represent SD.

Next, primary human macrophages were treated with the GSK3 inhibitor CHIR99021. Human monocytes isolated from peripheral blood were plated and differentiated into macrophages in the presence of granulocyte-macrophage colony-stimulating factor (GM-CSF) and interleukin 34 (IL-34) for 14 days. The differentiation conditions were adopted from a study by Ohgidani *et al. (*Ohgidani *et al.* 2014*).* These authors reported that GM-CSF and IL-34 -treated cells showed microglial properties, such as cytokine production, expression of microglial markers, and a characteristic ramified morphology (Ohgidani et al. 2014). However, in our experiments under identical conditions, the combination of GM-CSF and IL-34 resulted in a macrophage-like amoeboid morphology, with an enlarged cell volume compared to the untreated monocytes (Figure 11 A, B). These induced primary macrophages were treated with CHIR99021 for 48 h prior to the Aß uptake assay. Exposure to 5 µM CHIR99021 resulted in an approximately 50 % increase

in Aß uptake (Figure 11 C). Again, internalization of Aß was strongly reduced in the presence of cytochalasin D, indicating an actin-dependent mechanism. While the stimulation of Aß uptake by CHIR99021 was weaker, the outcome of these experiments with human macrophages was consistent with the results obtained with THP-1 macrophages and primary mouse microglia cells.

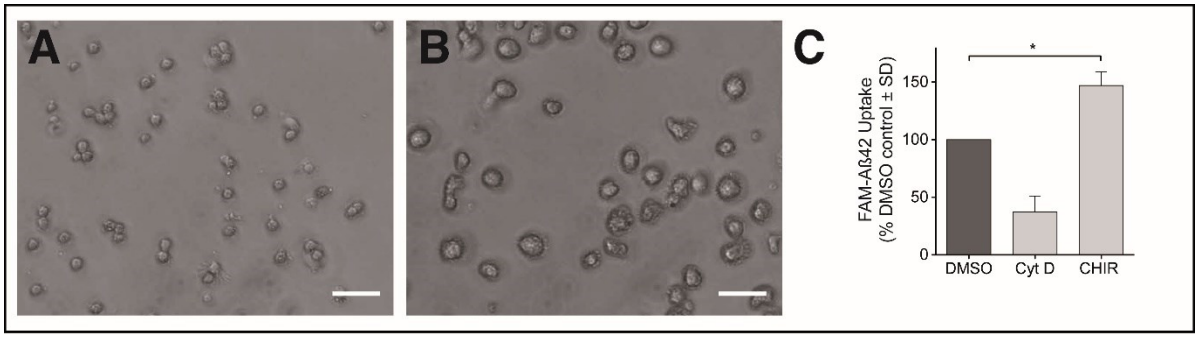

Figure 11: Inhibition of GSK3 stimulates the uptake of FAM-Aß$_{42}$ by primary human macrophages. (A) Representative light microscopy image of human monocytes 24 h after isolation. **(B)** Representative light microscopy image of induced human macrophages after 14 days of treatment with 10 ng/ml GM-CSF and 100 ng/ml IL-34. Scale bar 40 µm **(C)** Quantification of FAM-Aß$_{42}$ uptake by human macrophages after 48 h treatment with GSK3 inhibitor CHIR99021 (CHIR) (5 µM). Aß uptake was impaired in the presence of 10 µM cytochalasin D (CytD). n=2 independent biological experiments, with 3 technical replicates for each experimental condition. Averaged values for each experimental condition were normalized to the control condition. Statistical analysis was performed using two-tailed *t* test (* $p<0.05$). Error bars represent SD.

To investigate whether the increase in cellular uptake activity after treatment with GSK3 inhibitors is specific for the ligand Aß$_{42}$, the uptake assays were repeated with fluorescein-labeled *E. coli* particles instead of FAM-Aß$_{42}$. Following GSK3 inhibitor treatment, THP-1 cells or primary microglia cells were exposed to *E. coli* particles for 45 min. As decribed for the Aß uptake assay, extracellular fluorescence was quenched and the intracellular fluorescence was recorded to quantify the cellular uptake. Both THP-1 cells and primary microglia showed an increased uptake of fluorescently labeled *E. coli* particles after treatment with GSK3 inhibitors (Figure 12). The increase was approximately 2-fold at the highest concentration of CHIR99021, while SB216763 showed weaker effects. As seen with Aß, the uptake of *E. coli* particles was reduced in the presence of cytochalasin D. These results indicated that the increase in cellular uptake activity observed after treatment with GSK3 inhibitors is not specific for Aß$_{42}$. Rather, GSK3 inhibitors appeared to stimulate a cellular uptake mechanism that is used to internalize different types of molecules and particles.

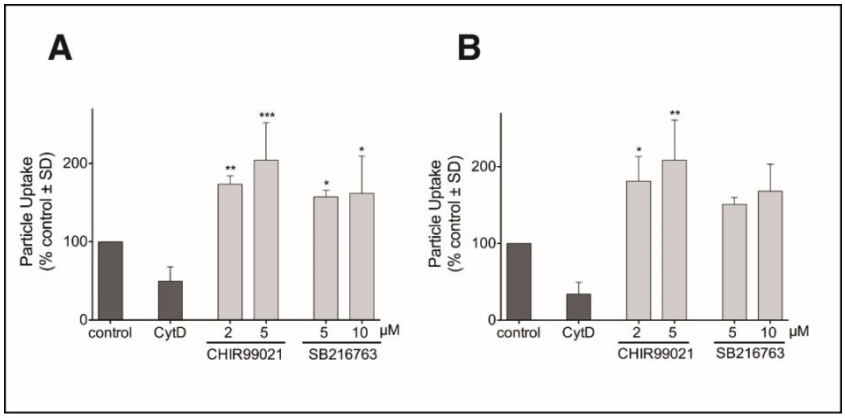

Figure 12: Inhibition of GSK3 stimulates the uptake of *E. coli* particles by THP-1 cells and primary microglia. (A) Uptake of *E. coli* particles by THP-1 cells after 48 h GSK3 inhibitor treatment. **(B)** Uptake of *E. coli* particles by primary microglia cells after 72 h GSK3 inhibitor treatment. Uptake was impaired in the presence of 10 µM cytochalasin D (CytD). n=3-5 independent biological experiments, with 3 technical replicates for each experimental condition. Averaged values for each experimental condition were normalized to the control condition. Statistical analysis was performed by one-way ANOVA, followed by Dunnett`s multiple comparison test (* p<0.05, ** p<0.01, *** p<0.001). Error bars represent SD.

4.2 Effects of GSK3 inhibitors on intracellular Aß degradation

Macrophages and microglia cells are able to internalize Aß aggregates and to degrade these peptides via the endo-lysosomal system (Sole-Domenech *et al.* 2016). The results in figures 9 and 10 showed that treatment of THP-1 macrophages and primary microglia cells with GSK3 inhibitors stimulated the cellular uptake of FAM-Aß$_{42}$. Next, we examined whether GSK3 inhibitors might also affect the rate of Aß$_{42}$ degradation within cells. THP-1 cells were treated with GSK3 inhibitors and then incubated in the presence of unlabeled, non-aggregated Aß$_{42}$. Western blotting of cell lysates with the monoclonal anti-Aß antibody IC16 showed that intracellular Aß$_{42}$ levels were increased after treatment with CHIR99021 and SB216763 compared to the DMSO control condition (Figure 13 A), supporting the findings of the uptake assays with fluorescently-labelled FAM-Aß$_{42}$. To assess the impact of GSK3 inhibitors on the degradation of internalized Aß$_{42}$, cells were treated with CHIR99021 or DMSO vehicle, incubated for 2 h with 2 µM Aß$_{42}$, and Aß$_{42}$ levels were then compared in cell lysates at 4 different time points with an Aß$_{42}$-specific ELISA assay.

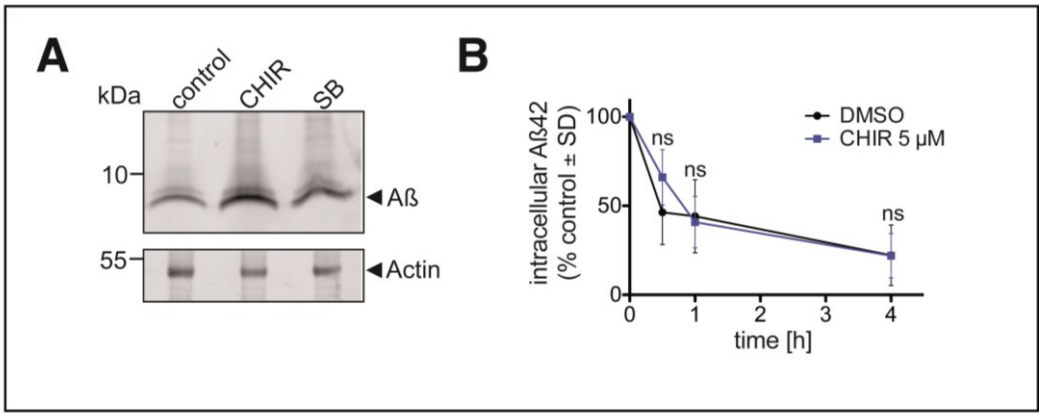

Figure 13: Treatment with GSK3 inhibitors increases the cellular uptake of Aß$_{42}$ but does not enhance Aß$_{42}$ degradation. THP-1 cells were treated with 5 µM CHIR99021 (CHIR) or 10 µM SB216763 (SB) for 48 h followed by incubation with 2 µM Aß$_{42}$ for 2 h. **(A)** Representative Western blots showing Aß levels in THP-1 cell lysates as detected with the monoclonal anti-Aß antibody IC16. n=3 independent biological experiments. **(B)** ELISA measurements of Aß$_{42}$ levels in cell lysates of CHIR99021 and DMSO-treated cells 0-4 h after incubation with 2 µM Aß$_{42}$. The amount of Aß$_{42}$ that was detected at time 0 in each experimental group was set to 100 %. n=3-6 independent biological experiments, with 3 technical replicates for each experimental condition. Statistical analysis was performed using two-tailed *t* test (* $p<0.05$). Error bars represent SD.

The results of the ELISA measurements showed a time-dependent decrease of intracellular Aß$_{42}$ levels in both CHIR99021 and DMSO treated cells (Figure 13 B). After 4 h, Aß levels in both experimental groups were reduced to approximately 25 % of the Aß$_{42}$ amount detected at time 0 h, indicating that Aß$_{42}$ was efficiently cleared in both control and GSK3 inhibitor treated cells. These findings demonstrated that GSK3 inhibitors stimulated the cellular uptake of Aß$_{42}$ but did not measurably enhance its intracellular degradation.

4.3 Effects of GSK3 inhibitors on metabolic activity and cell proliferation

GSK3 inhibition has been reported to stimulate the proliferation of specific cell types (Tseng *et al.* 2006, Cao *et al.* 2012). Increased cell numbers could potentially explain the increased Aß and *E. coli* particle uptake activity after treatment with GSK3 inhibitors. Therefore, alamarBlue and MTT assays were performed to detect cell proliferation and cell viability. In the alamarBlue assay the dye resazurin is converted to the fluorescent molecule resofurin by metabolically active cells. The MTT assay is based on the conversion of the tetrazolium dye MTT into formazan. Cellular tetrazolium reduction depends on the metabolic activity and has been linked to the activity of mitochondrial enzymes (Berridge & Tan 1993). The generation of both resofurin and formazan was quantified by absorbance measurement. For the alamarBlue assay, THP-1 cells were

treated with increasing concentrations of the GSK3 inhibitors. No cytotoxic effects of the compounds were observed for the concentration ranges and treatment periods used in this study (data not shown). For the MTT assay, THP-1 cells and primary microglia cells were treated with increasing concentrations of the GSK3 inhibitors for 48 h and 72 h, respectively. The results of the MTT assay indicated no toxic effects of the compounds on THP-1 and primary microglia cells (Figure 14). In contrast, treatment of primary microglia resulted in an increased rate of MTT conversion (Figure 14 B). This result was consistent with either increased cell numbers at the end of the treatment period or unchanged cell numbers with increased metabolic activity of individual cells. However, staining of cells with the nuclear dye Hoechst 33342 at the end of the Aß uptake assays as shown in figure 9 for THP-1 cells and figure 10 for primary microglia cells had not provided evidence for increased cell proliferation stimulated by GSK3 inhibitors.

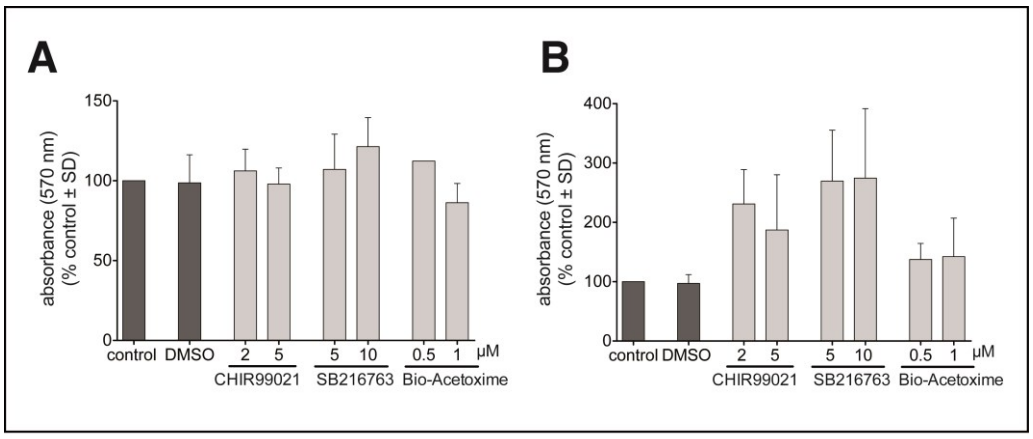

Figure 14: Treatment with GSK3 inhibitors reveals no cytotoxic effects but increases the metabolic activity of primary microglia cells. Conversion of MTT to formazan by **(A)** THP-1 cells and **(B)** primary microglia cells was quantified after GSK3 inhibitor treatment for 48 h and 72 h, respectively. Cells treated with medium only (untreated) served as control. THP-1 Bio-Acetoxime 0.5 µM: n=1, others: n=4-8 independent experiments, with 3 technical replicates for each experimental condition. Averaged values for each experimental condition were normalized to the control condition. Error bars represent SD.

To further exclude that changes in cell numbers affect the uptake activity of THP-1 and primary microglia cells, total cell numbers were determined after GSK3 inhibitor treatment with an automated Vi-Cell cell counter. Viable and non-viable cells were distinguished via the trypan blue exclusion method. In line with the results of the nuclear Hoechst 33342 staining, counting of cells revealed no changes in numbers of THP-1 and primary microglia cells treated with GSK3 inhibitors or DMSO vehicle (Figure 15). In conclusion, these results demonstrated that GSK3 inhibitors did not stimulate cellular proliferation but might increase overall metabolic activity of primary microglia cells.

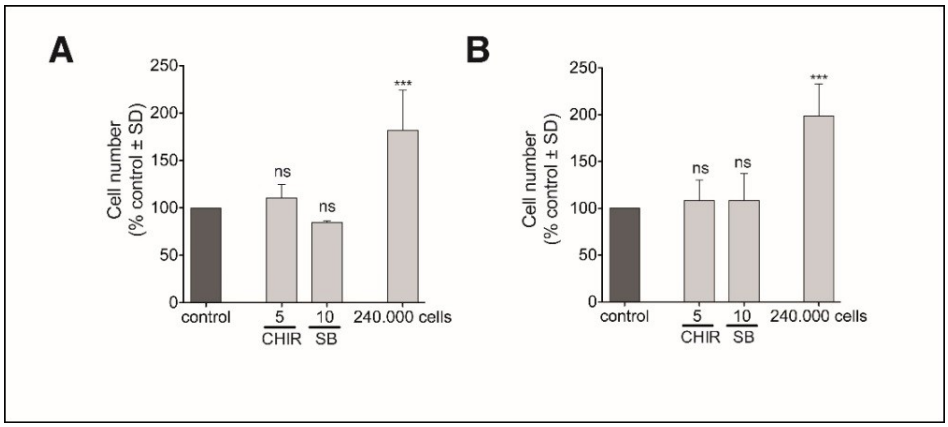

Figure 15: Inhibition of GSK3 has no impact on the proliferation of THP-1 and primary microglia cells. Cell numbers were determined after 48 h (THP-1, **A**) and 72 h (primary microglia, **B**) exposure to 5 µM CHIR99021 (CHIR) or 10 µM SB216763 (SB) with an automated Vi-Cell cell counter. As a control for appropriate cell counting, in one experimental condition twice the number of cells (240.000 cells) was plated. THP-1: n=2-5, primary microglia: n=7-9 independent biological experiments, with 3 technical replicates for each experimental condition. Averaged values for each experimental condition were normalized to the control condition. Statistical analysis was performed by one-way ANOVA, followed by Dunnett`s multiple comparison test (ns = non significant $p>0.05$, *** $p<0.001$). Error bars represent SD.

4.4 Phenotypic characterization of primary microglia cells treated with GSK3 inhibitors

Microglia can acquire a range of morphological and functional phenotypes, which have frequently been categorized into two extremes: the M1 phenotype, which is associated with cytotoxic effects, and the M2 phenotype, which is thought to be involved in neuroprotective actions (Colton & Wilcock 2010). The M2 state is related to an activation state induced by the cytokines IL-4 and IL-13. In addition, the release of anti-inflammatory and neurotrophic factors and enhanced uptake of cellular debris and misfolded proteins have been attributed to M2 microglia (Tang & Le 2016, Cherry *et al.* 2014). The morphology of microglia is very dynamic and related to their functional phenotype, ranging between a highly ramified and an amoeboid form completely lacking processes. The amoeboid form is generally considered to be “reactive”, whereas the ramified form is associated with a resting state engaged in physiological functions (Karperien et al. 2013).

As described above, treatment with GSK3 inhibitors enhanced the uptake activity of primary microglia (chapter 4.1). To investigate a potential relationship between GSK3 inhibition and the morphological and functional state of primary microglia, cell morphology was determined after 72 h treatment with GSK3 inhibitors. DMSO treated

microglia mostly exhibited an amoeboid or rod-like shape. In contrast, a large number of microglia cells treated with CHIR99021 or SB216763 displayed a ramified morphology with several long processes (Figure 16 A).

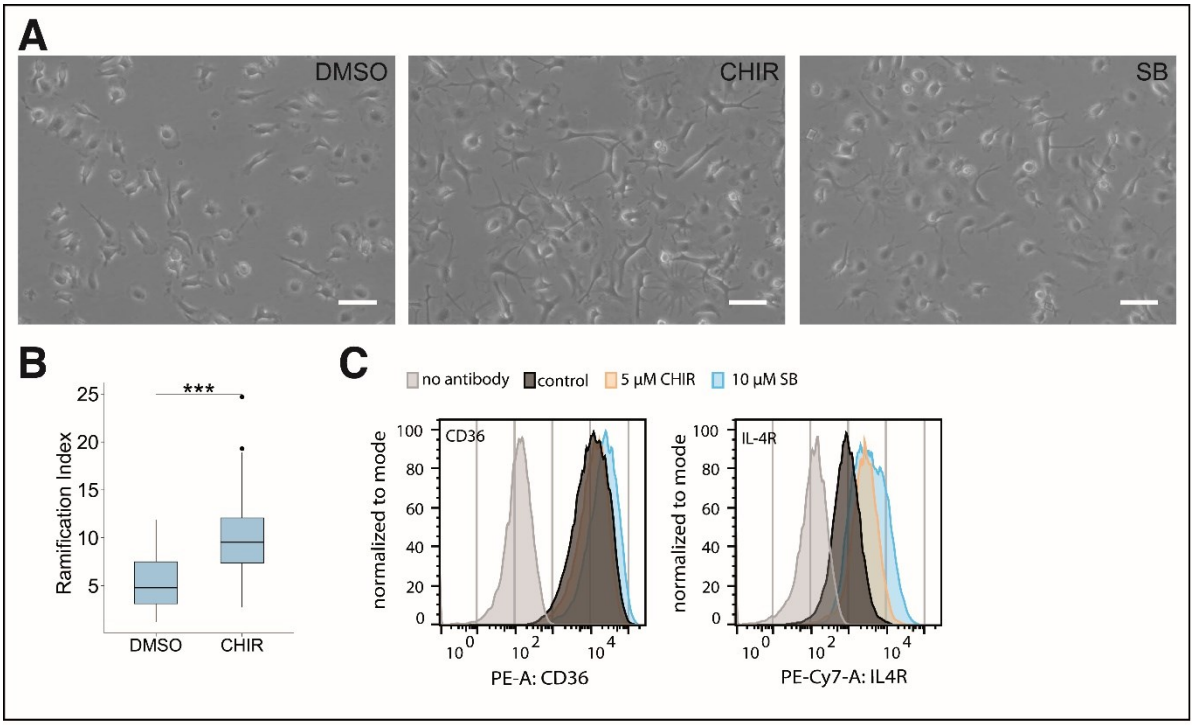

Figure 16: Morphological and functional characterization of GSK3 inhibitor treated primary microglia cells. (A) Representative microscopic picture for the morphology of primary microglia that were treated for 72h with DMSO or the GSK3 inhibitors CHIR99021 (CHIR) or SB216763 (SB). Scale bar 50 µm. **(B)** The Schoenen ramification index (RI) was calculated for microglia cells treated with DMSO or CHIR99021 (CHIR) for 72h, by dividing the maximum process number by the number of primary branches originating at the cell soma. Number of cells, DMSO=85, CHIR99021=70. n=1. Statistical analysis was performed by using two-tailed *t* test (*** $p<0.001$). Error bars represent interquartile range. **(C)** Representative flow cytometry analysis of CD36 and IL-4 receptor (IL-4R) expression levels on the surface of primary microglia after 72 h treatment with DMSO (control), CHIR99021 (CHIR) or SB216763 (SB). The number of primary microglia cells was normalized to mode (cell numbers). n=2 independent biological experiments were performed. Analysis of cell morphology and flow cytometry analysis were performed by our collaborative partner at the group of Michael Heneka (Department of Neurodegenerative Diseases and Gerontopsychiatry at the University of Bonn).

To quantify the shape changes of the cells, the ramification index (RI) of DMSO and CHIR99021 treated cells was determined by image analysis. CHIR99021 treated ramified microglia showed a significantly higher RI than DMSO treated cells, indicating enhanced branching in response to GSK3 inhibition (Figure 16 B). To further evaluate the functional phenotype of microglia, DMSO and GSK3 inhibitor treated cells were subjected to fluorescence activating cell sorting (FACS) analysis to determine the levels of the IL-4-receptor (IL4-R) and CD36, two receptors that have been linked to the M2 phenotype. Signaling of IL-4R is induced by binding of the cytokines IL-4 and IL-13 and triggers downstream anti-inflammatory actions (Gadani et al. 2012). CD36 is a scavenger

receptor that is part of the receptor complex for Aß and has been defined as an M2 alternative activation marker (Martinez et al. 2006, Yamanaka et al. 2012). FACS analysis showed that both receptors were upregulated on the surface of microglia cells treated with CHIR99021 or SB216763 in comparison to the DMSO control (Figure 16 C). These data are consistent with the hypothesis that microglia polarize towards an alternative M2 activation state upon treatment with GSK3 inhibitors, resulting in altered morphology and function and increased uptake activity.

4.5 Co-stimulation of THP-1 cells with lipopolysaccharides (LPS) and GSK3 inhibitors

In AD, microglia functions including phagocytosis and clearance of soluble and insoluble Aß peptides appear to be impaired, and it is believed that this is at least in part due to the chronic inflammatory state of the AD brain. Therefore, we wanted to investigate whether inflammatory co-stimulation would affect and potentially diminish the stimulatory effect of GSK3 inhibitors on FAM-A$ß_{42}$ uptake activity. Based on *in vitro* and *in vivo* studies, it is well established that macrophage and microglia activation can be induced by lipopolysaccharides (LPS), a component of the outer membrane of gram-negative bacteria. Upon activation by LPS, macrophages and microglia release inflammatory cytokines such as TNFα, IL-1ß and IL-6 (Sebire *et al.* 1993, Lee *et al.* 1993, Sharif *et al.* 2007, Chanput *et al.* 2010). To assess whether LPS treatment would affect Aß uptake under basal and stimulated conditions, THP-1 cells were co-incubated with CHIR99021 and LPS for 48 h and the uptake of FAM-A$ß_{42}$ was quantified (Figure 17).

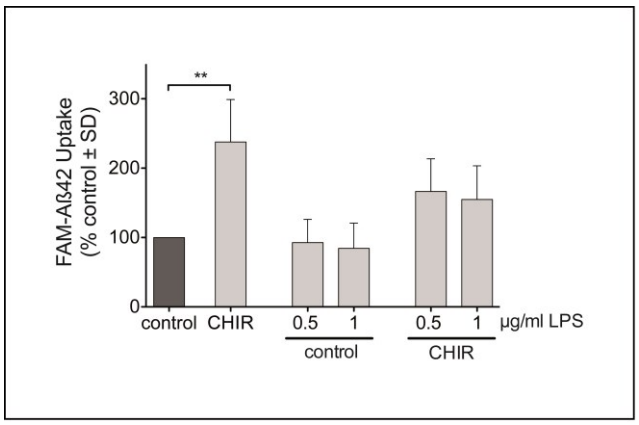

Figure 17: LPS stimulation reduced the stimulation of Aß uptake activity by GSK3 inhibitors. THP-1 cells were incubated with 5 µM CHIR99021 (CHIR) or DMSO vehicle (control) either in the presence or absence of 0.5-1 µg/ml LPS. FAM-A$ß_{42}$ uptake was quantified at the end of the 48 h treatment period. n=3 independent biological experiments, with 3 technical replicates for each experimental condition. Averaged values for each experimental condition were normalized to the control condition (cells treated only with DMSO). Statistical analysis was performed by using one-way ANOVA with Tukey`s post test (ns = non significant $p>0.05$, $^{**}p<0.01$). Error bars represent SD.

LPS stimulation did not affect the basal Aß uptake activity as compared to control cells treated only with DMSO vehicle. After simultaneous exposure to LPS and CHIR99021, THP-1 cells still showed a tendency to increase their Aß uptake activity (Figure 17). However, the effect was not significant. The results indicated that the stimulatory effect of GSK3 inhibitors is reduced but might still be effective even under inflammatory conditions as induced by LPS.

4.6 Effects of cyclin-dependent kinase (CDK) inhibitors on Aß uptake activity

As a first to step to investigate the molecular mechanism by which GSK3 inhibitors might stimulate the cellular uptake of Aß we attempted to exclude known off-target activities of this group of kinase inhibitors. Many ATP-competitive GSK3 inhibitors show promiscuous inhibitory activity towards other protein kinases (Meijer *et al.* 2004). Especially cyclin-dependent protein kinases (CDKs) are known off-targets of GSK3 inhibitors. This results from the structural similarity within the ATP-binding domain of GSK3 and CDKs (Eldar-Finkelman & Martinez 2011). To exclude that the stimulatory effects of GSK3 inhibitors on Aß uptake activity might be mediated by inhibition of CDKs, THP-1 cells were treated with Roscovitine and Purvalanol A, two compounds that inhibit multiple CDKs but do not target GSK3 (Bain *et al.* 2003). The toxicity of the compounds was assessed using the alamarBlue cell viability assay (data not shown). Subsequently, THP-1 cells were treated for 48 h with non-toxic concentrations of the CDK inhibitors followed by an Aß uptake assay. CDK inhibitor treatment had no effect on Aß uptake by THP-1 cells, indicating that CDKs are not involved in the modulation of uptake activity (Figure 18).

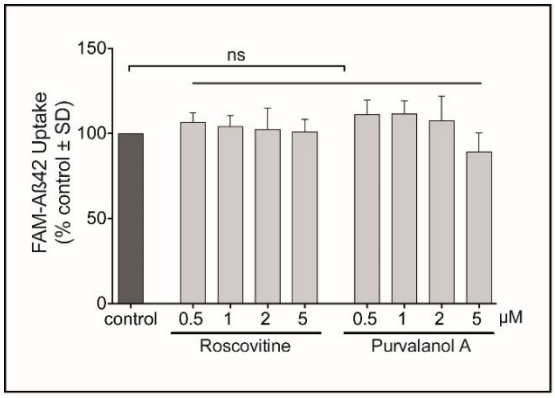

Figure 18: Inhibition of CDKs has no effect on Aß uptake by THP-1 cells. FAM-$Aß_{42}$ uptake by THP-1 cells was quantified after 48 h treatment with Roscovitine or Purvalanol A. n=3-4 independent biological experiments, with 3 technical replicates for each experimental condition. Averaged values for each experimental condition were normalized to the control condition. Statistical analysis was performed by one-way ANOVA, followed by Dunnett`s multiple comparison test (ns = non significant p>0.05). Error bars represent SD.

4.7 Role of GSK3ß in the stimulation of Aß uptake activity by GSK3 inhibitors

To further exclude off-target drug effects and to confirm that the stimulatory effect of GSK3 inhibitors on Aß uptake activity is mediated by their primary targets GSK3α/ß, endogenous GSK3 expression was knocked-down in RNAi experiments. THP-1 cells were transfected with siRNAs specific for GSK3α/ß. In addition, endoribonuclease-prepared siRNA (esiRNA) directed against GSK3ß was used. While siRNAs are chemically synthesized oligonucleotides, esiRNAs are prepared *in vitro* through endonucleolytic cleavage of target specific long double-stranded RNAs by RNase III. The cleavage results in a diverse pool of siRNA-like oligonucleotides. Both siRNA and esiRNA can trigger potent silencing of target-genes. However, esiRNAs have been proposed to cause less off-target effects (Kittler *et al.* 2007). Western blotting analysis showed that 72 h after GSK3α/ß siRNA or esiRNA transfection, protein levels of both GSK3α and GSK3ß were decreased to approximately 50 % as compared to control cells transfected with a non-targeting siRNA (Figure 19 A, B). Importantly, when the Aß uptake assay was performed after the knock-down of GSK3ß by siRNA or esiRNA, a small but significant increase of uptake activity was observed (Figure 19 C). In contrast, knock-down of GSK3α alone had no significant impact on Aß uptake activity. Likewise, the combined knock-down of both isoforms did not increase the effect size as compared to the single GSK3ß knock-down (Figure 19 C). These results supported that the stimulation of Aß uptake activity by GSK3 inhibitors is mediated by reduced activity of GSK3ß. Furthermore, they indicated that GSK3α is not involved in the modulation of uptake activity, at least in THP-1 cells.

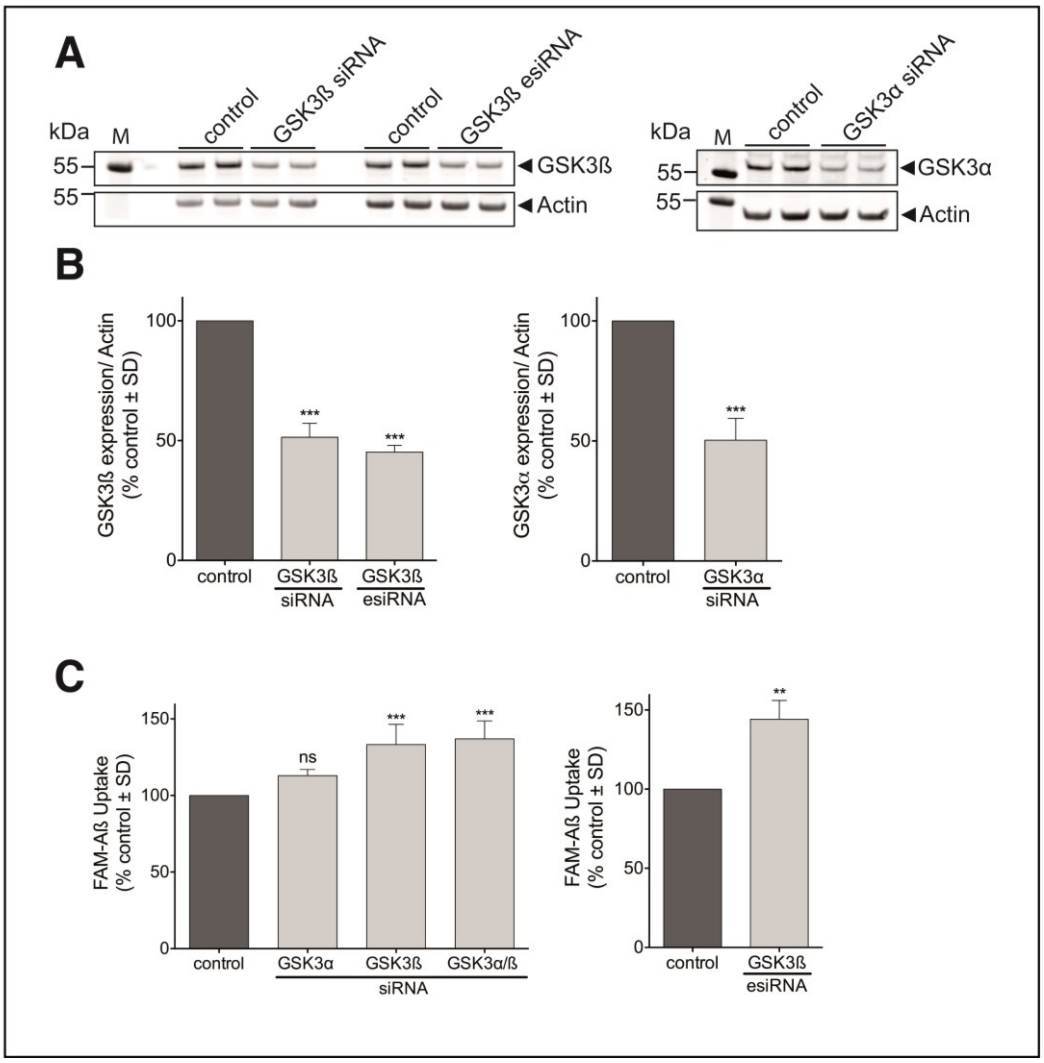

Figure 19: Knock-down of endogenous GSK3ß increased Aß uptake by THP-1 cells. THP-1 cells were transfected with either siRNA or esiRNA targeting GSK3ß, GSK3α or with a non-targeting control siRNA. **(A)** Representative Western blot analysis showing the expression of GSK3ß and GSK3α in THP-1 cell lysates 72 h post-transfection. **(B)** For semiquantitative analysis of protein levels, the signal intensity of Western blotting bands was measured with a LI-COR Odyssey CLx Imager system. n=3 independent biological experiments, with 2 technical replicates for each experimental condition. **(C)** FAM-A$ß_{42}$ uptake by THP-1 cells was quantified 72 h after single siRNA/esiRNA or combined siRNA (GSK3α/ß) transfections. n=3-5 independent biological experiments, with 3 technical replicates for each experimental condition. Averaged values for each experimental condition were normalized to the control condition. Statistical analysis was performed by either two-tailed *t* test or one-way ANOVA, followed by Dunnett`s multiple comparison test (ns = non significant $p>0.05$, ** $p<0.01$, *** $p<0.001$). Error bars represent SD.

The stimulatory effects of the GSK3ß knock-down on Aß uptake activity were much smaller compared to treatment with GSK3 inhibitors. This could be explained by the fact that the expression of GSK3 was only partially reduced after siRNA/esiRNA transfection with substantial residual enzyme activity remaining. Therefore, we wanted to obtain additional evidence to support the mechanistic role GSK3ß through the use of knock-out (KO) cell lines generated with the Clustered Regularly Interspaced Short Palindromic

Repeats/Cas9 (CRISPR/Cas9) system. The CRISPR/Cas9 system has emerged in recent years as a highly efficient tool to edit the cellular genome (Mali *et al.* 2013, Cong *et al.* 2013). It is is derived from a bacterial defence system (Jinek *et al.* 2012) and requires the co-expression of two components: the endonuclease Cas9 and a 20 bp single guide RNA (sgRNA) that is complementary to the genomic target. The most commonly used Cas9 endonuclease is from *Streptococcus pyogenes* (SpCas9). The sgRNA sequence allows for gene-specific targeting and needs to be positioned next to a protospacer adjacent motif (PAM). In *S. pyogenes*, the target DNA must immediately precede the PAM sequence "NGG," where N can be any nucleotide. The sgRNA forms a complex with Cas9 and directs it to the target DNA site, where Cas9 generates a double strand break (DSB) near the PAM. The DSB can be repaired by either of the two major cellular repair mechanisms: non-homologous end joining (NHEJ) or homology-directed repair (HDR). NHEJ repair is the most active but error-prone repair pathway, which often causes the introduction of insertion/deletion mutations within the target gene. Resulting frameshift mutations can lead to a premature stop codon in the open reading frame, generating a knock-out (KO) of the target gene. Throughout this study, the CRISPR/Cas9 technology was repeatedly used to validate candidate genes putatively involved in the modulation of Aß uptake activity. First, CRISPR/Cas9 was applied to generate THP-1 cells deficient for GSK3ß. The lentiviral vector lentiCRISPRv2 was used, which is a single-vector system for co-expression of Cas9 and sgRNA (Sanjana et al. 2014). The cloning vector is described in figure 20 A. Two individual sgRNAs were designed targeting different exons of the GSK3ß gene. As a non-targeting control, a sgRNA specific for EGFP was used. After cloning of sgRNAs into lentiCRISPRv2 and production of lentiviral particles, THP-1 cells were infected and subjected to puromycin selection. Limited dilution cloning of puromycin-selected cells was performed to obtain single cell clones. Individual cell clones were isolated and expanded prior to a western blot analysis. It is important to mention here that since THP-1 cells are growing in solution the isolation of true single cell clones is technically challenging, meaning that in some cases the isolated cell populations were likely heterogenous and derived from more than one cell. However, as shown by Western blotting in figure 20 B, for GSK3ß KO cell clones could be identified for both sgRNAs targeting exon 1 (Ex1) and exon 4 (Ex4) that completely lacked GSK3ß expression as compared to the control cell line expressing the sgRNA against EGFP. Subsequently, the KO cell lines were evaluated in the Aß uptake assay. KO and control cells were treated for 48 h with DMSO or 5 µM CHIR99021 and FAM-A$ß_{42}$ uptake was measured.

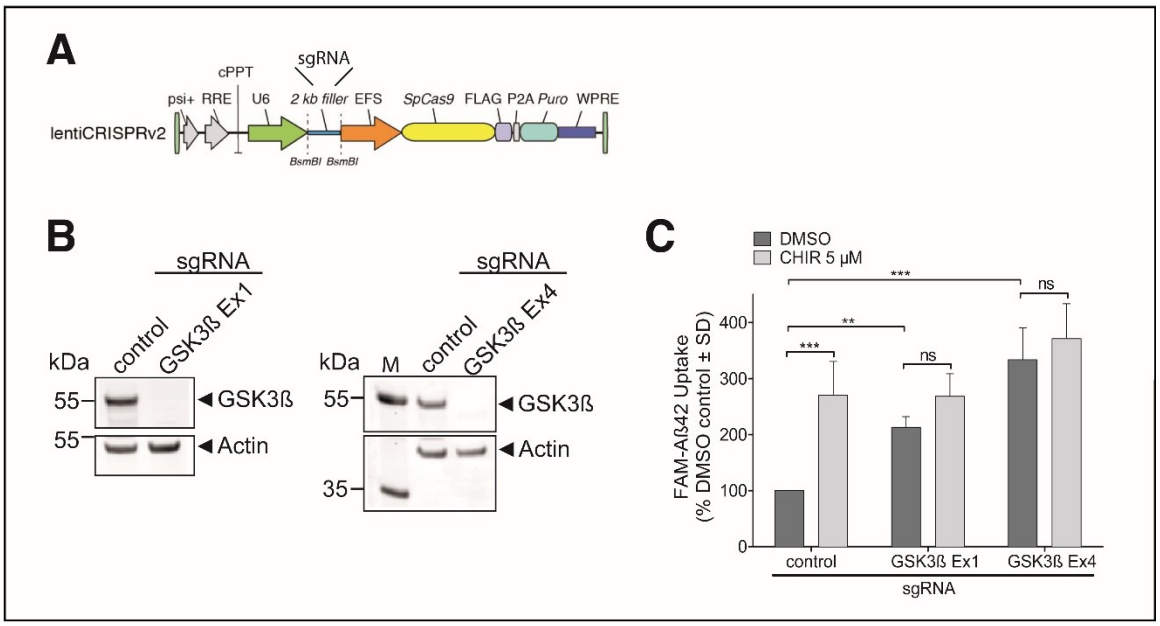

Figure 20: CRISPR/Cas9 mediated knock-out (KO) of GSK3ß increases the basal Aß uptake activity of THP-1 cells and abolishes the stimulatory effect of GSK3 inhibitors. (A) Schematic of the CRISPR/Cas9 lentiviral cloning vector containing a U6 promoter-driven sgRNA expression cassette, elongation factor-1α short (EFS) promoter-driven *SpCas9* with FLAG tag, Psi packaging signal (psi+), rev response element (RRE), central polypurine tract (cPPT), 2A self-cleaving peptide (P2A), puromycin selection marker (puro) and posttranscriptional regulatory element (WPRE) (Sanjana et al. 2014). **(B)** Representative Western blot analysis of endogenous GSK3ß protein levels in CRISPR/Cas9 generated THP-1 cells expressing a sgRNA against EGFP (control) or a target sequence in exons 1 or 4 of GSK3ß (GSK3ß Ex1, GSK3ß Ex4). Actin protein levels were used as a loading control. n=3 independent biological experiments. **(C)** Quantification of FAM-Aß$_{42}$ uptake by GSK3ß KO cells (GSK3ß Ex1 and Ex4) and control cells expressing EGFP sgRNA (control). Prior to the uptake assay the cells were treated for 48 h with 5 µM CHIR99021 or DMSO vehicle. n=3 independent biological experiments, with 3 technical replicates for each experimental condition. Averaged values for each experimental condition were normalized to the control condition (cells expressing sgRNA against EGFP treated with DMSO). Statistical analysis was performed by using one-way ANOVA with Tukey`s post test (ns = non significant p>0.05, ** p<0.01, *** p<0.001). Error bars represent SD.

In line with the RNAi experiments shown in figure 19, GSK3ß KO increased the basal level of Aß uptake (Figure 20 C, compare the two DMSO treated GSK3ß KO cell lines with the DMSO treated control line). However, the effect sizes were substantially larger and the KO cell lines generated with either of the two GSK3ß sgRNAs showed a 2-3 fold higher Aß uptake compared to the control cell line, likely because of the complete elimination of GSK3ß expression. Moreover, after treatment of the KO cell lines with the GSK3 inhibitor CHIR99021 the uptake of Aß was not significantly increased as compared to the DMSO control condition. In contrast, the control cell line expressing the sgRNA against EGFP displayed a > 2 fold increase in Aß uptake activity after treatment with 5 µM CHIR99021, similar to the effects shown in figure 9. Taken together, the results of the RNAi experiments and the CRISPR/Cas9 generated KO cell lines confirmed that GSK3ß activity is limiting the basal Aß uptake capacity of THP-1 cells, and that the stimulatory

effect of GSK3 inhibitors is due to inhibition of their main target GSK3ß with likely negligible contribution from off-targets.

4.8 Role of the Wnt/ß-catenin pathway in the stimulation of Aß uptake activity by GSK3 inhibitors

As GSK3 is a central kinase in the ß-catenin dependent canonical Wnt pathway, the role of this pathway in the stimulation of Aß uptake was investigated. The Wnt/ß-catenin pathway plays an important role in a wide range of developmental and physiological processes including cell proliferation, cell polarity and cell fate determination (Logan & Nusse 2004). In this pathway, GSK3 acts as a negative regulator. In the absence of a Wnt ligand, GSK3 mediates the phosphorylation of ß-catenin, which leads to the proteasomal degradation of ß-catenin. Upon Wnt stimulation, phosphorylation of ß-catenin by GSK3 is inhibited. This allows cytoplasmic accumulation of ß-catenin and its translocation into the nucleus, where ß-catenin serves as a transcriptional co-activator and interacts with TCF/LEF (T-cell factor/lymphoid enhancing factor) transcription factors to induce the transcription of target genes (Figure 21).

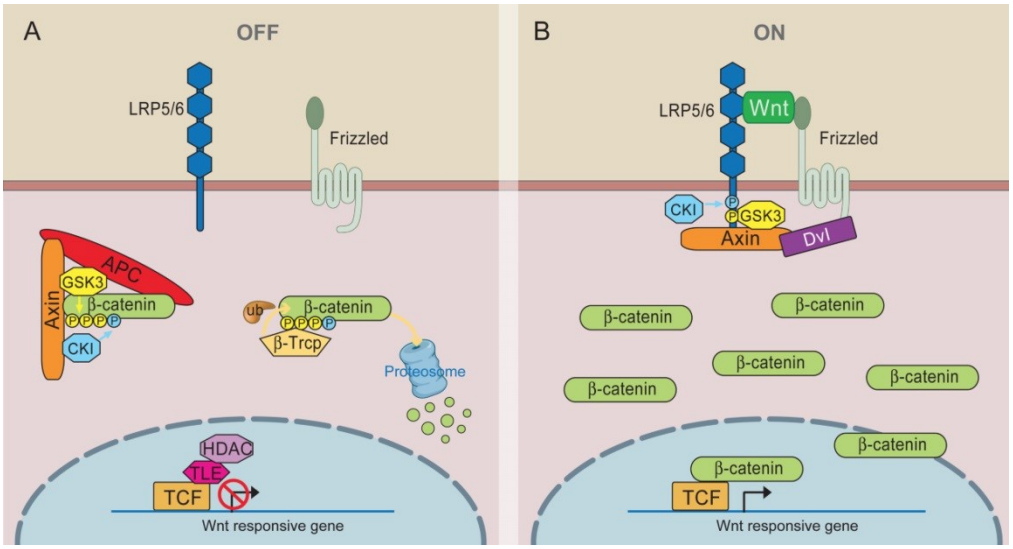

Figure 21: Simplified overview of the canonical Wnt/ß-catenin signaling pathway. (A) In the absence of a Wnt ligand, ß-catenin is associated with a multi-protein complex (destruction complex) consisting of Axin (axis inhibition protein), APC (adenomatous polyposis coli protein) and the kinases CK1 (casein kinase 1) and GSK3. In this complex, ß-catenin is sequentially phosphorylated by CK1 and GSK3, which leads to the ubiquitin-dependent degradation of ß-catenin by the proteasome. **(B)** Binding of a Wnt ligand to a Frizzled receptor and its co-receptors (LRP5/6) leads to the inactivation of the destruction complex and inhibition of ß-catenin phosphorylation. ß-catenin accumulates in the cytoplasm and translocates into the nucleus where it activates transcription of Wnt target genes (MacDonald *et al.* 2009).

Similarly, inhibition of GSK3 by GSK3 inhibitors enables ß-catenin accumulation and the activation of transcription. To confirm the accumulation of ß-catenin in THP-1 cells, the cells were treated with GSK3 inhibitors or a Wnt ligand, and ß-catenin protein levels were determined by Western blotting. Wnt-3a was chosen as a representative Wnt ligand that was shown to activate canonical β-catenin signaling (van Amerongen & Nusse 2009, Oderup *et al.* 2013). Both GSK3 inhibitor and Wnt-3a treatment resulted in a strong accumulation of ß-catenin in THP-1 cells (Figure 22 A, D). To assess putative effects of ß-catenin accumulation and downstream ß-catenin-mediated transcription on cellular Aß uptake, an activated form of mouse ß-catenin was stably overexpressed by infecting THP-1 cells with a ß-catenin-expressing retrovirus and selection of stable mass cultures (Figure 22 B).

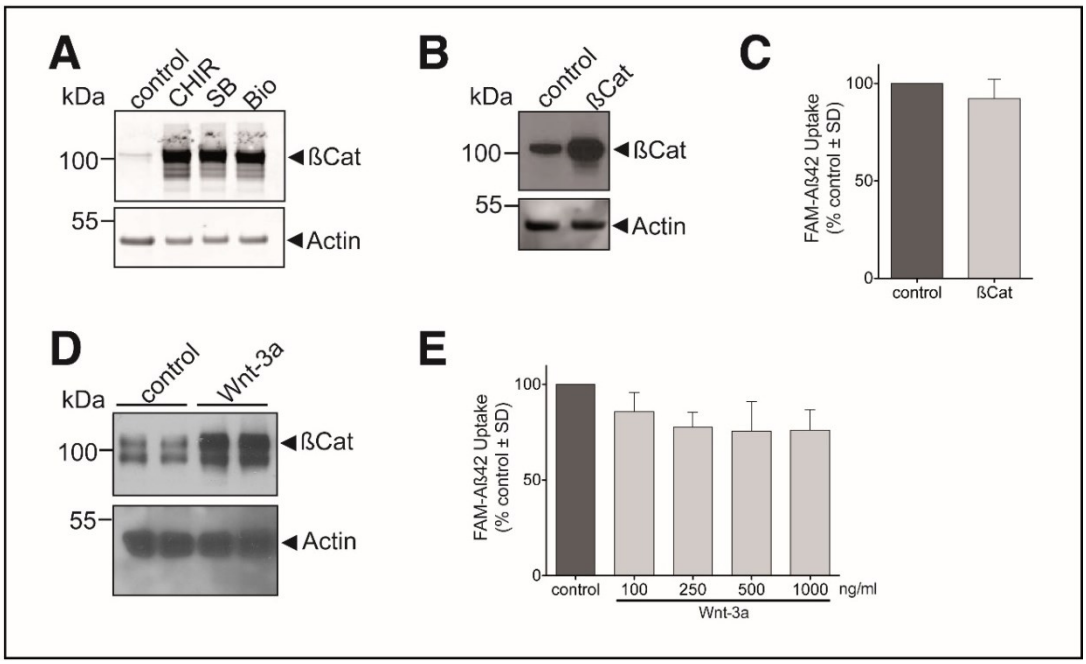

Figure 22: Increased ß-catenin protein levels did not affect Aß uptake by THP-1 cells. (A) Representative Western blot analysis of ß-catenin protein levels in THP-1 cells after 48 h treatment with GSK3 inhibitors CHIR99021 (CHIR), SB216763 (SB), Bio-Acetoxime (Bio) or DMSO vehicle (control). Actin protein levels were determined as a loading control. n=2-3 independent biological experiments. **(B)** Representative Western blot analysis of ß-catenin protein levels in THP-1 cells infected with the retroviral vector pLHCX-ß-catenin (ßCat) or empty control vector. Stable mass cultures were selected with hygromycin. Actin protein levels were determined as a loading control. n=3 independent biological experiments. **(C)** Quantification of FAM-A$ß_{42}$ uptake by THP-1 cells with stable overexpression of an activated form of ß-catenin (ßCat) and control cells with endogenous ß-catenin expression levels (control). n=4 independent biological experiments, with 3 technical replicates for each experimental condition. **(D)** Representative Western blot analysis of ß-catenin protein levels in THP-1 cells after 24 h treatment with 250 ng/ml human Wnt-3a. n=3 independent biological experiments. **(E)** Quantification of FAM-A$ß_{42}$ uptake by THP-1 cells treated for 72 h with increasing concentrations of the human Wnt-3a ligand. n=3 independent biological experiments, with 3 technical replicates for each experimental condition. Error bars represent SD.

Stable overexpression of an activated form of ß-catenin in THP-1 cells showed no effect on FAM-Aß$_{42}$ uptake as compared to the control cell line (Figure 22 C). Next, THP-1 cells were treated with increasing concentrations of Wnt-3a and FAM-Aß$_{42}$ uptake was quantified. Again, no effect on Aß uptake was observed (Figure 22 E). In addition, ß-catenin KO cells were generated using CRISPR/Cas9. A sgRNA targeting exon 2 (Ex2) of ß-catenin was cloned into lentiCRISPRv2 and lentiviral particles were produced. Subsequently, THP-1 cells were infected, subjected to puromycin selection, and single cell clones were obtained by limited dilution cloning. As shown in figure 23 A, Western blotting confirmed the complete absence of ß-catenin expression as compared to control cells expressing a sgRNA against EGFP. In contrast to the result with GSK3ß KO cells shown in figure 20, cells lacking ß-catenin expression displayed similar basal FAM-Aß$_{42}$ uptake as the control cells. Furthermore, after treatment with the GSK3 inhibitor CHIR99021 both ß-catenin KO cells and control cells showed a significant increase in FAM-Aß$_{42}$ uptake activity compared to the DMSO vehicle treated cells. Taken together, these results indicated that the stimulation of Aß uptake by GSK3 inhibitors was not mediated by enhanced Wnt/ß-catenin signalling and transcription of ß-catenin target genes.

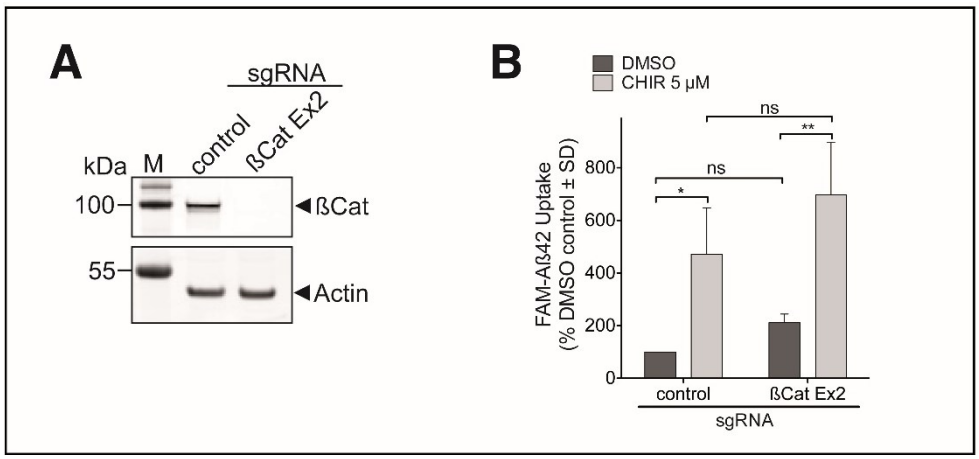

Figure 23: CRISPR/Cas9 mediated knock-out (KO) of ß-catenin did not affect basal or GSK3 inhibitor stimulated Aß uptake activity. (A) Representative Western blot analysis of endogenous ß-catenin protein levels in CRISPR/Cas9 generated THP-1 cells expressing a sgRNA against EGFP (control) or a target sequence in exon 2 of ß-catenin (ßCat Ex2). Actin protein levels were determined as a loading control. n=3 independent biological experiments. **(B)** Quantification of FAM-Aß$_{42}$ uptake by ß-catenin KO cells (ßCat Ex2) in comparison to control cells expressing EGFP sgRNA (control). Prior to the uptake assay the cells were treated for 48 h with 5 µM CHIR99021 or DMSO vehicle. n=3 independent biological experiments, with 3 technical replicates for each experimental condition. Averaged values for each experimental condition were normalized to the control condition (cells expressing sgRNA against EGFP treated with DMSO). Statistical analysis was performed by using one-way ANOVA with Tukey`s post test (ns = non significant p>0.05, *p<0.05, ** p<0.01). Error bars represent SD.

4.9 Role of *de novo* transcription in the stimulation of Aß uptake activity by GSK3 inhibitors

The observation that the effects of GSK3 inhibitors on Aß uptake activity were time-dependent and that, at least for primary microglia cells, the effects sizes increased with longer treatment periods (figures 9 and 10) indicated that the stimulatory effect might require transcription and the synthesis of novel proteins. Furthermore, GSK3 is know to regulate immune responses and transcriptional activity through the phosphorylation of several classes of transcription factors and co-activators/repressors including NF-κB (nuclear factor kappa-light-chain-enhancer of activated B-cells), CREB (cAMP response element-binding protein), NFAT (nuclear factor of activated T-cells), STATs (signal transducer and activator of transcription) and SMADs (Beurel *et al.* 2010). Therefore, to determine whether the stimulation of $Aß_{42}$ uptake activity after treatment with GSK3 inhibitors was dependent on *de novo* synthesis of mRNA, THP-1 cells were stimulated with the GSK3 inhibitor CHIR99021 in the presence of the transcriptional inhibitor actinomycin D followed by an FAM-$Aß_{42}$ uptake assay. Actinomycin D intercalates into the DNA and prevents RNA polymerase progression (Trask & Muller 1988). In preliminary experiments, a non-toxic concentration of actinomycin D was determined by an alamarBlue assay and it was found that THP-1 cells could tolerate a concentration of 0.05 µg/ml actinomycin D for a short period of time (7.5 h) without measurable toxicity (data not shown). Treatment of THP-1 cells with 5 µM CHIR99021 for only 7.5 h caused a smaller but significant increase in FAM-$Aß_{42}$ uptake (figure 24, compare to the 48 h treatment in figure 9). However, coincubation with actinomycin D abolished the increasing effect of CHIR99021 on Aß uptake, indicating that *de novo* mRNA synthesis was indeed required for the stimulation (figure 24). In contrast, actinomycin D did not affect the basal level of FAM-$Aß_{42}$ uptake.

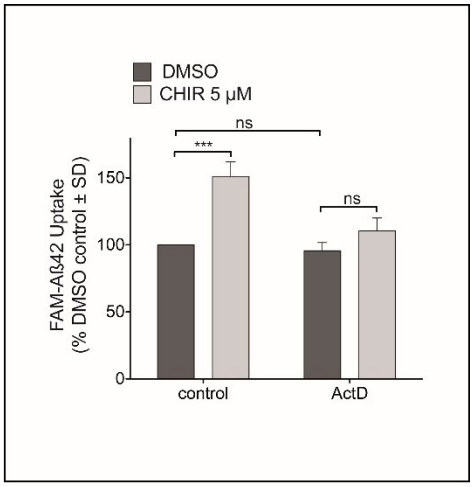

Figure 24: The stimulation of FAM-$Aß_{42}$ uptake by the GSK3 inhibitor CHIR99021 is abolished by coincubation with a transcriptional inhibitor. The Aß uptake by THP-1 cells was quantified after treatment with 5 µM CHIR99021 or DMSO vehicle in the presence or absence of 0.05 µg/ml actinomycin D (ActD) for 7.5 h. While actinomycin D blocked the stimulatory effect of CHIR99021 it did not affect basal levels of Aß uptake activity. n=3 independent biological experiments, with 3 technical replicates for each experimental condition. Averaged values for each experimental condition were normalized to the control condition (cells treated only with DMSO). Statistical analysis was performed by one-way ANOVA with Tukey`s post test (ns = non significant $p>0.05$, *** $p<0.001$). Error bars represent SD.

4.10 Microarray-based gene expression analysis

The results with the transcriptional inhibitor actinomycin D had indicated that *de novo* gene expression was required for the stimulation of Aß uptake activity by GSK3 inhibitors. Therefore, to further address the underlying mechanism and to identify differentially expressed genes, a DNA microarray-based gene expression analysis of GSK3 inhibitor treated THP-1 cells was performed. RNA was isolated from THP-1 cells treated with CHIR99021, SB216763, Bio-Acetoxime or DMSO vehicle as a control. All RNA samples were of high quality with a RNA Integrity Number (RIN) of 10. RIN is an algorithm used by the Agilent 2100 Bioanalyzer and allows for standardized determination of RNA quality with values ranging from 1 (totally degraded RNA) to 10 (completely intact RNA). RNA from GSK3 inhibitor treated and control cells was subjected to analysis using Affymetrix PrimeView Human Gene Expression microarrays, and the resulting gene expression profiles were compared.

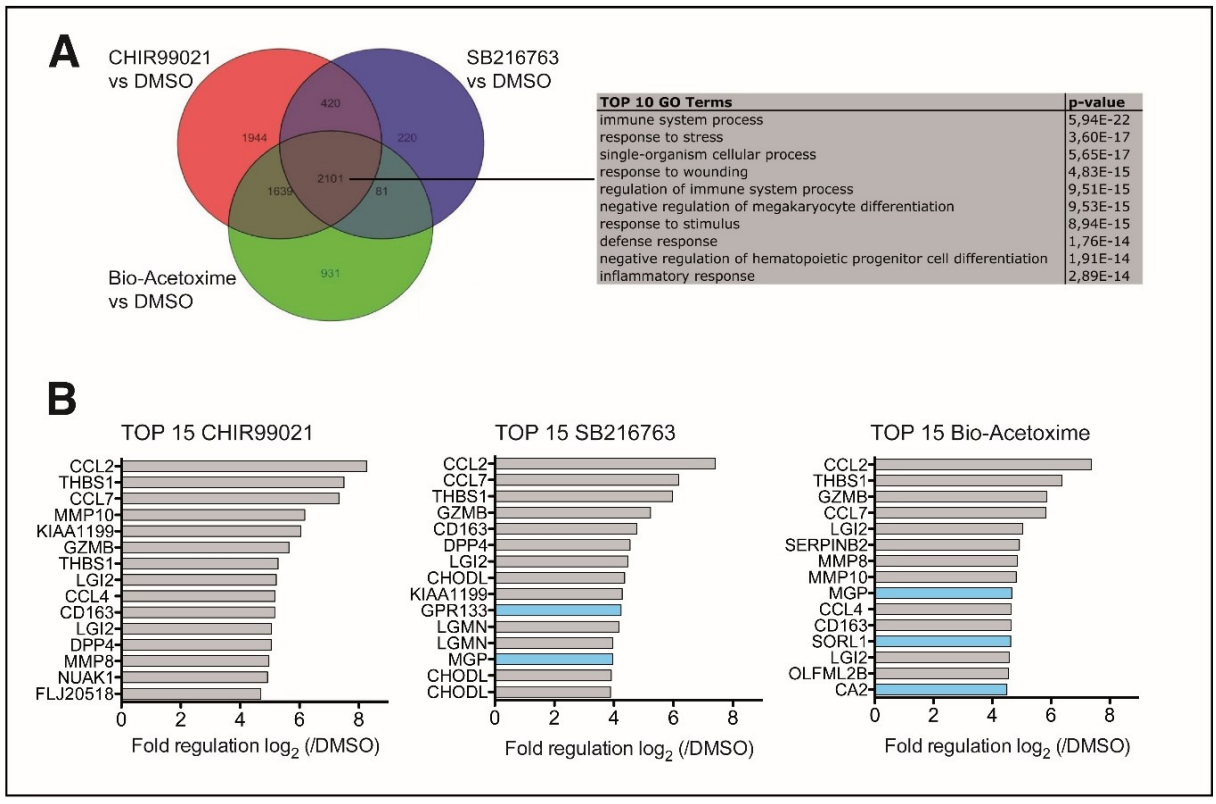

Figure 25: Microarray analysis comparing the gene expression profiles of THP-1 cells treated with three different GSK3 inhibitors to DMSO vehicle treated control cells. (A) Venn diagram displaying number and overlap of differentially expressed genes in THP-1 cells treated with GSK3 inhibitors. Gene ontology (GO) analysis was performed on the differentially expressed gene set common to all three inhibitors. The top ten significantly enriched GO terms with lowest *p*-values are shown (p(corr)<0.01). **(B)** Bar graphs showing the top 15 genes most significantly changed by each of the three GSK3 inhibitors from the overlapping set of 2101 genes (p(corr)<0.01). Upregulated genes are shown in grey; downregulated genes are shown in blue. Multiple entries of a gene indicate different gene probe sets that recognize alternative transcripts.

Treatment with GSK3 inhibitors caused both the induction and the repression of a large number of genes. The microarray results revealed 6104 genes that were differentially regulated in CHIR99021 treated THP-1 cells, while 2822 and 4752 differentially expressed genes were detected in SB216763 and Bio-Acetoxime treated cells, respectively (p(corr)<0.01). In total, an overlapping set of 2101 genes was found that were similarly regulated by all three GSK3 inhibitors in comparison to the DMSO control as displayed in the Venn diagram (Figure 25 A). Of note, the direction of gene expression regulation (upregulation or downregulation) among the overlapping 2101 genes was almost 100 % concordant between the three treatment groups, with only four genes regulated in opposite directions. The overlapping genes were categorized into functional GeneOntology (GO) classes. Several immune function related terms showed significant enrichment of differentially expressed genes and were among the ten most significantly regulated GO classes, including immune system response, response to stress, response to wounding, defense response and inflammatory response (Figure 25 A). The group of 2101 genes similarly up- or downregulated by all three inhibitors was ranked by fold change. Figure 25 B displays the top 15 up- and down-regulated genes. The most highly induced gene in response to all three GSK3 inhibitors was the chemokine *CCL2* (chemokine C-C motif ligand 2) with a mean fold change of approximately 200. Likewise, expression of *CCL7* (chemokine C-C motif ligand 7), *THBS1* (thrombospondin 1), *GZMB* (granzyme B), *LGI2* (leucin-rich repeat LGI family member 2) and *CD163* was highly upregulated with fold changes ranging from 22 (*LGI2*, SB216763) to 181 (*THBS1*, CHIR99021), further supporting a high concordance between the three treatment groups.

To further analyze the overlap between the transcriptional profiles induced by CHIR99021, SB216763 and Bio-Acetoxime, an Ingenuity Pathway Analysis (IPA) was performed. The IPA software allows the identification of gene networks and the analysis of gene expression patterns using a literature based database. Genes with a fold change greater than 5 were evaluated by IPA and categorized to related canonical pathways. The top five canonical pathways and their associated genes are listed in table 1. IPA revealed that pathways related to immune response and cytokine signaling were particularly enriched in the overlapping set of differentially expressed genes.

Table 1: The top five canonical pathways and their associated genes identified by IPA (minimum 5-fold change, $p<0.01$).

Canonical pathway	-log (*p*-value)	Associated gene
Agranulocyte Adhesion and Diapedesis	7.86	MMP7, IL1A, FN1, CCL2, MMP8, MMP10, CCL3, CCL4L1/CCL4L2, CCL7
Granulocyte Adhesion and Diapedesis	6.83	MMP7, IL1A, CCL2, MMP8, MMP10, CCL3, CCL4L1/CCL4L2, CCL7
Differential Regulation of Cytokine Production in Intestinal Epithelial Cells by IL-17A and IL-17F	5.92	IL-1A, CCL2, IL10, CCL3
TREM1 Signaling	5.22	TREM1, CCL2, IL10, CCL3, CCL7
Differential Regulation of Cytokine Production in Macrophages and T Helper Cells by IL-17A and IL-17F	4.49	CCL2, IL10, CCL3

The identified pathways included the migration of leukocytes towards site of injury/infection (Agranulocyte/granulocyte adhesion and diapedesis), interleukin-17 (IL-17) signaling and TREM1 (triggering receptor expressed on myeloid cells 1) signaling. The cytokines IL-17A and IL-17F share identical receptors and are associated with the induction of cytokine and chemokine production (Kawaguchi *et al.* 2004, Jin & Dong 2013). TREM1 is an immune receptor that was reported to be involved in inflammatory signaling (Bouchon *et al.* 2000, Bouchon *et al.* 2001, Bleharski *et al.* 2003). In AD, TREM1 is thought to play a role in microglial Aβ clearance. Overexpression of TREM1 was shown to facilitate Aß phagocytosis in primary mouse microglia (Jiang et al. 2016). In the microarray analysis, TREM1 expression was found to be induced between 9 (SB216763) to 15 fold (CHIR99021), making *TREM1* an interesting candidate gene potentially involved in the regulation of Aß uptake activity. In addition to *TREM1*, another eleven candidates from the overlapping set of differentially expressed genes were selected for further investigation. These genes were chosen based on literature associations with AD, endocytosis, microglia/macrophage activation and/or their strong regulation in the microarray analysis. Table 2 shows a list of all the candidate genes that were selected for further investigation.

Table 2: List of candidate genes selected for further analysis. Blue values indicate downregulation.

Gene name	Gene symbol	Fold change (*p*-value) CHIR99021	SB216763	Bio-Acetoxime
chemokine (C-C motif) ligand 2	CCL2	305,61 (0.0000223)	168,96 (0.00000538)	164,96 (0.000115)
thrombospondin 1	THBS1	180,80 (0.0000998)	62,43 (0.0000337)	82,57 (0.000115)
chemokine (C-C motif) ligand 7	CCL7	160,38 (0.0000552)	72,25 (0.000145)	56,66 (0.000372)
matrix metallopeptidase 10	MMP10	72,33 (0.00011)	5,37 (0.000838)	28,08 (0.000252)
CD163 molecule	CD163	35,82 (0.0000887)	27,30 (0.0000323)	24,81 (0.000115)
triggering receptor expressed on myeloid cells 1	TREM1	15,41 (0.000155)	9,36 (0.000163)	11,83 (0.000273)
chemokine (C-C motif) ligand 3	CCL3	11,51 (0.000301)	6,12 (0.000338)	9,22 (0.000593)
low density lipoprotein receptor	LDLR	3,88 (0.000310)	2,73 (0.00104)	3,48 (0.000372)
stabilin 1	STAB1	2,89 (0.00314)	2,06 (0.00775)	2,68 (0.00254)
CD44 molecule	CD44	2,71 (0.000509)	2,10 (0.00114)	1,95 (0.00278)
NLR family, pyrin domain containing 3	NLRP3	2,64 (0.00137)	2,15 (0.00171)	2,99 (0.000504)
cell division cycle 42	CDC42	2,03 (0.00275)	1,62 (0.00909)	2,09 (0.00113)

The list included the three chemokines CCL2, CCL3 and CCL7, which mediate the recruitment of microglia and macrophages to sites of inflammation (Shi & Pamer 2011). Besides, these chemokines were associated with TREM1 signaling in the IPA analysis (Table 1). A number of studies support, in particular, a role for CCL2 in microglia immune responses relevant to AD pathogenesis (Ishizuka *et al.* 1997, El Khoury et al. 2007, Kiyota *et al.* 2009, Naert & Rivest 2011). In a study by Kiyota *et al.*, CCL2-deficient AD mice showed increased Aß deposition in the brain, which was linked to impaired Aß clearance (Kiyota *et al.* 2013). *THBS1* appeared in the top three most substantially regulated genes for all three GSK3 inhibitors. It is a matrix glycoprotein that is involved in the regulation of macrophage function via its interaction with several cell surface receptors, including CD36 and CD47 (Lopez-Dee *et al.* 2011, Li *et al.* 2013b, Stein *et al.* 2016). The interaction of THBS1 with CD36 was shown to play a role in the uptake of apoptotic cells by macrophages (Savill *et al.* 1992). The matrix metallopeptidase 10 (MMP10), another strongly regulated matrix protein in the microarray analysis, has also been linked to the modulation of macrophage activity (Murray *et al.* 2013, McMahan *et al.* 2016). Moreover, a recent study provided evidence for a role of MMP10 in AD pathology (Duits *et al.* 2015). Besides TREM1, the cell surface receptors CD163, low density

lipoprotein receptor (LDLR), stabilin 1 (STAB1) and CD44 have all been connected to the endocytotic uptake of soluble factors or particles, and were selected for further investigations (Li *et al.* 2001, Kzhyshkowska *et al.* 2006, Thankamony & Knudson 2006, Vachon *et al.* 2006, Schaer *et al.* 2007, Park *et al.* 2009). The only downregulated gene listed in table 2, NLR Family Pyrin Domain Containing 3 (*NLRP3)*, encodes a cytosolic pattern recognition receptor. NLRP3 is involved in the formation of the NLRP3 inflammasome and triggers the release of pro-inflammatory cytokines such as IL-1ß (Latz *et al.* 2013). NLRP3-deficient AD mice showed enhanced Aß clearance and improved cognitive performance (Heneka et al. 2013). Finally, *CDC42* (cell division cycle 42), which encodes a small GTPase of the Rho family, is involved in the rearrangement of the actin cytoskeleton and has been directly implicated in the regulation of phagocytosis by monocytic cells (Cox *et al.* 1997, Massol *et al.* 1998, Hoppe & Swanson 2004).

4.11 Validation of the microarray results by quantitative PCR (qPCR)

To verify the results of the microarray analysis, quantitative PCR (qPCR) was performed for 8 of the 12 similarly regulated candidate genes listed in table 2. Confirmation of up- or downregulation of the candidate genes was performed with mRNA isolated from DMSO- and CHIR99021 treated THP-1 cells. At least three independent qPCR measurements were conducted for each gene and the data were analyzed using the comparative C_T method (Livak & Schmittgen 2001). A comparison of the fold changes obtained in the microarray analysis and by qPCR is shown in figure 26. The fold changes obtained by qPCR were in good agreement with the microarray data for each of the eight selected genes, indicating that the microarray data were reliable and reproducible.

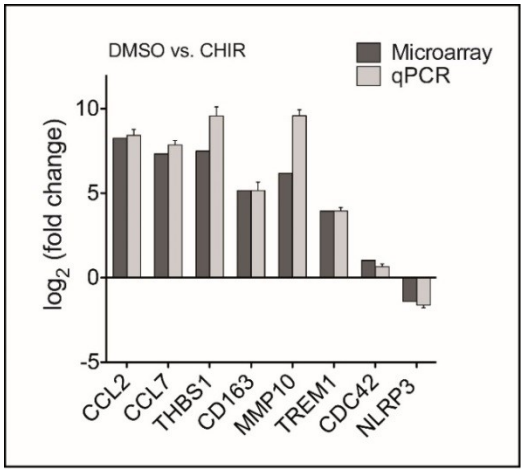

Figure 26: Validation of microarray data by qPCR. mRNA for qPCR analysis was isolated from THP-1 cells treated for 48 h with CHIR99021 (CHIR) or DMSO. The results from the qPCR and microarray analysis are depicted as relative fold change on a log scale. Details of the qPCR analysis are described in the method section. n=3-4 independent biological experiments, with 3 technical replicates for each gene. Error bars represent SD.

4.12 The role of secreted proteins in the stimulation of Aß uptake activity by GSK3 inhibitors

In a recent study, amyloid plaques in brain slices from old AD mice were reduced when these slices were co-cultured with brain slices from young wild type mice (Daria et al. 2016). The co-culturing caused the proliferation and clustering of old microglia around amyloid plaques, suggesting that dysfunction of old microglia might be restored by factors secreted by young microglia. Further studies identified the growth factor M-CSF as the responsible secreted protein (Daria et al. 2016) These and other studies indicate that secreted factors might be able to stimulate the phagocytic capacity of macrophages and microglia cells. While we did not observe proliferation of THP-1 or primary microglia cells after treatment with GSK3 inhibitors (figure 15), we wanted to investigate the contribution of soluble factors to the stimulation of Aß uptake activity. For this purpose, THP-1 cells were treated with conditioned media (CM) collected from cells that were treated for 48 h with either CHIR99021 or DMSO vehicle. Remaining CHIR99021 compound was removed from the CM via ultrafiltration using a 4 kDa molecular weight cut-off membrane. Addition of this CM to THP-1 cells did not result in increased uptake of FAM-Aß$_{42}$ (Figure 27 A). To exclude that small molecular weight stimulatory factors might be removed by the ultrafiltration, CM obtained from cells pre-treated with CHIR99021 was also tested. In these experiments, after treatment of THP-1 cells with CHIR99021 for 48 h, the medium was replaced by fresh medium and conditioned for another 24 h (24 h CM). THP-1 cells were then cultured for 48 h in the presence of this 24 h CM, which did not contain CHIR99021 but potentially increased levels of secreted factors stimulated by GSK3 inhibitor treatment. The addition of undiluted 24 h CM resulted in a decrease of FAM-Aß$_{42}$ uptake, likely indicating toxicity of the pure CM (Figure 27 B). Therefore, the 24 h CM was diluted 1:1 with fresh medium. Again, no effect on FAM-Aß$_{42}$ uptake was observed after treatment of THP-1 cells with the diluted 24h CM (Figure 27 B). These results suggested that increased levels of secreted factors were not responsible for the stimulation of Aß uptake activity by GSK3 inhibitors.

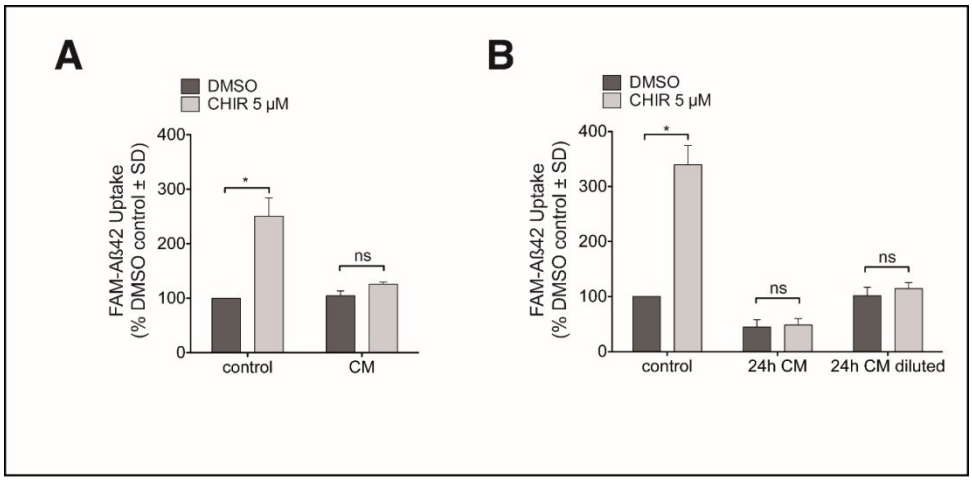

Figure 27: Conditioned media from CHIR99021 treated cells did not promote Aß uptake. (A) THP-1 cells were exposed to CM obtained from THP-1 cells treated for 48 h with DMSO or CHIR99021 (CHIR). Remaining CHIR99021 compound was removed by ultrafiltration. As a control, FAM-A$ß_{42}$ uptake by THP-1 cells directly treated for 48 h with DMSO or 5 µM CHIR99021 was quantified. **(B)** In an alternative approach, THP-1 cells were pre-treated with DMSO or 5 µM CHIR99021 (CHIR) for 48 h, the culture medium was changed and conditioned for another 24 h. This 24 CM was then used to treat another culture of THP-1 cells. Since the 24 h CM seemed to induce toxicity, the CM was also applied diluted in a ratio of 1:1 with fresh culture medium (24h CM diluted). A similar control experiment with direct treatment of THP-1 cells as in (A) was performed to prove the biological activity of the CHIR99021 compound. n=2 independent biological experiments, with 3 technical replicates for each experimental condition. Statistical analysis was performed by using two-tailed *t* test (ns = non significant $p>0.05$; * $p<0.05$). Error bars represent SD.

4.13 Validation of candidate genes by CRISPR/Cas9-mediated genome editing

The results for GSK3ß and ß-catenin shown in sections 4.7 and 4.8 had indicated that CRISPR/Cas9 mediated gene silencing in THP-1 cells followed by an Aß uptake assay was a straightforward and appropriate method to validate putative candidate genes that might be linked to the underlying molecular mechanism. Therefore, to assess the role of the selected microarray candidate genes in the stimulation of Aß uptake by GSK3 inhibitors, two sgRNAs per gene targeting different exons were designed and cloned into lentiCRISPRv2. Lentiviral particles were generated and used to transduce THP-1 cells as described above. After limited dilution cloning of puromycin-selected cells, none of the final cell populations displayed a complete knock-out as determined by qPCR. As mentioned above, this was likely due to the technical difficulties in isolating true single cell clones from THP-1 cells growing in suspension. Hence, the resulting cell populations consisted of a mixture of wild type cells (due to lack of efficient target cleavage) and mutant cells with heterozygously and homozygously mutated target genes. Cell lines and sgRNAs, which showed the strongest partial KO for a specific target gene, were chosen for subsequent analysis in the Aß uptake assay. Prior to the qPCR analysis of target

gene expression in the partial KO cell lines, the cells were treated with CHIR99021 for 48 h to assess the stimulated mRNA levels (either upregulated or downregulated) of each specific gene as determined in the microarray analysis. The qPCR analysis of cell lines expressing sgRNAs targeting the cytokines CCL2, CCL3 and CCL7, and the matrix proteins THBS1 and MMP10 revealed a strong reduction of target gene mRNA levels of 70-90 % (Figure 28, A, C-F). To examine the impact of the partial gene KO, cells were treated for 48 h with CHIR99021 or DMSO vehicle followed by the FAM-Aß$_{42}$ uptake assay. Assuming that the effect of CHIR99021 is due to the upregulation of one of the targeted proteins, even a partial KO of the responsible gene would be expected to reduce or abolish the stimulation of FAM-Aß$_{42}$ uptake activity by GSK3 inhibitors. Therefore, only the CHIR99021-induced stimulation of the Aß uptake activity was compared between the partial KO and the control cell line and statistically evaluated. However, the Aß uptake assays revealed no significant differences in the uptake activity induced by CHIR99021 in partial KO cell lines for CCL2, CCL3, CCL7, THBS1 and MMP10 in comparison to wild type THP-1 control cells, indicating that the stimulation in uptake activity was not mediated by the upregulation of any of these candidate proteins (Figure 28, A, C-F). Since *CCL2* was the most highly induced gene in response to all three inhibitors in the microarray analysis (Figure 25), the role of this cytokine was further validated by treatment of THP-1 cells with recombinant CCL2 for 48 h. Treatment with increasing concentrations of purified CCL2 did not show effects in the Aß uptake assay (Figure 28 B), supporting the results of the CRISPR cell line. Likewise, longer (72 h) and shorter (3 h) treatment periods with CCL2 had no impact (data not shown).

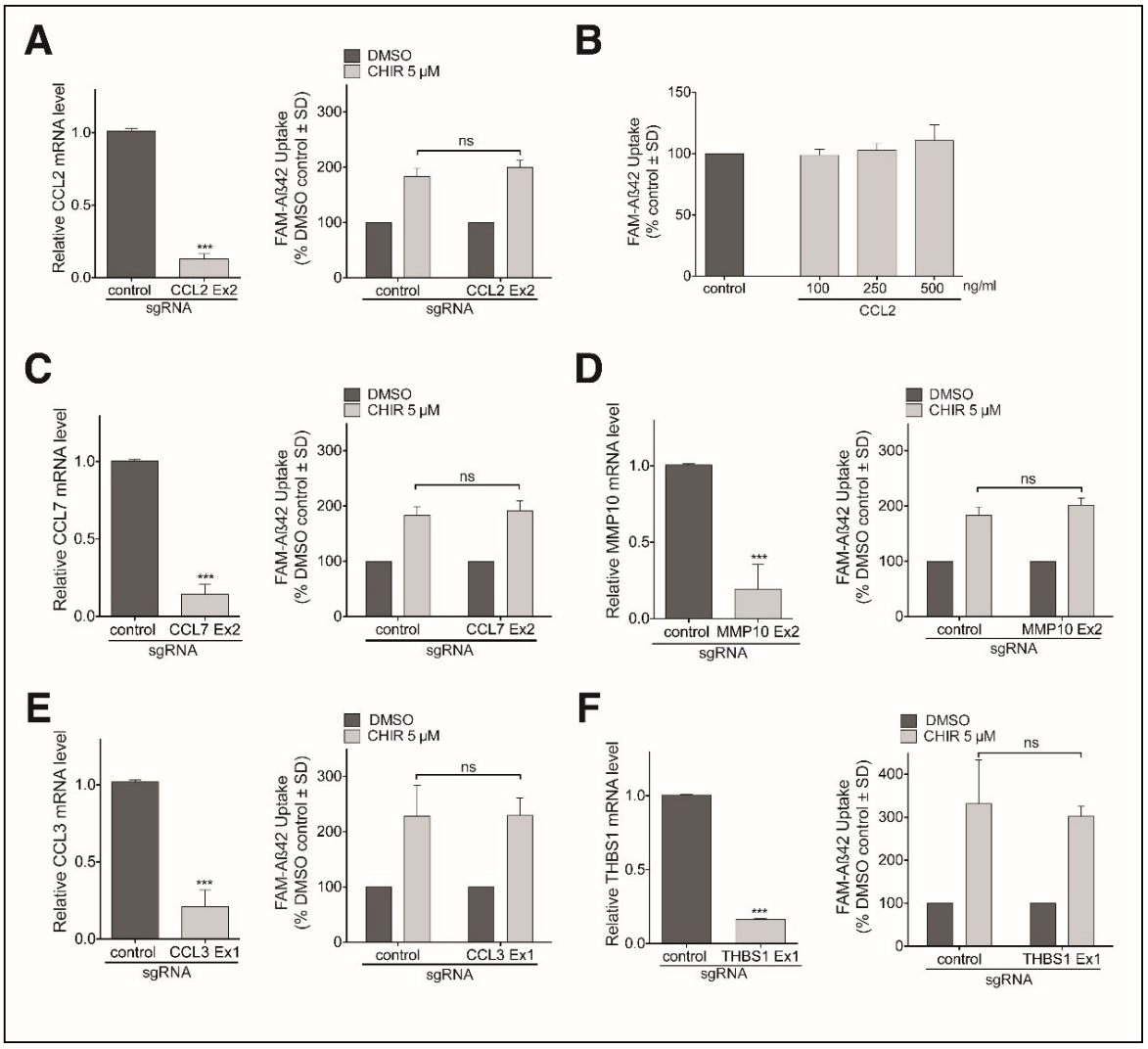

Figure 28: Functional validation of cytokine and matrix protein encoding candidate genes with CRISPR/Cas9 generated KO cell lines. (**A**) CCL2, **(C)** CCL7, **(D)** MMP10, **(E)** CCL3, **(F)** THBS1. Prior to the analysis of target genes expression by qPCR, the putative KO and control cells were treated for 48 h with CHIR99021 (CHIR) to compare the stimulated mRNA levels. For the functional analysis, the KO and the corresponding control cells were treated with CHIR99021 or DMSO vehicle for 48 h, and the stimulation of FAM-Aß$_{42}$ uptake activity was compared. Note that for the statistical analysis the FAM-Aß$_{42}$ uptake values after CHIR99021 treatment were normalized to the same cell line treated with DMSO. n=3 independent biological experiments, with 3 technical replicates for each experimental condition. **(B)** FAM-Aß$_{42}$ uptake by THP-1 cells after 48 h treatment with CCL2. Statistical analysis was performed by two-tailed *t* test (ns = non significant $p>0.05$; *** $p<0.001$). Error bars represent SD.

Subsequently, the same approach was used to validate additional genes from the list of putative candidates identified in the microarray analysis (Table 2). THP-1 cell lines expressing sgRNAs targeting the receptors CD163, CD44, NLRP3, TREM1, LDLR, STAB1, and the small GTPase CDC42 were generated as described above. Partial KO of the targeted genes was confirmed by either Western blotting or qPCR, and the cell lines were analyzed in the Aß uptake assay (Figure 29 A-C; Figure 30 A-D). Protein or mRNA levels were reduced by 70- 90% for CD163, CD44, TREM1, STAB1 and CDC42. A weaker reduction of approximately 60 % was observed for NLRP3 and LDLR mRNA

levels. Among the targeted receptors, NLRP3 was the only candidate gene that was downregulated in the microarray analysis (Table 2). After treatment with CHIR99021, none of the KO cell lines for CD163, CD44, NLRP3, LDLR and STAB1 showed a significant difference in the FAM-Aß$_{42}$ uptake activity in comparison to wildtype control cells (Figure 29 A-C; Figure 30 A-D), indicating that these receptors were not involved in the upregulation of Aß uptake activity by GSK3 inhibitors.

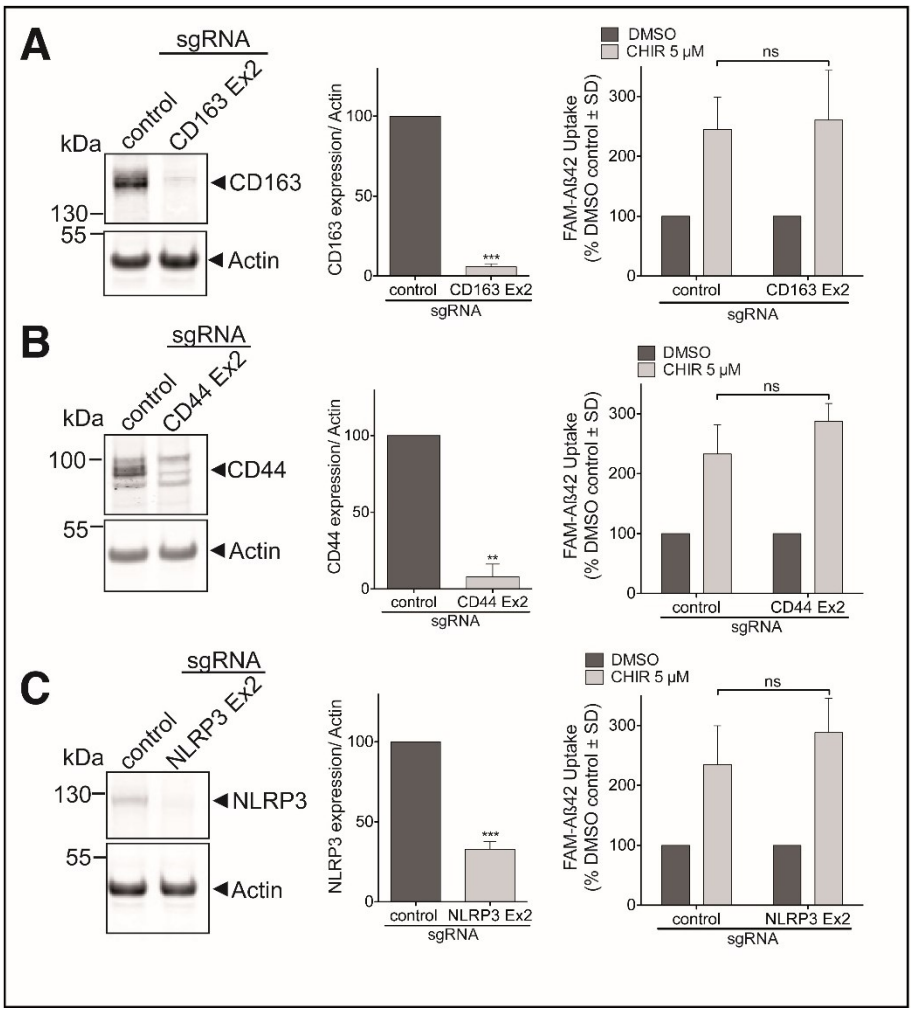

Figure 29: Functional validation of the candidate genes CD163 (A), CD44 (B) and NLRP3 (C) with CRISPR/Cas9 generated KO cell lines. Prior to expression analysis by Western blotting, the putative KO and control cells were treated for 48 h with CHIR99021 (CHIR) to compare the stimulated protein levels. The functional validation in the Aß uptake assay and the statistical analysis were performed as described in figure 28. n=3 independent biological experiments, with 1-3 technical replicates for each experimental condition. Statistical analysis was performed by two-tailed *t* test (ns = non significant $p>0.05$; ** $p<0.01$; *** $p<0.001$). Error bars represent SD.

In contrast, partial KO of the TREM1 receptor and the small GTPase CDC42 appeared to reduce the stimulating effect of the GSK3 inhibitor on Aß uptake activity (Figure 30 A, D). Here, after CHIR99021 treatment, a significant difference in the Aß uptake activity between the KO cell lines and the control cells was observed. These results indicated

that TREM1 and CDC42 might be involved in the stimulation of Aß uptake by GSK3 inhibitors.

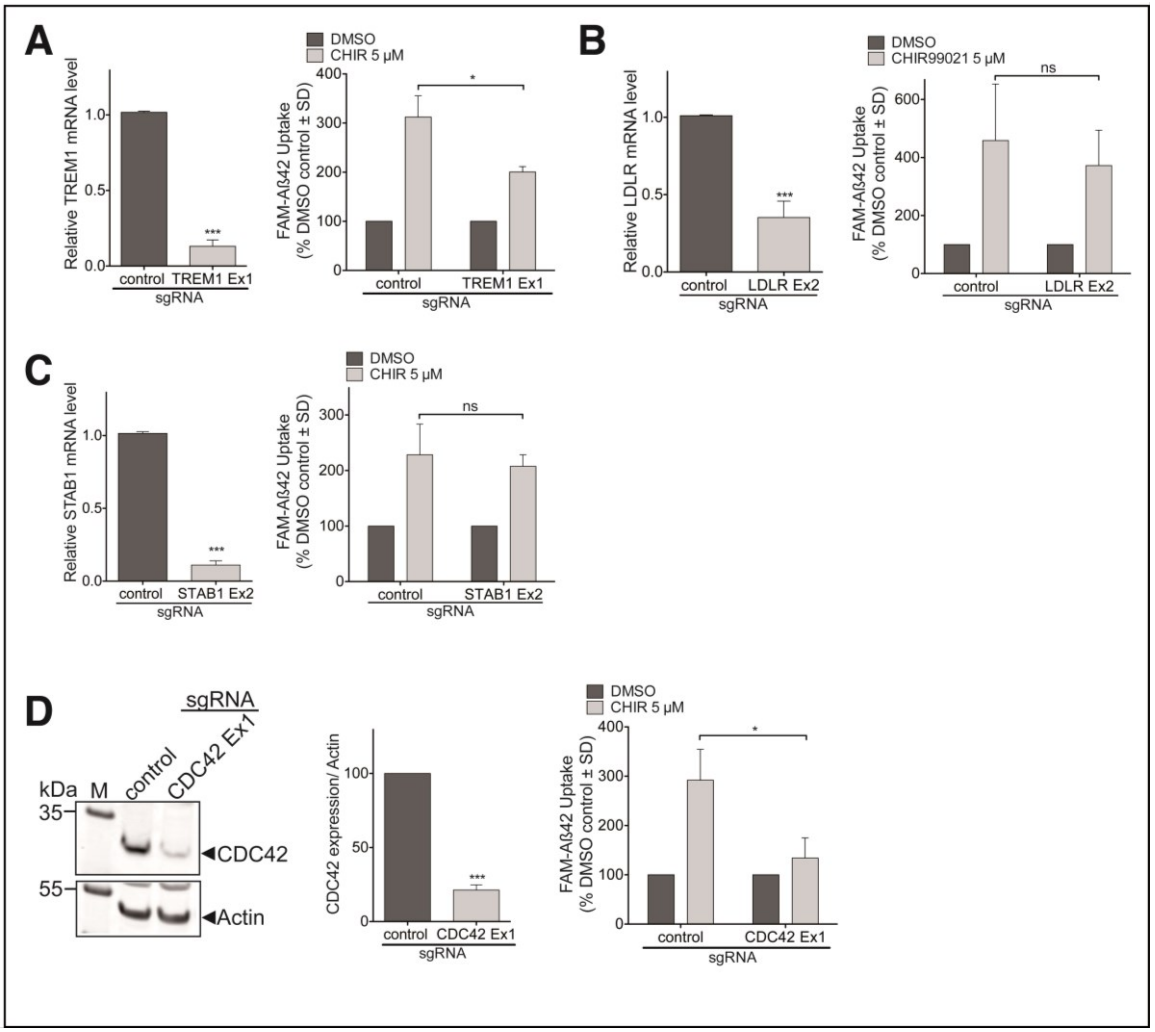

Figure 30: Functional validation of the candidate genes TREM1 (A), LDLR (B), STAB1 (C) and CDC42 (D) with CRISPR/Cas9 generated KO cells lines. Expression analysis of the candidate genes by Western blotting or qPCR, functional validation in the Aß uptake assay, and the statistical analysis were performed as described in figure 28. n=3 independent biological experiments, with 1-3 technical replicates for each experimental condition. Statistical analysis was performed by two-tailed *t* test (ns = non significant $p>0.05$; * $p<0.05$; *** $p<0.001$). Error bars represent SD.

To exclude potential false positive results due to clonal or off-target effects, additional sgRNAs targeting different parts of the *CDC42* and *TREM1* gene sequences were designed and additional KO cell lines were generated. Single cell clones were obtained for two sgRNAs targeting TREM1 (exon 1 and exon 2) and one sgRNA targeting CDC42 (exon 1), which showed partial KOs between 85 - 95 % as determined by qPCR (Figure 31 A, B) and Western blotting (Figure 31 C). In addition, as shown by Western blotting in figure 31 D, a CDC42 KO cell clone was identified for the sgRNA targeting exon 1. These cell lines were again treated for 48 h with CHIR99021 or DMSO vehicle followed by the Aß uptake assay.

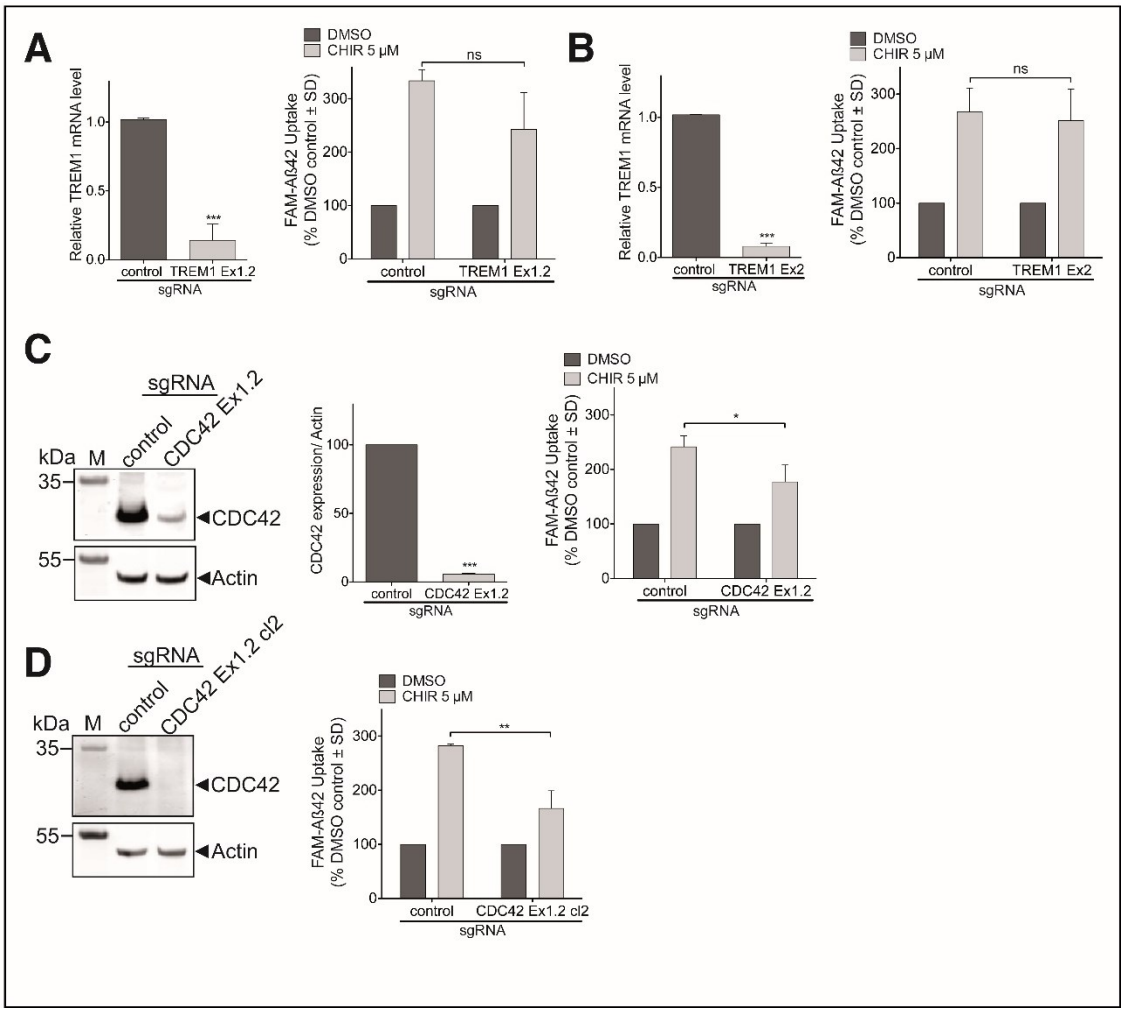

Figure 31: Additional validation experiments for the candidate genes TREM1 (A,B) and CDC42 (C,D) with CRISPR/Cas9 generated KO cells lines. Expression analysis of TREM1 and CDC42 by Western blotting or qPCR, functional validation in the Aß uptake assay, and the statistical analysis were performed as described in figure 28. qPCR n=2-3, others n=3 independent biological experiments, with 1-3 technical replicates for each experimental condition. Statistical analysis was performed by two-tailed *t* test (ns = non significant $p>0.05$; * $p<0.05$; ** $p<0.01$; *** $p<0.001$). Error bars represent SD.

Both TREM1 KO cell lines revealed no significant differences in their CHIR99021 stimulated FAM-Aß$_{42}$ uptake activity in comparison to the control cells (Figure 31 A, B). These results contradicted the positive findings with the first sgRNA targeting exon 1 (Figure 30 A), indicating that these previous observations were likely a false positive result. In contrast, the partial KO and the complete KO cell line generated with the second sgRNA against CDC42 displayed a significantly reduced FAM-Aß$_{42}$ uptake activity after CHIR99021 treatment (Figure 31 C, D), which was consistent with the phenotype induced by the previous sgRNA (Figure 30 D). These results suggested that CDC42 might indeed play a critical role in the upregulation of Aß uptake activity by GSK3 inhibitors.

The impact of GSK3 inhibitors on the expression levels of the two candidate genes TREM1 and CDC42 was further investigated in primary microglia. Cells were treated for

72 h with CHIR99021 and the expression of TREM1 and CDC42 was assessed by qPCR. While CDC42 mRNA expression was 2 fold upregulated in the microarray analysis, the expression level was unchanged in primary microglia following CHIR99021 treatment (Figure 32 B). In contrast, TREM1 expression was induced approximately 2 fold in CHIR99021 treated microglia (Figure 32 A). This corresponded to the upregulation of TREM1 in the microarray analysis, although the induction was weaker. In addition to TREM1, the expression levels of TREM2 were investigated. TREM1 and TREM2 belong to a family of structural related receptors and variants in either of the two genes have been associated with AD pathology (Guerreiro et al. 2013, Jonsson et al. 2013, Replogle et al. 2015). Interestingly, qPCR analysis showed that TREM2 expression was significantly reduced after treatment of THP-1 cells and primary microglia with CHIR99021 (Figure 32, C: primary microglia, D: THP-1).

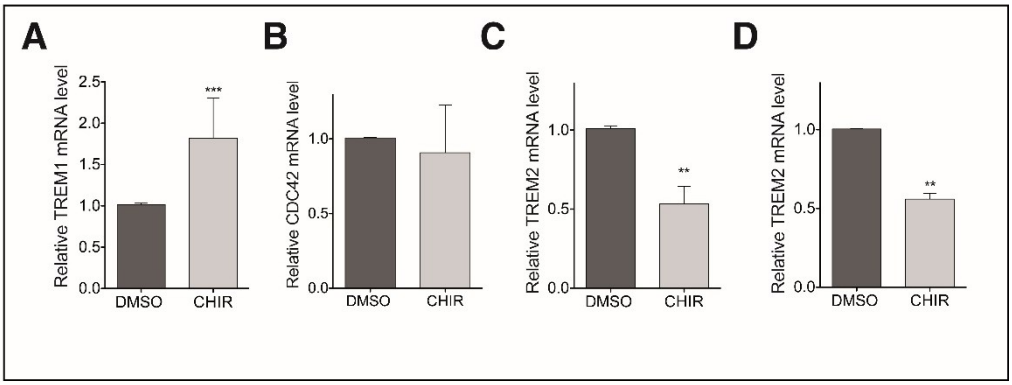

Figure 32: Analysis of TREM1, TREM2 and CDC42 expression in THP-1 and primary microglia cells by qPCR. mRNA was isolated from primary microglia treated for 72 h with CHIR99021 (CHIR) or DMSO vehicle. Expression levels of TREM1 **(A)**, CDC42 **(B)** and TREM2 **(C)** were measured by qPCR. **(D)** mRNA was isolated from THP-1 cells treated for 48 h with CHIR99021 (CHIR) or DMSO vehicle and TREM2 expression was analyzed by qPCR. n=3-7 independent biological experiments, with 3 technical replicates for each experimental condition. Statistical analysis was performed by two-tailed *t* test (ns = non significant $p>0.05$; ** $p<0.01$; *** $p<0.001$). Error bars represent SD.

In summary, the microarray analysis revealed a large set of genes that were consistently regulated by all three GSK3 inhibitors in THP-1 cells. 12 candidate genes associated with endocytic processes and/or other macrophage and microglia functions were selected for further validation experiments with CRISPR/Cas9 generated KO cell lines. Out of these, only CDC42 KO cell lines showed significant and consistent effects in the Aß uptake assays supporting that CDC42 might be mechanistically involved in the stimulation of Aß uptake activity by GSK3 inhibitors. However, qPCR measurements did not confirm upregulation of CDC42 expression in primary microglia cells after

CHIR99021 treatment, indicating potential differences in the response to GSK3 inhibitors between the two cell types.

5 Discussion

Microglia, the brain-resident immune cells, are now regarded as a central factor in the pathogenesis of AD. In the brains of AD patients, microglia cells have been shown to be closely associated with Aß deposits (Itagaki et al. 1989). Activated microglia mediate Aß-induced inflammation through the production of inflammatory cytokines and reactive oxygen species, which may contribute to neuronal cell death (Giulian et al. 1996, Lue et al. 2001a). Furthermore, numerous studies indicate that microglia are involved in the clearance of Aß peptides and amyloid deposits. They are able to internalize and degrade Aß and might therefore play a beneficial role in AD (Paresce et al. 1996, Koenigsknecht & Landreth 2004, Bolmont et al. 2008, Liu et al. 2010). Failure of Aß clearance is assumed to be a crucial factor in AD pathogenesis. Age-related alterations and specific pathological conditions in the AD brain have been suggested to be responsible for impaired microglia function and inefficient Aß clearance (Streit et al. 2004, Krabbe et al. 2013). Consequently, modulation of microglia behavior might be of benefit for AD and further understanding of molecular clearance mechanisms is of great relevance.

In the present study, the role of GSK3 in the modulation of microglia functions was investigated. GSK3 is a constitutively active serine-threonine kinase that exists in two isoforms, GSK3α und GSK3ß (Woodgett 1990). GSK3 was found to be a key regulator of the insulin and Wnt signaling pathways and is involved in numerous other cellular processes, including the regulation of apoptosis, cell polarity and migration (Jope et al. 2007). Importantly, dysregulation of this kinase has been implicated at multiple steps in the pathogenesis of AD (Figure 33) (Hooper et al. 2008). It has been shown that Aß activates GSK3 signaling in an AD mouse model, and increased GSK3 activity has been observed in the brains of AD patients (Leroy *et al.* 2007, Terwel *et al.* 2008). AD-related proteins such as microtubule-associated protein tau, presenilin and ß-catenin are known substrates of GSK3 and GSK3-mediated, aberrant phosphorylation of these targets has been proposed to contribute to both neurofibrillary tangle (NFT) and amyloid plaque formation (Phiel *et al.* 2003, Uemura *et al.* 2007, Hanger *et al.* 2009, Llorens-Maritin *et al.* 2014). Tau hyperphosphorylation and neurodegeneration have been observed in transgenic mice overexpressing GSK3, whereas inhibition of GSK3 prevented tau hyperphosphorylation and NFT formation (Lucas *et al.* 2001, Engel *et al.* 2006). Several studies have reported reduced Aß deposition in AD mouse models after treatment with GSK3 inhibitors or silencing of GSK3 with hairpin RNA constructs, and have further indicated a potential direct role of GSK3 in the regulation of APP cleavage (Sun *et al.*

2002, Phiel et al. 2003, Su *et al.* 2004, Sereno *et al.* 2009, Hurtado *et al.* 2012). It has been proposed that GSK3 might affect the proteolytic processing of APP by the γ-secretase complex, since both APP and presenilin are substrates of GSK3 (Aplin *et al.* 1996, Rockenstein *et al.* 2007, Uemura et al. 2007, Cai *et al.* 2012). However, the contribution of GSK3 to Aβ production remains controversial. A report by Jaworski *et al.* showed that knock-out of GSK3 in the mouse brain had no impact on the steady-state levels of APP metabolites or Aβ peptides (Jaworski *et al.* 2011). Increased activity of GSK3 has also been associated with learning and memory impairment. Overexpression of GSK3 in transgenic mice was shown to block the induction of long term potentiation (LTP), the long-lasting enhancement of synaptic efficacy, and caused a decrease in spatial learning (Hernandez *et al.* 2002, Hooper *et al.* 2007).

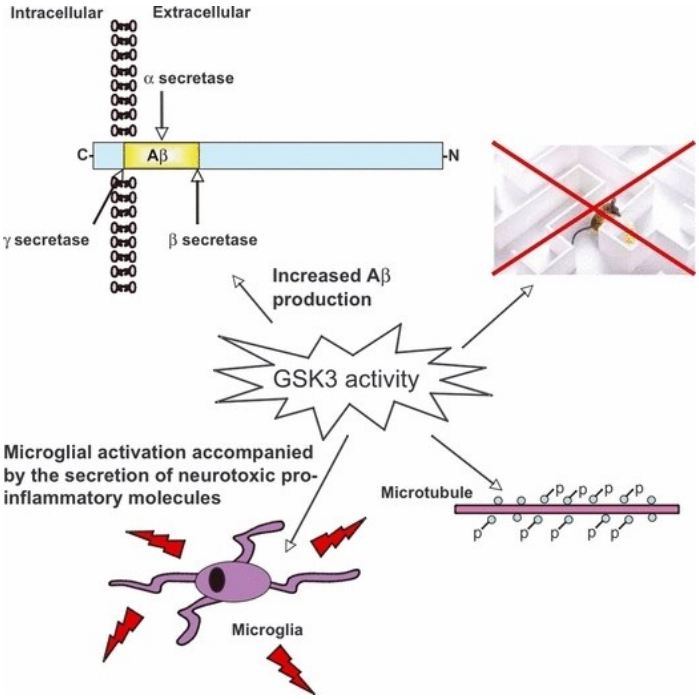

Figure 33: Role of GSK3 in AD pathogenesis. Multiple links have been proposed between GSK3 activity and neuropathological features of AD. Hyperphosphorylation of tau by GSK3 might result in decreased microtubule binding and formation of neurofibrillary tangles. Furthermore, enhanced activity of GSK3 has been associated with memory impairments, increased production of Aß peptides, and microglia-mediated inflammatory responses (adopted from Hooper et al. 2008).

Neuroinflammation plays a fundamental role in AD pathogenesis and GSK3ß was found to be a strong regulator of the inflammatory response in immune cells including microglia (Beurel & Jope 2009, Yuskaitis & Jope 2009). Microglia were shown to secrete a range of cytokines and chemokines upon activation by Aß, including IL-6, IL-8, TNFα, inflammatory protein-1 (MIP-1) and monocyte chemotactic protein-1 (MCP-1) (Rogers & Lue 2001). These secretory products regulate the intensity and duration of the immune response and might contribute to neuronal death observed in AD (Hanisch 2002, von Bernhardi *et al.* 2010). Strikingly, GSK3ß activity was found to be required to induce the

production of pro-inflammatory cytokines in monocytes and LPS-stimulated microglia (Martin et al. 2005, Beurel & Jope 2009, Cheng et al. 2009).

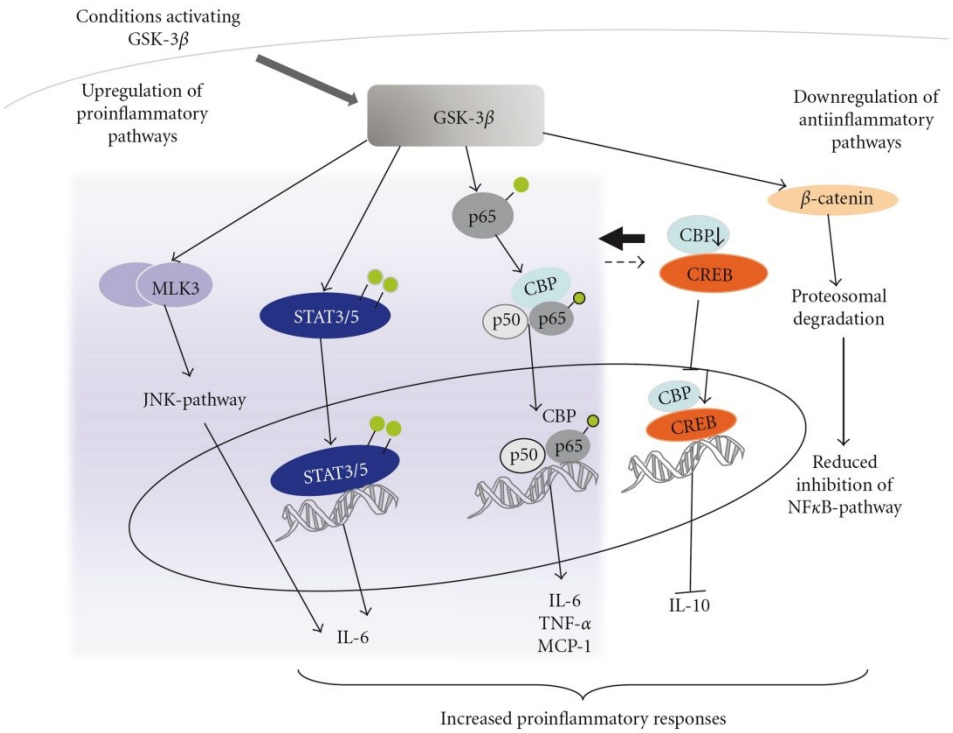

Figure 34: GSK3ß regulates the inflammatory response in microglia. GSK3ß-mediated phosphorylation increases the production of pro-inflammatory molecules via upregulation of multiple signaling pathways, including JNK-, STAT3/5- and NF-κB pathways. Moreover, phosphorylation by GSK3ß triggers the downregulation of anti-inflammatory pathways, such as CREB-mediated induction of IL-10 and ß-catenin mediated inhibition of the NF-κB pathway (adopted from Koistinaho *et al.* 2011).

The activation of the inflammatory response by GSK3ß in microglia involves several signaling pathways (Figure 34). LPS and other stimuli activate the c-Jun N-terminal kinase (JNK)- pathway via GSK3ß-mediated phosphorylation of mixed lineage kinase 3 (MLK3), which eventually leads to IL-6 and TNFα synthesis (Wang et al. 2010). Intracellular signaling induced by IL-6 receptors leads to the GSK3ß-mediated phosphorylation and activation of signal transducer and activator of transcription 3 and 5 (STAT3/5). These transcription factors translocate into the nucleus where they regulate the expression of proinflammatory molecules, including IL-6 itself (Beurel & Jope 2008, Beurel & Jope 2009). The transcription factor nuclear factor κB (NF-κB) is a protein complex that forms DNA-binding dimers and controls the transcription of numerous target genes. In mammals, the NF-κB family is composed of p50, p52, RelA (p65), c-Rel and RelB (Hayden & Ghosh 2004). NF-κB activation can be mediated at multiple steps. Phosphorylation of the p65 subunit of NF-κB by GSK3ß increases the binding of p65 to the coactivator CREB-binding protein (CBP) and induces NF-κB transcriptional activity (Steinbrecher *et al.* 2005). Activated NF-κB triggers the expression of pro-inflammatory

molecules, including IL-6, TNFα, MCP-1 and inducible nitric oxide synthase (iNOS) (Arias-Salvatierra *et al.* 2011). The transcription factor cAMP response element-binding protein (CREB) competes with p65 for CBP binding. GSK3ß phosphorylation of p65 shifts the balance in favor of NF-κB activation, thereby reducing CREB-mediated expression of interleukin 10 (IL-10) (Martin et al. 2005), which was shown to play an anti-inflammatory role by limiting excessive production of pro-inflammatory cytokines (Williams *et al.* 2004, Park *et al.* 2007). ß-catenin is a transcriptional coactivator of the Wnt pathway and a negative regulator of NF-κB activity. ß-catenin is a direct target of GSK3ß phosphorylation, leading to the proteasomal degradation of ß-catenin. Decreased ß-catenin levels, in turn, result in reduced inhibition of NF-κB-mediated inflammatory responses (Ma & Hottiger 2016). Consequently, pro-inflammatory GSK3ß signaling mediates both the upregulation of pro-inflammatory pathways and downregulation of anti-inflammatory pathways. These findings are consistent with published studies demonstrating benefits of GSK3 inhibitors in animal models of sepsis and organ injuries (Martin et al. 2005, Dugo *et al.* 2005, Ko *et al.* 2010, Noh *et al.* 2012). Mice treated with the GSK3 inhibitor SB216763 were protected from sepsis caused by the inflammatory stimulans LPS (Martin et al. 2005). A similar outcome has been observed with the GSK3 inhibitor SB415286 (Noh et al. 2012). Moreover, GSK3 inhibitor treated mice showed a significant reduction in the expression of pro-inflammatroy cytokines and an increase of anti-inflammatory cytokines when compared to control mice treated with only LPS (Martin et al. 2005, Ko et al. 2010). These results indicated that GSK3 inhibitors could effectively suppress the production of pro-inflammatory cytokines *in vivo*. In studies by Tay *et al.* and Tsao *et al.,* GSK3 inhibition decreased the mortality of bacteria-infected mice. The authors reported lower bacterial counts in the organs of infected mice after GSK3 inhibitor treatment when compared to untreated control mice (Tay *et al.* 2012, Tsao *et al.* 2015). This effect was attributed to enhanced bactericidal activity of macrophages (Tsao et al. 2015). Evidently, an increase in the phagocytic uptake of bacteria by macrophages could also provide a mechanistic explanation for the beneficial effect of GSK3 inhibition in these model systems.

Due to its role in AD pathophysiological processes, a reduction in GSK3 activity has been considered as a potential therapeutic strategy in AD, and GSK3 inhibitors have gained attention as a treatment approach. Treatment with the uncompetitive GSK3 inhibitor lithium and classical ATP-competitive inhibitors such as AR-014418 and indirubin reduced tau phosphorylation and amyloid deposition in several APP-transgenic mouse models of AD (Rockenstein et al. 2007, Sereno et al. 2009, Ding *et al.* 2010, Toledo & Inestrosa 2010). These promising results of GSK3 inhibitors in mouse models

of AD supported the initiation of several clinical trails in AD patients (Macdonald *et al.* 2008, Leyhe *et al.* 2009, Forlenza *et al.* 2011, del Ser *et al.* 2013, Lovestone *et al.* 2015). However, these studies produced either negative results, they were not designed or powered to observe clinical benefits, or they did not progress beyond early clinical stages.

In this study, human THP-1 macrophages, primary human macrophages and primary mouse microglia were used to examine the effects of GSK3 inhibition. THP-1 is a well-established human monocytic cell line, which was derived from the peripheral blood of an acute monocytic leukemia patient (Tsuchiya et al. 1980). In the presence of PMA, these cells differentiate into macrophage-like cells. It remains controversial whether monocytes interact with the brain under physiological conditions. However, under pathological conditions it was shown that monocytes are able to infiltrate the brain and differentiate into macrophages that produce inflammatory factors and internalize molecules, including Aß (Malm *et al.* 2010, Mildner *et al.* 2011). Furthermore, macrophages derived from infiltrated peripheral monocytes have been reported to be more efficient in clearing Aß deposits than resident microglia in AD mouse models (Simard et al. 2006). These findings make macrophages an appropriate surrogate model to study the impact of GSK3 inhibition on the regulation of Aß uptake.

Three commercially available GSK3 inhibitors, CHIR99021, SB216763 and Bio-Acetoxime were used to block GSK3 activity. They differ in their selectivity for GSK3 over other kinases and in their potency, and they inhibit both isoforms, GSK3α and GSK3ß. The high sequence homology of the two isoforms, which share 98 % sequence identity in their kinase domains, complicates the development of small molecule inhibitors that can discriminate between them (Kaidanovich-Beilin & Woodgett 2011). To date, all known GSK3 inhibitors inhibit both isoforms (Beurel *et al.* 2015). Especially, CHIR99021 was found to be a very potent and specific GSK3 inhibitor showing high selectivity towards GSK3α/ß over 359 other kinases, whereas Bio-Acetoxime and SB216763 were found to be less selective (Ring et al. 2003, Pan *et al.* 2011).
The results of the Aß uptake assay demonstrated that GSK3 inhibitors were able to stimulate the internalization of Aß. GSK3 inhibitor treatment of both THP-1 macrophages and primary microglia resulted in a substantial, dose-dependent increase of Aß uptake up to 2-3 fold. CHIR99021 treatment showed the strongest effects, likely due to its potent and specific inhibition of GSK3. Whereas treatment of THP-1 cells resulted in the strongest increase of Aß uptake after 48 h, primary microglia showed the strongest effect

after 72 h of treatment. An overall weaker increase was observed for primary macrophages differentiated from human monocytes. These observations suggest cell type specific differences in the molecular response to GSK3 inhibition.

For the Aß uptake assay, synthetic, N-terminally labeled carboxyfluorescein-Aß$_{42}$ peptides (FAM-Aß$_{42}$) were used, which were pre-incubated at 37° to enable the formation of aggregates. Similar fluorophore-labeled Aß preparations have been extensively used by numerous other research groups to quantify the cellular uptake of Aß (Paresce et al. 1996, Chung *et al.* 1999, Majumdar *et al.* 2008, Hickman et al. 2008, Jiang *et al.* 2008, Terwel *et al.* 2011, Li *et al.* 2013a). However, differences in the solubilization and preparation methods have been reported, and in many cases the structures of the peptide assemblies have not been well characterized. It can be assumed that the molecular properties of the fluorophores such as charged groups and size might influence the Aß aggregation process. In a study by Jungbauer *et al.*, the presence of an N-terminal fluorophore resulted in atypical oligomer and fibril formation when compared to unlabeled Aß preparations as demonstrated by atomic force microscopy (Jungbauer *et al.* 2009). In contrast, SDS-PAGE gel analysis of a FAM-Aß$_{42}$ preparation showed a similar pattern to the unlabeled peptide with bands corresponding to the monomer, oligomers and higher molecular weight Aß assemblies (Jungbauer et al. 2009). Consequently, despite small differences in fibril forming conditions, it appears likely that the FAM-Aß$_{42}$ preparations used in our present study contained monomers, dimers and oligomers as well as fibrillar aggregates. Moreover, in another study, the functional characterization of N-terminally fluorescein labeled and unlabeled Aß preparations revealed similar potencies to induce neuronal apoptosis, indicating similar toxic behaviour of those Aß preparations (Saavedra *et al.* 2007).

A number of critical control experiments were performed, which demonstrated that the increase in Aß uptake activity was indeed mediated by the inhibition of GSK3. Importantly, Hoechst 33342 stainings and cell counting experiments demonstrated that the increase in Aß uptake activity after GSK3 inhibitor treatment was not simply due to changes in the cellular proliferation of THP-1 cells and primary microglia cells. However, the MTT assays suggested an increase in the metabolic activity of primary microglia cells following GSK3 inhibitor treatment. This assay is based on the conversion of the tetrazolium dye MTT into formazan (Mueller *et al.* 2004). The rate of tetrazolium reduction reflects the metabolic activity and has been associated with the activity of mitochondrial enzymes (Berridge & Tan 1993). In this respect, it has been reported that

drug-induced changes in cell size and mitochondrial content could yield misleading results when screening compounds for proliferative activity (Chan *et al.* 2013). This is consistent with our findings as treatment of primary microglia cultures with GSK3 inhibitors led to enhanced formazan formation but not to increased cell numbers. This was also clearly different from a recent study in which an increase in Aß uptake by primary microglia cells after treatment with granulocyte-macrophage colony stimulating factor (GM-CSF) appeared to be largely driven by enhanced microglia proliferation (Daria et al. 2016). Interestingly, several studies have implicated GSK3ß in the regulation of mitochondrial proteins (Lim *et al.* 2016). However, it remains to be clarified how GSK3 inhibitiors influence the metabolic activity of primary microglia cells and how this might affect their Aß uptake activity.

In addition, the role of CDKs was investigated. Most of the ATP competitive GSK3 inhibitors also inhibit CDKs, due to the high sequence similarity of up to 86 % between the ATP binding sites of theses kinases (Eldar-Finkelman & Martinez 2011). CDKs are serine/threonine kinases that are involved in the regulation of the cell cycle and transcription (Malumbres 2014). In AD, dysregulation of CDK5 activity has been implicated in the disease pathogenesis through aberrant phosphorylation of its subtrates, including tau and APP (Liu *et al.* 2016a). Moreover, treatment of the microglia cell line BV-2 or primary microglia cultures with the CDK inhibitor roscovitine had been reported to reduce the uptake of Aß peptides (Ma *et al.* 2013b). In the present study, inhibition of CDKs in THP-1 cells by roscovitine or purvalanol A, two potent inhibitors of CDK1, CDK2 and CDK5 (Bain et al. 2003), showed no effect on the Aß uptake activity. Thus, a role for these CDKs in the cellular uptake of Aß could no be confirmed, at least in the THP-1 cellular model. More importantly, this indicated that the increase in Aß uptake after GSK3 inhibitor treatment did not result from an off-target effect of these compounds on CDK activity.

To confirm that the upregulation of Aß uptake activity after GSK3 inhibitor treatment was indeed mediated through their primary target GSK3, knock-down experiments were performed. SiRNA or esiRNA knock-down of the GSK3ß isoform in THP-1 cells by approximately 50% resulted in a significant upregulation of Aß uptake activity, albeit with a much smaller effect size compared to GSK3 inhibitor treatment. This might be explained by the remaining enzyme activity as GSK3ß protein levels were only partially reduced. In contrast, knock-down of the GSK3α isoform by 50 % showed no significant effects in the Aß uptake assay. Likewise, the combined knock-down of both isoforms showed no additive effects as compared to the single GSK3ß knock-down. These results suggest that GSK3ß but not GSK3α inhibition is critical for the observed effects of GSK3

inhibitors. Although both isoforms have been suggested to be involved in AD pathogenesis, differences in their tissue-specific distribution and functions have been reported. Whereas GSK3α has been implicated in the amyloidogenic processing of APP, GSK3ß has been associated with tau hyperphosphorylation (Kosik 1992, Phiel et al. 2003, Muyllaert *et al.* 2008). Both isoforms are highly expressed in neurons and glia cells, with GSK3α being particularly enriched in the hippocampus, cerebral cortex, striatum and cerebellum, whereas GSK3ß is found in nearly all human brain regions (Pandey *et al.* 2009, Kaidanovich-Beilin & Woodgett 2011). Deletion of the GSK3ß gene in mice was shown to be embryonically lethal, while GSK3α knock-out mice are viable and appear normal (Hoeflich *et al.* 2000, MacAulay *et al.* 2007). Furthermore, distinct changes in substrate phosphorylation were observed after GSK3 isoform-specific genetic deletion in the mouse brain, indicating differences in substrate specificity for each isoform (Soutar *et al.* 2010). GSK3 itself is differentially regulated by tyrosine and serine phosphorylation. Tyrosine phosphorylation leads to the activation of the enzyme (Tyr279 for GSK3α and Tyr216 for GSK3β), while phosphorylation of serine residues triggers inactivation (Ser21 for GSK3α and Ser9 for GSK3β) (Hughes *et al.* 1993, Sutherland *et al.* 1993). In a study by Gulen *et al*., it was reported that inactivation of GSK3α but not GSK3ß by phosphorylation selectively modulated IL-1-mediated regulation of the Th17 subtype of T cells (Gulen *et al.* 2012). Overall, the GSK3 isoforms appear to differ in certain regulatory functions, which might also apply to the modulation of Aß uptake activity.

Results of the GSK3ß knock-down experiments were further validated by CRISPR/Cas9-mediated knock-out of GSK3ß in THP-1 cells. Two specific sgRNAs targeting exons 1 and 4 of the *GSK3B* genomic region were designed and sequences were blasted to ensure minimal off-target potential. For each sgRNA one cell clone was obtained that likely represented a complete knock-out as GSK3ß expression was undetectable by Western blotting. Both GSK3ß knock-out cell lines demonstrated a considerable increase in Aß uptake activity as compared to the control cell line expressing a non-targeting sgRNA against EGFP. Importantly, after treatment of the GSK3ß knock-out cell lines with the GSK3 inhibitor CHIR99021, no further upregulation of Aß uptake activity was observed, showing that the GSK3ß knock-out phenotype indeed mimiced the effect of GSK3ß inhibitor treatment. Taken together, the confirmation of the GSK3ß knock-down phenotype with the CRISPR/Cas9 knock-out cell lines provided strong evidence that GSK3ß is mechanistically involved in the regulation of Aß uptake activity, and that GSK3 inhibitors upregulate Aß uptake through inhibition of their primary target GSK3.

The best characterized pathway that involves GSK3 is the canonical Wnt signaling pathway. GSK3 serves as a negative regulator of this pathway by constitutively phosphorylating ß-catenin, which targets the protein for proteasomal degradation (Doble & Woodgett 2003, Wu & Pan 2010). In the presence of a Wnt signal, phosphorylation of ß-catenin by GSK3 is inhibited, and stabilized ß-catenin translocates into the nucleus where it initiates the transcription of Wnt-responsive target genes. Consequently, changes in GSK3 activity are expected to alter ß-catenin levels. In the present study, it was assessed whether the Wnt pathway and ß-catenin-induced transcription had any mechanistic role in the upregulation of Aß uptake activity after GSK3 inhibitor treatment. Inhibition of GSK3 activity either by Wnt-3a stimulation or by GSK3 inhibitors resulted in a substantial increase in ß-catenin levels. However, Wnt-3a treatment alone had no effect on the Aß uptake activity of THP-1 macrophages. This result was further validated by overexpression of an active form of ß-catenin and a CRISPR/Cas9-mediated knock-out for ß-catenin in THP-1 macrophages. Neither overexpression nor a knock-out of ß-catenin had any impact on the basal Aß uptake activity of THP-1 cells. Moreover, the CHIR99021-mediated upregulation of Aß uptake activity was not different in wild type and ß-catenin knock-out THP-1 cells. These results indicated that the upregulation of Aß uptake activity was not dependent on ß-catenin or the transcription of ß-catenin responsive genes. In the context of AD, several studies have reported a downregulation of Wnt/ß-catenin signaling due to decreased ß-catenin levels or increased activity of Wnt signaling inhibitors like GSK3 (Rosi *et al.* 2010, Inestrosa *et al.* 2012, Oliva *et al.* 2013). Moreover, activation of Wnt signaling was reported to mediate neuroprotective effects in AD (Alvarez *et al.* 2004, Quintanilla *et al.* 2005). In rat hippocampal neurons, activation of the Wnt pathway by Wnt-3a was shown to block Aß-dependent toxic effects (Alvarez et al. 2004). In a more recent study, the authors reported similar effects with a GSK3 inhibitor for the indirect activation of Wnt signaling. They observed recovered ß-catenin levels and protection of hippocampal neurons from Aβ oligomer-induced neurotoxicity and apoptosis (Silva-Alvarez *et al.* 2013). Although our results did not provide evidence for an involvement of Wnt signaling in the cellular uptake of Aß, these studies suggest that activation of the Wnt pathway via Wnt ligands or inhibition of GSK3 might still represent a potential approach for AD treatment.

Numerous studies have investigated the internalization and degradation of Aß by microglia cells. Nevertheless, it has remained controversial how effective microglia are in the degradation of Aß. A study using *in vivo* imaging in an AD mouse model showed that microglia internalize Aß, and the ingested Aß was found to be localized to lysosomal

compartments of the cells, suggesting that microglia are engaged in the proteolytic degradation of Aß (Bolmont et al. 2008). In an earlier study by Frackowiak *et al.*, electron microscopy had been used to demonstrate the uptake of fibrillar Aß by microglia cells *in vitro*. These authors reported that the ingested Aß was stored in phagosomes for up to 20 days, indicating only limited effectiveness of microglia in degrading Aß fibrils (Frackowiak *et al.* 1992). In a study by Paresce *et al.*, the authors compared microglia degradation of Aß microaggregates with the degradation of acetylated low density lipoprotein and α2-macroglobulin. In line with the findings by Frackowiak *et al.,* they reported that, while Aß was ingested effectively and trafficked to the lysosomal compartment, degradation was very slow in comparison to the two other proteins (Paresce et al. 1997). Another study found that macrophages degraded fibrillar Aß efficiently, but limited digestion of the identical material was observed in microglia cells (Majumdar et al. 2008). In contrast, data from Mandrekar *et al*. showed efficient uptake and degradation of soluble Aß by microglia (Mandrekar et al. 2009). These discrepancies might have resulted from differences in the properties of the Aß preparations, in particular the use of aggregated, fibrillar versus soluble Aß peptides. Moreover, differences in the activation state of the cells might have played a role (Majumdar et al. 2008). In support of this idea, it has been shown that interferon-γ (IFN-γ) increased the intracellular retention of fibrillar Aß, whereas treatment with the anti-inflammatory cytokines IL-4, IL-10 and transforming growth factor-β1 (TGF-β1) enhanced Aß degradation by macrophages *in vitro* (Yamamoto *et al.* 2008). Furthermore, poor degradation of fibrillar Aß by cultured microglia has been suggested to result from low activity of lysosomal enzymes. Treatment with the cytokine macrophage colony stimulating factor (M-CSF) stimulated degradation of fibrillar Aß, which was attributed to increased acidity and hydrolytic activity of microglia lysosomes (Majumdar *et al.* 2007, Majumdar et al. 2008). In a study by Avrahami *et al.*, the authors reported that treatment with the GSK3 inhibitor L803-mts restored lysosomal acidification and reduced Aß deposition in an AD mouse model. *In vitro* studies confirmed that GSK3 activity impaired lysosomal acidification (Avrahami *et al.* 2013). We also investigated the impact of GSK3 inhibition on Aß degradation by THP-1 macrophages. Western blot analysis showed increased levels of intracellular Aß in cells treated with GSK3 inhibitors, indicating increased Aß uptake and confirming the results of the uptake assays with FAM-A$ß_{42}$. However, GSK3 inhibition had no effect on the degradation rate of the internalized peptides in THP-1 cells as monitored by ELISA. After 4 h, intracellular Aß levels were reduced by approximately 75 % in both the control and CHIR99021-treated THP-1 cells, indicating that intracellular Aß was degraded in both experimental groups with similar

efficacy. For these degradation assays, unlabeled $Aß_{42}$ was used, which was not subjected to fibrillization. Similar to our findings, Mandrekar *et al.* observed that approximately 50 % of internalized soluble Aß peptides were degraded after 3 h in a microglial cell line and in primary microglia cells (Mandrekar et al. 2009). Of note, in an earlier study by Chung *et al.*, it was reported that over 80 % of the internalized soluble Aß peptides were re-secreted back into the culture medium (Chung et al. 1999). In contrast, this was not observed in the study by Mandrekar *et al.* (Mandrekar et al. 2009).

To test whether a proinflammatory environment would block or attenuate the upregulation of Aß uptake activity by GSK3 inhibitors, THP-1 macrophages were treated with the bacterial membrane component LPS, which has been commonly used to model inflammation (Lien *et al.* 2000, Lehnardt *et al.* 2003, Koenigsknecht-Talboo & Landreth 2005, Awada *et al.* 2014). Stimulation of microglia cells and THP-1 macrophages with LPS triggers the production of inflammatory cytokines, and the activation of microglia by LPS has been shown to result in neuronal loss *in vitro* and in *in vivo* models (Chanput et al. 2010, Lehnardt et al. 2003). Moreover, it has been shown that LPS exposure could suppress phagocytosis by primary mouse macrophages, which was attributed to the effect of LPS on the cytoskeletal network (Wonderling *et al.* 1996). In another study by Feng *et al*., it has been demonstrated that LPS-mediated suppression of macrophage phagocytosis was partly due to the induction of TNF-α (Feng *et al.* 2011). These data indicated that a pro-inflammatory environment might suppress the uptake activity of macrophages and microglia cells, and thereby inhibit the clearance of Aß deposits in the AD brain. Further supporting this idea, cellular uptake capacity could be be restored by coincubation with anti-inflammatory cytokines and the non-steroidal anti-inflammatory drug ibuprofen (Koenigsknecht-Talboo & Landreth 2005). In most studies, LPS doses between 10 ng and 1 µg/ml had been used to induce a neuroinflammatory response. We used 0.5 and 1 µg/ml LPS, and LPS treatment did not impair the basal Aß uptake activity of THP-1 macrophages. These seemingly contradictory results might reflect differences in the LPS response between mouse and human macrophages and in the LPS concentrations used in the studies mentioned above. In this respect, it has been reported that different human macrophage cell lines showed dramatically different changes in gene expression in response to LPS treatment (Sharif et al. 2007, Genin *et al.* 2015). Moreover, LPS treatment reduced the upregulation of Aß uptake activity in response to the GSK3 inhibitor CHIR99021. Overall, these observations indicated that inflammatory conditions induced by LPS might negatively affect Aß uptake activity but that the stimulatory effect of GSK3 inhibitors was still detectable.

Intriguingly, our experiments also indicated that treatment with GSK3 inhibitors had a modifiying effect on the activation state of primary microglia cells. Microglia can undergo diverse morphological and functional changes in response to various environmental signals (Karperien et al. 2013). The complexity of the microglia response to different stimuli has been simplified and categorized into two functional phenotypes, known as the classical pro-inflammatory M1 phenotype and the alternative anti-inflammatory M2 state (Tang & Le 2016). Interestingly, oligomeric Aß was found to be a more potent M1-inducer than fibrillar Aß (Michelucci *et al.* 2009). Studies investigating the activation state of microglia in cortical tissues from AD mouse models and AD patients demonstrated a mixed profile of alternative activation and classical activation genes, indicating heterogeneous, functional phenotypes of microglia cells in AD (Colton *et al.* 2006, Sudduth *et al.* 2013). In a recent study by Keren-Shaul *et al.*, single-cell RNA sequencing was used to identify molecular characteristics of microglia subtypes in an AD mouse model and wild-type control animals (Keren-Shaul *et al.* 2017). The authors discovered two additional microglia subtypes in the AD mice, defined as disease-associated microglia (DAMs), which were absent from the healthy animals. These DAM microglia showed a reduction in the expression levels of certain homeostatic genes, e.g. the chemokine receptor Cx3Cr1 and the purinergic receptors P2ry12/P2ry13, whereas several AD-related genes, including *APOE* and *TREM2*, were upregulated. Furthermore, these cells were found to be localized near Aß plaques and contained intracellular Aß particles. Multiple studies have hypothesized that TREM2 is important for the phagocytic activity of microglia cells (Kleinberger et al. 2014, Xiang *et al.* 2016, Yeh *et al.* 2016). Moreover, several studies in AD mouse models have consistently reported that TREM2 deficiency leads to reduced microglia and macrophage accumulation around amyloid deposits (Ulrich et al. 2014, Jay et al. 2015, Wang et al. 2015). Knock-out of TREM2 also reduced the efficacy of antibody-mediated Aβ clearance in an AD mouse model (Xiang et al. 2016). Consequently, the DAM profile has been suggested to reflect a protective state of microglia cells (Keren-Shaul et al. 2017). However, in another recent report, the TREM2-APOE pathway was shown to induce a phenotypic switch from a homeostatic to a neurodegenerative microglia phenotype (Krasemann *et al.* 2017). Thus, further investigations are required to clarify whether the TREM2-dependent transcriptional profile of microglia cells is beneficial or detrimental. In addition, it is not clear how these novel microglia activation states exemplified by the DAM profile conform to the older categorization of microglia into M1 and M2 states. In our study, treatment of primary microglia with GSK3 inhibitors resulted in a transition from an amoeboid or rod-like shape to a ramified morphology with several long processes and enhanced branching. This

change in morphology was accompanied by the upregulation of two cell surface receptors CD36 and IL-4R, which have been linked to the anti-inflammatory M2 activation state (Martinez et al. 2006, Zhao *et al.* 2015, Liu *et al.* 2016b). These findings indicated that GSK3 inhibitors were able to induce a morphological and functional transition of primary microglia towards an anti-inflammatory (M2-like) state with increased Aß uptake activity. This result is also consistent with GSK3 being a central regulator of inflammatory processes, and with previous reports, which had demonstrated that GSK3 inhibitors can attenuate inflammatory actions of microglia cells (Beurel & Jope 2008, Yuskaitis & Jope 2009, Wang et al. 2010). Interestingly, TREM2 expression was downregulated after the treatment of THP-1 macrophages and primary microglia cells with CHIR99021, indicating that the Aß uptake mechanism was likely not dependent on TREM2.

Different endocytic mechanisms have been proposed for the uptake of Aß peptides by microglia cells. It is widely accepted that microglia internalize fibrillar Aß via phagocytosis, a process that enables the uptake of larger particles through the interaction with cell surface receptors (Stuart & Ezekowitz 2005). A range of cell surface receptors have been implicated in the interaction with fibrillar Aß, including a receptor complex consisting of CD36, α6β1 integrin and the integrin associated protein CD47 (Bamberger et al. 2003, Koenigsknecht & Landreth 2004). In contrast, soluble Aß was cleared by microglia cells through a macropinocytic mechanism (Mandrekar et al. 2009). Macropinocytosis allows the efficient and non-selective cellular uptake of solute macromolecules from the extracellular milieu and involves the formation and internalization of vesicles from membrane ruffles, which is an actin and tubulin dependent process (Swanson & Watts 1995). Interestingly, treatment with GSK3 inhibitors also resulted in increased uptake of *E. coli* particles by THP-1 macrophages and mouse primary microglia, indicating that the uptake mechanism was not specific for Aß. The uptake of both Aß and *E. coli* particles was markedly reduced in the presence of the actin polymerization inhibitor cytochalasin D, which strongly supported a role for actin polymerization in the uptake mechanism. Cytochalasin D is a metabolite known to block both the polymerization and depolymerization of actin subunits, resulting in inhibition of actin-dependent endocytic pathways (Flanagan & Lin 1980, Cooper 1987, Lamaze *et al.* 1997). The increased uptake of both Aß and *E. coli* particles suggested the induction of a non-specific and receptor-independent internalization process, likely a macropinocytic uptake mechanism rather than receptor-mediated phagocytosis. In a study by Bosedasgupta *et al.*, macropinocytosis was shown to be responsible for the uptake of

microbial material and particles by macrophages (Bosedasgupta & Pieters 2014). However, further efforts are needed to better characterize the Aß uptake mechanism that is stimulated by GSK3 inhibitors. In this respect, amiloride, an inhibitor of Na^+/H^+-exchangers, was shown to effectively block membrane ruffling and macropinocytosis and might therefore be useful to distinguish between the different uptake mechanisms (Meier *et al.* 2002, Koivusalo *et al.* 2010).

A number of studies had indicated that secreted factors might be able to stimulate the uptake activity of macrophages and microglia cells. For instance, neuropeptides, which can be secreted by neurons, were shown to increase Aβ uptake by microglia in a concentration-dependent manner (Fleisher-Berkovich et al. 2010). In a more recent study by Daria *et al.*, the dysfunction of old microglia was reported to be restored by factors secreted by young microglia (Daria et al. 2016). To test whether the stimulation of Aß uptake activity by GSK3 inhibitors was potentially mediated by a secreted protein, experiments with conditioned media collected from GSK3 inhibitor-treated cells were performed. Treatment of THP-1 cells with these conditioned media did not stimulate the uptake of Aß indicating that the effect of GSK3 inhibitors was likely not mediated by a secreted protein. However, these experiments might not be fully conclusive for two reasons. First, the concentration of the secreted proteins could have been too low as the conditioned media had to be diluted with fresh medium to avoid cytotoxic effects. Second, it cannot be excluded that potentially relevant small proteins were eliminated by filtration through a 4 kDa molecular weight cut-off filter, which was used to remove the GSK3 inhibitor CHIR99021 from the conditioned media.

Importantly, the stimulatory effect of GSK3 inhibitors on Aß uptake activity was abolished by coincubation with Actinomycin D, a widely used transcriptional inhibitor (Trang *et al.* 2009, Koscso *et al.* 2012, Yamanaka et al. 2012). This suggested that the stimulatory effect was dependent on *de novo* mRNA and protein synthesis. Therefore, to gain further insight into the molecular pathways by which GSK3 inhibition might stimulate Aß uptake activity, a DNA microarray-based gene expression analysis of GSK3 inhibitor-treated THP-1 macrophages was performed. Microarray technology had been widely used in previous reports to study the response of macrophages to different stimuli (McGuire & Glass 2005, Martinez et al. 2006, Xue *et al.* 2014, Yoshida *et al.* 2016). The microarray data identified a set of 2101 overlapping genes that were similarly regulated by three different GSK3 inhibitors with almost 100 % concordance regarding the up- or downregulation of gene expression. Quantitative PCR analysis verified the results of the

microarray analysis for all examined genes, indicating that the microarray provided a robust and reproducible comparison of transcript levels. Gene Ontology (GO) classification and Ingenuity Pathway Analysis (IPA) were performed for the set of overlapping genes and revealed that pathways related to the immune response and cytokine signaling were particularly enriched. Moreover, several of the identified, differentially expressed genes were closely associated with microglia/macrophage activation, endocytosis and AD, and therefore represented potentially interesting candidate proteins. Out of these, the chemokines CCL2, CCL3 and CCL7, the cell surface receptors TREM1, CD163, LDLR, STAB1 and CD44, the matrix proteins THBS1 and MMP10, the cytosolic receptor NLRP3 and the small GTPase CDC42 were chosen to further investigate their potential role in the stimulation of Aß uptake activity.

Using CRISPR/Cas9 gene editing, THP-1 macrophages with a partial knock-out for all of the selected microarray candidate genes were obtained, on average showing 60-90 % reduction of target gene expression. The efficacy to generate homozygous knock-outs can vary due to differences in sgRNA production, complex formation with Cas9, and cleavage efficiency (Wang *et al.* 2014). Cas9-induced double strand DNA breaks can be repaired via endogenous DNA repair mechanisms, resulting in a mixture of wild type alleles and hetero- and homozygously mutated target genes. Consequently, single cell cloning is required to obtain a uniformly modified cell population. In our study, the isolation of true single cell clones was complicated due to the fact that THP-1 cells are growing in suspension. Thus, in many cases, the obtained cell populations were likey derived from more than one cell leading to a mixture of different genotypes. Clearly, it cannot be excluded that for some genes a complete knock-out would have been required to uncover a phenotype. Nevertheless, even a partial knock-out of a gene mechanistically involved in the upregulation of Aß uptake activity would have been expected to at least reduce the stimulatory effect of GSK3 inhibitors. The cytokine CCL2 was the most highly induced gene in response to all three GSK3 inhibitors. CCL2 mediates its effects through the receptor CC chemokine receptor 2 (CCR2), and it is one of the central chemokines that promote the migration of microglia and macrophages to sites of inflammation. In numerous studies, CCL2 has been associated with both inflammatory and anti-inflammatory activities, indicating a complex role of CCL2 in the regulation of cytokine-specific immune responses (Deshmane *et al.* 2009). The CCL2-CCR2 axis has been implicated in the downregulation of pro-inflammatory cytokine production in macrophages (Sierra-Filardi *et al.* 2014). In contrast, in a recent study by Carson *et al.,* CCL2 was implicated in the classical activation of macrophages by stimulating pro-inflammatory gene expression (Carson *et al.* 2017). In AD patients, CCL2

levels have been found to be elevated in the serum and cerebrospinal fluid (CSF) (Galimberti *et al.* 2006b, Galimberti *et al.* 2006a). At early stages of the disease, higher CSF CCL2 levels were associated with faster cognitive decline (Westin *et al.* 2012). Likewise, CCL2 overexpression in mouse models of AD increased Aß deposition and accelerated deficits in spatial and working memory (Kiyota et al. 2009, Yamamoto *et al.* 2005). Interestingly, the authors reported that the uptake of Aß by microglia cells was significantly enhanced by CCL2 (Kiyota et al. 2009). In agreement, significant impairments in the clearance of both monomeric and oligomeric Aβ by CCL2-deficient microglia cells were demonstrated, resulting in increased Aß deposition in the brain (Kiyota et al. 2013). Taken together, similar outcomes were demonstrated in CCL2-overexpressing and deficient AD mice. However, in our study, neither a partial knock-out of CCL2 nor the treatment of THP-1 cells with recombinant CCL2 had any impact on the Aß uptake activity, indicating that this chemokine is not responsible for the stimulatory effect of GSK3 inhibitors.

Out of the 11 remaining candidate genes for which THP-1 cell lines with substantially reduced expression were generated, two appeared to have an impact in the FAM-Aß uptake assay. In intial experiments, partial knock-out cell lines for the TREM1 receptor and the small GTPase CDC42 displayed a smaller effect size after treatment with the GSK3 inhibitor CHIR99021 as compared to wild type cells, suggesting that these two candidates might be involved in the stimulation of Aß uptake activity by GSK3 inhibitors. In particular, *TREM1* represented an interesting candidate gene potentially involved in the regulation of Aß uptake activity. In the microarray analysis, TREM1 expression was induced up to 15 fold by the GSK3 inhibitor CHIR99021. In 2015, Replogle *et al.* had provided evidence for a genetic link between a common, intronic sequence variant of *TREM1* and increased amyloid plaque burden in the brains of AD patients (Replogle et al. 2015). This *TREM1* variant was further associated with decreased expression of TREM1 on the surface of myeloid cells. In addition, in a recent study by Jiang *et al.,* the same *TREM1* variant reduced the ability of human monocytes for Aß phagocytosis (Jiang et al. 2016). These authors observed a 50 % reduction of internalized $Aß_{42}$ in primary mouse microglia after *TREM1* knock-down, while overexpression of *TREM1* increased the internalization of Aß42 1.7 fold. *In vivo* experiments revealed significantly increased levels of insoluble and soluble $Aß_{42}$ in the cerebral cortex of an AD mouse model after *TREM1* knock-down. In contrast, *TREM1* overexpression significantly reduced the total amyloid burden in the brains of these mice by around 60 % (Jiang et al. 2016). *TREM1* shares relatively low sequence homology with its family member *TREM2* (Radaev *et al.* 2003). While the genetic and functional findings for *TREM1* are clearly not

as strong and convincing as the studies implicating *TREM2* in the pathogenesis of AD (Kleinberger et al. 2014, Ulrich et al. 2014, Jay et al. 2015, Wang et al. 2015, Xiang et al. 2016), they nevertheless indicate that high surface expression of *TREM1* might promote Aß uptake by macrophages and microglia cells. In addition, other research groups have also reported that silencing of *TREM1* expression impaired the phagocytic capacity of macrophages (Hommes et al. 2014, Li et al. 2016). However, in our studies, the initially observed TREM1 phenotype could not be confirmed in two additional knock-out cell lines with sgRNAs targeting different regions of the *TREM1* gene, which indicated a false positive result. Although Cas9-induced gene mutations occur at target sites localized adjacent to a PAM sequence, the relatively short 20-bp sgRNA can lead to off-target mutations by targeting sites in different genes that share a similar sequence (Kuscu *et al.* 2014). In addition, the stress of cell cloning and antibiotic treatment can promote the selection of unwanted phenotypes. Consequently, to reduce the risk of non-specific phenotypes either due to off-target mutations or to clonal effects, at least two sgRNAs should be investigated for each target gene.

In contrast to TREM1, two cell clones expressing a second sgRNA against CDC42 also reduced the stimulatory effect of the GSK inhibitor CHIR99021, confirming the phenotype seen with the first sgRNA. These results suggested that CDC42 might indeed be involved in the stimulation of Aß uptake activity by GSK3 inhibitors. In the microarray analysis, CDC42 expression was up to 2 fold upregulated (CHIR99021, Bio-Acetoxime). *CDC42* (cell division cycle 42) encodes a small GTPase protein that belongs to the Rho (Ras homologue) GTPase family and plays an important role in the rearrangement of the actin cytoskeleton (Tapon & Hall 1997). Rho GTPases share a highly conserved GTPase domain and act as molecular switches that cycle between an active GTP-bound and an inactive GDP-bound state. Among the 25 known human Rho GTPase proteins, the roles of RhoA, Rac1 (Ras-related C3 botulinum toxin substrate 1) and CDC42 in controlling actin organization are best understood (Caron & Hall 1998, Wennerberg & Der 2004, Mao & Finnemann 2015). Rho GTPase activity in cells is tightly controlled by three types of regulators. The formation of the GTP-bound, active state is catalysed by upstream guanine nucleotide exchange factors (GEFs), while GTP hydrolysis is induced by GTPase activating proteins (GAPs). The third type of regulators, the guanine nucleotide dissociation inhibitors (GDIs), stabilize the GDP-bound form and prevent activation (Cherfils & Zeghouf 2013). Activated CDC42 regulates downstream functions by interacting with different cytosolic effector proteins. Besides cytoskeleton organization, CDC42 activity has been implicated in numerous other cell functions including

transcription, cell cycle progression and vesicle trafficking (Melendez *et al.* 2011). Activation of CDC42 was shown to induce the formation of short actin filaments and is required for the formation of highly dynamic cell surface protrusions called filopodia (Nobes & Hall 1995). Activated CDC42 binds actin regulatory proteins and induces the Arp2/3-mediated polymerisation of new actin filaments (Pollard 2007). Due to its role in actin remodeling, CDC42 has been implicated in the regulation of phagocytosis and macropinocytosis, two actin-dependent processes (Kerr & Teasdale 2009, Mao & Finnemann 2015). Using fluorescence resonance energy transfer (FRET) imaging, active CDC42 was found to colocalize with filamentous actin (F-actin) during the formation of the phagocytic cup, which engulfs target particles (Hoppe & Swanson 2004). In line with this observation, inhibition of CDC42 as well as expression of a dominant-negative mutant form of CDC42 decreased the phagocytosis of apoptotic cells by macrophages (Leverrier & Ridley 2001, Nakaya *et al.* 2006). CDC42 was also shown to drive the actin remodeling required for macropinocytosis (Koivusalo et al. 2010). In mature dendritic cells, which downregulate macropinocytosis after differentiation, the levels of GTP-bound CDC42 were markedly reduced in comparison to immature cells (Garrett *et al.* 2000). Intriguingly, the authors observed reactivation of macropinocytosis in mature dendritic cells following injection of constitutively active CDC42. Taken together, these results strongly support a central role of CDC42 in the regulation of both phago- and macropinocytosis.

To further confirm a role for CDC42 in the upregulation of Aß uptake activity by GSK3 inhibitors, CDC42 activity could also be experimentally manipulated by overexpression of either constitutively active or dominant negative mutants of CDC42 in THP-1 cells. It might also be of interest to investigate the role of CDC42 downstream effector proteins, which could result in the identification of additional protein targets that are mechanistically involved in the regulation of Aß uptake activity. While CDC42 mRNA expression was upregulated in THP-1 cells following GSK3 inhibitor treatment, qPCR measurements did not confirm upregulation of CDC42 expression in primary microglia after CHIR99021 treatment. The discrepancy of these results might arise from potential differences in the response to GSK3 inhibitors between human macrophages and mouse microglia cells. The two cell types might share GSK3 as the main upstream regulator but might differ in the expression and activation of downstream effectors. In this regard, the other closely related Rho GTPases might be of particular relevance. For example, it has recently been reported that RhoA is involved in the regulation of phagocytosis by the murine microglial cell line BV-2 (Scheiblich & Bicker 2017). In addition, CDC42 regulatory proteins like GEFs, GAPs and GDIs might be differentially expressed in primary microglia

cells after GSK3 inhibitor treatment, leading to the same outcome (increased CDC42 activity and Aß uptake activity) through a slightly different molecular mechanism. In this respect, it would be informative to determine whether the amount of the active GTP-bound form of CDC42 is increased in primary microglia cells after GSK3 inhibition despite the unchanged mRNA expression of CDC42.

Aside from further mechanistic studies, it would seem important to confirm that GSK3 inhibitors are indeed able to modulate the uptake and clearance of Aß and the behaviour of microglia cells *in vivo*. Improved GSK3 inhibitors, which are available today, should allow to perform more definitive pharmacological treatment experiments in AD animal models. For example, CHIR99021 has been shown to modulate behavioural phenotypes in mice following intraperitoneal administration (Pan et al. 2011). In addition, intravenous injection of CHIR98014, another aminopyrimidine derivative from the CHIR series of GSK3 inhibitors, resulted in a dose-dependent reduction of tau phosphorylation in the cortex and hippocampus of a postnatal rat model (Selenica *et al.* 2007). These data indicated effective crossing of the blood-brain barrier by these compounds. The effects of GSK3 inhibition could also be further characterized *ex vivo* by culturing brain slices of amyloid plaque-bearing mice with primary microglia cells in the presence of GSK3 inhibitors (Daria et al. 2016). In such experiments it might also be of interest to cultivate microglia cells from aged animals to examine whether GSK3 inhibitors could improve or reverse the dysfunction of old microglia cells in the uptake and clearance of Aß deposits (Krabbe et al. 2013, Hellwig et al. 2015, Daria et al. 2016). Furthermore, the characterization of microglia cells from GSK3ß knock-out mice might represent another interesting approach.

In summary, the experiments performed in this thesis demonstrated that structurally divergent GSK3 inhibitors stimulated the uptake of Aß peptides by human THP-1 macrophages and primary murine microglia cells in a dose-dependent manner, without effects on the cellular degradation rate of Aß. In primary microglia, this was accompanied by a ramified morphology and upregulation of the CD36 and IL-4R cell surface receptors, indicating the transition to an anti-inflammatory activation state. GSK3 inhibitors similarly enhanced the uptake of *E. Coli* particles suggesting a receptor-independent, macropinocytic uptake mechanism. Importantly, both siRNA knockdown and CRISPR/Cas9 knockout experiments in THP-1 cells confirmed that the stimulatory effect of GSK3 inhibitors was mediated by their primary target GSK3, with a critical role for the GSK3ß isoform. Further studies showed that the stimulation of Aß uptake by GSK3

inhibitors required *de novo* transcription. A microarray-based gene expression analysis of THP-1 cells identified a subset of genes similarly altered by three different GSK3 inhibitors, including genes encoding cytokines and surface receptors implicated in the regulation of microglia activation and endocytosis. Subsequently, extensive CRISPR/Cas9 candidate gene analysis revealed a role for CDC42 in the stimulation of Aß uptake by GSK3 inhibitors. In agreement with GSK3 being a central regulator of inflammatory pathways (Beurel & Jope 2008, Yuskaitis & Jope 2009, Wang et al. 2010), our findings that GSK3 inhibitors stimulate the uptake of Aß peptides by microglia cells provide a novel molecular explanation for their beneficial effects in AD animal models. They further indicate that pharmacological targeting of GSK3 or its downstream effector pathways could provide a way to overcome impaired Aß clearance and limit its accumulation in AD.

6 References

Abraha, A., Ghoshal, N., Gamblin, T. C., Cryns, V., Berry, R. W., Kuret, J. and Binder, L. I. (2000) C-terminal inhibition of tau assembly in vitro and in Alzheimer's disease. *Journal of cell science,* **113 Pt 21,** 3737-3745.

Aderem, A. and Underhill, D. M. (1999) Mechanisms of phagocytosis in macrophages. *Annual review of immunology,* **17,** 593-623.

Aizenstein, H. J., Nebes, R. D., Saxton, J. A. et al. (2008) Frequent amyloid deposition without significant cognitive impairment among the elderly. *Archives of neurology,* **65,** 1509-1517.

Ajami, B., Bennett, J. L., Krieger, C., McNagny, K. M. and Rossi, F. M. (2011) Infiltrating monocytes trigger EAE progression, but do not contribute to the resident microglia pool. *Nature neuroscience,* **14,** 1142-1149.

Ajami, B., Bennett, J. L., Krieger, C., Tetzlaff, W. and Rossi, F. M. (2007) Local self-renewal can sustain CNS microglia maintenance and function throughout adult life. *Nature neuroscience,* **10,** 1538-1543.

Alvarez, A. R., Godoy, J. A., Mullendorff, K., Olivares, G. H., Bronfman, M. and Inestrosa, N. C. (2004) Wnt-3a overcomes beta-amyloid toxicity in rat hippocampal neurons. *Experimental cell research,* **297,** 186-196.

Alzheimer, A. (1907) Über eine eigenartige Erkrankung der Hirnrinde. *Allgemeine Zeitschrift für Psychiatrie und Psychisch-gerichtliche Medizin,* **64,** 146-148.

Andrew, R. J., Kellett, K. A., Thinakaran, G. and Hooper, N. M. (2016) A Greek Tragedy: The Growing Complexity of Alzheimer Amyloid Precursor Protein Proteolysis. *The Journal of biological chemistry,* **291,** 19235-19244.

Anthony, J. C., Breitner, J. C., Zandi, P. P., Meyer, M. R., Jurasova, I., Norton, M. C. and Stone, S. V. (2000) Reduced prevalence of AD in users of NSAIDs and H2 receptor antagonists: the Cache County study. *Neurology,* **54,** 2066-2071.

Aplin, A. E., Gibb, G. M., Jacobsen, J. S., Gallo, J. M. and Anderton, B. H. (1996) In vitro phosphorylation of the cytoplasmic domain of the amyloid precursor protein by glycogen synthase kinase-3beta. *Journal of neurochemistry,* **67,** 699-707.

Araki, N., Johnson, M. T. and Swanson, J. A. (1996) A role for phosphoinositide 3-kinase in the completion of macropinocytosis and phagocytosis by macrophages. *The Journal of cell biology,* **135,** 1249-1260.

Arias-Salvatierra, D., Silbergeld, E. K., Acosta-Saavedra, L. C. and Calderon-Aranda, E. S. (2011) Role of nitric oxide produced by iNOS through NF-kappaB pathway in migration of cerebellar granule neurons induced by Lipopolysaccharide. *Cellular signalling,* **23,** 425-435.

Arnold, S. E., Hyman, B. T., Flory, J., Damasio, A. R. and Van Hoesen, G. W. (1991) The topographical and neuroanatomical distribution of neurofibrillary tangles and neuritic plaques in the cerebral cortex of patients with Alzheimer's disease. *Cerebral cortex,* **1,** 103-116.

Avrahami, L., Farfara, D., Shaham-Kol, M., Vassar, R., Frenkel, D. and Eldar-Finkelman, H. (2013) Inhibition of glycogen synthase kinase-3 ameliorates beta-amyloid pathology and restores lysosomal acidification and mammalian target of rapamycin activity in the Alzheimer disease mouse model: in vivo and in vitro studies. *The Journal of biological chemistry,* **288,** 1295-1306.

Awada, R., Saulnier-Blache, J. S., Gres, S., Bourdon, E., Rondeau, P., Parimisetty, A., Orihuela, R., Harry, G. J. and d'Hellencourt, C. L. (2014) Autotaxin downregulates LPS-induced microglia activation and pro-inflammatory cytokines production. *Journal of cellular biochemistry,* **115,** 2123-2132.

Bacskai, B. J., Kajdasz, S. T., Christie, R. H., Carter, C., Games, D., Seubert, P., Schenk, D. and Hyman, B. T. (2001) Imaging of amyloid-beta deposits in brains of

living mice permits direct observation of clearance of plaques with immunotherapy. *Nature medicine,* **7,** 369-372.

Bain, J., McLauchlan, H., Elliott, M. and Cohen, P. (2003) The specificities of protein kinase inhibitors: an update. *The Biochemical journal,* **371,** 199-204.

Bamberger, M. E., Harris, M. E., McDonald, D. R., Husemann, J. and Landreth, G. E. (2003) A cell surface receptor complex for fibrillar beta-amyloid mediates microglial activation. *The Journal of neuroscience : the official journal of the Society for Neuroscience,* **23,** 2665-2674.

Bard, F., Barbour, R., Cannon, C. et al. (2003) Epitope and isotype specificities of antibodies to beta -amyloid peptide for protection against Alzheimer's disease-like neuropathology. *Proceedings of the National Academy of Sciences of the United States of America,* **100,** 2023-2028.

Bard, F., Cannon, C., Barbour, R. et al. (2000) Peripherally administered antibodies against amyloid beta-peptide enter the central nervous system and reduce pathology in a mouse model of Alzheimer disease. *Nature medicine,* **6,** 916-919.

Benilova, I., Gallardo, R., Ungureanu, A. A. et al. (2014) The Alzheimer disease protective mutation A2T modulates kinetic and thermodynamic properties of amyloid-beta (Abeta) aggregation. *The Journal of biological chemistry,* **289,** 30977-30989.

Bergmans, B. A. and De Strooper, B. (2010) gamma-secretases: from cell biology to therapeutic strategies. *The Lancet. Neurology,* **9,** 215-226.

Berridge, M. V. and Tan, A. S. (1993) Characterization of the cellular reduction of 3-(4,5-dimethylthiazol-2-yl)-2,5-diphenyltetrazolium bromide (MTT): subcellular localization, substrate dependence, and involvement of mitochondrial electron transport in MTT reduction. *Archives of biochemistry and biophysics,* **303,** 474-482.

Bertram, L. and Tanzi, R. E. (2005) The genetic epidemiology of neurodegenerative disease. *The Journal of clinical investigation,* **115,** 1449-1457.

Beurel, E. (2011) Regulation by glycogen synthase kinase-3 of inflammation and T cells in CNS diseases. *Frontiers in molecular neuroscience,* **4,** 18.

Beurel, E., Grieco, S. F. and Jope, R. S. (2015) Glycogen synthase kinase-3 (GSK3): regulation, actions, and diseases. *Pharmacology & therapeutics,* **148,** 114-131.

Beurel, E. and Jope, R. S. (2008) Differential regulation of STAT family members by glycogen synthase kinase-3. *The Journal of biological chemistry,* **283,** 21934-21944.

Beurel, E. and Jope, R. S. (2009) Lipopolysaccharide-induced interleukin-6 production is controlled by glycogen synthase kinase-3 and STAT3 in the brain. *Journal of neuroinflammation,* **6,** 9.

Beurel, E., Michalek, S. M. and Jope, R. S. (2010) Innate and adaptive immune responses regulated by glycogen synthase kinase-3 (GSK3). *Trends in immunology,* **31,** 24-31.

Bleharski, J. R., Kiessler, V., Buonsanti, C., Sieling, P. A., Stenger, S., Colonna, M. and Modlin, R. L. (2003) A role for triggering receptor expressed on myeloid cells-1 in host defense during the early-induced and adaptive phases of the immune response. *Journal of immunology,* **170,** 3812-3818.

Blennow, K., Mattsson, N., Scholl, M., Hansson, O. and Zetterberg, H. (2015) Amyloid biomarkers in Alzheimer's disease. *Trends in pharmacological sciences,* **36,** 297-309.

Block, M. L., Zecca, L. and Hong, J. S. (2007) Microglia-mediated neurotoxicity: uncovering the molecular mechanisms. *Nature reviews. Neuroscience,* **8,** 57-69.

Blum-Degen, D., Muller, T., Kuhn, W., Gerlach, M., Przuntek, H. and Riederer, P. (1995) Interleukin-1 beta and interleukin-6 are elevated in the cerebrospinal fluid of Alzheimer's and de novo Parkinson's disease patients. *Neuroscience letters,* **202,** 17-20.

Boissonneault, V., Filali, M., Lessard, M., Relton, J., Wong, G. and Rivest, S. (2009) Powerful beneficial effects of macrophage colony-stimulating factor on beta-amyloid deposition and cognitive impairment in Alzheimer's disease. *Brain : a journal of neurology,* **132,** 1078-1092.

Bolmont, T., Haiss, F., Eicke, D., Radde, R., Mathis, C. A., Klunk, W. E., Kohsaka, S., Jucker, M. and Calhoun, M. E. (2008) Dynamics of the microglial/amyloid interaction indicate a role in plaque maintenance. *The Journal of neuroscience : the official journal of the Society for Neuroscience,* **28,** 4283-4292.

Bolstad, B. M., Irizarry, R. A., Astrand, M. and Speed, T. P. (2003) A comparison of normalization methods for high density oligonucleotide array data based on variance and bias. *Bioinformatics,* **19,** 185-193.

Bosedasgupta, S. and Pieters, J. (2014) Inflammatory stimuli reprogram macrophage phagocytosis to macropinocytosis for the rapid elimination of pathogens. *PLoS pathogens,* **10,** e1003879.

Bouchon, A., Dietrich, J. and Colonna, M. (2000) Cutting edge: inflammatory responses can be triggered by TREM-1, a novel receptor expressed on neutrophils and monocytes. *Journal of immunology,* **164,** 4991-4995.

Bouchon, A., Facchetti, F., Weigand, M. A. and Colonna, M. (2001) TREM-1 amplifies inflammation and is a crucial mediator of septic shock. *Nature,* **410,** 1103-1107.

Brawek, B., Schwendele, B., Riester, K., Kohsaka, S., Lerdkrai, C., Liang, Y. and Garaschuk, O. (2014) Impairment of in vivo calcium signaling in amyloid plaque-associated microglia. *Acta neuropathologica,* **127,** 495-505.

Bruttger, J., Karram, K., Wortge, S. et al. (2015) Genetic Cell Ablation Reveals Clusters of Local Self-Renewing Microglia in the Mammalian Central Nervous System. *Immunity,* **43,** 92-106.

Burdick, D., Soreghan, B., Kwon, M., Kosmoski, J., Knauer, M., Henschen, A., Yates, J., Cotman, C. and Glabe, C. (1992) Assembly and aggregation properties of synthetic Alzheimer's A4/beta amyloid peptide analogs. *The Journal of biological chemistry,* **267,** 546-554.

Burns, A. and Iliffe, S. (2009) Alzheimer's disease. *Bmj,* **338,** b158.

Burns, A., Jacoby, R. and Levy, R. (1990) Psychiatric phenomena in Alzheimer's disease. IV: Disorders of behaviour. *The British journal of psychiatry : the journal of mental science,* **157,** 86-94.

Burns, J. C., Friedmann, T., Driever, W., Burrascano, M. and Yee, J. K. (1993) Vesicular stomatitis virus G glycoprotein pseudotyped retroviral vectors: concentration to very high titer and efficient gene transfer into mammalian and nonmammalian cells. *Proceedings of the National Academy of Sciences of the United States of America,* **90,** 8033-8037.

Cacabelos, R., Barquero, M., Garcia, P., Alvarez, X. A. and Varela de Seijas, E. (1991) Cerebrospinal fluid interleukin-1 beta (IL-1 beta) in Alzheimer's disease and neurological disorders. *Methods and findings in experimental and clinical pharmacology,* **13,** 455-458.

Cacace, R., Sleegers, K. and Van Broeckhoven, C. (2016) Molecular genetics of early-onset Alzheimer disease revisited. *Alzheimers Dement*.

Cai, H., Wang, Y., McCarthy, D., Wen, H., Borchelt, D. R., Price, D. L. and Wong, P. C. (2001) BACE1 is the major beta-secretase for generation of Abeta peptides by neurons. *Nature neuroscience,* **4,** 233-234.

Cai, X. D., Golde, T. E. and Younkin, S. G. (1993) Release of excess amyloid beta protein from a mutant amyloid beta protein precursor [see comments]. *Science,* **259,** 514-516.

Cai, Z., Zhao, Y. and Zhao, B. (2012) Roles of glycogen synthase kinase 3 in Alzheimer's disease. *Current Alzheimer research,* **9,** 864-879.

Cao, H., Chu, Y., Lv, X. et al. (2012) GSK3 inhibitor-BIO regulates proliferation of immortalized pancreatic mesenchymal stem cells (iPMSCs). *PloS one,* **7,** e31502.

Caron, E. and Hall, A. (1998) Identification of two distinct mechanisms of phagocytosis controlled by different Rho GTPases. *Science,* **282,** 1717-1721.

Carson, W. F. t., Salter-Green, S. E., Scola, M. M., Joshi, A., Gallagher, K. A. and Kunkel, S. L. (2017) Enhancement of macrophage inflammatory responses by CCL2 is correlated with increased miR-9 expression and downregulation of the ERK1/2 phosphatase Dusp6. *Cellular immunology,* **314,** 63-72.

Castano, E. M., Prelli, F., Wisniewski, T., Golabek, A., Kumar, R. A., Soto, C. and Frangione, B. (1995) Fibrillogenesis in Alzheimer's disease of amyloid beta peptides and apolipoprotein E. *The Biochemical journal,* **306 (Pt 2),** 599-604.

Castellano, J. M., Kim, J., Stewart, F. R. et al. (2011) Human apoE Isoforms Differentially Regulate Brain Amyloid-{beta} Peptide Clearance. *Science translational medicine,* **3,** 89ra57.

Chakrabarty, P., Herring, A., Ceballos-Diaz, C., Das, P. and Golde, T. E. (2011) Hippocampal expression of murine TNFalpha results in attenuation of amyloid deposition in vivo. *Molecular neurodegeneration,* **6,** 16.

Chakrabarty, P., Jansen-West, K., Beccard, A. et al. (2010) Massive gliosis induced by interleukin-6 suppresses Abeta deposition in vivo: evidence against inflammation as a driving force for amyloid deposition. *FASEB journal : official publication of the Federation of American Societies for Experimental Biology,* **24,** 548-559.

Chakrabarty, P., Li, A., Ceballos-Diaz, C. et al. (2015) IL-10 alters immunoproteostasis in APP mice, increasing plaque burden and worsening cognitive behavior. *Neuron,* **85,** 519-533.

Chan, G. K., Kleinheinz, T. L., Peterson, D. and Moffat, J. G. (2013) A simple high-content cell cycle assay reveals frequent discrepancies between cell number and ATP and MTS proliferation assays. *PloS one,* **8,** e63583.

Chanput, W., Mes, J., Vreeburg, R. A., Savelkoul, H. F. and Wichers, H. J. (2010) Transcription profiles of LPS-stimulated THP-1 monocytes and macrophages: a tool to study inflammation modulating effects of food-derived compounds. *Food & function,* **1,** 254-261.

Chartier, H. M., Crawford, F., Houlden, H. et al. (1991) Early-onset Alzheimer's disease caused by mutations at codon 717 of the beta-amyloid precursor protein gene. *Nature,* **353,** 844-846.

Cheng, Y. L., Wang, C. Y., Huang, W. C., Tsai, C. C., Chen, C. L., Shen, C. F., Chi, C. Y. and Lin, C. F. (2009) Staphylococcus aureus induces microglial inflammation via a glycogen synthase kinase 3beta-regulated pathway. *Infection and immunity,* **77,** 4002-4008.

Cherfils, J. and Zeghouf, M. (2013) Regulation of small GTPases by GEFs, GAPs, and GDIs. *Physiological reviews,* **93,** 269-309.

Cherry, J. D., Olschowka, J. A. and O'Banion, M. K. (2014) Neuroinflammation and M2 microglia: the good, the bad, and the inflamed. *Journal of neuroinflammation,* **11,** 98.

Chow, V. W., Mattson, M. P., Wong, P. C. and Gleichmann, M. (2010) An overview of APP processing enzymes and products. *Neuromolecular medicine,* **12,** 1-12.

Chung, H., Brazil, M. I., Soe, T. T. and Maxfield, F. R. (1999) Uptake, degradation, and release of fibrillar and soluble forms of Alzheimer's amyloid beta-peptide by microglial cells. *The Journal of biological chemistry,* **274,** 32301-32308.

Citron, M., Oltersdorf, T., Haass, C., McConlogue, L., Hung, A. Y., Seubert, P., Vigo, P. C., Lieberburg, I. and Selkoe, D. J. (1992) Mutation of the beta-amyloid precursor protein in familial Alzheimer's disease increases beta-protein production. *Nature,* **360,** 672-674.

Clifford, J. R. (2012) Alzheimer Disease: New Concepts on Its Neurobiology and the Clinical Role Imaging Will Play. *Radiology,* **263,** 344–361.

Coghlan, M. P., Culbert, A. A., Cross, D. A. et al. (2000) Selective small molecule inhibitors of glycogen synthase kinase-3 modulate glycogen metabolism and gene transcription. *Chemistry & biology,* **7,** 793-803.

Colton, C. and Wilcock, D. M. (2010) Assessing activation states in microglia. *CNS & neurological disorders drug targets,* **9,** 174-191.

Colton, C. A. (2009) Heterogeneity of microglial activation in the innate immune response in the brain. *Journal of neuroimmune pharmacology : the official journal of the Society on NeuroImmune Pharmacology,* **4,** 399-418.

Colton, C. A., Mott, R. T., Sharpe, H., Xu, Q., Van Nostrand, W. E. and Vitek, M. P. (2006) Expression profiles for macrophage alternative activation genes in AD and in mouse models of AD. *Journal of neuroinflammation,* **3,** 27.

Combs, C. K., Johnson, D. E., Cannady, S. B., Lehman, T. M. and Landreth, G. E. (1999) Identification of microglial signal transduction pathways mediating a neurotoxic response to amyloidogenic fragments of beta-amyloid and prion proteins. *The Journal of neuroscience : the official journal of the Society for Neuroscience,* **19,** 928-939.

Combs, C. K., Karlo, J. C., Kao, S. C. and Landreth, G. E. (2001) beta-Amyloid stimulation of microglia and monocytes results in TNFalpha-dependent expression of inducible nitric oxide synthase and neuronal apoptosis. *The Journal of neuroscience : the official journal of the Society for Neuroscience,* **21,** 1179-1188.

Cong, L., Ran, F. A., Cox, D. et al. (2013) Multiplex genome engineering using CRISPR/Cas systems. *Science,* **339,** 819-823.

Cooper, J. A. (1987) Effects of cytochalasin and phalloidin on actin. *The Journal of cell biology,* **105,** 1473-1478.

Corder, E. H., Saunders, A. M., Strittmatter, W. J., Schmechel, D. E., Gaskell, P. C., Small, G. W., Roses, A. D., Haines, J. L. and Pericak, V. M. (1993) Gene dose of apolipoprotein E type 4 allele and the risk of Alzheimer's disease in late onset families [see comments]. *Science,* **261,** 921-923.

Cox, D., Chang, P., Zhang, Q., Reddy, P. G., Bokoch, G. M. and Greenberg, S. (1997) Requirements for both Rac1 and Cdc42 in membrane ruffling and phagocytosis in leukocytes. *The Journal of experimental medicine,* **186,** 1487-1494.

Cuzzocrea, S., Genovese, T., Mazzon, E. et al. (2006) Glycogen synthase kinase-3 beta inhibition reduces secondary damage in experimental spinal cord trauma. *The Journal of pharmacology and experimental therapeutics,* **318,** 79-89.

Da Mesquita, S., Ferreira, A. C., Sousa, J. C., Correia-Neves, M., Sousa, N. and Marques, F. (2016) Insights on the pathophysiology of Alzheimer's disease: The crosstalk between amyloid pathology, neuroinflammation and the peripheral immune system. *Neuroscience and biobehavioral reviews,* **68,** 547-562.

Daria, A., Colombo, A., Llovera, G., Hampel, H., Willem, M., Liesz, A., Haass, C. and Tahirovic, S. (2016) Young microglia restore amyloid plaque clearance of aged microglia. *The EMBO journal*.

Davalos, D., Grutzendler, J., Yang, G., Kim, J. V., Zuo, Y., Jung, S., Littman, D. R., Dustin, M. L. and Gan, W. B. (2005) ATP mediates rapid microglial response to local brain injury in vivo. *Nature neuroscience,* **8,** 752-758.

Daviglus, M. L., Bell, C. C., Berrettini, W. et al. (2010) NIH state-of-the-science conference statement: Preventing Alzheimer's disease and cognitive decline. *NIH consensus and state-of-the-science statements,* **27,** 1-30.

De Sarno, P., Axtell, R. C., Raman, C., Roth, K. A., Alessi, D. R. and Jope, R. S. (2008) Lithium prevents and ameliorates experimental autoimmune encephalomyelitis. *Journal of immunology,* **181,** 338-345.

De Strooper, B. and Annaert, W. (2000) Proteolytic processing and cell biological functions of the amyloid precursor protein. *Journal of cell science,* **113,** 1857-1870.

De Strooper, B., Iwatsubo, T., Wolfe, M.S. (2012) Presenilins and γ-Secretase: Structure, Function, and Role in Alzheimer Disease. *Cold Spring Harbor perspectives in medicine,* **2.1**.

del Rio-Hortega, P. (1919) Notas tecnicas. Coloracion rapida de tejidos normales y patologicos con carbonato de Plata amoniacal. *Trab Lab Invest Biol Univ Madrid,* **17,** 29-235.

del Ser, T., Steinwachs, K. C., Gertz, H. J. et al. (2013) Treatment of Alzheimer's disease with the GSK-3 inhibitor tideglusib: a pilot study. *Journal of Alzheimer's disease : JAD,* **33,** 205-215.

Deshmane, S. L., Kremlev, S., Amini, S. and Sawaya, B. E. (2009) Monocyte chemoattractant protein-1 (MCP-1): an overview. *Journal of interferon & cytokine research : the official journal of the International Society for Interferon and Cytokine Research,* **29,** 313-326.

Ding, Y., Qiao, A. and Fan, G. H. (2010) Indirubin-3'-monoxime rescues spatial memory deficits and attenuates beta-amyloid-associated neuropathology in a mouse model of Alzheimer's disease. *Neurobiology of disease,* **39,** 156-168.

Doble, B. W. and Woodgett, J. R. (2003) GSK-3: tricks of the trade for a multi-tasking kinase. *Journal of cell science,* **116,** 1175-1186.

Doens, D. and Fernandez, P. L. (2014) Microglia receptors and their implications in the response to amyloid beta for Alzheimer's disease pathogenesis. *Journal of neuroinflammation,* **11,** 48.

Dugo, L., Collin, M., Allen, D. A. et al. (2005) GSK-3beta inhibitors attenuate the organ injury/dysfunction caused by endotoxemia in the rat. *Critical care medicine,* **33,** 1903-1912.

Duits, F. H., Hernandez-Guillamon, M., Montaner, J. et al. (2015) Matrix Metalloproteinases in Alzheimer's Disease and Concurrent Cerebral Microbleeds. *Journal of Alzheimer's disease : JAD,* **48,** 711-720.

Dull, T., Zufferey, R., Kelly, M., Mandel, R. J., Nguyen, M., Trono, D. and Naldini, L. (1998) A third-generation lentivirus vector with a conditional packaging system. *Journal of virology,* **72,** 8463-8471.

Earle, W. R. (1943) Production of malignancy in vitro. IV. The mouse fibroblast cultures and changes seen in the living cells. . *J. Nat. Cancer Inst.,* **4,** 165-212.

Eikelenboom, P., Zhan, S. S., van Gool, W. A. and Allsop, D. (1994) Inflammatory mechanisms in Alzheimer's disease. *Trends in pharmacological sciences,* **15,** 447-450.

El Khoury, J., Toft, M., Hickman, S. E., Means, T. K., Terada, K., Geula, C. and Luster, A. D. (2007) Ccr2 deficiency impairs microglial accumulation and accelerates progression of Alzheimer-like disease. *Nature medicine,* **13,** 432-438.

El Khoury, J. B., Moore, K. J., Means, T. K., Leung, J., Terada, K., Toft, M., Freeman, M. W. and Luster, A. D. (2003) CD36 mediates the innate host response to beta-amyloid. *The Journal of experimental medicine,* **197,** 1657-1666.

Eldar-Finkelman, H. and Martinez, A. (2011) GSK-3 Inhibitors: Preclinical and Clinical Focus on CNS. *Frontiers in molecular neuroscience,* **4,** 32.

Embi, N., Rylatt, D. B. and Cohen, P. (1980) Glycogen synthase kinase-3 from rabbit skeletal muscle. Separation from cyclic-AMP-dependent protein kinase and phosphorylase kinase. *European journal of biochemistry,* **107,** 519-527.

Emi, N., Friedmann, T. and Yee, J. K. (1991) Pseudotype formation of murine leukemia virus with the G protein of vesicular stomatitis virus. *Journal of virology,* **65,** 1202-1207.

Engel, T., Goni-Oliver, P., Lucas, J. J., Avila, J. and Hernandez, F. (2006) Chronic lithium administration to FTDP-17 tau and GSK-3beta overexpressing mice prevents tau hyperphosphorylation and neurofibrillary tangle formation, but pre-formed neurofibrillary tangles do not revert. *Journal of neurochemistry,* **99,** 1445-1455.

Fang, F., Lue, L. F., Yan, S. et al. (2010) RAGE-dependent signaling in microglia contributes to neuroinflammation, Abeta accumulation, and impaired learning/memory in a mouse model of Alzheimer's disease. *FASEB journal : official publication of the Federation of American Societies for Experimental Biology,* **24,** 1043-1055.

Fassbender, K., Walter, S., Kuhl, S. et al. (2004) The LPS receptor (CD14) links innate immunity with Alzheimer's disease. *FASEB journal : official publication of the Federation of American Societies for Experimental Biology,* **18,** 203-205.

Feng, X., Deng, T., Zhang, Y., Su, S., Wei, C. and Han, D. (2011) Lipopolysaccharide inhibits macrophage phagocytosis of apoptotic neutrophils by regulating the production of tumour necrosis factor alpha and growth arrest-specific gene 6. *Immunology,* **132,** 287-295.

Fiala, M., Lin, J., Ringman, J. et al. (2005) Ineffective phagocytosis of amyloid-beta by macrophages of Alzheimer's disease patients. *Journal of Alzheimer's disease : JAD,* **7,** 221-232; discussion 255-262.

Flanagan, M. D. and Lin, S. (1980) Cytochalasins block actin filament elongation by binding to high affinity sites associated with F-actin. *The Journal of biological chemistry,* **255,** 835-838.

Fleisher-Berkovich, S., Filipovich-Rimon, T., Ben-Shmuel, S., Hulsmann, C., Kummer, M. P. and Heneka, M. T. (2010) Distinct modulation of microglial amyloid beta phagocytosis and migration by neuropeptides. *Journal of neuroinflammation,* **7,** 61.

Floden, A. M. and Combs, C. K. (2006) Beta-amyloid stimulates murine postnatal and adult microglia cultures in a unique manner. *The Journal of neuroscience : the official journal of the Society for Neuroscience,* **26,** 4644-4648.

Forlenza, O. V., Diniz, B. S., Radanovic, M., Santos, F. S., Talib, L. L. and Gattaz, W. F. (2011) Disease-modifying properties of long-term lithium treatment for amnestic mild cognitive impairment: randomised controlled trial. *The British journal of psychiatry : the journal of mental science,* **198,** 351-356.

Frackowiak, J., Wisniewski, H. M., Wegiel, J., Merz, G. S., Iqbal, K. and Wang, K. C. (1992) Ultrastructure of the microglia that phagocytose amyloid and the microglia that produce beta-amyloid fibrils. *Acta neuropathologica,* **84,** 225-233.

Frank, S., Burbach, G. J., Bonin, M., Walter, M., Streit, W., Bechmann, I. and Deller, T. (2008) TREM2 is upregulated in amyloid plaque-associated microglia in aged APP23 transgenic mice. *Glia,* **56,** 1438-1447.

Frautschy, S. A., Yang, F., Irrizarry, M., Hyman, B., Saido, T. C., Hsiao, K. and Cole, G. M. (1998) Microglial response to amyloid plaques in APPsw transgenic mice. *The American journal of pathology,* **152,** 307-317.

Friedland, J. S., Shattock, R. J. and Griffin, G. E. (1993) Phagocytosis of Mycobacterium tuberculosis or particulate stimuli by human monocytic cells induces equivalent monocyte chemotactic protein-1 gene expression. *Cytokine,* **5,** 150-156.

Fuerer, C. and Nusse, R. (2010) Lentiviral vectors to probe and manipulate the Wnt signaling pathway. *PloS one,* **5,** e9370.

Gadani, S. P., Cronk, J. C., Norris, G. T. and Kipnis, J. (2012) IL-4 in the brain: a cytokine to remember. *Journal of immunology,* **189,** 4213-4219.

Galimberti, D., Fenoglio, C., Lovati, C. et al. (2006a) Serum MCP-1 levels are increased in mild cognitive impairment and mild Alzheimer's disease. *Neurobiology of aging,* **27,** 1763-1768.

Galimberti, D., Schoonenboom, N., Scheltens, P., Fenoglio, C., Venturelli, E., Pijnenburg, Y. A., Bresolin, N. and Scarpini, E. (2006b) Intrathecal chemokine levels in Alzheimer disease and frontotemporal lobar degeneration. *Neurology,* **66,** 146-147.

Garrett, W. S., Chen, L. M., Kroschewski, R., Ebersold, M., Turley, S., Trombetta, S., Galan, J. E. and Mellman, I. (2000) Developmental control of endocytosis in dendritic cells by Cdc42. *Cell,* **102,** 325-334.

Genin, M., Clement, F., Fattaccioli, A., Raes, M. and Michiels, C. (2015) M1 and M2 macrophages derived from THP-1 cells differentially modulate the response of cancer cells to etoposide. *BMC cancer,* **15,** 577.

Ghiso, J. and Frangione, B. (2002) Amyloidosis and Alzheimer's disease. *Advanced drug delivery reviews,* **54,** 1539-1551.

Ginhoux, F., Greter, M., Leboeuf, M. et al. (2010) Fate Mapping Analysis Reveals That Adult Microglia Derive from Primitive Macrophages. *Science*.

Giulian, D., Haverkamp, L. J., Yu, J. H., Karshin, W., Tom, D., Li, J., Kirkpatrick, J., Kuo, L. M. and Roher, A. E. (1996) Specific domains of beta-amyloid from Alzheimer plaque elicit neuron killing in human microglia. *The Journal of neuroscience : the official journal of the Society for Neuroscience,* **16,** 6021-6037.

Glabe, C. (2001) Intracellular mechanisms of amyloid accumulation and pathogenesis in Alzheimer's disease. *Journal of molecular neuroscience : MN,* **17,** 137-145.

Glenner, G. G. and Wong, C. W. (1984) Alzheimer's disease: initial report of the purification and characterization of a novel cerebrovascular amyloid protein. *Biochem Biophys Res Commun,* **120,** 885-890.

Goate, A., Chartier, H. M., Mullan, M. et al. (1991) Segregation of a missense mutation in the amyloid precursor protein gene with familial Alzheimer's disease [see comments]. *Nature,* **349,** 704-706.

Gong, Y., Chang, L., Viola, K. L., Lacor, P. N., Lambert, M. P., Finch, C. E., Krafft, G. A. and Klein, W. L. (2003) Alzheimer's disease-affected brain: presence of oligomeric A beta ligands (ADDLs) suggests a molecular basis for reversible memory loss. *Proceedings of the National Academy of Sciences of the United States of America,* **100,** 10417-10422.

Gorevic, P. D., Goni, F., Pons-Estel, B., Alvarez, F., Peress, N. S. and Frangione, B. (1986) Isolation and partial characterization of neurofibrillary tangles and amyloid plaque core in Alzheimer's disease: immunohistological studies. *Journal of neuropathology and experimental neurology,* **45,** 647-664.

Gotz, J., Chen, F., van Dorpe, J. and Nitsch, R. M. (2001) Formation of neurofibrillary tangles in P301l tau transgenic mice induced by Abeta 42 fibrils. *Science,* **293,** 1491-1495.

Gouras, G. K., Tsai, J., Naslund, J. et al. (2000) Intraneuronal Abeta42 accumulation in human brain. *The American journal of pathology,* **156,** 15-20.

Gray, N. S., Wodicka, L., Thunnissen, A. M. et al. (1998) Exploiting chemical libraries, structure, and genomics in the search for kinase inhibitors. *Science,* **281,** 533-538.

Greenberg, S. M., Gurol, M. E., Rosand, J. and Smith, E. E. (2004) Amyloid angiopathy-related vascular cognitive impairment. *Stroke; a journal of cerebral circulation,* **35,** 2616-2619.

Greter, M. and Merad, M. (2013) Regulation of microglia development and homeostasis. *Glia,* **61,** 121-127.

Griciuc, A., Serrano-Pozo, A., Parrado, A. R. et al. (2013) Alzheimer's disease risk gene CD33 inhibits microglial uptake of amyloid beta. *Neuron,* **78,** 631-643.

Griffin, W. S., Stanley, L. C., Ling, C., White, L., MacLeod, V., Perrot, L. J., White, C. L., 3rd and Araoz, C. (1989) Brain interleukin 1 and S-100 immunoreactivity are elevated in Down syndrome and Alzheimer disease. *Proceedings of the National Academy of Sciences of the United States of America,* **86,** 7611-7615.

Grundke-Iqbal, I., Iqbal, K., Tung, Y. C., Quinlan, M., Wisniewski, H. M. and Binder, L. I. (1986) Abnormal phosphorylation of the microtubule-associated protein tau (tau) in Alzheimer cytoskeletal pathology. *Proceedings of the National Academy of Sciences of the United States of America,* **83,** 4913-4917.

Guerreiro, R., Wojtas, A., Bras, J. et al. (2013) TREM2 variants in Alzheimer's disease. *The New England journal of medicine,* **368,** 117-127.

Guillot-Sestier, M. V., Doty, K. R., Gate, D., Rodriguez, J., Jr., Leung, B. P., Rezai-Zadeh, K. and Town, T. (2015) Il10 deficiency rebalances innate immunity to mitigate Alzheimer-like pathology. *Neuron,* **85,** 534-548.

Gulen, M. F., Bulek, K., Xiao, H. et al. (2012) Inactivation of the enzyme GSK3alpha by the kinase IKKi promotes AKT-mTOR signaling pathway that mediates interleukin-1-induced Th17 cell maintenance. *Immunity,* **37,** 800-812.

Haass, C., Kaether, C., Thinakaran, G. and Sisodia, S. (2012) Trafficking and proteolytic processing of APP. *Cold Spring Harbor perspectives in medicine,* **2,** a006270.

Haass, C. and Selkoe, D. J. (2007) Soluble protein oligomers in neurodegeneration: lessons from the Alzheimer's amyloid beta-peptide. *Nature reviews. Molecular cell biology,* **8,** 101-112.

Hanger, D. P., Anderton, B. H. and Noble, W. (2009) Tau phosphorylation: the therapeutic challenge for neurodegenerative disease. *Trends in molecular medicine,* **15,** 112-119.

Hanisch, U. K. (2002) Microglia as a source and target of cytokines. *Glia,* **40,** 140-155.

Hanisch, U. K. and Kettenmann, H. (2007) Microglia: active sensor and versatile effector cells in the normal and pathologic brain. *Nature neuroscience,* **10,** 1387-1394.

Hardy, J. and Selkoe, D. J. (2002) The amyloid hypothesis of Alzheimer's disease: progress and problems on the road to therapeutics. *Science,* **297,** 353-356.

Hardy, J. A. and Higgins, G. A. (1992) Alzheimer's disease: the amyloid cascade hypothesis. *Science,* **256,** 184-185.

Hayden, M. S. and Ghosh, S. (2004) Signaling to NF-kappaB. *Genes & development,* **18,** 2195-2224.

Hellwig, S., Masuch, A., Nestel, S., Katzmarski, N., Meyer-Luehmann, M. and Biber, K. (2015) Forebrain microglia from wild-type but not adult 5xFAD mice prevent amyloid-beta plaque formation in organotypic hippocampal slice cultures. *Scientific reports,* **5,** 14624.

Heneka, M. T., Kummer, M. P., Stutz, A. et al. (2013) NLRP3 is activated in Alzheimer's disease and contributes to pathology in APP/PS1 mice. *Nature,* **493,** 674-678.

Heneka, M. T., Sastre, M., Dumitrescu-Ozimek, L. et al. (2005) Acute treatment with the PPAR{gamma} agonist pioglitazone and ibuprofen reduces glial inflammation and A{beta}1-42 levels in APPV717I transgenic mice. *Brain : a journal of neurology,* **128,** 1442-1453.

Hernandez, F., Borrell, J., Guaza, C., Avila, J. and Lucas, J. J. (2002) Spatial learning deficit in transgenic mice that conditionally over-express GSK-3beta in the brain but do not form tau filaments. *Journal of neurochemistry,* **83,** 1529-1533.

Hickman, S. E., Allison, E. K. and El Khoury, J. (2008) Microglial dysfunction and defective beta-amyloid clearance pathways in aging Alzheimer's disease mice. *The Journal of neuroscience : the official journal of the Society for Neuroscience,* **28,** 8354-8360.

Hickman, S. E. and El Khoury, J. (2014) TREM2 and the neuroimmunology of Alzheimer's disease. *Biochemical pharmacology,* **88,** 495-498.

Hoeflich, K. P., Luo, J., Rubie, E. A., Tsao, M. S., Jin, O. and Woodgett, J. R. (2000) Requirement for glycogen synthase kinase-3beta in cell survival and NF-kappaB activation. *Nature,* **406,** 86-90.

Hommes, T. J., Hoogendijk, A. J., Dessing, M. C., Van't Veer, C., Florquin, S., Colonna, M., de Vos, A. F. and van der Poll, T. (2014) Triggering receptor expressed on myeloid cells-1 (TREM-1) improves host defence in pneumococcal pneumonia. *The Journal of pathology,* **233,** 357-367.

Hooper, C., Killick, R. and Lovestone, S. (2008) The GSK3 hypothesis of Alzheimer's disease. *Journal of neurochemistry,* **104,** 1433-1439.

Hooper, C., Markevich, V., Plattner, F. et al. (2007) Glycogen synthase kinase-3 inhibition is integral to long-term potentiation. *The European journal of neuroscience,* **25,** 81-86.

Hoppe, A. D. and Swanson, J. A. (2004) Cdc42, Rac1, and Rac2 display distinct patterns of activation during phagocytosis. *Molecular biology of the cell,* **15,** 3509-3519.

Hsieh, C. L., Koike, M., Spusta, S. C., Niemi, E. C., Yenari, M., Nakamura, M. C. and Seaman, W. E. (2009) A role for TREM2 ligands in the phagocytosis of apoptotic neuronal cells by microglia. *Journal of neurochemistry,* **109,** 1144-1156.

Huang da, W., Sherman, B. T. and Lempicki, R. A. (2009a) Bioinformatics enrichment tools: paths toward the comprehensive functional analysis of large gene lists. *Nucleic acids research,* **37,** 1-13.

Huang da, W., Sherman, B. T. and Lempicki, R. A. (2009b) Systematic and integrative analysis of large gene lists using DAVID bioinformatics resources. *Nature protocols,* **4,** 44-57.

Hughes, K., Nikolakaki, E., Plyte, S. E., Totty, N. F. and Woodgett, J. R. (1993) Modulation of the glycogen synthase kinase-3 family by tyrosine phosphorylation. *The EMBO journal,* **12,** 803-808.

Hull, M., Sadowsky, C., Arai, H. et al. (2017) Long-Term Extensions of Randomized Vaccination Trials of ACC-001 and QS-21 in Mild to Moderate Alzheimer's Disease. *Current Alzheimer research*.

Hurtado, D. E., Molina-Porcel, L., Carroll, J. C., Macdonald, C., Aboagye, A. K., Trojanowski, J. Q. and Lee, V. M. (2012) Selectively silencing GSK-3 isoforms reduces plaques and tangles in mouse models of Alzheimer's disease. *The Journal of neuroscience : the official journal of the Society for Neuroscience,* **32,** 7392-7402.

Inestrosa, N. C., Montecinos-Oliva, C. and Fuenzalida, M. (2012) Wnt signaling: role in Alzheimer disease and schizophrenia. *Journal of neuroimmune pharmacology : the official journal of the Society on NeuroImmune Pharmacology,* **7,** 788-807.

Inoue, H., Nojima, H. and Okayama, H. (1990) High efficiency transformation of Escherichia coli with plasmids. *Gene,* **96,** 23-28.

Ishizuka, K., Kimura, T., Igata-yi, R., Katsuragi, S., Takamatsu, J. and Miyakawa, T. (1997) Identification of monocyte chemoattractant protein-1 in senile plaques and reactive microglia of Alzheimer's disease. *Psychiatry and clinical neurosciences,* **51,** 135-138.

Itagaki, S., McGeer, P. L., Akiyama, H., Zhu, S. and Selkoe, D. (1989) Relationship of microglia and astrocytes to amyloid deposits of Alzheimer disease. *J Neuroimmunol,* **24,** 173-182.

Jack, C. R., Jr., Knopman, D. S., Jagust, W. J. et al. (2013) Tracking pathophysiological processes in Alzheimer's disease: an updated hypothetical model of dynamic biomarkers. *The Lancet. Neurology,* **12,** 207-216.

Jarrett, J. T., Berger, E. P. and Lansbury, P. T., Jr. (1993) The carboxy terminus of the beta amyloid protein is critical for the seeding of amyloid formation: implications for the pathogenesis of Alzheimer's disease. *Biochemistry,* **32,** 4693-4697.

Jaworski, T., Dewachter, I., Lechat, B. et al. (2011) GSK-3alpha/beta kinases and amyloid production in vivo. *Nature,* **480,** E4-5; discussion E6.

Jay, T. R., Miller, C. M., Cheng, P. J. et al. (2015) TREM2 deficiency eliminates TREM2+ inflammatory macrophages and ameliorates pathology in Alzheimer's disease mouse models. *The Journal of experimental medicine,* **212,** 287-295.

Jiang, Q., Lee, C. Y., Mandrekar, S. et al. (2008) ApoE promotes the proteolytic degradation of Abeta. *Neuron,* **58,** 681-693.

Jiang, T., Tan, L., Zhu, X. C. et al. (2014) Upregulation of TREM2 ameliorates neuropathology and rescues spatial cognitive impairment in a transgenic mouse model of Alzheimer's disease. *Neuropsychopharmacology : official publication of the American College of Neuropsychopharmacology,* **39,** 2949-2962.

Jiang, T., Zhang, Y. D., Gao, Q. et al. (2016) TREM1 facilitates microglial phagocytosis of amyloid beta. *Acta neuropathologica,* **132,** 667-683.

Jin, W. and Dong, C. (2013) IL-17 cytokines in immunity and inflammation. *Emerging microbes & infections,* **2,** e60.

Jinek, M., Chylinski, K., Fonfara, I., Hauer, M., Doudna, J. A. and Charpentier, E. (2012) A programmable dual-RNA-guided DNA endonuclease in adaptive bacterial immunity. *Science,* **337,** 816-821.

Jonsson, T., Atwal, J. K., Steinberg, S. et al. (2012) A mutation in APP protects against Alzheimer's disease and age-related cognitive decline. *Nature,* **488,** 96-99.

Jonsson, T., Stefansson, H., Steinberg, S. et al. (2013) Variant of TREM2 associated with the risk of Alzheimer's disease. *The New England journal of medicine,* **368,** 107-116.

Jope, R. S., Yuskaitis, C. J. and Beurel, E. (2007) Glycogen synthase kinase-3 (GSK3): inflammation, diseases, and therapeutics. *Neurochemical research,* **32,** 577-595.

Jungbauer, L. M., Yu, C., Laxton, K. J. and LaDu, M. J. (2009) Preparation of fluorescently-labeled amyloid-beta peptide assemblies: the effect of fluorophore conjugation on structure and function. *Journal of molecular recognition : JMR,* **22,** 403-413.

K. W. Menting, J. C. (2014) β-secretase inhibitor; a promising novel therapeutic drug in Alzheimer's disease. *Frontiers in Aging Neuroscience,* **6,** 165.

Kaidanovich-Beilin, O. and Woodgett, J. R. (2011) GSK-3: Functional Insights from Cell Biology and Animal Models. *Frontiers in molecular neuroscience,* **4,** 40.

Kapetanovic, R., Nahori, M. A., Balloy, V., Fitting, C., Philpott, D. J., Cavaillon, J. M. and Adib-Conquy, M. (2007) Contribution of phagocytosis and intracellular sensing for cytokine production by Staphylococcus aureus-activated macrophages. *Infection and immunity,* **75,** 830-837.

Karperien, A., Ahammer, H. and Jelinek, H. F. (2013) Quantitating the subtleties of microglial morphology with fractal analysis. *Frontiers in cellular neuroscience,* **7,** 3.

Katsumoto, A., Lu, H., Miranda, A. S. and Ransohoff, R. M. (2014) Ontogeny and functions of central nervous system macrophages. *Journal of immunology,* **193,** 2615-2621.

Kawaguchi, M., Adachi, M., Oda, N., Kokubu, F. and Huang, S. K. (2004) IL-17 cytokine family. *The Journal of allergy and clinical immunology,* **114,** 1265-1273; quiz 1274.

Keren-Shaul, H., Spinrad, A., Weiner, A. et al. (2017) A Unique Microglia Type Associated with Restricting Development of Alzheimer's Disease. *Cell,* **169,** 1276-1290 e1217.

Kerr, M. C. and Teasdale, R. D. (2009) Defining macropinocytosis. *Traffic,* **10,** 364-371.

Kettenmann, H., Hanisch, U. K., Noda, M. and Verkhratsky, A. (2011) Physiology of microglia. *Physiological reviews,* **91,** 461-553.

Kettenmann, H., Kirchhoff, F. and Verkhratsky, A. (2013) Microglia: new roles for the synaptic stripper. *Neuron,* **77,** 10-18.

Kim, J., Basak, J. M. and Holtzman, D. M. (2009) The role of apolipoprotein E in Alzheimer's disease. *Neuron,* **63,** 287-303.

Kim, J. Y., Kim, D. H., Kim, J. H. et al. (2012) Soluble intracellular adhesion molecule-1 secreted by human umbilical cord blood-derived mesenchymal stem cell reduces amyloid-beta plaques. *Cell death and differentiation,* **19,** 680-691.

Kimberly, W. T., LaVoie, M. J., Ostaszewski, B. L., Ye, W., Wolfe, M. S. and Selkoe, D. J. (2003) Gamma-secretase is a membrane protein complex comprised of presenilin, nicastrin, Aph-1, and Pen-2. *Proceedings of the National Academy of Sciences of the United States of America,* **100,** 6382-6387.

Kittler, R., Surendranath, V., Heninger, A. K. et al. (2007) Genome-wide resources of endoribonuclease-prepared short interfering RNAs for specific loss-of-function studies. *Nature methods,* **4,** 337-344.

Kiyota, T., Gendelman, H. E., Weir, R. A., Higgins, E. E., Zhang, G. and Jain, M. (2013) CCL2 affects beta-amyloidosis and progressive neurocognitive dysfunction in a mouse model of Alzheimer's disease. *Neurobiology of aging,* **34,** 1060-1068.

Kiyota, T., Yamamoto, M., Xiong, H., Lambert, M. P., Klein, W. L., Gendelman, H. E., Ransohoff, R. M. and Ikezu, T. (2009) CCL2 accelerates microglia-mediated Abeta oligomer formation and progression of neurocognitive dysfunction. *PloS one,* **4,** e6197.

Kleinberger, G., Yamanishi, Y., Suarez-Calvet, M. et al. (2014) TREM2 mutations implicated in neurodegeneration impair cell surface transport and phagocytosis. *Science translational medicine,* **6,** 243ra286.

Ko, R., Jang, H. D. and Lee, S. Y. (2010) GSK3beta Inhibitor Peptide Protects Mice from LPS-induced Endotoxin Shock. *Immune network,* **10,** 99-103.

Koenigsknecht-Talboo, J. and Landreth, G. E. (2005) Microglial phagocytosis induced by fibrillar beta-amyloid and IgGs are differentially regulated by proinflammatory cytokines. *The Journal of neuroscience : the official journal of the Society for Neuroscience,* **25,** 8240-8249.

Koenigsknecht-Talboo, J., Meyer-Luehmann, M., Parsadanian, M., Garcia-Alloza, M., Finn, M. B., Hyman, B. T., Bacskai, B. J. and Holtzman, D. M. (2008) Rapid microglial response around amyloid pathology after systemic anti-Abeta antibody administration in PDAPP mice. *The Journal of neuroscience : the official journal of the Society for Neuroscience,* **28,** 14156-14164.

Koenigsknecht, J. and Landreth, G. (2004) Microglial phagocytosis of fibrillar beta-amyloid through a beta1 integrin-dependent mechanism. *The Journal of neuroscience : the official journal of the Society for Neuroscience,* **24,** 9838-9846.

Kohsaka, S., Hamanoue, M. and Nakajima, K. (1996) Functional implication of secretory proteases derived from microglia in the central nervous system. *The Keio journal of medicine,* **45,** 263-269.

Koistinaho, J., Malm, T. and Goldsteins, G. (2011) Glycogen synthase kinase-3beta: a mediator of inflammation in Alzheimer's disease? *International journal of Alzheimer's disease,* **2011,** 129753.

Koivusalo, M., Welch, C., Hayashi, H., Scott, C. C., Kim, M., Alexander, T., Touret, N., Hahn, K. M. and Grinstein, S. (2010) Amiloride inhibits macropinocytosis by lowering submembranous pH and preventing Rac1 and Cdc42 signaling. *The Journal of cell biology,* **188,** 547-563.

Kopke, E., Tung, Y. C., Shaikh, S., Alonso, A. C., Iqbal, K. and Grundke-Iqbal, I. (1993) Microtubule-associated protein tau. Abnormal phosphorylation of a non-paired helical filament pool in Alzheimer disease. *The Journal of biological chemistry,* **268,** 24374-24384.

Korzhevskii, D. E. and Kirik, O. V. (2016) Brain Microglia and Microglial Markers. *Neuroscience and Behavioral Physiology,* **46**.

Koscso, B., Csoka, B., Selmeczy, Z., Himer, L., Pacher, P., Virag, L. and Hasko, G. (2012) Adenosine augments IL-10 production by microglial cells through an A2B adenosine receptor-mediated process. *Journal of immunology,* **188,** 445-453.

Kosik, K. S. (1992) Cellular aspects of Alzheimer neurofibrillary pathology. *Progress in clinical and biological research,* **379,** 183-193.

Kosik, K. S., Joachim, C. L. and Selkoe, D. J. (1986) Microtubule-associated protein tau (tau) is a major antigenic component of paired helical filaments in Alzheimer disease. *Proceedings of the National Academy of Sciences of the United States of America,* **83,** 4044-4048.

Krabbe, G., Halle, A., Matyash, V. et al. (2013) Functional impairment of microglia coincides with Beta-amyloid deposition in mice with Alzheimer-like pathology. *PloS one,* **8,** e60921.

Krasemann, S., Madore, C., Cialic, R. et al. (2017) The TREM2-APOE Pathway Drives the Transcriptional Phenotype of Dysfunctional Microglia in Neurodegenerative Diseases. *Immunity,* **47,** 566-581 e569.

Kuhn, P. H., Wang, H., Dislich, B., Colombo, A., Zeitschel, U., Ellwart, J. W., Kremmer, E., Rossner, S. and Lichtenthaler, S. F. (2010) ADAM10 is the physiologically relevant, constitutive alpha-secretase of the amyloid precursor protein in primary neurons. *The EMBO journal,* **29,** 3020-3032.

Kumar, D. K., Choi, S. H., Washicosky, K. J. et al. (2016) Amyloid-beta peptide protects against microbial infection in mouse and worm models of Alzheimer's disease. *Science translational medicine,* **8,** 340ra372.

Kuscu, C., Arslan, S., Singh, R., Thorpe, J. and Adli, M. (2014) Genome-wide analysis reveals characteristics of off-target sites bound by the Cas9 endonuclease. *Nature biotechnology,* **32,** 677-683.

Kzhyshkowska, J., Workman, G., Cardo-Vila, M., Arap, W., Pasqualini, R., Gratchev, A., Krusell, L., Goerdt, S. and Sage, E. H. (2006) Novel function of alternatively activated macrophages: stabilin-1-mediated clearance of SPARC. *Journal of immunology,* **176,** 5825-5832.

Lai, A., Sisodia, S. S. and Trowbridge, I. S. (1995) Characterization of sorting signals in the beta-amyloid precursor protein cytoplasmic domain. *The Journal of biological chemistry,* **270,** 3565-3573.

Lamaze, C., Fujimoto, L. M., Yin, H. L. and Schmid, S. L. (1997) The actin cytoskeleton is required for receptor-mediated endocytosis in mammalian cells. *The Journal of biological chemistry,* **272,** 20332-20335.

Lambert, J. C., Heath, S., Even, G. et al. (2009) Genome-wide association study identifies variants at CLU and CR1 associated with Alzheimer's disease. *Nature genetics,* **41,** 1094-1099.

Lambert, J. C., Ibrahim-Verbaas, C. A., Harold, D. et al. (2013) Meta-analysis of 74,046 individuals identifies 11 new susceptibility loci for Alzheimer's disease. *Nature genetics,* **45,** 1452-1458.

Lammich, S., Kojro, E., Postina, R., Gilbert, S., Pfeiffer, R., Jasionowski, M., Haass, C. and Fahrenholz, F. (1999) Constitutive and regulated alpha-secretase cleavage of Alzheimer's amyloid precursor protein by a disintegrin metalloprotease. *Proceedings of the National Academy of Sciences of the United States of America,* **96,** 3922-3927.

Latz, E., Xiao, T. S. and Stutz, A. (2013) Activation and regulation of the inflammasomes. *Nature reviews. Immunology,* **13,** 397-411.

Lawson, L. J., Perry, V. H., Dri, P. and Gordon, S. (1990) Heterogeneity in the distribution and morphology of microglia in the normal adult mouse brain. *Neuroscience,* **39,** 151-170.

Lee, J. K., Jin, H. K., Endo, S., Schuchman, E. H., Carter, J. E. and Bae, J. S. (2010) Intracerebral transplantation of bone marrow-derived mesenchymal stem cells reduces amyloid-beta deposition and rescues memory deficits in Alzheimer's disease mice by modulation of immune responses. *Stem cells,* **28,** 329-343.

Lee, S. C., Liu, W., Dickson, D. W., Brosnan, C. F. and Berman, J. W. (1993) Cytokine production by human fetal microglia and astrocytes. Differential induction by lipopolysaccharide and IL-1 beta. *Journal of immunology,* **150,** 2659-2667.

Lee, V. M., Balin, B. J., Otvos, L., Jr. and Trojanowski, J. Q. (1991) A68: a major subunit of paired helical filaments and derivatized forms of normal Tau. *Science,* **251,** 675-678.

Lehnardt, S., Massillon, L., Follett, P., Jensen, F. E., Ratan, R., Rosenberg, P. A., Volpe, J. J. and Vartanian, T. (2003) Activation of innate immunity in the CNS triggers

neurodegeneration through a Toll-like receptor 4-dependent pathway. *Proceedings of the National Academy of Sciences of the United States of America,* **100,** 8514-8519.

Leroy, K., Yilmaz, Z. and Brion, J. P. (2007) Increased level of active GSK-3beta in Alzheimer's disease and accumulation in argyrophilic grains and in neurones at different stages of neurofibrillary degeneration. *Neuropathology and applied neurobiology,* **33,** 43-55.

Lesne, S., Koh, M. T., Kotilinek, L., Kayed, R., Glabe, C. G., Yang, A., Gallagher, M. and Ashe, K. H. (2006) A specific amyloid-beta protein assembly in the brain impairs memory. *Nature,* **440,** 352-357.

Leverrier, Y. and Ridley, A. J. (2001) Requirement for Rho GTPases and PI 3-kinases during apoptotic cell phagocytosis by macrophages. *Current biology : CB,* **11,** 195-199.

Lewis, J., Dickson, D. W., Lin, W. L. et al. (2001) Enhanced neurofibrillary degeneration in transgenic mice expressing mutant tau and APP. *Science,* **293,** 1487-1491.

Leyhe, T., Eschweiler, G. W., Stransky, E., Gasser, T., Annas, P., Basun, H. and Laske, C. (2009) Increase of BDNF serum concentration in lithium treated patients with early Alzheimer's disease. *Journal of Alzheimer's disease : JAD,* **16,** 649-656.

Li, H., Hong, F., Pan, S., Lei, L. and Yan, F. (2016) Silencing Triggering Receptors Expressed on Myeloid Cells-1 Impaired the Inflammatory Response to Oxidized Low-Density Lipoprotein in Macrophages. *Inflammation,* **39,** 199-208.

Li, H. Q., Chen, C., Dou, Y. et al. (2013a) P2Y4 receptor-mediated pinocytosis contributes to amyloid beta-induced self-uptake by microglia. *Molecular and cellular biology,* **33,** 4282-4293.

Li, R., Lindholm, K., Yang, L. B. et al. (2004) Amyloid beta peptide load is correlated with increased beta-secretase activity in sporadic Alzheimer's disease patients. *Proceedings of the National Academy of Sciences of the United States of America,* **101,** 3632-3637.

Li, R., Shen, Y., Yang, L. B., Lue, L. F., Finch, C. and Rogers, J. (2000) Estrogen enhances uptake of amyloid beta-protein by microglia derived from the human cortex. *Journal of neurochemistry,* **75,** 1447-1454.

Li, Y., Cam, J. and Bu, G. (2001) Low-density lipoprotein receptor family: endocytosis and signal transduction. *Molecular neurobiology,* **23,** 53-67.

Li, Y., Qi, X., Tong, X. and Wang, S. (2013b) Thrombospondin 1 activates the macrophage Toll-like receptor 4 pathway. *Cellular & molecular immunology,* **10,** 506-512.

Lien, E., Means, T. K., Heine, H. et al. (2000) Toll-like receptor 4 imparts ligand-specific recognition of bacterial lipopolysaccharide. *The Journal of clinical investigation,* **105,** 497-504.

Lim, S., Smith, K. R., Lim, S. T., Tian, R., Lu, J. and Tan, M. (2016) Regulation of mitochondrial functions by protein phosphorylation and dephosphorylation. *Cell & bioscience,* **6,** 25.

Liu, S. L., Wang, C., Jiang, T., Tan, L., Xing, A. and Yu, J. T. (2016a) The Role of Cdk5 in Alzheimer's Disease. *Molecular neurobiology,* **53,** 4328-4342.

Liu, X., Liu, J., Zhao, S. et al. (2016b) Interleukin-4 Is Essential for Microglia/Macrophage M2 Polarization and Long-Term Recovery After Cerebral Ischemia. *Stroke; a journal of cerebral circulation,* **47,** 498-504.

Liu, Z., Condello, C., Schain, A., Harb, R. and Grutzendler, J. (2010) CX3CR1 in Microglia Regulates Brain Amyloid Deposition through Selective Protofibrillar Amyloid-{beta} Phagocytosis. *The Journal of neuroscience : the official journal of the Society for Neuroscience,* **30,** 17091-17101.

Livak, K. J. and Schmittgen, T. D. (2001) Analysis of relative gene expression data using real-time quantitative PCR and the 2(-Delta Delta C(T)) Method. *Methods,* **25,** 402-408.

Llorens-Maritin, M., Jurado, J., Hernandez, F. and Avila, J. (2014) GSK-3beta, a pivotal kinase in Alzheimer disease. *Frontiers in molecular neuroscience,* **7,** 46.

Logan, C. Y. and Nusse, R. (2004) The Wnt signaling pathway in development and disease. *Annual review of cell and developmental biology,* **20,** 781-810.

Lopez-Dee, Z., Pidcock, K. and Gutierrez, L. S. (2011) Thrombospondin-1: multiple paths to inflammation. *Mediators of inflammation,* **2011,** 296069.

Lovestone, S., Boada, M., Dubois, B. et al. (2015) A phase II trial of tideglusib in Alzheimer's disease. *Journal of Alzheimer's disease : JAD,* **45,** 75-88.

Lucas, J. J., Hernandez, F., Gomez-Ramos, P., Moran, M. A., Hen, R. and Avila, J. (2001) Decreased nuclear beta-catenin, tau hyperphosphorylation and neurodegeneration in GSK-3beta conditional transgenic mice. *The EMBO journal,* **20,** 27-39.

Lue, L. F., Brachova, L., Civin, W. H. and Rogers, J. (1996) Inflammation, A beta deposition, and neurofibrillary tangle formation as correlates of Alzheimer's disease neurodegeneration. *Journal of neuropathology and experimental neurology,* **55,** 1083-1088.

Lue, L. F., Rydel, R., Brigham, E. F. et al. (2001a) Inflammatory repertoire of Alzheimer's disease and nondemented elderly microglia in vitro. *Glia,* **35,** 72-79.

Lue, L. F., Walker, D. G., Brachova, L., Beach, T. G., Rogers, J., Schmidt, A. M., Stern, D. M. and Yan, S. D. (2001b) Involvement of microglial receptor for advanced glycation endproducts (RAGE) in Alzheimer's disease: identification of a cellular activation mechanism. *Experimental neurology,* **171,** 29-45.

Luo, Y., Bolon, B., Damore, M. A., Fitzpatrick, D., Liu, H., Zhang, J., Yan, Q., Vassar, R. and Citron, M. (2003) BACE1 (beta-secretase) knockout mice do not acquire compensatory gene expression changes or develop neural lesions over time. *Neurobiology of disease,* **14,** 81-88.

Ma, B. and Hottiger, M. O. (2016) Crosstalk between Wnt/beta-Catenin and NF-kappaB Signaling Pathway during Inflammation. *Frontiers in immunology,* **7,** 378.

Ma, J., Yee, A., Brewer, H. B., Jr., Das, S. and Potter, H. (1994) Amyloid-associated proteins alpha 1-antichymotrypsin and apolipoprotein E promote assembly of Alzheimer beta-protein into filaments. *Nature,* **372,** 92-94.

Ma, T., Gong, K., Ao, Q., Yan, Y., Song, B., Huang, H., Zhang, X. and Gong, Y. (2013a) Intracerebral transplantation of adipose-derived mesenchymal stem cells alternatively activates microglia and ameliorates neuropathological deficits in Alzheimer's disease mice. *Cell transplantation,* **22 Suppl 1,** S113-126.

Ma, Y., Bao, J., Zhao, X. et al. (2013b) Activiated cyclin-dependent kinase 5 promotes microglial phagocytosis of fibrillar beta-amyloid by up-regulating lipoprotein lipase expression. *Molecular & cellular proteomics : MCP*.

MacAulay, K., Doble, B. W., Patel, S., Hansotia, T., Sinclair, E. M., Drucker, D. J., Nagy, A. and Woodgett, J. R. (2007) Glycogen synthase kinase 3alpha-specific regulation of murine hepatic glycogen metabolism. *Cell metabolism,* **6,** 329-337.

Macdonald, A., Briggs, K., Poppe, M., Higgins, A., Velayudhan, L. and Lovestone, S. (2008) A feasibility and tolerability study of lithium in Alzheimer's disease. *International journal of geriatric psychiatry,* **23,** 704-711.

MacDonald, B. T., Tamai, K. and He, X. (2009) Wnt/beta-catenin signaling: components, mechanisms, and diseases. *Developmental cell,* **17,** 9-26.

Mahley, R. W. (1988) Apolipoprotein E: cholesterol transport protein with expanding role in cell biology. *Science,* **240,** 622-630.

Mahley, R. W. and Rall, S. C., Jr. (2000) Apolipoprotein E: far more than a lipid transport protein. *Annual review of genomics and human genetics,* **1,** 507-537.

Majumdar, A., Chung, H., Dolios, G., Wang, R., Asamoah, N., Lobel, P. and Maxfield, F. R. (2008) Degradation of fibrillar forms of Alzheimer's amyloid beta-peptide by macrophages. *Neurobiology of aging,* **29,** 707-715.

Majumdar, A., Cruz, D., Asamoah, N., Buxbaum, A., Sohar, I., Lobel, P. and Maxfield, F. R. (2007) Activation of microglia acidifies lysosomes and leads to degradation of Alzheimer amyloid fibrils. *Molecular biology of the cell,* **18,** 1490-1496.

Malek-Ahmadi, M., Perez, S. E., Chen, K. and Mufson, E. J. (2016) Neuritic and Diffuse Plaque Associations with Memory in Non-Cognitively Impaired Elderly. *Journal of Alzheimer's disease : JAD,* **53,** 1641-1652.

Mali, P., Yang, L., Esvelt, K. M., Aach, J., Guell, M., DiCarlo, J. E., Norville, J. E. and Church, G. M. (2013) RNA-guided human genome engineering via Cas9. *Science,* **339,** 823-826.

Malm, T., Koistinaho, M., Muona, A., Magga, J. and Koistinaho, J. (2010) The role and therapeutic potential of monocytic cells in Alzheimer's disease. *Glia,* **58,** 889-900.

Malumbres, M. (2014) Cyclin-dependent kinases. *Genome biology,* **15,** 122.

Mandrekar-Colucci, S., Karlo, J. C. and Landreth, G. E. (2012) Mechanisms underlying the rapid peroxisome proliferator-activated receptor-gamma-mediated amyloid clearance and reversal of cognitive deficits in a murine model of Alzheimer's disease. *The Journal of neuroscience : the official journal of the Society for Neuroscience,* **32,** 10117-10128.

Mandrekar, S., Jiang, Q., Lee, C. Y., Koenigsknecht-Talboo, J., Holtzman, D. M. and Landreth, G. E. (2009) Microglia mediate the clearance of soluble Abeta through fluid phase macropinocytosis. *The Journal of neuroscience : the official journal of the Society for Neuroscience,* **29,** 4252-4262.

Manocha, G. D., Floden, A. M., Rausch, K. et al. (2016) APP Regulates Microglial Phenotype in a Mouse Model of Alzheimer's Disease. *The Journal of neuroscience : the official journal of the Society for Neuroscience,* **36,** 8471-8486.

Mao, Y. and Finnemann, S. C. (2015) Regulation of phagocytosis by Rho GTPases. *Small GTPases,* **6,** 89-99.

Martin, M., Rehani, K., Jope, R. S. and Michalek, S. M. (2005) Toll-like receptor-mediated cytokine production is differentially regulated by glycogen synthase kinase 3. *Nat Immunol,* **6,** 777-784.

Martinez, F. O., Gordon, S., Locati, M. and Mantovani, A. (2006) Transcriptional profiling of the human monocyte-to-macrophage differentiation and polarization: new molecules and patterns of gene expression. *Journal of immunology,* **177,** 7303-7311.

Martinez, F. O., Helming, L. and Gordon, S. (2009) Alternative activation of macrophages: an immunologic functional perspective. *Annual review of immunology,* **27,** 451-483.

Massol, P., Montcourrier, P., Guillemot, J. C. and Chavrier, P. (1998) Fc receptor-mediated phagocytosis requires CDC42 and Rac1. *The EMBO journal,* **17,** 6219-6229.

Masters, C. L., Simms, G., Weinman, N. A., Multhaup, G., McDonald, B. L. and Beyreuther, K. (1985) Amyloid plaque core protein in Alzheimer disease and Down syndrome. *Proceedings of the National Academy of Sciences of the United States of America,* **82,** 4245-4249.

Matsui, T., Ingelsson, M., Fukumoto, H., Ramasamy, K., Kowa, H., Frosch, M. P., Irizarry, M. C. and Hyman, B. T. (2007) Expression of APP pathway mRNAs and proteins in Alzheimer's disease. *Brain research,* **1161,** 116-123.

Mattson, M. P., Cheng, B., Culwell, A. R., Esch, F. S., Lieberburg, I. and Rydel, R. E. (1993) Evidence for excitoprotective and intraneuronal calcium-regulating roles for secreted forms of the beta-amyloid precursor protein. *Neuron,* **10,** 243-254.

Mawuenyega, K. G., Sigurdson, W., Ovod, V., Munsell, L., Kasten, T., Morris, J. C., Yarasheski, K. E. and Bateman, R. J. (2010) Decreased clearance of CNS beta-amyloid in Alzheimer's disease. *Science,* **330,** 1774.

McGeer, P. L. and McGeer, E. G. (2015) Targeting microglia for the treatment of Alzheimer's disease. *Expert opinion on therapeutic targets,* **19,** 497-506.

McGuire, K. and Glass, E. J. (2005) The expanding role of microarrays in the investigation of macrophage responses to pathogens. *Veterinary immunology and immunopathology,* **105,** 259-275.

McMahan, R. S., Birkland, T. P., Smigiel, K. S., Vandivort, T. C., Rohani, M. G., Manicone, A. M., McGuire, J. K., Gharib, S. A. and Parks, W. C. (2016) Stromelysin-2 (MMP10) Moderates Inflammation by Controlling Macrophage Activation. *Journal of immunology,* **197,** 899-909.

Meda, L., Cassatella, M. A., Szendrei, G. I., Otvos Jr, L., Baron, P., Villalba, M., Ferrari, D. and Rossi, F. (1995) Activation of microglial cells by ß-amyloid protein and interferon-y. *Nature,* **374,** 647-650.

Meier, O., Boucke, K., Hammer, S. V., Keller, S., Stidwill, R. P., Hemmi, S. and Greber, U. F. (2002) Adenovirus triggers macropinocytosis and endosomal leakage together with its clathrin-mediated uptake. *The Journal of cell biology,* **158,** 1119-1131.

Meijer, L., Borgne, A., Mulner, O., Chong, J. P., Blow, J. J., Inagaki, N., Inagaki, M., Delcros, J. G. and Moulinoux, J. P. (1997) Biochemical and cellular effects of roscovitine, a potent and selective inhibitor of the cyclin-dependent kinases cdc2, cdk2 and cdk5. *European journal of biochemistry,* **243,** 527-536.

Meijer, L., Flajolet, M. and Greengard, P. (2004) Pharmacological inhibitors of glycogen synthase kinase 3. *Trends in pharmacological sciences,* **25,** 471-480.

Melendez, J., Grogg, M. and Zheng, Y. (2011) Signaling role of Cdc42 in regulating mammalian physiology. *The Journal of biological chemistry,* **286,** 2375-2381.

Meyer-Luehmann, M., Spires-Jones, T. L., Prada, C. et al. (2008) Rapid appearance and local toxicity of amyloid-beta plaques in a mouse model of Alzheimer's disease. *Nature,* **451,** 720-724.

Michelucci, A., Heurtaux, T., Grandbarbe, L., Morga, E. and Heuschling, P. (2009) Characterization of the microglial phenotype under specific pro-inflammatory and anti-inflammatory conditions: Effects of oligomeric and fibrillar amyloid-beta. *J Neuroimmunol,* **210,** 3-12.

Mildner, A., Schlevogt, B., Kierdorf, K. et al. (2011) Distinct and Non-Redundant Roles of Microglia and Myeloid Subsets in Mouse Models of Alzheimer's Disease. *The Journal of neuroscience : the official journal of the Society for Neuroscience,* **31,** 11159-11171.

Mildner, A., Schmidt, H., Nitsche, M. et al. (2007) Microglia in the adult brain arise from Ly-6C(hi)CCR2(+) monocytes only under defined host conditions. *Nature neuroscience,* **10,** 1544-1553.

Morgan, S. C., Taylor, D. L. and Pocock, J. M. (2004) Microglia release activators of neuronal proliferation mediated by activation of mitogen-activated protein kinase, phosphatidylinositol-3-kinase/Akt and delta-Notch signalling cascades. *Journal of neurochemistry,* **90,** 89-101.

Morkuniene, R., Zvirbliene, A., Dalgediene, I. et al. (2013) Antibodies bound to Abeta oligomers potentiate the neurotoxicity of Abeta by activating microglia. *Journal of neurochemistry,* **126,** 604-615.

Morris, G. P., Clark, I. A. and Vissel, B. (2014) Inconsistencies and controversies surrounding the amyloid hypothesis of Alzheimer's disease. *Acta neuropathologica communications,* **2,** 135.

Mueller, H., Kassack, M. U. and Wiese, M. (2004) Comparison of the usefulness of the MTT, ATP, and calcein assays to predict the potency of cytotoxic agents in various human cancer cell lines. *Journal of biomolecular screening,* **9,** 506-515.

Muller, T., Meyer, H. E., Egensperger, R. and Marcus, K. (2008) The amyloid precursor protein intracellular domain (AICD) as modulator of gene expression, apoptosis, and cytoskeletal dynamics-relevance for Alzheimer's disease. *Progress in neurobiology,* **85,** 393-406.

Murray, M. Y., Birkland, T. P., Howe, J. D., Rowan, A. D., Fidock, M., Parks, W. C. and Gavrilovic, J. (2013) Macrophage migration and invasion is regulated by MMP10 expression. *PloS one,* **8,** e63555.

Muyllaert, D., Kremer, A., Jaworski, T., Borghgraef, P., Devijver, H., Croes, S., Dewachter, I. and Van Leuven, F. (2008) Glycogen synthase kinase-3beta, or a link between amyloid and tau pathology? *Genes, brain, and behavior,* **7 Suppl 1,** 57-66.

N'Diaye, E. N., Branda, C. S., Branda, S. S., Nevarez, L., Colonna, M., Lowell, C., Hamerman, J. A. and Seaman, W. E. (2009) TREM-2 (triggering receptor expressed on myeloid cells 2) is a phagocytic receptor for bacteria. *The Journal of cell biology,* **184,** 215-223.

Naert, G. and Rivest, S. (2011) CC chemokine receptor 2 deficiency aggravates cognitive impairments and amyloid pathology in a transgenic mouse model of Alzheimer's disease. *The Journal of neuroscience : the official journal of the Society for Neuroscience,* **31,** 6208-6220.

Naj, A. C., Jun, G., Beecham, G. W. et al. (2011) Common variants at MS4A4/MS4A6E, CD2AP, CD33 and EPHA1 are associated with late-onset Alzheimer's disease. *Nature genetics,* **43,** 436-441.

Nakamura, T., Hemmi, H., Aso, H. and Ishida, N. (1986) Variants of a human monocytic leukemia cell line (THP-1): induction of differentiation by retinoic acid, interferon-gamma, and T-lymphocyte-derived differentiation-inducing activity. *Journal of the National Cancer Institute,* **77,** 21-27.

Nakaya, M., Tanaka, M., Okabe, Y., Hanayama, R. and Nagata, S. (2006) Opposite effects of rho family GTPases on engulfment of apoptotic cells by macrophages. *The Journal of biological chemistry,* **281,** 8836-8842.

Naldini, L., Blomer, U., Gage, F. H., Trono, D. and Verma, I. M. (1996) Efficient transfer, integration, and sustained long-term expression of the transgene in adult rat brains injected with a lentiviral vector. *Proceedings of the National Academy of Sciences of the United States of America,* **93,** 11382-11388.

Nicoll, J. A., Barton, E., Boche, D. et al. (2006) Abeta species removal after abeta42 immunization. *Journal of neuropathology and experimental neurology,* **65,** 1040-1048.

Nicoll, J. A., Wilkinson, D., Holmes, C., Steart, P., Markham, H. and Weller, R. O. (2003) Neuropathology of human Alzheimer disease after immunization with amyloid-beta peptide: a case report. *Nature medicine,* **9,** 448-452.

Nilsberth, C., Westlind-Danielsson, A., Eckman, C. B. et al. (2001) The 'Arctic' APP mutation (E693G) causes Alzheimer's disease by enhanced Abeta protofibril formation. *Nature neuroscience,* **4,** 887-893.

Nimmerjahn, A., Kirchhoff, F. and Helmchen, F. (2005) Resting microglial cells are highly dynamic surveillants of brain parenchyma in vivo. *Science,* **308,** 1314-1318.

Nobes, C. D. and Hall, A. (1995) Rho, rac, and cdc42 GTPases regulate the assembly of multimolecular focal complexes associated with actin stress fibers, lamellipodia, and filopodia. *Cell,* **81,** 53-62.

Noh, K. T., Son, K. H., Jung, I. D., Kang, H. K., Hwang, S. A., Lee, W. S., You, J. C. and Park, Y. M. (2012) Protein kinase C delta (PKCdelta)-extracellular signal-regulated kinase 1/2 (ERK1/2) signaling cascade regulates glycogen synthase kinase-3 (GSK-3) inhibition-mediated interleukin-10 (IL-10) expression in lipopolysaccharide (LPS)-induced endotoxemia. *The Journal of biological chemistry,* **287,** 14226-14233.

Oakley, H., Cole, S. L., Logan, S. et al. (2006) Intraneuronal beta-amyloid aggregates, neurodegeneration, and neuron loss in transgenic mice with five familial Alzheimer's disease mutations: potential factors in amyloid plaque formation. *The Journal of neuroscience : the official journal of the Society for Neuroscience,* **26,** 10129-10140.

Oderup, C., LaJevic, M. and Butcher, E. C. (2013) Canonical and noncanonical Wnt proteins program dendritic cell responses for tolerance. *Journal of immunology,* **190,** 6126-6134.

Ogorek, I. (2011) Modulation of phagocytosis by microglia cells. In: *(unpublished Master`s thesis)*. Heinrich-Heine University Düsseldorf, Germany.

Ohgidani, M., Kato, T. A., Setoyama, D. et al. (2014) Direct induction of ramified microglia-like cells from human monocytes: dynamic microglial dysfunction in Nasu-Hakola disease. *Scientific reports,* **4,** 4957.

Oliva, C. A., Vargas, J. Y. and Inestrosa, N. C. (2013) Wnt signaling: role in LTP, neural networks and memory. *Ageing research reviews,* **12,** 786-800.

Orre, M., Kamphuis, W., Osborn, L. M., Jansen, A. H., Kooijman, L., Bossers, K. and Hol, E. M. (2014) Isolation of glia from Alzheimer's mice reveals inflammation and dysfunction. *Neurobiology of aging,* **35,** 2746-2760.

Pan, J. Q., Lewis, M. C., Ketterman, J. K. et al. (2011) AKT Kinase Activity Is Required for Lithium to Modulate Mood-Related Behaviors in Mice. *Neuropsychopharmacology : official publication of the American College of Neuropsychopharmacology,* **36,** 1397-1411.

Pandey, G. N., Dwivedi, Y., Rizavi, H. S., Teppen, T., Gaszner, G. L., Roberts, R. C. and Conley, R. R. (2009) GSK-3beta gene expression in human postmortem brain: regional distribution, effects of age and suicide. *Neurochemical research,* **34,** 274-285.

Paolicelli, R. C., Bolasco, G., Pagani, F. et al. (2011) Synaptic pruning by microglia is necessary for normal brain development. *Science,* **333,** 1456-1458.

Paresce, D. M., Chung, H. and Maxfield, F. R. (1997) Slow degradation of aggregates of the Alzheimer's disease amyloid beta-protein by microglial cells. *The Journal of biological chemistry,* **272,** 29390-29397.

Paresce, D. M., Ghosh, R. N. and Maxfield, F. R. (1996) Microglial cells internalize aggregates of the Alzheimer's disease amyloid beta-protein via a scavenger receptor. *Neuron,* **17,** 553-565.

Park, K. W., Lee, H. G., Jin, B. K. and Lee, Y. B. (2007) Interleukin-10 endogenously expressed in microglia prevents lipopolysaccharide-induced neurodegeneration in the rat cerebral cortex in vivo. *Experimental & molecular medicine,* **39,** 812-819.

Park, S. Y., Jung, M. Y., Lee, S. J., Kang, K. B., Gratchev, A., Riabov, V., Kzhyshkowska, J. and Kim, I. S. (2009) Stabilin-1 mediates phosphatidylserine-dependent clearance of cell corpses in alternatively activated macrophages. *Journal of cell science,* **122,** 3365-3373.

Patel, N. S., Paris, D., Mathura, V., Quadros, A. N., Crawford, F. C. and Mullan, M. J. (2005) Inflammatory cytokine levels correlate with amyloid load in transgenic mouse models of Alzheimer's disease. *Journal of neuroinflammation,* **2,** 9.

Perlmutter, L. S., Barron, E. and Chui, H. C. (1990) Morphologic association between microglia and senile plaque amyloid in Alzheimer's disease. *Neuroscience letters,* **119,** 32-36.

Perry, V. H. (1998) A revised view of the central nervous system microenvironment and major histocompatibility complex class II antigen presentation. *Journal of Neuroimmunology,* **90,** 113–121.

Perry, V. H. and Teeling, J. (2013) Microglia and macrophages of the central nervous system: the contribution of microglia priming and systemic inflammation to chronic neurodegeneration. *Seminars in immunopathology,* **35,** 601-612.

Phiel, C. J., Wilson, C. A., Lee, V. M. and Klein, P. S. (2003) GSK-3alpha regulates production of Alzheimer's disease amyloid-beta peptides. *Nature,* **423,** 435-439.

Plant, L. D., Boyle, J. P., Smith, I. F., Peers, C. and Pearson, H. A. (2003) The production of amyloid beta peptide is a critical requirement for the viability of central neurons. *The Journal of neuroscience : the official journal of the Society for Neuroscience,* **23,** 5531-5535.

Pollard, T. D. (2007) Regulation of actin filament assembly by Arp2/3 complex and formins. *Annual review of biophysics and biomolecular structure,* **36,** 451-477.

Polychronopoulos, P., Magiatis, P., Skaltsounis, A. L. et al. (2004) Structural basis for the synthesis of indirubins as potent and selective inhibitors of glycogen synthase kinase-3 and cyclin-dependent kinases. *Journal of medicinal chemistry,* **47,** 935-946.

Ponomarev, E. D., Maresz, K., Tan, Y. and Dittel, B. N. (2007) CNS-derived interleukin-4 is essential for the regulation of autoimmune inflammation and induces a state of alternative activation in microglial cells. *The Journal of neuroscience : the official journal of the Society for Neuroscience,* **27,** 10714-10721.

Prasher, V. P., Farrer, M. J., Kessling, A. M., Fisher, E. M., West, R. J., Barber, P. C. and Butler, A. C. (1998) Molecular mapping of Alzheimer-type dementia in Down's syndrome. *Annals of neurology,* **43,** 380-383.

Prinz, M. and Priller, J. (2014) Microglia and brain macrophages in the molecular age: from origin to neuropsychiatric disease. *Nature reviews. Neuroscience*.

Quintanilla, R. A., Munoz, F. J., Metcalfe, M. J., Hitschfeld, M., Olivares, G., Godoy, J. A. and Inestrosa, N. C. (2005) Trolox and 17beta-estradiol protect against amyloid beta-peptide neurotoxicity by a mechanism that involves modulation of the Wnt signaling pathway. *The Journal of biological chemistry,* **280,** 11615-11625.

Radaev, S., Kattah, M., Rostro, B., Colonna, M. and Sun, P. D. (2003) Crystal structure of the human myeloid cell activating receptor TREM-1. *Structure,* **11,** 1527-1535.

Raivich, G., Bohatschek, M., Kloss, C. U., Werner, A., Jones, L. L. and Kreutzberg, G. W. (1999) Neuroglial activation repertoire in the injured brain: graded response, molecular mechanisms and cues to physiological function. *Brain research. Brain research reviews,* **30,** 77-105.

Rebeck, G. W., Reiter, J. S., Strickland, D. K. and Hyman, B. T. (1993) Apolipoprotein E in sporadic Alzheimer's disease: allelic variation and receptor interactions. *Neuron,* **11,** 575-580.

Reed-Geaghan, E. G., Savage, J. C., Hise, A. G. and Landreth, G. E. (2009) CD14 and toll-like receptors 2 and 4 are required for fibrillar A{beta}-stimulated microglial activation. *The Journal of neuroscience : the official journal of the Society for Neuroscience,* **29,** 11982-11992.

Replogle, J. M., Chan, G., White, C. C. et al. (2015) A TREM1 variant alters the accumulation of Alzheimer-related amyloid pathology. *Annals of neurology,* **77,** 469-477.

Ring, D. B., Johnson, K. W., Henriksen, E. J. et al. (2003) Selective glycogen synthase kinase 3 inhibitors potentiate insulin activation of glucose transport and utilization in vitro and in vivo. *Diabetes,* **52,** 588-595.

Ring, S., Weyer, S. W., Kilian, S. B. et al. (2007) The secreted beta-amyloid precursor protein ectodomain APPs alpha is sufficient to rescue the anatomical, behavioral, and electrophysiological abnormalities of APP-deficient mice. *The Journal of neuroscience : the official journal of the Society for Neuroscience,* **27,** 7817-7826.

Rockenstein, E., Torrance, M., Adame, A., Mante, M., Bar-on, P., Rose, J. B., Crews, L. and Masliah, E. (2007) Neuroprotective effects of regulators of the glycogen synthase kinase-3beta signaling pathway in a transgenic model of Alzheimer's disease are associated with reduced amyloid precursor protein phosphorylation. *The Journal of neuroscience : the official journal of the Society for Neuroscience,* **27,** 1981-1991.

Rogers, J. and Lue, L. F. (2001) Microglial chemotaxis, activation, and phagocytosis of amyloid beta-peptide as linked phenomena in Alzheimer's disease. *Neurochemistry international,* **39,** 333-340.

Rogers, J., Strohmeyer, R., Kovelowski, C. J. and Li, R. (2002) Microglia and inflammatory mechanisms in the clearance of amyloid beta peptide. *Glia,* **40,** 260-269.

Rogers, J., Webster, S., Lue, L. F., Brachova, L., Civin, W. H., Emmerling, M., Shivers, B., Walker, D. and McGeer, P. (1996) Inflammation and Alzheimer's disease pathogenesis. *Neurobiology of aging,* **17,** 681-686.

Rosi, M. C., Luccarini, I., Grossi, C. et al. (2010) Increased Dickkopf-1 expression in transgenic mouse models of neurodegenerative disease. *Journal of neurochemistry,* **112,** 1539-1551.

Rygiel, K. (2016) Novel strategies for Alzheimer's disease treatment: An overview of anti-amyloid beta monoclonal antibodies. *Indian journal of pharmacology,* **48,** 629-636.

Saavedra, L., Mohamed, A., Ma, V., Kar, S. and de Chaves, E. P. (2007) Internalization of beta-amyloid peptide by primary neurons in the absence of apolipoprotein E. *The Journal of biological chemistry,* **282,** 35722-35732.

Saijo, K. and Glass, C. K. (2011) Microglial cell origin and phenotypes in health and disease. *Nature reviews. Immunology,* **11,** 775-787.

Saitoh, T., Sundsmo, M., Roch, J. M., Kimura, N., Cole, G., Schubert, D., Oltersdorf, T. and Schenk, D. B. (1989) Secreted form of amyloid beta protein precursor is involved in the growth regulation of fibroblasts. *Cell,* **58,** 615-622.

Sandbrink, R., Masters, C. L. and Beyreuther, K. (1996) APP gene family. Alternative splicing generates functionally related isoforms. *Annals of the New York Academy of Sciences,* **777,** 281-287.

Sanjana, N. E., Shalem, O. and Zhang, F. (2014) Improved vectors and genome-wide libraries for CRISPR screening. *Nature methods,* **11,** 783-784.

Savill, J., Hogg, N., Ren, Y. and Haslett, C. (1992) Thrombospondin cooperates with CD36 and the vitronectin receptor in macrophage recognition of neutrophils undergoing apoptosis. *The Journal of clinical investigation,* **90,** 1513-1522.

Schaer, D. J., Alayash, A. I. and Buehler, P. W. (2007) Gating the radical hemoglobin to macrophages: the anti-inflammatory role of CD163, a scavenger receptor. *Antioxidants & redox signaling,* **9,** 991-999.

Scheiblich, H. and Bicker, G. (2017) Regulation of Microglial Phagocytosis by RhoA/ROCK-Inhibiting Drugs. *Cellular and molecular neurobiology,* **37,** 461-473.

Schenk, D., Barbour, R., Dunn, W. et al. (1999) Immunization with amyloid-beta attenuates Alzheimer-disease-like pathology in the PDAPP mouse. *Nature,* **400,** 173-177.

Schiff, D. E., Kline, L., Soldau, K., Lee, J. D., Pugin, J., Tobias, P. S. and Ulevitch, R. J. (1997) Phagocytosis of gram-negative bacteria by a unique CD14-dependent mechanism. *Journal of leukocyte biology,* **62,** 786-794.

Schoenen, J. (1982) The dendritic organization of the human spinal cord: the dorsal horn. *Neuroscience,* **7,** 2057-2087.

Sebire, G., Emilie, D., Wallon, C., Hery, C., Devergne, O., Delfraissy, J. F., Galanaud, P. and Tardieu, M. (1993) In vitro production of IL-6, IL-1 beta, and tumor necrosis factor-alpha by human embryonic microglial and neural cells. *Journal of immunology,* **150,** 1517-1523.

Selenica, M. L., Jensen, H. S., Larsen, A. K., Pedersen, M. L., Helboe, L., Leist, M. and Lotharius, J. (2007) Efficacy of small-molecule glycogen synthase kinase-3 inhibitors in the postnatal rat model of tau hyperphosphorylation. *British journal of pharmacology,* **152,** 959-979.

Selkoe, D. J. (2001a) Alzheimer's disease: genes, proteins, and therapy. *Physiological reviews,* **81,** 741-766.

Selkoe, D. J. (2001b) Clearing the brain's amyloid cobwebs. *Neuron,* **32,** 177-180.

Selkoe, D. J. (2011) Alzheimer's disease. *Cold Spring Harb Perspect Biol,* **3**.

Selkoe, D. J. and Hardy, J. (2016) The amyloid hypothesis of Alzheimer's disease at 25 years. *EMBO Mol Med*.

Sengupta, A., Kabat, J., Novak, M., Wu, Q., Grundke-Iqbal, I. and Iqbal, K. (1998) Phosphorylation of tau at both Thr 231 and Ser 262 is required for maximal

inhibition of its binding to microtubules. *Archives of biochemistry and biophysics,* **357,** 299-309.

Sereno, L., Coma, M., Rodriguez, M. et al. (2009) A novel GSK-3beta inhibitor reduces Alzheimer's pathology and rescues neuronal loss in vivo. *Neurobiology of disease,* **35,** 359-367.

Serrano-Pozo, A., Frosch, M. P., Masliah, E. and Hyman, B. T. (2011) Neuropathological alterations in Alzheimer disease. *Cold Spring Harbor perspectives in medicine,* **1,** a006189.

Sessa, G., Podini, P., Mariani, M., Meroni, A., Spreafico, R., Sinigaglia, F., Colonna, M., Panina, P. and Meldolesi, J. (2004) Distribution and signaling of TREM2/DAP12, the receptor system mutated in human polycystic lipomembraneous osteodysplasia with sclerosing leukoencephalopathy dementia. *The European journal of neuroscience,* **20,** 2617-2628.

Seubert, P., Oltersdorf, T., Lee, M. G. et al. (1993) Secretion of beta-amyloid precursor protein cleaved at the amino terminus of the beta-amyloid peptide. *Nature,* **361,** 260-263.

Sevigny, J., Chiao, P., Bussiere, T. et al. (2016) The antibody aducanumab reduces Abeta plaques in Alzheimer's disease. *Nature,* **537,** 50-56.

Shaftel, S. S., Kyrkanides, S., Olschowka, J. A., Miller, J. N., Johnson, R. E. and O'Banion, M. K. (2007) Sustained hippocampal IL-1 beta overexpression mediates chronic neuroinflammation and ameliorates Alzheimer plaque pathology. *The Journal of clinical investigation,* **117,** 1595-1604.

Shalem, O., Sanjana, N. E., Hartenian, E. et al. (2014) Genome-scale CRISPR-Cas9 knockout screening in human cells. *Science,* **343,** 84-87.

Shankar, G. M., Li, S., Mehta, T. H. et al. (2008) Amyloid-beta protein dimers isolated directly from Alzheimer's brains impair synaptic plasticity and memory. *Nature medicine*.

Sharif, O., Bolshakov, V. N., Raines, S., Newham, P. and Perkins, N. D. (2007) Transcriptional profiling of the LPS induced NF-kappaB response in macrophages. *BMC immunology,* **8,** 1.

Shi, C. and Pamer, E. G. (2011) Monocyte recruitment during infection and inflammation. *Nature reviews. Immunology,* **11,** 762-774.

Sierra-Filardi, E., Nieto, C., Dominguez-Soto, A. et al. (2014) CCL2 shapes macrophage polarization by GM-CSF and M-CSF: identification of CCL2/CCR2-dependent gene expression profile. *Journal of immunology,* **192,** 3858-3867.

Silva-Alvarez, C., Arrazola, M. S., Godoy, J. A., Ordenes, D. and Inestrosa, N. C. (2013) Canonical Wnt signaling protects hippocampal neurons from Abeta oligomers: role of non-canonical Wnt-5a/Ca(2+) in mitochondrial dynamics. *Frontiers in cellular neuroscience,* **7,** 97.

Simard, A. R., Soulet, D., Gowing, G., Julien, J. P. and Rivest, S. (2006) Bone marrow-derived microglia play a critical role in restricting senile plaque formation in Alzheimer's disease. *Neuron,* **49,** 489-502.

Slunt, H. H., Thinakaran, G., Von Koch, C., Lo, A. C., Tanzi, R. E. and Sisodia, S. S. (1994) Expression of a ubiquitous, cross-reactive homologue of the mouse beta-amyloid precursor protein (APP). *The Journal of biological chemistry,* **269,** 2637-2644.

Sole-Domenech, S., Cruz, D. L., Capetillo-Zarate, E. and Maxfield, F. R. (2016) The endocytic pathway in microglia during health, aging and Alzheimer's disease. *Ageing research reviews,* **32,** 89-103.

Solito, E. and Sastre, M. (2012) Microglia function in Alzheimer's disease. *Frontiers in pharmacology,* **3,** 14.

Sorkin, A. and von Zastrow, M. (2009) Endocytosis and signalling: intertwining molecular networks. *Nature reviews. Molecular cell biology,* **10,** 609-622.

Soscia, S. J., Kirby, J. E., Washicosky, K. J. et al. (2010) The Alzheimer's disease-associated amyloid beta-protein is an antimicrobial peptide. *PloS one,* **5,** e9505.

Soutar, M. P., Kim, W. Y., Williamson, R., Peggie, M., Hastie, C. J., McLauchlan, H., Snider, W. D., Gordon-Weeks, P. R. and Sutherland, C. (2010) Evidence that glycogen synthase kinase-3 isoforms have distinct substrate preference in the brain. *Journal of neurochemistry,* **115,** 974-983.

Stein, E. V., Miller, T. W., Ivins-O'Keefe, K., Kaur, S. and Roberts, D. D. (2016) Secreted Thrombospondin-1 Regulates Macrophage Interleukin-1beta Production and Activation through CD47. *Scientific reports,* **6,** 19684.

Steinbrecher, K. A., Wilson, W., 3rd, Cogswell, P. C. and Baldwin, A. S. (2005) Glycogen synthase kinase 3beta functions to specify gene-specific, NF-kappaB-dependent transcription. *Molecular and cellular biology,* **25,** 8444-8455.

Stence, N., Waite, M. and Dailey, M. E. (2001) Dynamics of microglial activation: a confocal time-lapse analysis in hippocampal slices. *Glia,* **33,** 256-266.

Stewart, S. A., Dykxhoorn, D. M., Palliser, D. et al. (2003) Lentivirus-delivered stable gene silencing by RNAi in primary cells. *Rna,* **9,** 493-501.

Streit, W. J. (2006) Microglial senescence: does the brain's immune system have an expiration date? *Trends Neurosci,* **29,** 506-510.

Streit, W. J., Sammons, N. W., Kuhns, A. J. and Sparks, D. L. (2004) Dystrophic microglia in the aging human brain. *Glia,* **45,** 208-212.

Stuart, L. M. and Ezekowitz, R. A. (2005) Phagocytosis: elegant complexity. *Immunity,* **22,** 539-550.

Su, Y., Ryder, J., Li, B. et al. (2004) Lithium, a common drug for bipolar disorder treatment, regulates amyloid-beta precursor protein processing. *Biochemistry,* **43,** 6899-6908.

Sudduth, T. L., Schmitt, F. A., Nelson, P. T. and Wilcock, D. M. (2013) Neuroinflammatory phenotype in early Alzheimer's disease. *Neurobiology of aging,* **34,** 1051-1059.

Sun, X., Sato, S., Murayama, O., Murayama, M., Park, J. M., Yamaguchi, H. and Takashima, A. (2002) Lithium inhibits amyloid secretion in COS7 cells transfected with amyloid precursor protein C100. *Neuroscience letters,* **321,** 61-64.

Sutherland, C., Leighton, I. A. and Cohen, P. (1993) Inactivation of glycogen synthase kinase-3 beta by phosphorylation: new kinase connections in insulin and growth-factor signalling. *The Biochemical journal,* **296 (Pt 1),** 15-19.

Suzuki, N., Cheung, T. T., Cai, X. D., Odaka, A., Otvos, L. J., Eckman, C., Golde, T. E. and Younkin, S. G. (1994) An increased percentage of long amyloid beta protein secreted by familial amyloid beta protein precursor (beta APP717) mutants. *Science,* **264,** 1336-1340.

Swanson, J. A. and Watts, C. (1995) Macropinocytosis. *Trends in cell biology,* **5,** 424-428.

Tahara, K., Kim, H. D., Jin, J. J., Maxwell, J. A., Li, L. and Fukuchi, K. (2006) Role of toll-like receptor signalling in Abeta uptake and clearance. *Brain : a journal of neurology,* **129,** 3006-3019.

Takahashi, K., Rochford, C. D. and Neumann, H. (2005) Clearance of apoptotic neurons without inflammation by microglial triggering receptor expressed on myeloid cells-2. *The Journal of experimental medicine,* **201,** 647-657.

Tang, Y. and Le, W. (2016) Differential Roles of M1 and M2 Microglia in Neurodegenerative Diseases. *Molecular neurobiology,* **53,** 1181-1194.

Tapon, N. and Hall, A. (1997) Rho, Rac and Cdc42 GTPases regulate the organization of the actin cytoskeleton. *Current opinion in cell biology,* **9,** 86-92.

Tay, T. F., Maheran, M., Too, S. L., Hasidah, M. S., Ismail, G. and Embi, N. (2012) Glycogen synthase kinase-3beta inhibition improved survivability of mice infected with Burkholderia pseudomallei. *Tropical biomedicine,* **29,** 551-567.

Teller, J. K., Russo, C., DeBusk, L. M. et al. (1996) Presence of soluble amyloid beta-peptide precedes amyloid plaque formation in Down's syndrome. *Nature medicine,* **2,** 93-95.

Terwel, D., Muyllaert, D., Dewachter, I., Borghgraef, P., Croes, S., Devijver, H. and Van Leuven, F. (2008) Amyloid activates GSK-3beta to aggravate neuronal tauopathy in bigenic mice. *The American journal of pathology,* **172,** 786-798.

Terwel, D., Steffensen, K. R., Verghese, P. B., Kummer, M. P., Gustafsson, J. A., Holtzman, D. M. and Heneka, M. T. (2011) Critical Role of Astroglial Apolipoprotein E and Liver X Receptor-{alpha} Expression for Microglial A{beta} Phagocytosis. *The Journal of neuroscience : the official journal of the Society for Neuroscience,* **31,** 7049-7059.

Thankamony, S. P. and Knudson, W. (2006) Acylation of CD44 and its association with lipid rafts are required for receptor and hyaluronan endocytosis. *The Journal of biological chemistry,* **281,** 34601-34609.

Theriault, P., ElAli, A. and Rivest, S. (2015) The dynamics of monocytes and microglia in Alzheimer's disease. *Alzheimer's research & therapy,* **7,** 41.

Tokuda, T., Fukushima, T., Ikeda, S., Sekijima, Y., Shoji, S., Yanagisawa, N. and Tamaoka, A. (1997) Plasma levels of amyloid beta proteins Abeta1-40 and Abeta1-42(43) are elevated in Down's syndrome. *Annals of neurology,* **41,** 271-273.

Toledo, E. M. and Inestrosa, N. C. (2010) Activation of Wnt signaling by lithium and rosiglitazone reduced spatial memory impairment and neurodegeneration in brains of an APPswe/PSEN1DeltaE9 mouse model of Alzheimer's disease. *Molecular psychiatry,* **15,** 272-285, 228.

Town, T., Laouar, Y., Pittenger, C., Mori, T., Szekely, C. A., Tan, J., Duman, R. S. and Flavell, R. A. (2008) Blocking TGF-beta-Smad2/3 innate immune signaling mitigates Alzheimer-like pathology. *Nature medicine,* **14,** 681-687.

Trang, T., Beggs, S., Wan, X. and Salter, M. W. (2009) P2X4-receptor-mediated synthesis and release of brain-derived neurotrophic factor in microglia is dependent on calcium and p38-mitogen-activated protein kinase activation. *The Journal of neuroscience : the official journal of the Society for Neuroscience,* **29,** 3518-3528.

Trask, D. K. and Muller, M. T. (1988) Stabilization of type I topoisomerase-DNA covalent complexes by actinomycin D. *Proceedings of the National Academy of Sciences of the United States of America,* **85,** 1417-1421.

Tremblay, M. E., Lowery, R. L. and Majewska, A. K. (2010) Microglial interactions with synapses are modulated by visual experience. *PLoS biology,* **8,** e1000527.

Tsao, N., Kuo, C. F., Chiu, C. C., Lin, W. C., Huang, W. H. and Chen, L. Y. (2015) Protection against Klebsiella pneumoniae using lithium chloride in an intragastric infection model. *Antimicrobial agents and chemotherapy,* **59,** 1525-1533.

Tseng, A. S., Engel, F. B. and Keating, M. T. (2006) The GSK-3 inhibitor BIO promotes proliferation in mammalian cardiomyocytes. *Chemistry & biology,* **13,** 957-963.

Tsuchiya, S., Yamabe, M., Yamaguchi, Y., Kobayashi, Y., Konno, T. and Tada, K. (1980) Establishment and characterization of a human acute monocytic leukemia cell line (THP-1). *International journal of cancer,* **26,** 171-176.

Uemura, K., Kuzuya, A., Shimozono, Y., Aoyagi, N., Ando, K., Shimohama, S. and Kinoshita, A. (2007) GSK3beta activity modifies the localization and function of presenilin 1. *The Journal of biological chemistry,* **282,** 15823-15832.

Ulrich, J. D., Finn, M. B., Wang, Y. et al. (2014) Altered microglial response to Abeta plaques in APPPS1-21 mice heterozygous for TREM2. *Molecular neurodegeneration,* **9,** 20.

Vachon, E., Martin, R., Plumb, J. et al. (2006) CD44 is a phagocytic receptor. *Blood,* **107,** 4149-4158.

van Amerongen, R. and Nusse, R. (2009) Towards an integrated view of Wnt signaling in development. *Development,* **136,** 3205-3214.

Van Cauwenberghe, C., Van Broeckhoven, C. and Sleegers, K. (2016) The genetic landscape of Alzheimer disease: clinical implications and perspectives. *Genetics in medicine : official journal of the American College of Medical Genetics,* **18,** 421-430.

Vassar, R., Bennett, B. D., Babu-Khan, S. et al. (1999a) Beta-secretase cleavage of Alzheimer's amyloid precursor protein by the transmembrane aspartic protease BACE. *Science,* **286,** 735-741.

Vassar, R., Bennett, B. D., Babu-Khan, S. et al. (1999b) Beta-secretase cleavage of Alzheimer's amyloid precursor protein by the transmembrane aspartic protease BACE. *Science,* **286,** 735-741.

von Bernhardi, R., Tichauer, J. E. and Eugenin, J. (2010) Aging-dependent changes of microglial cells and their relevance for neurodegenerative disorders. *Journal of neurochemistry,* **112,** 1099-1114.

Wang, M. J., Huang, H. Y., Chen, W. F., Chang, H. F. and Kuo, J. S. (2010) Glycogen synthase kinase-3beta inactivation inhibits tumor necrosis factor-alpha production in microglia by modulating nuclear factor kappaB and MLK3/JNK signaling cascades. *Journal of neuroinflammation,* **7,** 99.

Wang, T., Wei, J. J., Sabatini, D. M. and Lander, E. S. (2014) Genetic screens in human cells using the CRISPR-Cas9 system. *Science,* **343,** 80-84.

Wang, Y., Cella, M., Mallinson, K. et al. (2015) TREM2 lipid sensing sustains the microglial response in an Alzheimer's disease model. *Cell,* **160,** 1061-1071.

Webster, S., Lue, L. F., Brachova, L. et al. (1997) Molecular and cellular characterization of the membrane attack complex, C5b-9, in Alzheimer's disease. *Neurobiology of aging,* **18,** 415-421.

Weggen, S. and Beher, D. (2012) Molecular consequences of amyloid precursor protein and presenilin mutations causing autosomal-dominant Alzheimer's disease. *Alzheimer's research & therapy,* **4,** 9.

Weingarten, M. D., Lockwood, A. H., Hwo, S. Y. and Kirschner, M. W. (1975) A protein factor essential for microtubule assembly. *Proceedings of the National Academy of Sciences of the United States of America,* **72,** 1858-1862.

Wennerberg, K. and Der, C. J. (2004) Rho-family GTPases: it's not only Rac and Rho (and I like it). *Journal of cell science,* **117,** 1301-1312.

Westin, K., Buchhave, P., Nielsen, H., Minthon, L., Janciauskiene, S. and Hansson, O. (2012) CCL2 is associated with a faster rate of cognitive decline during early stages of Alzheimer's disease. *PloS one,* **7,** e30525.

WHO, W. H. O. (2016) Dementia Fact sheet April 2016. http://www.who.int/mediacentre/factsheets/fs362/en/.

Wilcock, D. M., Rojiani, A., Rosenthal, A. et al. (2004) Passive amyloid immunotherapy clears amyloid and transiently activates microglia in a transgenic mouse model of amyloid deposition. *The Journal of neuroscience : the official journal of the Society for Neuroscience,* **24,** 6144-6151.

Willem, M., Lammich, S. and Haass, C. (2009) Function, regulation and therapeutic properties of beta-secretase (BACE1). *Semin Cell Dev Biol,* **20,** 175-182.

Williams, L. M., Ricchetti, G., Sarma, U., Smallie, T. and Foxwell, B. M. (2004) Interleukin-10 suppression of myeloid cell activation--a continuing puzzle. *Immunology,* **113,** 281-292.

Wilquet, V. and De Strooper, B. (2004) Amyloid-beta precursor protein processing in neurodegeneration. *Curr Opin Neurobiol,* **14,** 582-588.

Winslow, B. T., Onysko, M. K., Stob, C. M. and Hazlewood, K. A. (2011) Treatment of Alzheimer disease. *American family physician,* **83,** 1403-1412.

Wirths, O., Multhaup, G., Czech, C., Blanchard, V., Moussaoui, S., Tremp, G., Pradier, L., Beyreuther, K. and Bayer, T. A. (2001) Intraneuronal Abeta accumulation

precedes plaque formation in beta-amyloid precursor protein and presenilin-1 double-transgenic mice. *Neuroscience letters,* **306,** 116-120.

Wolf, S. A., Boddeke, H. W. and Kettenmann, H. (2016) Microglia in Physiology and Disease. *Annual review of physiology*.

Wonderling, R. S., Ghaffar, A. and Mayer, E. P. (1996) Lipopolysaccharide-induced suppression of phagocytosis: effects on the phagocytic machinery. *Immunopharmacology and immunotoxicology,* **18,** 267-289.

Wood, J. G., Mirra, S. S., Pollock, N. J. and Binder, L. I. (1986) Neurofibrillary tangles of Alzheimer disease share antigenic determinants with the axonal microtubule-associated protein tau (tau). *Proceedings of the National Academy of Sciences of the United States of America,* **83,** 4040-4043.

Woodgett, J. R. (1990) Molecular cloning and expression of glycogen synthase kinase-3/factor A. *The EMBO journal,* **9,** 2431-2438.

Wu, D. and Pan, W. (2010) GSK3: a multifaceted kinase in Wnt signaling. *Trends Biochem Sci,* **35,** 161-168.

Wu, Y., Dissing-Olesen, L., MacVicar, B. A. and Stevens, B. (2015) Microglia: Dynamic Mediators of Synapse Development and Plasticity. *Trends in immunology,* **36,** 605-613.

Xiang, X., Werner, G., Bohrmann, B. et al. (2016) TREM2 deficiency reduces the efficacy of immunotherapeutic amyloid clearance. *EMBO Mol Med*.

Xue, J., Schmidt, S. V., Sander, J. et al. (2014) Transcriptome-based network analysis reveals a spectrum model of human macrophage activation. *Immunity,* **40,** 274-288.

Yamamoto, M., Horiba, M., Buescher, J. L., Huang, D., Gendelman, H. E., Ransohoff, R. M. and Ikezu, T. (2005) Overexpression of monocyte chemotactic protein-1/CCL2 in beta-amyloid precursor protein transgenic mice show accelerated diffuse beta-amyloid deposition. *The American journal of pathology,* **166,** 1475-1485.

Yamamoto, M., Kiyota, T., Walsh, S. M., Liu, J., Kipnis, J. and Ikezu, T. (2008) Cytokine-mediated inhibition of fibrillar amyloid-beta peptide degradation by human mononuclear phagocytes. *Journal of immunology,* **181,** 3877-3886.

Yamanaka, M., Ishikawa, T., Griep, A., Axt, D., Kummer, M. P. and Heneka, M. T. (2012) PPARgamma/RXRalpha-Induced and CD36-Mediated Microglial Amyloid-beta Phagocytosis Results in Cognitive Improvement in Amyloid Precursor Protein/Presenilin 1 Mice. *The Journal of neuroscience : the official journal of the Society for Neuroscience,* **32,** 17321-17331.

Yamazaki, T., Koo, E. H. and Selkoe, D. J. (1997) Cell surface amyloid beta-protein precursor colocalizes with beta 1 integrins at substrate contact sites in neural cells. *The Journal of neuroscience : the official journal of the Society for Neuroscience,* **17,** 1004-1010.

Yan, R. and Vassar, R. (2014) Targeting the beta secretase BACE1 for Alzheimer's disease therapy. *The Lancet. Neurology,* **13,** 319-329.

Yao, H. B., Shaw, P. C., Wong, C. C. and Wan, D. C. (2002) Expression of glycogen synthase kinase-3 isoforms in mouse tissues and their transcription in the brain. *Journal of chemical neuroanatomy,* **23,** 291-297.

Yates, S. L., Burgess, L. H., Kocsis-Angle, J., Antal, J. M., Dority, M. D., Embury, P. B., Piotrkowski, A. M. and Brunden, K. R. (2000) Amyloid beta and amylin fibrils induce increases in proinflammatory cytokine and chemokine production by THP-1 cells and murine microglia. *Journal of neurochemistry,* **74,** 1017-1025.

Yeh, F. L., Wang, Y., Tom, I., Gonzalez, L. C. and Sheng, M. (2016) TREM2 Binds to Apolipoproteins, Including APOE and CLU/APOJ, and Thereby Facilitates Uptake of Amyloid-Beta by Microglia. *Neuron,* **91,** 328-340.

Yip, A. G., Green, R. C., Huyck, M., Cupples, L. A., Farrer, L. A. and Group, M. S. (2005) Nonsteroidal anti-inflammatory drug use and Alzheimer's disease risk: the MIRAGE Study. *BMC geriatrics,* **5,** 2.

Yoshida, K., Renard-Guillet, C., Inoue, K., Shirahige, K., Okada-Hatakeyama, M. and Ishii, S. (2016) Microarray expression analysis of genes involved in innate immune memory in peritoneal macrophages. *Genomics data,* **7,** 90-91.

Young-Pearse, T. L., Chen, A. C., Chang, R., Marquez, C. and Selkoe, D. J. (2008) Secreted APP regulates the function of full-length APP in neurite outgrowth through interaction with integrin beta1. *Neural development,* **3,** 15.

Yuskaitis, C. J. and Jope, R. S. (2009) Glycogen synthase kinase-3 regulates microglial migration, inflammation, and inflammation-induced neurotoxicity. *Cellular signalling,* **21,** 264-273.

Zandi, P. P., Anthony, J. C., Hayden, K. M., Mehta, K., Mayer, L. and Breitner, J. C. (2002) Reduced incidence of AD with NSAID but not H2 receptor antagonists: the Cache County Study. *Neurology,* **59,** 880-886.

Zhang, Y. W., Thompson, R., Zhang, H. and Xu, H. (2011) APP processing in Alzheimer's disease. *Molecular brain,* **4,** 3.

Zhao, X., Wang, H., Sun, G., Zhang, J., Edwards, N. J. and Aronowski, J. (2015) Neuronal Interleukin-4 as a Modulator of Microglial Pathways and Ischemic Brain Damage. *The Journal of neuroscience : the official journal of the Society for Neuroscience,* **35,** 11281-11291.

Zheng, H., Jiang, M., Trumbauer, M. E. et al. (1995) ß-amyloid precursor protein-deficient mice show reactive gliosis and decreased locomotor activity. *Cell,* **81,** 525-531.

Zheng, H. and Koo, E. H. (2011) Biology and pathophysiology of the amyloid precursor protein. *Molecular neurodegeneration,* **6,** 27.

Zheng, X., Liu, D., Roychaudhuri, R., Teplow, D. B. and Bowers, M. T. (2015) Amyloid beta-Protein Assembly: Differential Effects of the Protective A2T Mutation and Recessive A2V Familial Alzheimer's Disease Mutation. *ACS chemical neuroscience,* **6,** 1732-1740.

Publications

Naumann EC, Göring S, **Ogorek I**, Weggen S, Schmidt B. *Membrane anchoring γ-secretase modulators with terpene-derived moieties.* **Bioorg Med Chem Lett**. 2013 Jul 1;23(13):3852-6.

Gowert NS, Donner L, Chatterjee M, Eisele YS, Towhid ST, Münzer P, Walker B, **Ogorek I**, Borst O, Grandoch M, Schaller M, Fischer JW, Gawaz M, Weggen S, Lang F, Jucker M, Elvers M. *Blood platelets in the progression of Alzheimer's disease.* **PLoS One**. 2014 Feb 28;9(2):e90523.

Flesch D, Ness J, Lamers C, Dehm F, Popella S, Steri R, **Ogorek I**, Hieke M, Dannhardt G, Werz O, Weggen S, Schubert-Zsilavecz M.
SAR-studies of γ-secretase modulators with PPARγ-agonistic and 5-lipoxygenase-inhibitory activity for Alzheimer's disease. **Bioorg Med Chem Lett**. 2015 Feb 15;25(4):841-6.

Goel P, Jumpertz T, Mikles DC, Tichá A, Nguyen MTN, Verhelst S, Hubalek M, Johnson DC, Bachovchin DA, **Ogorek I**, Pietrzik CU, Strisovsky K, Schmidt B, Weggen S. *Discovery and Biological Evaluation of Potent and Selective N-Methylene Saccharin-Derived Inhibitors for Rhomboid Intramembrane Proteases.* **Biochemistry**. 2017 Dec 26;56(51):6713-6725.

Goel P, Jumpertz T, Tichá A, **Ogorek I**, Mikles DC, Hubalek M, Pietrzik CU, Strisovsky K, Schmidt B, Weggen S. *Discovery and validation of 2-styryl substituted benzoxazin-4-ones as a novel scaffold for rhomboid protease inhibitors.* **Bioorg Med Chem Lett**. 2018 May 1;28(8):1417-1422.

Suwala A, Koch K, Herrera Rios D, Aretz P, Uhlmann C, **Ogorek I**, Felsberg J, Reifenberger G, Köhrer K, Deenen R, Steiger H, Kahlert U, Maciaczyk J. *Inhibition of Wnt/beta-catenin signaling downregulates expression of aldehyde dehydrogenase isoform 3A1 (ALDH3A1) to reduce resistance against temozolomide in glioblastoma in vitro.* **Oncotarget.** Accepted.

Walter S, Jumpertz T, Hüttenrauch M, Gerber H, **Ogorek I**, Lehmann S, Lepka K, Berndt C, Wiltfang J, Becker-Pauly C, Pietrzik C, Fraering P, Wirths O, Weggen S. *The metalloprotease ADAMTS4 generates N-truncated Aß4-x peptides and marks oligodendrocytes as a pro-amyloidogenic cell lineage in Alzheimer's disease.* **Submitted.**

Hüttenrauch M, **Ogorek I**, Klafki H, Otto M, Stadelmann-Nessler C, Weggen S, Wiltfang J, Wirths O. *Glycoprotein NMB: a novel Alzheimer's disease associated marker expressed in a subset of activated microglia.* **Submitted.**

Acknowledgements

First of all, I would like to thank Prof. Dr. Sascha Weggen for the opportunity to work on this project and for guiding and supporting me over the years.

I would like to thank Prof. Dr. Lutz Schmitt for being my second supervisor and mentor.

Many thanks to all the members of the Institute of Neuropathology, especially Sandra Lehmann and all former members of the Weggen lab, for their support and the great working atmosphere.

I thank Dr. Markus Kummer for collaborating with us and for his helpful advice. I thank our collaborative partners Prof. Dr. Karl Köhrer and Dr. René Deenen for conducting the microarray experiments and statistical analyses.

I am forever grateful to my family and friends for their loving support and constant encouragement, and for making me laugh just at the right times.